

Soil erosion and nitrogen leaching in northern Vietnam: Experimentation and modelling

Promotor: Prof. dr. ir. H. van Keulen
Hoogleraar bij de leerstoelgroep Plantaardige Productiesystemen
Wageningen Universiteit

Co-promotoren: Dr. R.P. Roetter
Senior onderzoeker,
Soil Science Centre, Alterra Green World Research,
Wageningen Universiteit en Researchcentrum
Dr. R. Hessel
Senior onderzoeker,
Soil Science Centre, Alterra Green World Research,
Wageningen Universiteit en Researchcentrum

Promotiecommissie:
Prof. dr. C.J. Ritsema (Wageningen Universiteit)
Dr. C.T. Hoanh (IWMI-SEA, Malaysia)
Dr. ir. M.E.F. van Mensvoort (Wageningen Universiteit)
Dr. ir. C.M.M. Mannaerts (ITC, Enschede)

Dit onderzoek is uitgevoerd binnen de C.T. de Wit onderzoekschool: Production Ecology and Resource Conservation.

Soil erosion and nitrogen leaching in northern Vietnam: Experimentation and modelling

Mai Van Trinh

Proefschrift
ter verkrijging van de graad van doctor
op gezag van de rector magnificus
van Wageningen Universiteit,
prof. dr. M.J. Kropff,
in het openbaar te verdedigen
op dinsdag 17 april 2007
des namiddags te half twee in de Aula.

Mai Van Trinh (2007)

Soil erosion and nitrogen leaching in northern Vietnam: Experimentation and modelling.

Mai Van Trinh –[S.l.:s.n.]. Ill.

PhD thesis Wageningen University. –With ref.–

With summaries in English, Dutch and Vietnamese.

ISBN: 90-8504-605-x

Abstract

Mai Van Trinh, 2007. Soil erosion and nitrogen leaching in northern Vietnam: Experimentation and modelling. PhD thesis, Wageningen University, Wageningen, The Netherlands. With summaries in English, Dutch, and Vietnamese, 182 pp.

Two years research has been conducted in Tam Duong district, Vinh Phuc province, upstream in the Red River Delta in northern Vietnam, comprising three geographical regions, i.e. mountainous areas, terraces in hilly land and flat land. The extent of soil degradation in the district was delineated, using the Red/Near-Infrared band ratio of satellite images, calibrated on the basis of soil maps and field checks. Results showed strong dynamics in soil degradation with the largest area of degraded soil of 3280 ha in 1992, associated with a substantial reduction in forest cover and expansion of the agricultural area from the mid-1980s. Subsequently (1996), re-forestation, particularly planting of eucalyptus plantations, led to a reduction, followed (2000) by expansion again, as a consequence of harvesting of production forests.

In the mountainous and hilly areas, soil erosion is the dominant degradation process, very severe at individual plot scale, but far less at sub-watershed and watershed scales (i.e. measured soil losses over eight events, with the same total rainfall, were 1360 and 773 kg ha⁻¹ in a cassava and an eucalyptus plot, while it was 45 in the sub-watershed and 125 in the main watershed). Performance of the soil erosion model LISEM was evaluated in the study area; results showed differences in performance at different spatial scales. In the main watershed, simulated total runoff and soil loss were underestimated, because of storage and release in terraces and rice fields. In the upland sub-watershed, total soil loss was overestimated due to overestimation of sediment concentration, as a result of high detachment and transport capacity.

In addition to soil erosion from the terraces, nitrogen leaching from the root zone in these sandy soils contributes to negative environmental impact of agriculture. A nitrogen balance model was developed, and calibrated on the basis of measured soil nitrogen concentrations in different cropping systems. Results from the model showed increased nitrogen leaching with increasing fertilizer doses, i.e. in a rice-rice-maize rotation, the traditional land use pattern in the district, annual nitrogen leaching losses varied from 52 to 60 kg ha⁻¹, 56 to 114 kg ha⁻¹, and 58 to 154 kg ha⁻¹ for low, intermediate, and high fertilizer inputs, respectively. In the lowland area, agriculture has diversified and intensified, and high value crops are cultivated with very high doses of fertilizer. In these cropping systems, nitrogen leaching is particularly high. Annual leaching losses were calculated of up to 193 kg ha⁻¹ in flowers and 115 kg ha⁻¹ in vegetables compared to about 50 kg ha⁻¹ in rice.

From a set of point measurements, spatial distributions of nitrate- and ammonium nitrogen for a small region were predicted, using regression block kriging. The method was based on a stepwise backward linear regression, combined with expert knowledge, taking into account

the weighted influences of various explanatory variables, i.e. elevation, soil type, and land use. Temporal variability in nitrogen concentrations in the groundwater were mainly the result of variations in rainfall and in land use, characterized by different irrigation and fertilizer regimes.

For exploration of the consequences of introduction of alternative land use types and crop management, a spatial dynamic model was developed to simulate nitrogen dynamics at the scale of a sub-region, consisting of a mosaic of different soil and land use types. The model was calibrated and validated on the basis of two years of measured mineral nitrogen (both NO_3 and NH_4) concentrations under different land use types with different irrigation and fertilizer regimes. Simulated results showed annual leaching losses varying from 88 to 122 kg N ha^{-1} in flowers, 64 to 82 in vegetables of the 'cabbage group' (i.e. paprika, cabbage, eggplant, kohlrabi), 51 to 76 in chili, 56 to 75 in vegetables of the 'squash group' (i.e. cucumber, tomato, pumpkin), and 36 to 55 in rice. The model, after further calibration and validation, is a useful tool for regional environmental assessment, and management support.

The study has indicated that current agricultural developments in Tam Duong district, that are strongly influenced by (short-term) economic drivers, present a serious threat for the quality of the natural resource base, particularly soil and water and thus for the sustainability of the production systems. The obvious conflicts between the various objectives need to be addressed through integrated analysis in which the various stakeholders are involved.

Keywords: Soil degradation, remote sensing, watershed, soil erosion model, paddy fields, terraces, water balance model, nitrogen balance model, geostatistics, rice-based systems, spatial dynamic model.

Preface

In 2002, I joined the Systems Research for Integrated Resource Management and Land Use Analysis in East and Southeast Asia (IRMLA) project that aimed at combining research into future-oriented design of agro-technologies with evaluation of stakeholder-negotiated choices for sustainable land use options at different decision levels (farm, district, and province) and supportive policy measures. I would like to thank Tran Thuc Son and Chu Thai Hoanh for introducing me to this project and the associated Wageningen scientists. Through this project I met Herman van Keulen and Reimund Roetter, who became my promotor and co-promotor, respectively. Thank you Herman, for your warm and patient support and for finding time to comment on both the English language and the substance of my draft chapters, until they finally were combined in this thesis. I would not have finished my thesis without your help. Many thanks go to Reimund Roetter for his guidance and comments. The discussions with you helped to keep my work on track, which greatly improved the quality and relevance of my research. I also want to thank Coen Ritsema, who first suggested the use of a soil erosion model and introduced me to his skilful and kind colleague, Rudi Hessel, who also became my co-promotor. I want to thank him for his guidance and the contributions to the thesis. Thank you very much Rudi, you are very kind and enthusiastic.

I benefited a lot from discussions with Chu Thai Hoanh during formulation of my project proposal, and on soil erosion and water balance modeling. He always motivated and inspired me to continued dedication to my research. I also want to express many thanks to Don Acton and Thai Phien for their strong support to my research.

From Alterra, I would like to thank Erik van den Elsen for helping me in ordering measuring equipment and Jannes Stolte for the many helpful suggestions about field measurements. Let me express my thanks also to Joost Wolf for his interest in my work and the many suggestions and discussions that helped in creating a clearer picture of my study, and to Tommie Ponsioen for sharing his technical coefficient generator and his knowledge of the study area.

This study involved many trips to Tam Duong, and the people there helped me in making the trips productive and pleasant. The IRMLA team in Vietnam provided valuable material and information on the study area. Mr. Dang Hai Trieu, vice-director of Vinh Phuc Soil and Fertilizer Research Center helped me in identifying the study area. Many thanks to Mr. Pham Dinh, who was a great help in taking care of the rain gauge and data logger, and in taking soil and water samples. Many thanks to Mr.

Nguyen Hue, the Head of Quan Dinh cooperative, who intensively supported me in selecting the watershed and the terraces for the experiments, provided me with expert information on soils, crops, and farming activities in the study area, and especially for the hospitality shown by him and his family, with very good food and an excellent atmosphere during my visits. Also many thanks to Mr. Nguyen Van Ke and his son for helping me in intensive soil and water sampling during two years in his own and his neighbour's fields.

I am indebted to Gon van Laar for doing a wonderful job in editing this thesis. I have appreciated very much your help with critical comments and ready and transparent answers.

Ken Giller, many thanks for your hospitality and guidance during lunch meetings and in meetings of the soil fertility discussion group. Thanks to Ria van Dijk and Charlotte Schils for providing excellent administrative support. I am grateful to Marcel Lubbers, Eelco Meuter, Bert Rijk and the staff from TUPEA for the operational help with computers and software.

Living in the Netherlands was an experience with very nice weather and people; I would like to thank Nico de Ridder and his wife for their hospitality and for organizing a wonderful dinner with my international friends. All my friends at the Haarweg building, Muhammed Ebrahim Shibu, Alice G. Laborte, Shamie Zingore, Bongani Ncube, Wen Jiang, Annie Boling, Myriam Adam, Ilse Geijzendorffer, Senthilkumar Kalimuthu, Eduardo Cittadini, and Benjamin Kibor, creating an international atmosphere, thank you all for your support and encouragement.

Living far away from one's country, family and relatives, we share similar feelings and care for each other. I would like to thank my Vietnamese-Dutch friends who helped me a lot with warm evenings and weekends, thank you ANH KE, CHI KHANH and CHI HUONG for your support. I especially thank my fellow Vietnamese students in Wageningen, both those that have already finished and that have not finished yet, for their friendship, and care and for sharing all things. Very best wishes to all of you in Wageningen and finish your study with good results.

I want to send special thanks to my late mother and my father for my upbringing and for stimulating me to attend University; I want to extend my warmest thanks to my wife for encouraging me to study and for taking care of our children; without you I would never have finished my PhD. Great thanks to my daughter and sons for being as good as gold during my absence; I have missed you very much and promise to bring you a lot of Dutch chocolate.

Last but not least, I would like to thank all of you, who are here with or without name for everything you gave me during our meetings, for joint experiences and for what we shared; my best wishes to you and your families.

Contents

Chapter 1	General introduction	1
Chapter 2	Using LANDSAT images for studying land use dynamics and soil degradation. Case study in Tam Duong district, Vinh Phuc province, Vietnam	9
Chapter 3	Soil erosion in Quan Dinh watershed, a hilly area in Tam Duong district, north Vietnam	17
Chapter 4	Simulation of soil erosion in Quan Dinh watershed in Tam Duong district, north Vietnam	35
Chapter 5	Nitrogen leaching in intensive cropping systems in Tam Duong district, Red River Delta of Vietnam	61
Chapter 6	Nitrogen leaching and nitrogen losses in rice-rice-maize systems on sandy loam soil in Tam Duong, Red River Delta, Vietnam	81
Chapter 7	Spatio-temporal prediction of nitrogen concentrations in shallow groundwater under intensive farming in northern Vietnam using regression-kriging	101
Chapter 8	Spatial dynamics of nitrogen in shallow groundwater under intensive farming in northern Vietnam	119
Chapter 9	General discussion	137
	References	147
	Summary	169
	Samenvatting	173
	Tóm tắt	177
	PE&RC PhD Education Statement Form	180
	Curriculum vitae	181
	Funding	182

List of acronyms and abbreviations

Aggrstab	Aggregate stability
ANSWERS	Areal Non-point Source Watershed Environmental Response Simulation model
BR	Band Ratio
CC	Colour Composite
Coh	Soil Cohesion
CREAMS	Chemicals, Runoff and Erosion from Agricultural Management Systems
D50	Mean soil particle size
DAS	Day after sowing
DAT	Day after transplanting
DEM	Digital Elevation Model
EPIC	Erosion-Productivity Impact Calculator
FYM	Farm Yard Manure
GIS	Geographic Information System
GLEAMS	Groundwater Loading Effects of Agricultural Management Systems
GSA	Geological Society of America
KINEROS2	KINematic runoff and EROSion model
LAI	Leaf Area Index
LISEM	Limburg Soil Erosion Model
Manning's n	Manning's value
MW	Main watershed
Obs	Observation
Qpeak	Peak runoff
Qtot	Total discharge
R/G	Red/Green
R/NIR	Red/Near Infra-Red
RGB	Red, Green, Blue
RR	Random Roughness
RRD	Red River Delta
RUSLE	Revised Universal Soil Loss Equation
SC	Sediment Concentration
Sim	Simulation
SW	Sub-watershed
SY	Sediment Yield
Theta-init	Initial soil moisture content
Tpeak	Time to peak
USLE	Universal Soil Loss Equation
UTM	Universal Transverse Mercator
WEPP	Water Erosion Prediction Project

CHAPTER 1

General introduction

BACKGROUND

Agricultural systems in East and South-east Asia have been changing dramatically in recent decades along with economic development of the region. Total production increased spectacularly, thanks to expansion of cultivated land, introduction of new varieties with associated, more intensive production technologies, and development of regional markets. However, the development of agriculture has not been successful in meeting the increasing needs, resulting from the ever-increasing population pressure (Hossain and Narciso, 2003). In many regions, agricultural production systems have become very intensive, with high inputs of irrigation water, fertilizers, herbicides, pesticides and insecticides, while in other areas non-rational and/or unsuitable land use systems are practiced. In the more marginal agricultural areas, often, the soil is exploited without attention for conservation, so that erosion is accelerating, resulting in declining crop yields due to depletion of soil fertility, leading to low efficiencies in the use of labour, land and other natural resources. To deal with the complex problems associated with unsustainable use of the natural resources, innovative approaches are necessary. One of the approaches for land use analysis in support of land use policy formulation that has been developed in recent years (Van Ittersum, 1998; Van Keulen et al., 2000; Van Ittersum et al., 2004), is based on systems research for optimizing land use. Exploring land use options has been used as a methodology to support agricultural and environmental policy formulation (Changhe, 2000). Current land use systems are quantified (Kruseman and Van Keulen, 2001) and future target crop yields are estimated, based on quantity and quality of available natural resources (Kalra et al., 2001), through crop growth simulation models (De Koning et al., 1995; Goudriaan et al., 1997; Boogaard et al., 1998) and expert systems (Roetter et al., 1998, 2005). These biophysical potentials are combined with social conditions and economic development targets or policies, applying techniques, such as Geographical Information System (GIS) and Multiple Goal Linear Programming (MGLP). Land use is optimized with respect to such targets as maximizing land productivity, total crop production and total income and/or minimizing total soil loss, nutrient losses, production costs, use of mineral fertilizers and/or biocides (Changhe, 2000). Comparison of the 'window of opportunities' (De Ridder et al., 2002) with current land use patterns generally shows substantial scope for improvement. However, considerable efforts are required to reach the targets, and transform the pictures of the future into reality. In the process, there are challenges in answering difficult questions: why is there such a big gap between potential and actual production? What are the most important yield-limiting or yield-reducing factors? And what measures to take, technically or in terms of policies, to bridge the yield gap, and maintain the quality of the natural resource base? The bridge to closing the gap between potential and actual production and between unsustainable

and environmentally sound and economically viable production systems is composed of sets of technical coefficients, that link various components of the land use system, such as soil type, cropping calendar, land use type and land use management, water balance, nutrient balance, technology level and labour, all affecting the use efficiencies of the production factors (Ponsioen, 2003; Ponsioen et al., 2006).

Nutrient balances, i.e. the differences between nutrient inputs and nutrient outputs from agricultural systems at various spatial scales, are considered central in land use analyses, because they affect soil fertility and thus productivity in the long run (Roy et al., 2003). In many regions, soils are eroding and become depleted, leading to low crop yields, whereas in other regions very high inputs of fertilizer result in low use efficiencies and environmental pollution (Witt, 2003). Much research has been carried out, but concentrated at field and plot scales. Quantifying nutrient losses at watershed and regional scales accurately, still constitutes a major methodological challenge – in general (Lesschen et al., 2004) and, particularly, in Vietnam, where relatively little research on the subject has been done so far.

Vietnam, with a population of 77 million, covers a total land area of 33,104 Mha (Nhuan, 1996), of which three fourths consists of high mountains with a complex topography and steep slopes. The Vietnamese economy has been growing remarkably since 1986, when the Sixth Party Congress introduced significant economic reforms with market economy elements, as part of a broad economic reform package called ‘đổi mới’. Private ownership was encouraged in industry, commerce, and agriculture. Vietnam realized around 8% annual GDP growth from 1990 to 1997 and continued at around 7% from 2000 to 2005, making it the world's second-fastest growing economy. Agriculture has been changing and growing thanks to three important events. Firstly, ‘Khoán 100’ (Directive 100) was released by the Government at the end of the 1970s as a new contract of production with households in certain regions. Secondly, ‘Khoán 10’ was launched in 1988, regulating land redistribution to households, at market prices. Farmers were free in crop selection and in purchase of inputs and sale of products to private traders. Collective contracts were abolished and farmers had to pay taxes directly. Thirdly, land was allocated to the farmers (20-year lease for agricultural land and 50-year for forestry land) which encouraged them to invest in land improvements to increase production potential. As a result, Vietnam has become the largest cashew nut exporter, and the second largest rice exporter in the world.

However, during the long period of a centrally-planned economy with cooperative land ownership, agricultural land in the uplands had been expanding to meet the increasing food demand. Very large forest and protected areas were deforested, leading to decreasing land cover and rapidly declining soil quality. Natural forest cover in 1945 was 19 Mha, in 1980 12 Mha, in 1985 9.6 Mha, and in 1992 9.3 Mha.

Non-cultivated land up to 1995 was 13 Mha, including 1.1 Mha of eroded lands, partially consisting of rock outcrops (Phong, 1995). Average natural and cultivated area per capita in 1995 was 0.41 and 0.12 ha, respectively. Between 1995 and 2000, agricultural land expanded by 1.35 Mha (Bat, 2001), forest land by 0.78 Mha, as a result of planting of production forest, such as eucalyptus, perennial crops by 0.74 Mha, and the area for infrastructure and industry by 0.24 Mha, associated with increasing population and urbanization. Non-cultivated land in the country in 2000 was reduced to 8.65 Mha (Khang, 2005). In the same period, average cropping intensity of annual crops increased from 1.4 in 1995 to 1.6 in 2000, as a result of shifting from double to triple crops, and introduction of leguminous crops in the rotations. Under the influence of population pressure, natural forest and fallow land has been replaced by upland crops, such as cassava, maize, upland rice, and coffee. Farmers cultivate these crops without applying soil conservation practices, so most cultivated upland soils are seriously eroded. This soil erosion associated with high runoff and soil loss is the main cause of soil degradation (Phong, 1995). Annual soil loss under forest is estimated at 3–12 Mg ha⁻¹, under coffee and tea 22–70 Mg, and under cassava and hill rice 175–260 Mg ha⁻¹ (Phong, 1995; Lanh, 1999; Hung, 2001). As a result of soil erosion, continuous rice cultivation and organic matter decomposition, soil nitrogen (N) contents in soils derived from basalt and schist rapidly declined from 0.25% in the first year to 0.13% in the fourth year (Hung, 2001). Farming without soil conservation and very low or no inputs of either organic or inorganic fertilizers, leads to continuously declining soil fertility, as observed in soils derived from magma bazo under long-term rice cultivation: pH declined by 0.2–0.5 units, and exchangeable calcium by 30% (Siem and Phien, 1992). After 15 years of cultivation, exchangeable calcium (Ca) and magnesium (Mg) in soils on schist were reduced from 150 to 70 and from 30 to 20 me kg⁻¹, respectively. In general, most degraded soils in Vietnam are sandy, acid, of very low fertility and cation exchange capacity (Khoa, 1993).

In Tam Duong district, Vinh Phuc province (21°18' to 21°27' N, 105°36' to 105°38' E), large areas of soil are degraded, with occasional areas of bare soil, where parent material is exposed. Soils are characterized by low organic matter (OM) contents varying from 0.54–1.8%, total phosphorus (P) contents of less than 0.06%, exchangeable Ca between 8–29 me kg⁻¹, CEC from 75 to 103 me kg⁻¹, and pH from 3.5 to 4.0. The most degraded soils in the province, subject to erosion under long-term eucalyptus plantations, are characterized by organic matter contents below 1.0%, pH_{KCl}-values below 4, total N less than 0.08%, total P below 0.04%, total potassium (K) below 1.0%, available P less than 10 ppm, CEC less than 55 me kg⁻¹, exchangeable Ca and Mg below 2 and 3 me kg⁻¹, respectively (Hoang et al., 1998).

One of the consequences of soil fertility depletion is a reduction in crop yields. Upland rice yields rapidly declined from 2250 and 1350 kg ha⁻¹ in the first year, via 1830 and 1200 in the second year, 570 and 680 in the third to 0 and 550 kg ha⁻¹ in the fourth year, respectively (Hung, 2001). Studies on slopes from 22 to 30 degrees with hill rice and maize crops, showed very high soil and nutrient losses in the first year after forest clearing (Phien et al., 2001). In subsequent years losses decreased, but hill rice yields continued to decline and were negligible after 4 to 5 years. Soil nutrient balances were negative throughout, because of nutrient losses and crop uptake that exceeded supply. The efficiencies of nutrient use are low, even in intensive agriculture; for instance, Dobermann et al. (2002) showed that in rice systems on degraded soils in the Red River Delta of Vietnam (RRD) nitrogen recovery efficiency (kg N taken up per kg N applied) was 0.39, agronomic efficiency (kg grain per kg fertilizer applied) was 0.18, while physiological efficiency (kg grain yield per kg increase in plant N accumulation) was 46. The study showed that although yield goal achievement, defined as the ratio of actual yield to potential, in RRD was as high as 95%, gross returns to fertilizer investments were very low, i.e. 38% compared to 82% in Jinhua, China.

The common problem in agriculture in this area is nutrient losses. These losses have become a major concern in relation to the sustainability of agricultural production systems. Nutrient losses can take various forms (Antikainen et al., 2005): The first is erosion, including surface runoff, where both topsoil and associated nutrients are washed off the fields to lower areas and into nearby water bodies (Lal, 1991; Daura et al., 1995; Hollger et al., 1998). Cho (2003) reported that in a paddy field in central Korea, annual runoff loading of total-N and total-P was 157.9 and 4.5 kg ha⁻¹, respectively. The risk for nutrient losses via runoff is highest when the soil is saturated with water, and bare, especially in sandy soils, low in organic matter (Miller and Gardiner, 2001). The second mechanism is leaching, through excess water from rainfall or irrigation (Jinno and Honna, 1999; Di and Cameron, 2002; Hauggaard-Nielsen et al., 2003; Verloop et al., 2006). The sources for nutrient leaching are commercial fertilizers, manure, sludge, fixation by legumes, crop residues, irrigation water, atmospheric deposition, and surface runoff from agricultural lands. The nutrients eventually end up in streams, lakes, estuaries and/or the groundwater. When soils are not cultivated, they are particularly vulnerable to nutrient leaching under heavy rains. For example, annual nutrient leaching losses from soils in the catchment of Bassenthwaite lake in Colombia (Lawlor and Tipping, 1996) were 0.16–0.34 kg ha⁻¹ for soluble reactive phosphorus, 10–210 for nitrate, and 24–45 for dissolved silica. In dryland areas in the US, due to inefficient use or over-application of fertilizer, after harvest up to 90 kg ha⁻¹ NO₃-N had leached below the root zone to between 1.5 and 2.5 m (Fuentes et al., 2003). For farmers, nutrient losses represent

losses in time and money (Pierzynski et al., 2005), as more fertilizer is needed to replace the nutrients that have leached. The third is loss to the air: in saturated soils, alkaline soils or when organic fertilizers are left on the soil surface, nitrogen can be lost to the atmosphere through denitrification and volatilization processes in the form of NO and NO₂ (Akiyama and Tsuruta, 2002; Hou and Tsuruta, 2003; Külling et al., 2003), N₂O (Xiong et al., 2002; Külling et al., 2003), N₂ and ammonia, NH₃ (Malhi et al., 2003). In a study on the fate of N fertilizer applied to a calcareous sandy loam soil in the north China plain (Cai et al., 2002), ammonia volatilization was found an important pathway of N loss, e.g. 30–39% of the applied N in rice, 11–48% in maize, and less than 20% in wheat. Unaccounted-for fertilizer N decreased in the order rice > maize > wheat.

Environmentally, nutrient losses may have various effects (Byrnes, 1990), e.g. the nutrients may enter groundwater and surface water bodies. Nitrate, phosphate, and other nutrients can trigger eutrophication and excessive algal growth in rivers, lakes, and estuaries, affecting both estuarine and freshwater habitats. Moreover, nutrient contamination of drinking water presents potential health risks. Long-term consumption of nitrite, a reaction product of nitrate, in drinking water has been linked with cancer and miscarriages (Amr and Hadidi, 2001). High doses (exceeding 10 mg l⁻¹ for nitrate and 1 mg l⁻¹ for nitrite) may lead to methemoglobinemia or ‘blue baby disease’ in infants (Fan and Steinberg, 1996).

Nutrient depletion is a serious threat to the sustainability of farming systems in northern Vietnam. Tam Duong district is one of the affected areas; geomorphologically three regions can be distinguished; mountainous, hilly and plain. The mountain areas with steep slopes are covered by forests. The hilly lands have been cleared since the 1980s for cultivation of annual crops, such as cassava, maize and beans, and for eucalyptus plantations. Soils are strongly eroded due to slope, high rainfall, and low soil cover (Thu et al., 1997; Hoang et al., 1998; Toan et al., 1998). Upland crop yields are very low, even when farmers use high fertilizer inputs. Agronomic and recovery efficiencies both are low, food production is insufficient and the agricultural systems appear unsustainable. The lowland areas consist of soils derived from old alluvial deposits, with low fertility. These areas are used for food production for most of the population. The high pressure on the land leads to increasing fertilizer use and shortened crop rotations. Nutrient leaching is potentially the dominant process in nutrient losses in this area.

OBJECTIVES

In Tam Duong district, erosion and leaching are the main processes leading to high nutrient losses and consequently uneconomic production and soil degradation.

Counteracting measures can be designed to reduce these losses, based on knowledge derived from quantitative studies of these processes in the various production systems. To increase insight in the basic processes underlying soil degradation at different spatial scales, our study pursued the following objectives:

- To survey soil degradation dynamics in the study area, using remote sensing, to delineate the extent of different soil degradation types as a basis for the design of effective soil conservation measures.
- To study soil erosion at different spatial scales in the hilly land watershed, effects of paddy fields on soil erosion in the watershed, and to simulate soil erosion in the watershed in the presence of paddy fields.
- To quantify nutrient losses due to leaching from different soils and agricultural systems through field experimentation and to develop a suitable model for estimation of nutrient leaching losses from these agricultural systems.
- To scale-up nitrogen dynamics and leaching losses in a small region, using geostatistics and a geographic information system (GIS).

CHAPTER 2

Using LANDSAT images for studying land use dynamics and soil degradation. Case study in Tam Duong district, Vinh Phuc province, Vietnam*

Mai Van Trinh^{1,3}, Nguyen Dinh Duong², Herman Van Keulen^{1,4}

- ¹ Plant Production Systems Group, Wageningen University, P.O. Box 430, 6700 AK, Wageningen, The Netherlands
- ² Department of Environmental Information Study and Analysis, Institute of Geography, Hanoi, Vietnam
- ³ Institute for Soils and Fertilizers, Dong Ngac, Tu Liem, Ha Noi, Vietnam
- ⁴ Plant Research International, Wageningen University and Research Centre, P.O. Box 16, 6700 AA Wageningen, The Netherlands

Abstract

Tam Duong district, Vinh Phuc province, is representative for vast areas in the north of Vietnam where soils are strongly degraded and erosion has led to patches of bare soil with exposure of parent material and crop yields on these soils are strongly reduced. The aims of this study are to apply satellite imagery for the assessment of the extent of soil degradation and implementing the results to the whole middle altitude area of north of Vietnam. Satellite images LANDSAT MSS in 1984 (4 bands), TM 1992, 1996 and 2000 (6 bands) were used for creating maps of the Colour Composite and Band Ratios. Bare and degraded soils were identified and extracted from the Colour Composite and Band Ratios images. The classified map of Band Ratios of the year 2000 was established on the basis of new soil maps and ground truth data, in combination with laboratory analysis of soil quality. The best band ratio was selected for continuously processing and classification base on its visual interpretation and accuracy. Results showed that the band ratio of Red/Near-Infrared bands was selected and classified map of degraded soils matched well with the soil survey map and the field checks with overall accuracy of 73.29%. Land use and soil degradation dynamics were delineated for the dates 1984, 1992, 1996 and 2000 and degraded soil area of district in these dates are: 2437, 3282, 2185 and 2576 respectively. Hot spots from the Band Ratio imagery appeared to accurately represent the degraded soil areas in the hilly land and the degraded sandy soils on high terraces, but not the agricultural lowland, because on hilly and sandy terraces soil organic matter and soil moisture content were very low. The study shows that satellite imagery is a very useful tool for soil degradation studies.

Keywords: Forest cover, soil erosion, band ratio, supervised classified, slicing

* This chapter has been published as:
Mai Van Trinh, Nguyen Dinh Duong and Herman van Keulen, 2005, Using LANDSAT images for studying land use dynamics and soil degradation. Case study in Tamduong district, Vinhphuc province, Vietnam, International Journal of Geoinformatics 1, 157-164.

INTRODUCTION

Deforestation, desertification and land degradation have been critical global environmental issues during the past decade. Monitoring of cover conditions and their changes is essential to the identification of environmental problems at both the local and global scale (Oldeman, 1994).

Vietnam, with a population of 77 million, covers a total land area of 33,104 Mha (Nhuan, 1996), of which three fourths consists of high steep mountains with a complex topography. Forest cover in 1945 was 19 Mha, gradually declining to 9.3 Mha in 1992 (Phong, 1995). Non-cultivated land comprised 13 Mha up to 1995, including 10.4 Mha bare land, distributed over 56 soil units of 12 soil groups, including ferrasols (65%), high mountain humus soils (12.6%), eroded land with partially rock outcrops (8.6%) and others (13.8%). A total of 5.5 Mha are strongly degraded, 4.6 Mha intermediately, and 4.6 Mha slightly (Siem and Phien, 1999). It is, therefore, important to monitor land and water management practices causing severe soil degradation. Remote sensing is one of the key tools in monitoring local, regional and global environmental issues. Recently, attention has been paid to spatial analysis via combinations of Geographic Information Systems (GIS) and satellite images for environmental research and applications (Harahsheh and Tateishi, 2000; Hill and Schütt, 2000; Harmsen, 2004). Examples of such studies are that of Tateishi (2003) for soil degradation, which yielded essential information for management of natural resources, that of Gad (2002) for obtaining land use and land cover maps on the basis of 132 field observations and 65 soil profiles to arrive at a map of soil degradation, and that of Zeleke and Hurni (2001), indicating the increase in soil degradation in Dembecha, Gojam, Ethiopia with declining cover of natural forest from 27% in 1957 via 2% in 1982 to 0.3% in 1995. At a more detailed level, Huete et al. (2002) combined EO-1 and air-born AVIRIS with field measurements of an ASD spectroradiometer to identify types and stages of soil degradation. Nizeyimana and Petersen (1997) distinguished different soil erosion classes using Bright Index (BI) derived from multi-spectral spot images. In this chapter a study is described in which multi-temporal LANDSAT digital data are used in combination with ground truth data to study land use dynamics and soil degradation in Tam Duong, an upstream district in the Red River Delta in the north of Vietnam.

METHODOLOGY

Study area

Tam Duong district in Vietnam is located upstream in the Red River Basin (21°18' to 21°27' N, 105°36' to 105°38' E), about 60 km north-east of Hanoi, in the transitional zone between almost flat lowlands and the mountainous regions (Figure 1). The flat

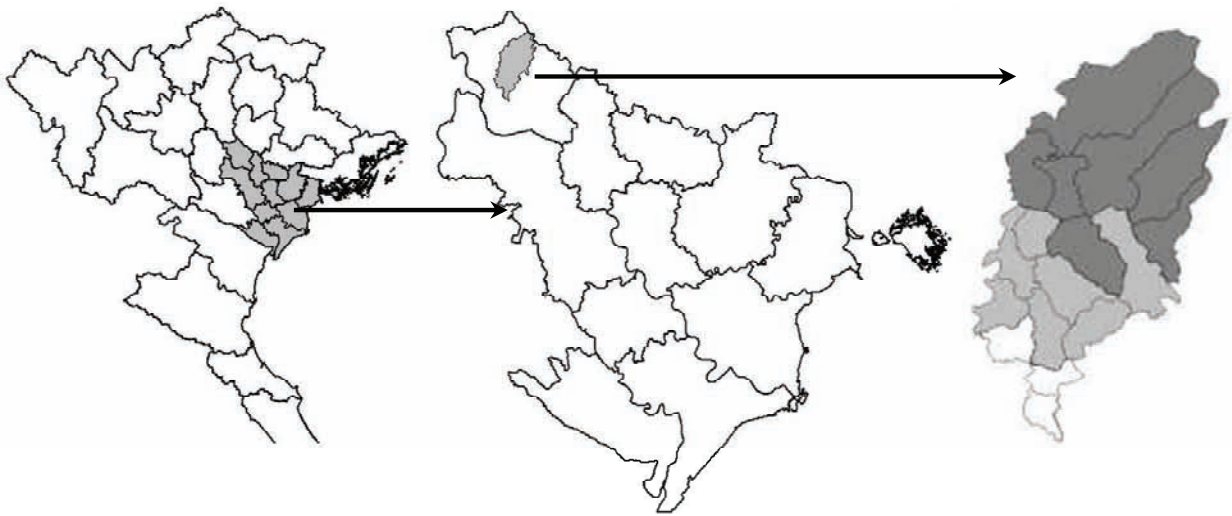


Figure 1. Location of (left) Red River Delta, (center) provinces in the Delta and Tam Duong district and (right) its sub-division into seven mountainous communes (dark-grey), seven midland communes (grey) and three flat low land communes (white).

southern part (3 communes) is characterized by paddy rice and vegetable cropping systems; the middle part (7 communes) consists of alternating flat and hilly land at altitudes between 20 and 100 m above sea level (asl). More than half of the district (7 communes in the northern part) is mountainous along the Tamdao range from north-west to south-east, at altitudes ranging from 100 to 1400 m asl. The district has a total area of 19,779 ha, with 7,838 ha of agricultural land (including 6,147 ha of annual crops and 1,691 ha of perennial crops), 6,744 ha of forest, while the remainder is non-cultivated land. Seven soil types were distinguished: Acrisols, Cambisols, Gleysols, Fluvisols, Plinthosols, Arenosols, and Leptosols.

Methodology

The data used in this study are one LANDSAT-MSS image (MSS84) operating in 4 bands with 80m spatial resolution acquired on 8th May 1984 and four LANDSAT-TM images operating in 6 bands with 30m spatial resolution acquired on 21st October 1992, 18th October 1996 and 11st April 2000 (TM92, TM96, and TM00). Although the images are acquired at difference dates, the land cover status is quite similar, because October is the early and April late dry seasons, both with low land cover, and May early rainy season, when biomass is still very low, as is soil water content. Colour Composites (CC) were generated using band combination of red, green and blue (RGB) of 4:3:2 for the MSS84 image and of 5:4:3 for the TM92, TM96 and TM00 images for visual interpretation of temporal changes in land use and land cover. Use of

band ratios (BRs), generated by dividing the pixels in one band by the corresponding pixels in a second band, to suppress illumination differences attributable to surface albedo, incidence angle and topographic effects, has long history of successful applications to multispectral data. In this study, two kinds of BR are generated by dividing the Red band by the Green band (ratio = R/G) and dividing the Red band by the Near-Infra Red band (ratio = R/NIR). The band ratio N/NIR is the inverse of the Ratio Vegetation Index (RVI), that has been widely and successfully used to map and/or monitor vegetation (Gilabert et al., 2002). The TM00 image was supervised classified to differentiate degraded soil from forest and arable soils and other land use types. The classified map was adjusted to match reality by comparison with the map of degraded soils derived from the district soil map (Khang et al., 1998) and field checks. The band ratio giving the best fit with ground truth data is selected for further works. Soil degradation was deduced from the supervised classified of selected BRs at each date, combined with the RGB colour combinations to simulate land use dynamics and changes in soil degradation in the study area.

RESULT AND DISCUSSION

Image preprocessing

Before performing digital processing, all images were radiometrically normalized. To compensate for variations in the sensor radiometric responses over time and for variations in natural conditions of solar irradiance and solar angles, digital numbers were first converted into exo-atmosphere reflectance values (Markham and Barker, 1985) and radiometrically corrected (Hall et al., 1991) by applying minimum subtraction method (Chavez, 1988) to remove the effect of haze. After radiometric normalization, images were geometrically corrected. The TM00 image was converted to the UTM coordinate system, using common control points extracted from a topographic map at the scale of 1:50,000. Using a first-degree polynomial rectification algorithm, this procedure yielded a registration accuracy equal to 0.8 pixel. Following this procedure, the other images were registered through an image-to-image tie-down algorithm using ILWIS 3.0 for Windows.

Image processing and Band Ratio selection

There are two reasons for using BR (Abdeen et al., 2001; Penn, 2002; Ren and Abdelsalam, 2003; Higgs, 2004): (i) differences between the spectral reflectance curves of surface types can be brought out, (ii) Illumination, and consequently radiance, may vary, but the ratio between an illuminated and a non-illuminated area of the same surface type will be the same. Based on this principle, vegetated soil and

bare/degraded soil can be differentiated by using the band ratios. For R/G ratio, bare and degraded soils show high reflectance in the red band but low in the green one, while vegetated soils show lower reflectance in the red band. Hence, the ratio of R/G will give high values for bare/degraded soils and low for vegetated areas.

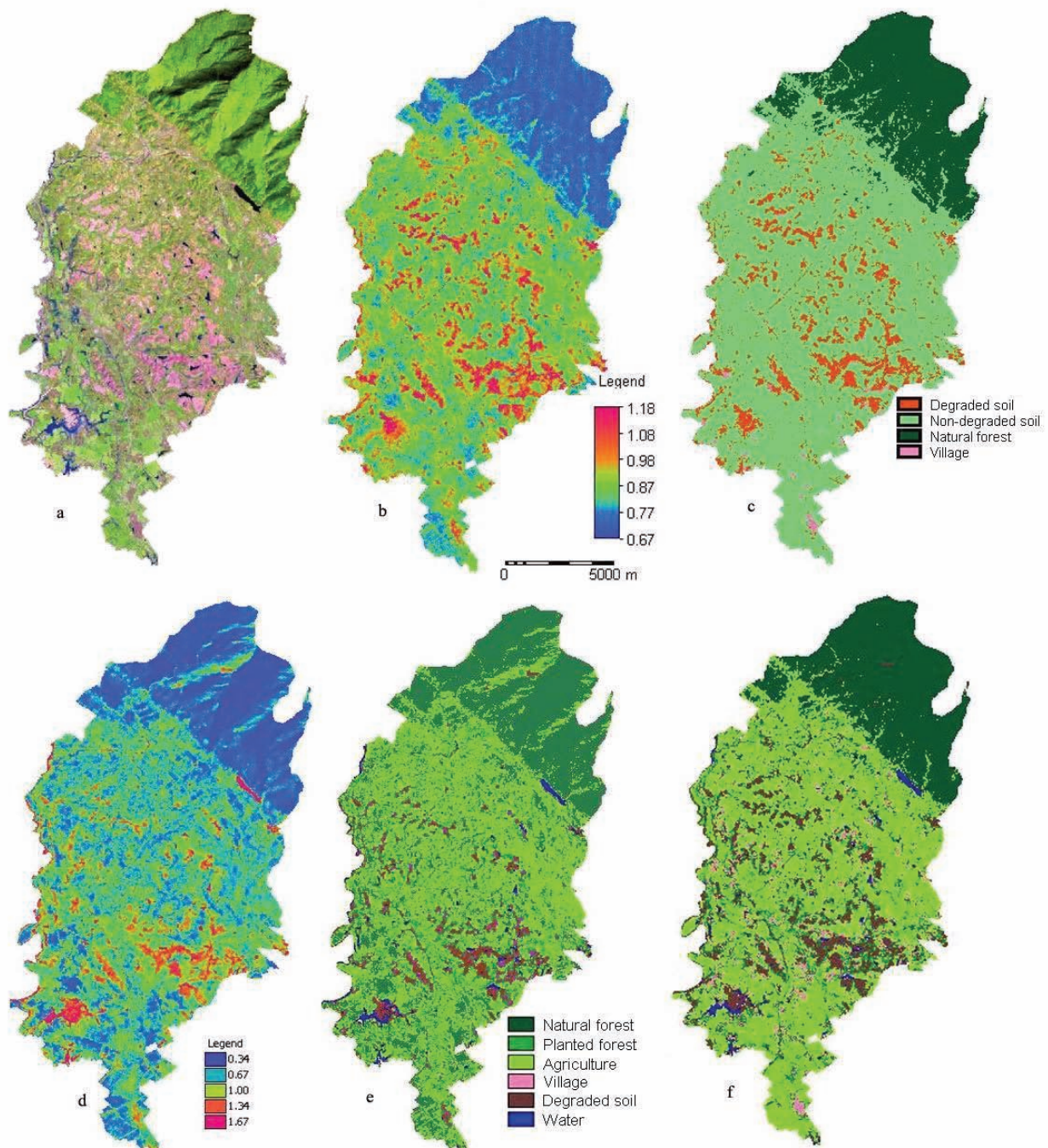


Figure 2. Result maps from LANDSAT TM 2000 (a) Colour Composite RGB 5:4:3, (b) Band ratio red/green (c) supervised classified map from band ratio red/green, (d) Band ratio red/near-infrared (e) Sliced classified map from band ratio red/near-infrared and (f) supervised classified map from band ratio red/near-infrared.

As for ratio R/NIR, features such as water reflect strongly in the R band and weakly in the NIR band, roads slightly stronger in the R band than in the NIR band, while features such as vegetation show relatively low reflectance in the R band and high reflectance in the NIR band (Lillesand and Kiefer, 1994). Therefore, the ratio R/NIR gives high values for water and bare soils and low values for vegetation (Figure 2).

On both BRs images (Figure 2), natural forest (low values, blue colour) and bare/degraded soils (high values, red colour) can easily distinguished visually. But the difference between two ratios is that in the R/G image the values for degraded soil and village and for planted forest and agriculture land are very close, while these features can be distinguished in band ratio R/NIR image with strongly red colours for water, light blue for agricultural land, green orange for planted forest and red orange for villages. This resulted in four classes in the classified map from BR R/G and in 6 classes in BR R/NIR, while recognizably maintaining the geometric features. In addition, BR R/NIR shows distinctly different values for different features; therefore slicing classified (Figure 2e) work well with this BR and gives comparable results to the supervised classified map (Figure 2f). Base on all these advantages, the band ratio of R/NIR is used for further image processing and classification.

Soil degradation

The soil degradation map for the area was derived from the soil map (Khang et al., 1998) in combination with field checks for each soil unit, based on the guidelines of Oldeman (1994) where soil degradation was classified into different types, causes, degrees, rates, and extent. According to this reference, the dominated soil degradation in the area is water erosion caused by forest cutting, agricultural land use on slopping land with very low or no fertilizer input and without soil conservation measures. Soils are mostly sandy, with very low organic carbon, and nutrient contents as well as Cation Exchange Capacity. Thu et al. (1997) found a wide range in soil erosion rates for different types of land cover in upland soils with slopes from 5 to 8 degrees in three years in Tam Duong with an annual rainfall exceeding 2000 mm (Table 1).

Soil erosion rate was very high on bare soil, eucalyptus forest and agricultural land. Not only surface soil was removed, but also many nutrients were lost, as in the experiment carried out by Toan et al. (1998) from 1992 to 1996 at another site within the district, with rainfall varying from 800 to 1890 mm yr⁻¹. In that experiment, soil loss, runoff and nutrient loss have been measured and the results showed that soil nutrient losses on bare soil are 599.2 kg ha⁻¹ yr⁻¹ of organic carbon, 52 kg nitrogen, 26.6 kg phosphorus and 34.6 kg potassium and on cassava 295.0, 28.3, 21.3 and 22.4 kg, respectively.

Table 1. Soil erosion rate for different land covers in Tam Duong.

Land cover	Soil erosion rate (ton ha ⁻¹ yr ⁻¹)
Bare soil	189.4
Eight-year <i>Acacia mungium</i> forest	34.8
Ten-year old regenerated mixed forest	38.9
Pineapple	85.2
<i>Eucalyptus</i> forest	158.8
Agroforestry (< 3 year olds, 8 degree slope)	75.0
Agroforestry (after 3 years, 19 degrees slope)	93.0

Source: Thu et al. (1997).

Field observations

For each of twenty one ground truth points we determined type, state, and degree of degradation. Results showed satisfactory agreement with the classified map (R/NIR band ratio), with nine strongly degraded observations, on bare soil, poor eucalyptus plantations, and sandy soil on terraces. Three points on upland soil with cassava and fruit tree plantations showed intermediate levels of soil degradation; while only two were part of the degraded domain on the classified map.

The classified map was compared to the soil degradation map derived from the soil map and ground truth data, showing that most land classified as degraded on the classified map was located in the degraded domain of the soil degradation map, but not all. The reason is that on the classified map the most strongly degraded soils were identified where soils were dry, with low organic matter content, high sand content and poor land cover. However, as explained before, parts of the degraded land have been reclaimed through reforestation, high organic matter applications to crops or through planting of productive fruit trees, with high land cover and biomass. In other words degraded sandy soils located on terraces are being cultivated, and their reflectance is thus reduced, as they are covered by crops, such as beans and rice.

Soil degradation dynamics

For classification, degraded land was identified by classifying BR R/NIR for all dates in 1984, 1992, 1996, and 2000. The results (Figure 3) yielded an attractive picture of soil degradation dynamics since 1984. The extent of soil degradation in Tam Duong fluctuated from 2440 ha in 1984 via 3280 ha in 1992 to 2190 ha in 1996 and 2580 ha in 2000. This trend is realistic and can be associated with real human activities in Tam Duong district: when forest was cut, soil degradation started and aggravated till 1992. During the years 1990–92, large-scale reforestation took place (mostly eucalyptus

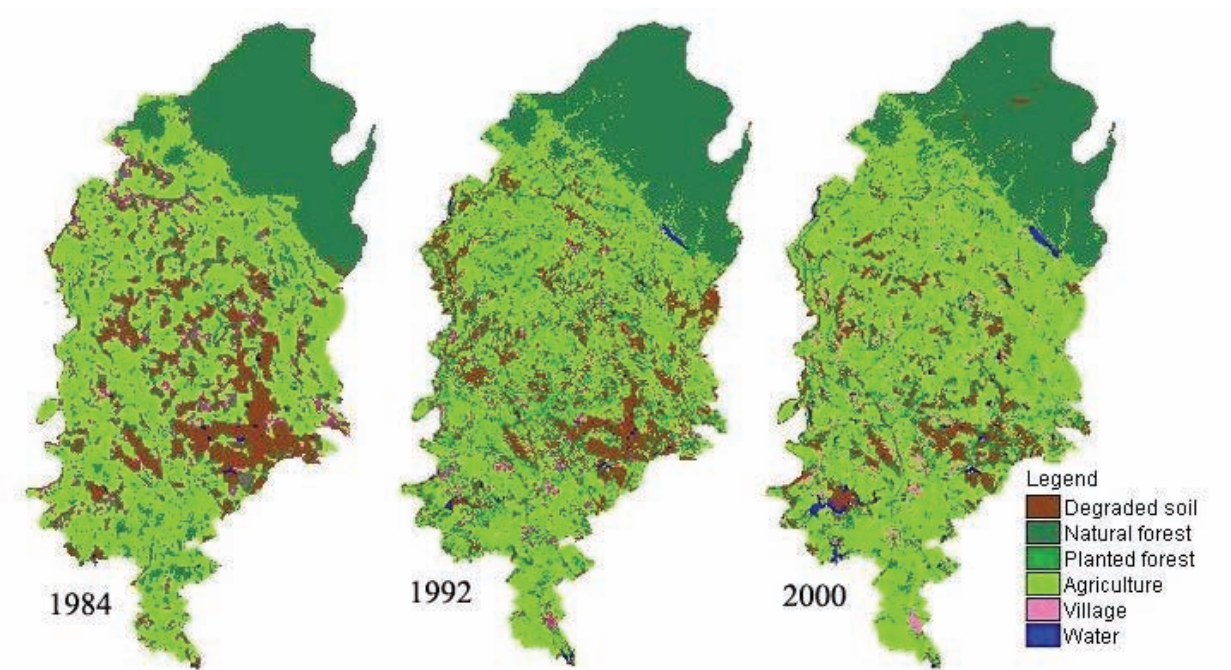


Figure 3. Classified maps derived from band ratio R/NIR in 1984, 1992 and 2000 in Tam Duong.

for supply to the paper mill), with the associated higher land cover and biomass, reducing erosion and soil degradation. The productive forest has been harvested since 1996, resulting in larger bare soil areas and increased soil degradation.

CONCLUSIONS

The band ratio red/near-infrared gave better result than band ratio red/green, because it showed different value ranges for different land use types. Colour Composite and supervised classified images of red/near-infrared band ratio showed that in Tam Duong district in Vietnam, most degraded soils, especially the strongly degraded and bare soils, with very high reflectance and distinct colours, are located on the hilly land and on high-level sandy terraces. Classified images from 1984, 1992, 1996, and 2000 clearly showed the trends in the extent of soil degradation with 2440 ha in 1984, 3280 ha in 1992, 2190 ha in 1996 and 2580 ha in 2000, a trend that is closely related to land use dynamics in the district, especially the forest cover and agricultural activities in the upland soils. These results illustrate the possibilities for use of satellite images for identification of degraded soils. Moreover, types, causes, and degrees of soil degradation could possibly be identified by testing more satellite images with different resolution and functions in combination with more ground truth data, including detailed soil properties.

CHAPTER 3

Soil erosion in Quan Dinh watershed, a hilly area in Tam Duong district, north Vietnam*

V.T. Mai^{1,4}, H. Van Keulen^{1,2}, R. Hessel³, C. Ritsema³, R.P. Roetter³, P. Thai⁴

¹ Plant Production Systems Group, Wageningen University, P.O. Box 430, 6700 AK Wageningen, The Netherlands

² Plant Research International, Wageningen University and Research centre, P.O. Box 16, 6700 AA Wageningen, The Netherlands

³ Soil Science Centre, Alterra Green World Research, Wageningen University and Research centre, P.O. Box 47, 6700 AA Wageningen, The Netherlands

⁴ National Institute for Soils and Fertilizers (NISF), Dong Ngac, Tu Liem, Hanoi, Vietnam

Abstract

Soil erosion is the main cause of soil degradation in northern Vietnam. In this study, soil erosion was measured in the period 2004–05 in the 248.9 ha Quan Dinh watershed in Tam Duong district, upstream in the Red River Delta, northern Vietnam, including lowland paddy fields, and representative for watersheds in the northern Vietnamese landscape. Soil erosion was measured for 9 events, at three scales, i.e. field plots of cassava and eucalyptus, a 19.1 ha sub-watershed and the main watershed to increase understanding of the effects of paddy fields within the main watershed. Total runoff and sediment yield from the plots were measured by tank collectors for each event. Total discharge was calculated from measured water height and flow velocity. Water samples were taken at the (sub-) watershed outlets, for determination of sediment concentration, and sediment yield was calculated as the product of total discharge and sediment concentration. The results show that total discharge and sediment yield in both the sub-watershed and watershed were much lower than those in the field plots. Total discharge in the main watershed was higher than in the sub-watershed. This is caused by the storage effect of rice fields and throughflow through the terraces during the cropping season. Sediment yield in the main watershed fluctuated, in dependence of the soil erosion contribution from many sub-watersheds. Annual rainfall in 2004 and 2005 was 1172 mm and 1560 mm, respectively, resulting in a total discharge of 538 and 3324 m³ ha⁻¹ yr⁻¹ and a total soil loss of 163 and 1722 kg ha⁻¹ yr⁻¹. Sediment concentration at the watershed outlet showed that April, June, the last 10 days of September and October, were the most susceptible periods for soil erosion in the study area. During these periods, land preparation after harvesting and weeding activities coincided with large rainfall amounts and high rainfall intensities.

Keywords: Paddy fields, terraces, scale effects

* This chapter has been submitted to CATENA Journal.

INTRODUCTION

Of the human-induced land degradation problems, permanent loss of soil productivity due to soil erosion is the worst at global scale. Asia has probably suffered more from human-induced soil erosion than any other continent (Morgan, 1995; Wani, 2001). Population growth has led to increasing pressure on increasingly marginal resources, particularly on the land and water resources in the upper parts of watersheds, on which many of the region's poorest people depend for their livelihoods (Maglinao and Valentin, 2003). In China, estimated annual soil loss in the Yellow River Basin and the Loess Plateau is of the order of 100 and 200 Mg ha⁻¹, respectively, leading to an annual sediment transport to the sea of around 5.0 Pg. Consequently, economic losses due to soil erosion over the last 50 years have been estimated at over 10 billion Yuan* in this area (Ritsema, 2003). Using recorded data from hydrological stations in Vietnam, Siem and Phien (1999) estimated annual losses of 1000 Mg of humus, 100 Mg of nitrogen, 60 Mg of phosphorus, and 200 Mg of potassium to the sea due to soil erosion. Loc et al. (1998) have reported annual runoff volumes of 1354 and 2162 m³ ha⁻¹ and soil losses of 11,303 and 22,655 kg ha⁻¹ from agricultural land with and without soil conservation measures, respectively in Hoa Binh province, in the mountain area in north-western Vietnam.

Soil erosion studies have started in Vietnam in the 1960s and have focused on: establishing soil erosion control measures (Quat and Nghan, 1964); studying the main factors affecting soil erosion and erosion control measures in hilly rice fields in the north-western mountains (Chung, 1978; Huyen and Toan, 1965); and country-wide monitoring of soil erosion (Can and My, 1982). Soil erosion at regional scale has been studied in northern Vietnam by Bac (1984) and in central Vietnam by Vi (1983), in small-scale studies, in which rough estimates of soil erosion were made, on the basis of changes in flow regimes in river systems, and crop damage in provincial domains. Recently, Ha (1996) analysed ten years' rainfall data, in combination with three years' observed soil erosion data, to identify the factors influencing soil erosion in six regions of northern Vietnam. In total almost 200 studies have been published (Ha, 1996), focusing on soil erosion (Loc et al., 1998; Phien et al., 2000), and implementing anti-erosion measures, such as contouring, alley cropping, green hedgerow construction (Truong et al., 1998), and agro-forestry (Thu et al., 1997; Toan et al., 1998).

On sloping lands, on-site effects of soil erosion at field plot and slope scales include removal of surface soil, associated with declines in soil fertility and crop yield, while at watershed, basin and regional scales off-site effects result in negative environmental impacts. In Vietnam, many soil erosion studies have been performed at plot and slope scales, but very few at watershed scale. At plot scale, runoff, soil loss and nutrient

* 1 US\$ = 8.25 Yuan (2005)

losses vary among crop systems, with the highest rates recorded for bare soil and monocultures. At this scale, soil conservation methods, such as hedgerows, intercropping, improved fallows (i.e. indigenous species or improved ones as *Tephrosia candida*), and agro-forestry significantly reduced soil erosion (Phien et al., 2000; Toan et al., 1998). At watershed scale, soil erosion rate is dependent on watershed size, and associated with differences in topography, slope steepness and shape, and land use types. A five-year study was carried out on a 49.7 ha watershed (Table 1), consisting of four sub-watersheds with different land use types (Phien et al., 2002; Toan et al., 2005). The study showed that soil loss from these watersheds was much lower than the annual values of 27.7 and 16.0 Mg ha⁻¹ for cassava and alley crops of cassava and *Tephrosia candida*, respectively, reported by Hue and Phien (2005) from plot and field slope studies, over the period 1995–2003, while soil erosion varied for different watershed sizes, land use types and years (Table 1). In particular, soil erosion was very high in the agricultural sub-watershed and lower in the forest sub-watershed. In 2001, soil erosion was extremely high because of very high rainfall in that year.

Tam Duong district (21°26' N, 105° 36' E) is situated in the transitional zone between flat lowland and mountainous areas, and consists of hilly land, mountains, and paddy lowlands. Soil erosion was very severe during the 1980–86 period (Mai et al., 2005), because of massive deforestation and expansion of agricultural activities, following the re-unification of Vietnam in 1975. As a result, there are large areas of degraded soils in the district, while soil erosion continues, even on soils that are already degraded. Annual runoff volume and soil loss in this area were 42,520 m³ ha⁻¹ and 37.2 Mg ha⁻¹ for bare soil, 32,628 and 24.5 for a pure cassava stand, 30,946 and 22.7 for a cassava and black bean intercrop, and 27,437 m³ ha⁻¹ and 17.5 Mg ha⁻¹ for a

Table 1. Annual rainfall (mm) and soil loss (kg ha⁻¹) at the outlets of (sub-)watershed(s) in Dong Cao watershed, Luong Son district, Hoa Binh province, Vietnam.

Watershed	Area (ha)	Dominant land use	Soil loss				
			1999	2000	2001	2002	2003
Rainfall			661	1202	2514	1047	1583
W ₁	2.64	Cassava + grass	1302	1724	9370	1816	586
W ₂	7.71	Cassava	679	687	5293	1923	2742
W ₃	9.92	Secondary forest + cassava	463	549	1824	856	571
W ₄	8.36	Grass + forest	303	424	2685	518	281
W _m	49.7		401	586	3617	419	512

Source: Toan et al. (2005); W₁, W₂, W₃, W₄: Sub-watersheds; W_m: Main watershed.

cassava and black bean intercrop with a green hedgerow of *Acacia* and *Tephrosia candida* (Toan et al., 1998). Moreover, Thu et al. (1997) reported erosion rates of 189 Mg ha⁻¹ yr⁻¹ for bare soil, 34 for *Acacia mungium* forest, 85 for pineapple and 75 for agroforestry, on slopes from 5 to 8 degrees during three years, with annual rainfall exceeding 2000 mm. Almost all erosion studies at watershed scale in the (sub)tropics deal with upland conditions, for instance, forest, grass, cassava, and fallow in Vietnam (Toan et al., 2005); maize, sugarcane, shrubs and forest in South Africa (De Roo and Jetten, 1999); wasteland, non-rice cropland and fallow in China (Hessel et al., 2003b); and maize, sugarcane, rangeland, tea, woodlots, grasslands, semi-deciduous vegetation, and forest in Kenya (Cohen et al., 2005). However, in the (sub)tropics, and especially in South-east Asia, paddy rice is an important land use type, as it is the main food source for the local communities, and is therefore present in almost all watersheds on sloping land in northern Vietnam. Quan Dinh watershed, located in the upper part of Tam Duong district, comprises many sub-watersheds and three villages, and consists of hilly lands, terraces and paddy lowlands. Paddy fields lie along the drainage systems from the middle terraces to the watershed outlet. The wide diversity in land use types and topography in the watershed may result in soil erosion patterns different from those observed in previous studies in upland watersheds. The objectives of this study were therefore: (i) to measure erosion at field, sub-watershed and main watershed scales and (ii) to evaluate the effect of paddy fields on runoff and erosion in the watershed.

MATERIALS AND METHODS

Study area

Quan Dinh main watershed (MW) is located in Quan Dinh village, in the hilly land of Tam Duong district, 72 km north of Hanoi (Figure 1). The watershed has a total area of 248.9 ha, elevation ranges from 28 to 70 meter (Figure 2) above sea level (asl). A small watershed of 19.1 ha, referred to as the sub-watershed (SW), located just north of the main watershed and sharing a drainage divide with MW, was also selected. Soil, land use and agricultural activities in SW are representative for the upland part of MW, while in MW, characterized by a more complex topography with hill lands, terraces and paddy lowlands, there are more soil types, land use types, slopes, roads and drainage systems.

Soil and land use

The study area is geomorphologically composed of hilly land and medium to low terraces. Soils are dominated by Arenosols and Acrisols (FAO, 1976; FAO/UNESCO,

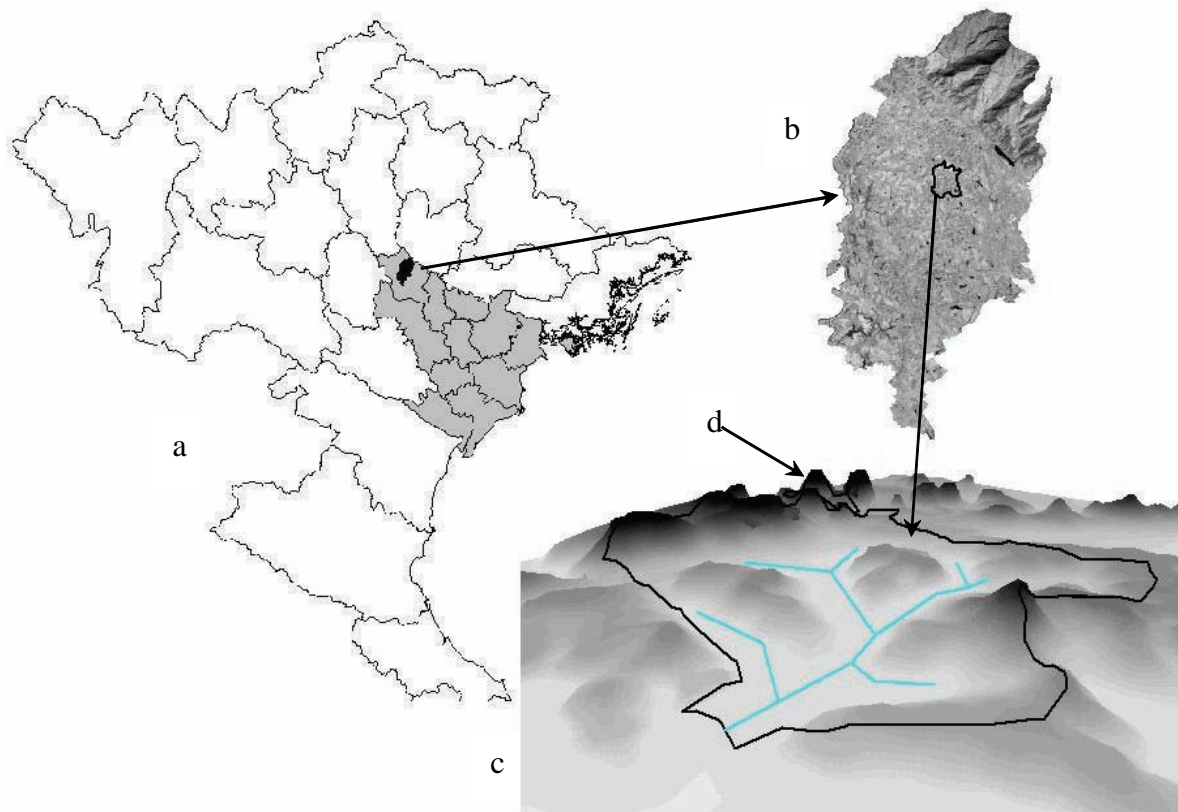


Figure 1. (a) Location of Red River Delta in northern Vietnam, (b) Satellite image (Landsat TM) of Tam Duong district, (c) 3D view of the main watershed (MW), (d) Sub-watershed (SW), where field plots of cassava and eucalyptus are located with arrow indicating the location.

1974). In the hilly land, soils have long been subject to erosion, especially the eucalyptus (*Eucalyptus globulus*) forests with their strongly compacted soils and low organic matter contents. In the lowlands, slopes are gentle and more clay and organic matter has accumulated in the soil. This part of the watershed is susceptible to temporary water logging during the cropping season. Selected soil properties were measured, such as particle size distribution by the pipette method (Day, 1965), soil organic matter with the Walkley-Black method (Nelson and Sommers, 1996), and saturated hydraulic conductivity using the constant head method (Stolte, 1997). Sand content tends to decrease, organic matter to increase and water conductivity to decrease going from the hills to the low terraces and paddy fields (Table 2).

In the upper hills, the dominant land use is second and third generation eucalyptus, regrowing after cutting of the first and second generations, that was planted widely in the late 1980s and the middle of the 1990s to supply raw materials to paper factories in the north. After a growth period of 10 to 20 years it was harvested at large scale (Mai et al., 2005). Regrowth was very slow, resulting in low soil cover for a prolonged

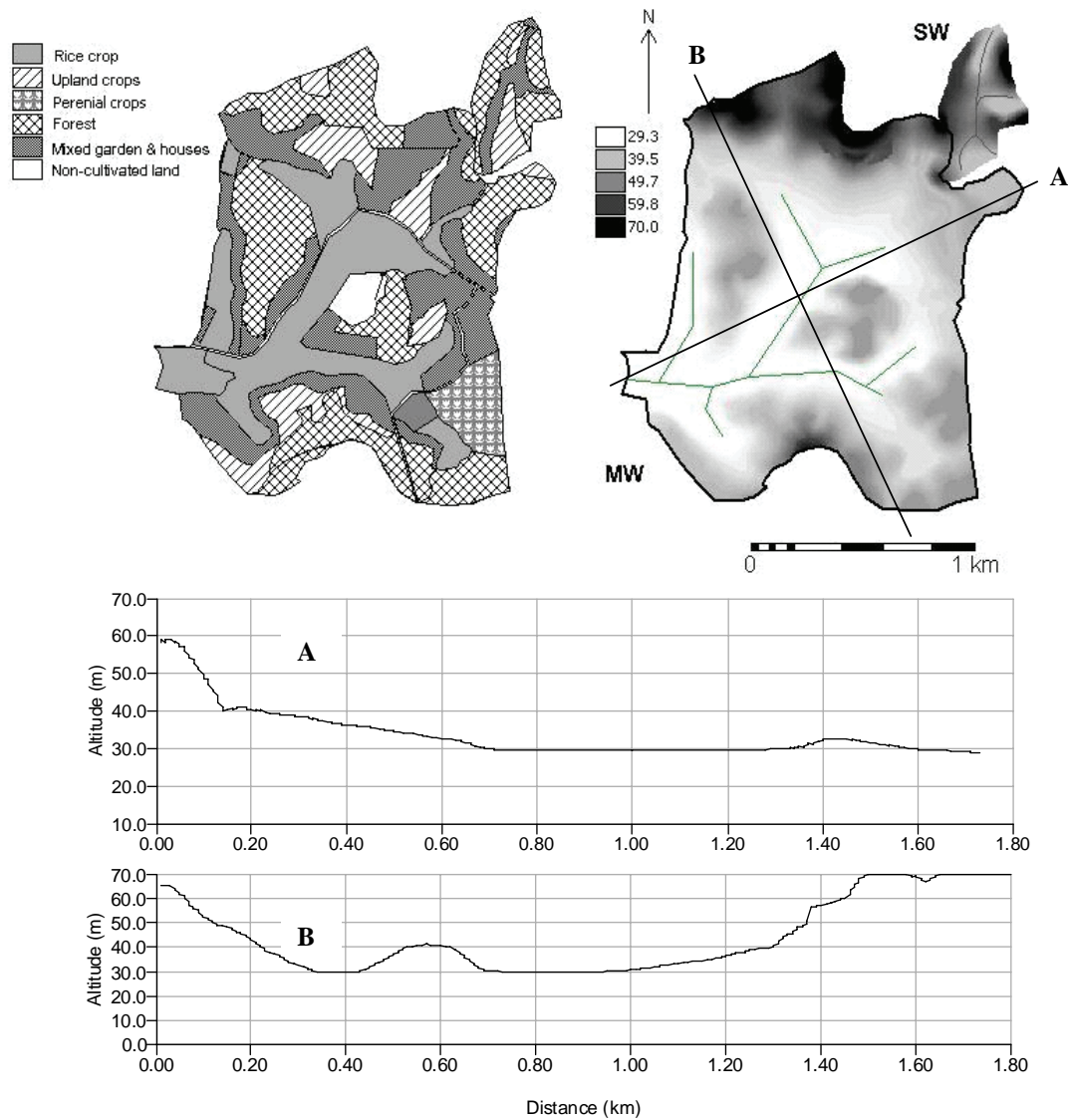


Figure 2. Land use map (left) and digital elevation map for main watershed (MW) and sub-watershed (SW). Cross-section along the watershed length (km) from north-east to south-west (A), and cross-section along the watershed width (km) from north-west to south-east (B) with altitude (m above sea level).

Table 2. Soil particle size distribution, organic matter content (OM) and saturated hydraulic conductivity (Ksat) for soils under rice, cassava and eucalyptus.

Land use	Particle size distribution (%)					OM (%)	Ksat (cm d ⁻¹)
	<0.002	0.002-0.02	0.02-0.20	0.2-0.5	0.5-2.0		
Rice on low terraces	7.0	12.4	46.6	14.5	19.5	3.2	16.5
Rice on middle terraces	20.8	9.8	5.2	26.6	37.6	2.4	40.0
Cassava on high terraces	12.8	2.6	30.5	30.2	23.9	1.5	143.2
Eucalyptus on high hill	16.8	8.5	5.2	27.9	41.6	1.1	646.0
Eucalyptus on low hill	16.4	7.8	34.4	22.9	18.5	1.3	51.8

period of time, which under the prevailing high intensity tropical rainfall pattern caused very strong soil erosion. As a result, the soil is strongly degraded, the soil surface is compacted and soil organic matter content is reduced. Land use in the watershed consists of eucalyptus and other forests in the upper hills; upland crops, such as cassava, peanut and beans on the high terraces; fruit trees, including litchi, longan, and custard in the low hills and mixed gardens around farmers' homesteads and rice on middle and low terraces (Figure 2). The middle and low terraces lie along the watershed drainage network, have gentle slopes and have a long history as paddy fields surrounded by bunds. The cropping pattern typically consists of spring rice from January/February to June, summer rice from July to September and winter maize from September 20th to the middle of January. Transition time between crops is 10 to 20 days for land preparation and transplanting/sowing, with substantial soil surface disturbance. The watershed is clearly different from watersheds in most other soil erosion studies, because of the presence of paddy fields, which are usually wet or waterlogged in the growing season. In the SW, however, there is only hilly land, suitable for forest, mixed gardens and upland crops.

Field measurements

Soil erosion measurements were carried out at three scales: main watershed (MW), sub-watershed (SW), and two field plots with cassava and eucalyptus, each 1 × 2 m in size. For the field plots, runoff and associated sediment per rainfall event were collected in a tank placed at the bottom of the plot. Discharge was recorded at the outlet of both MW and SW, for all rainfall events for the MW, and for main events for the SW, because of limitations of time, construction, and protection of equipment.

A 'stand-alone' tipping bucket rain gauge with data logger was placed at the outlet of the main watershed, to continuously record rainfall with an accuracy of 0.2 mm. The data were retrieved from the data logger using a notebook computer, or a data shuttle. The data were formatted to standard input files for any time step calculation and for soil erosion modelling. Water height at the outlet of both watershed and sub-watershed was measured with a water height data logger (WT-HR), using a capacitive sensor (Intech). Data resolution was formatted as five-minute interval for both SW and MW, for comparison of soil erosion. Flow velocity at the outlets was measured for various water levels and a linear relationship between water height and flow velocity was found. This relationship was used to estimate flow velocity for events for which flow velocity could not be measured. Discharge was calculated as product of wet area of the outlet, which depends on water height, and flow velocity.

Water samples were taken at the outlets for determination of sediment concentration from the start of runoff, every 10 minutes during the period of rapidly changing water

level, and every 30 minutes during more gradually changing conditions. Soil loss was calculated as the product of runoff volume and associated sediment concentration.

RESULTS

Soil erosion measurements at three scales

Soil erosion rates vary at different scales due to the specific surface characteristics, geometry, storage capacity, and drainage network at these scales (Van Dijk et al., 2005; Walling et al., 2002). At plot scale, soil loss originates from splash detachment, and sheet and rill erosion processes (Wezel et al., 2002). At sub-watershed scale, where more gullies and the edges of terraces are present, both soil erosion and deposition processes take place (Paringit and Nadaoka, 2003). At watershed scale, effects of terrain discontinuities, drainage network, and plant filters of densely vegetated fields play a role in deposition processes and transport capacity.

Table 3 shows that for almost all events, measured total runoff in both field plots was very high, as all runoff water from the slope is collected. At sub-watershed scale, various factors affect the runoff process, such as vegetation cover, different slope angles, infiltration capacity, and presence of depressions. As a result, a substantial part of rainfall eventually infiltrates, and total runoff at the outlet of the sub-watershed is low. At watershed scale, more runoff water was recorded at the outlet, also in relative terms, than at SW scale, but much less than at plot scale. This higher runoff is the result of the contribution from the paddy fields, where the soil is usually saturated or flooded, so that little or no water infiltrates. In particular two events (250804 and 260804) were examples. For MW, the runoff peaks of both events were superimposed, resulting in a single hydrograph, while at the SW outlet hydrographs were recorded for the two separate events. The event 3008-010904 was characterized by high rainfall volume and intensity on August 30th and extended rainfall with lower intensity on August 31st and September 1st. Both runoff and soil loss were very high in these events. To compare soil erosion rates among scales, the totals are given in Table 3 (total of 8 events with total rainfall of 173.2 mm, event 18-190905 was excluded, because there were no measurements at plot and SW-scales), showing that runoff (Q_{tot}) and soil loss (SY) from the plots ($656.2 \text{ m}^3 \text{ ha}^{-1}$ and $1067.4 \text{ kg ha}^{-1}$) were much higher than those from SW ($58.5 \text{ m}^3 \text{ ha}^{-1}$ and 44.6 kg ha^{-1}) and MW ($375.3 \text{ m}^3 \text{ ha}^{-1}$ and 125.2 kg ha^{-1}).

Table 3 also illustrates that the larger the watershed, the lower the sediment concentration in the runoff. In the field plots, all detached soil material from the slope face was collected. In SW, (part of) the sediment was trapped by vegetation, deposited in depressions and large particles settled through gravity during transport. Cerdan et al.

Table 3. Total runoff (Qtot), sediment concentration (SC) at peak discharge for the sub-watershed (SW) and the main watershed (MW) and sediment yield (SY) from cassava and eucalyptus field plots, SW and MW for 9 events. Rainfall (P) in mm; rain duration (T) in min.

Date	Measurements	Plot		SW MW		Plot			MW/
		Cassava	Eucalyptus			average	SW/P	MW/P	SW
170804	Qtot (m ³ ha ⁻¹)	140.00	140.00	35.11	67.86	140.00	0.25	0.48	1.93
P = 34.8	SC (g l ⁻¹)	1.70	1.51	0.91	0.70	1.61	0.57	0.44	0.77
T = 51	SY (kg ha ⁻¹)	238.00	211.40	27.36	22.16	224.70	0.12	0.10	0.81
250804	Qtot (m ³ ha ⁻¹)	32.00	24.00	0.70	-	28.00	0.02		
P = 31.0	SC (g l ⁻¹)	1.67	1.34	0.50	-	1.51	0.33		
T = 45	SY (kg ha ⁻¹)	53.40	32.20	0.27	-	42.80	0.01		
260804	Qtot (m ³ ha ⁻¹)	36.00	28.00	1.84	60.15*	32.00	0.06	1.88	32.64
P = 10.2	SC (g l ⁻¹)	1.28	1.15	0.50	0.30*	1.22	0.41	0.25	0.60
T = 33	SY (kg ha ⁻¹)	46.10	32.20	0.92	4.05*	39.15	0.02	0.10	4.40
3008-									
010904**	Qtot (m ³ ha ⁻¹)	180.00	84.00	2.43	187.84	132.00	0.02	1.39	77.30
P = 55.0	SC (g l ⁻¹)	2.52	1.70	0.73	0.52	2.11	0.35	0.25	0.71
T = 354	SY (kg ha ⁻¹)	453.60	142.80	1.72	79.71	298.20	0.01	0.27	46.34
100705	Qtot (m ³ ha ⁻¹)	80.40	69.00	3.35	4.63	74.70	0.03	0.06	2.46
P = 13.2	SC (g l ⁻¹)	2.58	2.17	0.63	0.43	2.38	0.27	0.18	0.68
T = 25	SY (kg ha ⁻¹)	207.40	149.70	1.94	1.77	178.55	0.01	0.01	1.90
250705	Qtot (m ³ ha ⁻¹)	92.00	75.00	7.16	25.31	83.50	0.09	0.30	3.53
P = 11.9	SC (g l ⁻¹)	1.12	1.09	0.86	0.56	1.11	0.78	0.51	0.65
T = 20	SY (kg ha ⁻¹)	103.00	81.80	5.63	13.50	92.40	0.06	0.15	2.40
310705	Qtot (m ³ ha ⁻¹)	180.00	84.00	6.82	10.46	132.00	0.05	0.08	1.53
P = 24.3	SC (g l ⁻¹)	1.08	1.08	0.96	0.56	1.08	0.89	0.52	0.59
T = 45	SY (kg ha ⁻¹)	194.40	90.70	6.34	2.23	142.55	0.04	0.02	0.35
040805	Qtot (m ³ ha ⁻¹)	42.00	26.00	1.06	19.39	34.00	0.10	0.57	5.79
P = 17.8	SC (g l ⁻¹)	1.57	1.24	0.43	0.15	1.41	0.31	0.11	0.35
T = 72	SY (kg ha ⁻¹)	65.94	32.24	0.43	1.80	49.09	0.04	0.04	0.93
18-190905	Qtot (m ³ ha ⁻¹)	ND	ND	ND	1337.50				
P = 156.6	SC (g l ⁻¹)	ND	ND	ND	1.46				
T = 2300	SY (kg ha ⁻¹)	ND	ND	ND	1168.30				
Sum	Qtot (m ³ ha ⁻¹)	782.40	530.00	58.50	375.30	656.20	0.09	0.57	6.42
(8 events)***	SY (kg ha ⁻¹)	1361.80	773.00	44.60	125.20	1067.40	0.04	0.12	2.81

* event 250804 and 260804 are in one hydrograph for the MW outlet.

** event 3008-010904 has taken place from August 30th to September 1st 2004, with the largest amount on August 30th and smaller amounts on August 31st and September 1st.

*** sum of 8 events, excluding event 18-190905 because no measurements were available for plot and SW.

ND = not determined.

(2002) observed deposition of sediment at sub-watershed scale, where it can be stored in gullies and in the streams (Van Dijk et al., 2005), when the sediment load exceeded the flow transport capacity, but not at plot scale. As MW comprises many sub-watersheds with different soils, land cover types and slopes, storage will also occur. As flow distances from the uphill plots to the watershed outlet are long, sediment is easily trapped and deposited on the terraces and in drainage systems. Within MW however, soil cover may be very low and the soil surface may be disturbed in some SWs, but not in others. For example, in the event 3008-010904, both Q_{tot} and SY in MW were much higher than in SW for various reasons. It was preceded by a heavy rain event on 250804 with high runoff and sediment yield, and subsequently it rained on the 26th, 27th, 28th and 29th, so that the soil was saturated at the start of the event and little infiltration took place. In our SW, plant cover on all land use types was high and the soil surface was undisturbed. In some of the other sub-watersheds, soil and hydrological conditions were different, e.g. with higher detachment and less opportunity for deposition, resulting in high runoff and soil loss. In addition, in MW more upland summer crops were cultivated with more tillage activities than in SW. The heavy rain immediately followed crop weeding, which results in high soil erodibility, and therefore caused very high sediment yields in this event. On the other hand, rice fields could not retain runoff water, following the rainfall of the preceding days. During the event 250705, rice fields contributed to high sediment yields, because this was weeding time for rice in the area, and the soil was strongly disturbed with a lot of sediment already suspended in the standing water before the event.

Total discharge

Total number of rainy days was 136 and 156, with annual rainfall of 1172 and 1560 mm in 2004 and 2005, respectively. In 2004, maximum daily rainfall was 70 mm. Maximum runoff volume was $187.8 \text{ m}^3 \text{ ha}^{-1}$ on August 30th – September 1st with 55.0 mm precipitation. In 2005, however, rainfall was concentrated in the July-September period with very high rainfall intensities. Maximum rainfall was 156.6 mm on September 18-19th, with a highest intensity (in five-minute intervals) of 112.8 mm h^{-1} , which generated a maximum runoff volume of $1337 \text{ m}^3 \text{ ha}^{-1}$.

In total (Figure 3), in 2004 there were 11 events that generated runoff at the MW outlet with an average runoff coefficient (ratio of Q_{tot} and precipitation) of 0.12 (ranging from 0.02 to 0.41). In 2005, there were 30 events that generated runoff at the MW outlet with an average runoff coefficient of 0.25 (ranging from 0.01 to 0.85). Most of the high runoff coefficients were associated with high soil moisture contents at the start of the rainfall event, resulting from rainfall on preceding days. In addition, the presence of paddy fields on the low terraces in MW influenced runoff regimes,

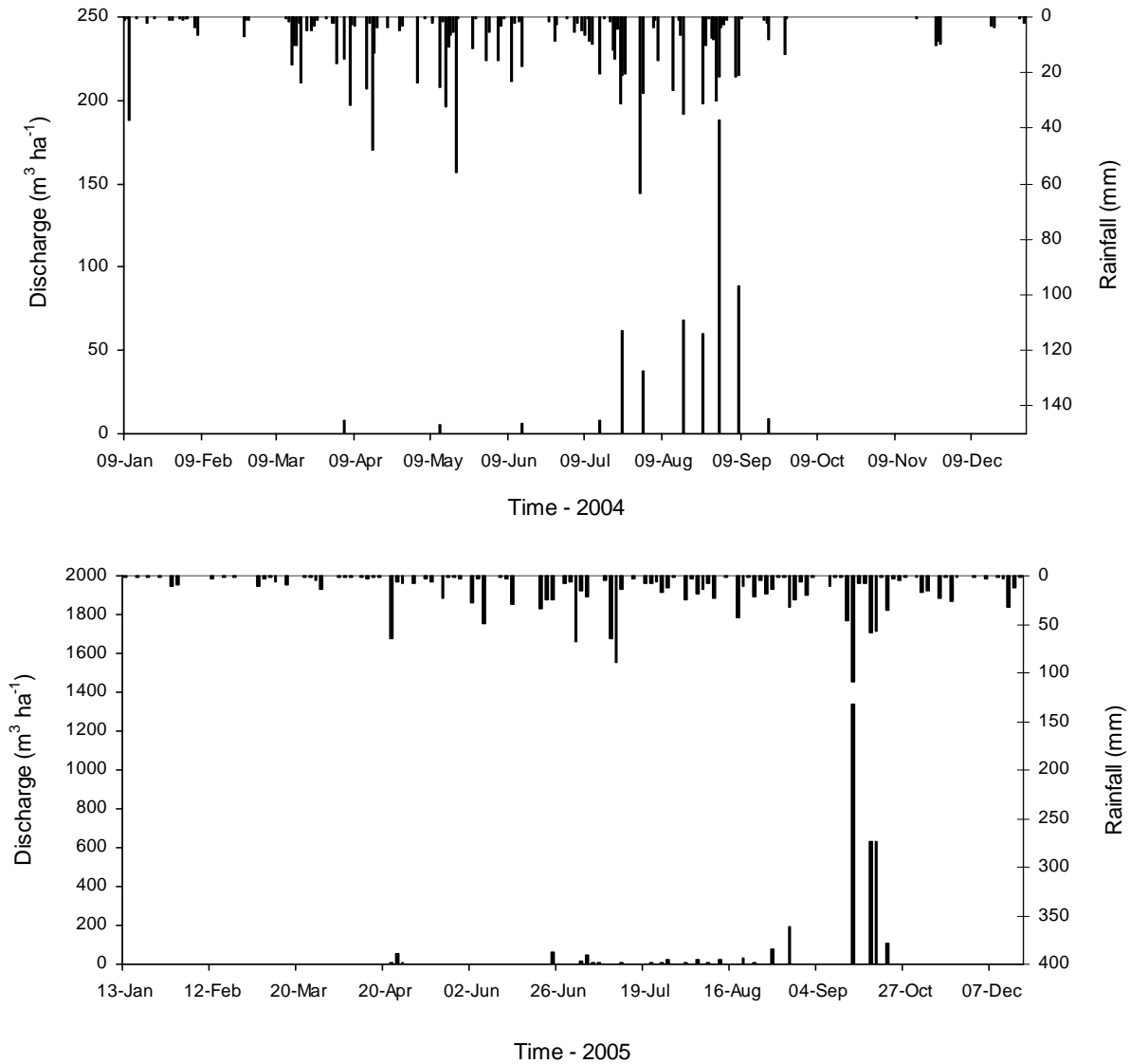


Figure 3. Precipitation in mm (downward bars) and discharge in $\text{m}^3 \text{ha}^{-1}$ (upward bars) of main watershed in 2004 (on top) and in 2005 (at bottom). Note the difference in scale for 2004 and 2005.

because of the occurrence of ponding (Chen et al., 2003) in the rice fields that are constructed as small reservoirs with bunds, varying in height from 0.05 to 0.3 m. If a rainfall event occurs when field storage capacity is (almost) completely utilized, almost all rainwater runs off towards the drainage system, and rapidly reaches the MW outlet. This pattern can be clearly recognized by comparing the runoff coefficients of MW and SW for the events 170804, 300804, 310705, and 040805, which were 0.19 and 0.01, 0.32 and 0.0008, 0.043 and 0.003, and 0.109 and 0.0005, respectively, keeping in mind that the soils in SW were mostly deep and dry.

Sediment Concentration (SC)

Sediment concentration at the outlet of MW varied strongly in both years (Figure 4) as a result of the wide variation in rainfall volume and intensity, but also in dependence of soil surface conditions, land cover, and stage of crop growth. In 2004, maximum SC was 0.87 g l^{-1} and maximum discharge 928 l s^{-1} ; in 2005, maximum SC was 1.60 g l^{-1} and maximum discharge 5400 l s^{-1} . However, SC in our watershed was low compared to that measured in Dong Cao watershed by Phien et al. (2002) that reached values up to 5 g l^{-1} . Many studies have shown a relation between sediment concentration and discharge. For example, Holtschlag (2001) in analysing the relation between suspended sediment concentration and stream flow for 10 selected sites, reported consistent positive correlations between the logarithm of both characteristics. Horowitz (2003) found the same when plotting sediment concentration versus discharge for various river basin sizes. Recently, Hessel (2006) also found an increase in sediment concentration with increasing discharge on the Chinese Loess Plateau. Moreover, SC strongly depends on rainfall energy, determined by drop size and intensity (Morgan, 1995; Wischmeier and Smith, 1978), flow detachment and soil moisture content. In this study, both rainfall volume and rainfall intensity were high, and most soils were silty loams and very fine sands, which are susceptible to detachment and transport. Therefore, high discharge rates are the result of large rainfall amounts and high rainfall intensity, resulting in strong detachment and transport and high SC.

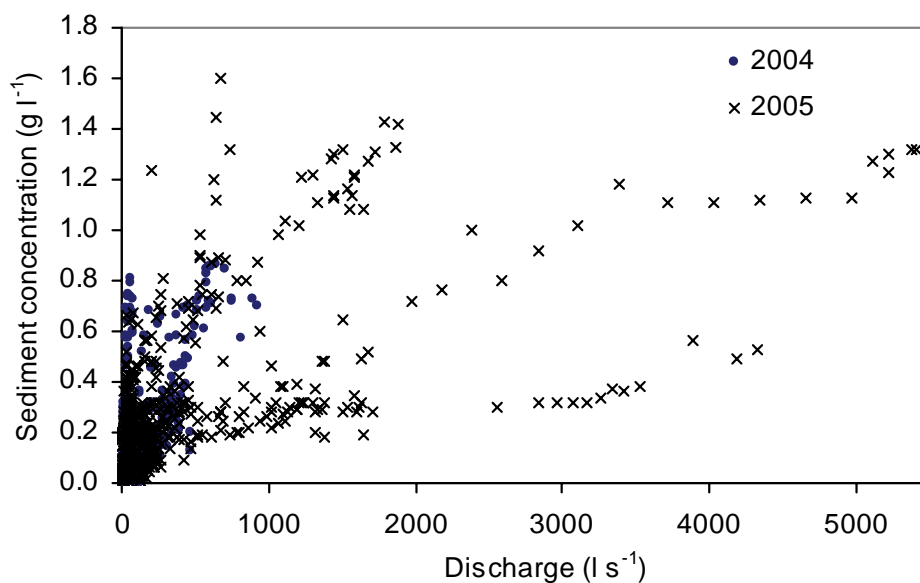


Figure 4. Sediment concentration (g l^{-1}) versus discharge (l s^{-1}) in the MW outlet.

Sediment Yield (SY)

Soil erosion in MW occurred between April and October and varied from year to year. In 2004, peak discharge and soil loss occurred in July and August, but the highest total runoff was in August and September. In 2005, peak discharge and highest total runoff and soil loss were recorded in August and September. In April, which is normally part of the dry season, characterized by very low rainfall and dry soils, soil erosion was observed in 2005, but not in 2004, because rain started early in 2005 with large rainfall volumes and high intensities. At that time, most soils in the hilly area were bare, and soil surfaces were strongly disturbed by land preparation. In the paddy fields, plant cover was less than 30%, while extensive weeding activities took place. After September 20th, the late growth period for all upland crops, soil cover is high and soils are dry, because of low rainfall and high crop transpiration. Thus, soil erosion did not happen in the hilly area, except at very high rainfall amount and/or rainfall intensity. In the paddy fields, however, summer rice had been harvested, and soils had been plowed and harrowed for planting winter crops, creating conditions conducive to soil erosion.

Comparing 2004 and 2005 (Table 4) shows that rainfall volume, peak discharge, total discharge and soil loss in 2005 were 1.3, 5.9, 6.2 and 11.5 times higher, respectively, than in 2004. The extraordinary event on September 18–19th 2005 with rainfall exceeding 156 mm, generated 1337 m³ ha⁻¹ runoff and 1168 kg ha⁻¹ sediment, comprising 40% of the total annual runoff and 67% of the total sediment yield. For the remainder of that year, discharge and sediment yield were comparable to 2004, although rainfall in 2004 was low, as expressed by farmers in the area, complaining about shortage of water for crop growth, due to below-average rainfall (1172 compared to 1400 mm yr⁻¹).

DISCUSSION

Plot measurements since 1990 yielded erosion rates in Tam Duong district ranging from 30 to 200 Mg ha⁻¹ yr⁻¹, showing soil erosion to be the main process in soil degradation (Siem and Phien, 1999). In a soil erosion zonation, based on calculated water erosivity and soil erodibility (Ha, 1996), Tam Duong district was classified as one of the 'hot spots' of soil erosion in Vietnam. The erosion rates measured on our plots (Table 3) are comparable to those reported by Toan et al. (1998) and Thu et al. (1997). Our study (Table 3) indicates that runoff and soil loss rates are much higher at plot (cassava and eucalyptus) scale than at (sub-)watershed scale, because almost all runoff and sediment are directly collected. Parcel boundaries, such as hedgerows, play an important role in reducing flow rates and retaining sediment (Hoang Fagerström et al., 2001). Total runoff and soil loss at the SW outlet were not very high, despite high runoff and soil loss from individual plots, such as our cassava and eucalyptus plots,

Table 4. Observed monthly precipitation, peak discharge, total discharge and soil loss from the main watershed (MW) in two observation years, 2004 and 2005.

Month	2004				2005			
	Preci- pitation (mm)	Discharge		Soil loss (kg ha ⁻¹)	Preci- pitation (mm)	Discharge		Soil loss (kg ha ⁻¹)
		Peak (l s ⁻¹)	Total runoff (m ³ ha ⁻¹)			Peak (l s ⁻¹)	Total runoff (m ³ ha ⁻¹)	
1	44.8	0.0	0.0	0.0	5.0	0.0	0.0	0.0
2	22.1	0.0	0.0	0.0	28.3	0.0	0.0	0.0
3	82.0	0.0	0.0	0.0	54.7	0.0	0.0	0.0
4	176.4	140.0	8.0	1.0	89.7	851.0	63.0	27.0
5	192.8	92.0	5.0	0.6	46.4	0.0	-	0.0
6	82.6	76.0	6.5	3.3	206.8	668.0	68.0	38.8
7	228.4	704.0	70.3	22.4	364.8	469.0	132.0	39.2
8	226.2	928.0	350.8	122.1	250.1	1899.0	367.0	232.7
9	76.6	389.0	97.6	13.4	326.4	5480.0	2586.0	1296.0
10	0.0	0.0	0.0	0.0	47.0	1521.0	108.0	88.2
11	29.4	0.0	0.0	0.0	87.4	0.0	0.0	0.0
12	10.2	0.0	0.0	0.0	53.8	0.0	0.0	0.0
Sum	1172.0	928.0*	538.1	162.8	1560.0	5480.0*	3324.0	1721.9

* peak (in the sum row) = highest peak.

because in moving from individual fields to the SW outlet, runoff water has to pass through many plant beds, furrows and parcel boundaries, where sediment is trapped and deposited (Paringit and Nadaoka, 2003). Moreover, depressions within the SW are important in reducing runoff and sediment yield, as illustrated by Fiener et al. (2005), who showed that up to 85% of the sediment can be trapped in small ponds. However, the amount of trapped sediment depends on number and size of ponds, concavity of the slope and slope length. Soil erosion rates also varied among slope segments, resulting in different influences on soil detachment, deposition, and transport (Pilotti and Bacchi, 1997). The magnitude of runoff and soil loss at the SW outlet agreed with results from other sites, e.g. from 0.3 to 9.4 Mg ha⁻¹ yr⁻¹ (Table 1) in Dong Cao watershed (Toan et al., 2001, 2005), while sediment yield in the field plot was up to 100 Mg ha⁻¹ yr⁻¹ (Phien et al., 2000).

Scaling up to watershed scale requires integration of many entities and their combinations, such as soil types, land use types, slopes, and drainage networks. In this study, terraces and paddy fields with their bunds and storage effects strongly affected the overall results. For MW, the upland crops in the low terraces retain the runoff

water coming from the hills, while the stored water in the paddy rice fields is gradually released. This process results in longer recession curves of the hydrograph, while the suspension also settles in the course of this process (Fiener et al., 2005). Paddy fields on the one hand, rapidly generate runoff from rainwater when fully flooded, and on the other hand, slow down water flowing from the hills and the upper terraces, so that soil particles are deposited. Within the watershed, these paddy fields act as biological filters or riparian zones, influencing hydrological processes as illustrated by Tabacchi et al. (2000) and Abu-Zreig et al. (2001).

Sediment concentration strongly depends on soil properties, soil detachment, plant cover and transport capacity. In most events, the magnitude of SC was in the order field plot > SW > MW. In practice, SC strongly depended on surface characteristics and plant cover (Cerdan et al., 2002), i.e. increasing with increasing surface roughness and decreasing with increasing crop cover. In the study area, upland crop fields contributed large amounts of sediment, because their soil particle size is very susceptible to detachment, and because low soil cover and strong soil surface disturbance due to land preparation and weeding often occur simultaneously. For example, the cassava fields were bare with very high surface roughness in April and May; plant cover increased slowly in the early stages and attained high values only in late August/early September. It was even worse on soils planted with peanut and beans, where crops were harvested in June and land was prepared for the subsequent crops in periods with concentrated high rainfall amounts. In paddy fields, the dynamics of soil and plant were repeated from spring rice to summer rice and winter maize, i.e. low cover in April with weeding activities, maximum cover in the middle of May, bare in June, low cover with weeding activities in July, harvesting after September 20th and bare with land preparation in October. This land use type is located along the stream network, very close to the MW outlet, and therefore contributed substantially to the sediment load during crop transitions, with intensive land preparation, and weeding in the tillering period.

SC at the MW outlet was highly variable in time (Figure 5) and was influenced by environmental conditions such as rainfall, soil type and crop type. In April, SC was high, because the soil was bare in the hilly areas and soil cover was low in the lowlands. In May, crop cover rapidly increased because of increasing radiation, temperature and rainfall, with minimum soil surface disturbance on hilly lands, resulting in very low SC. From June 20th to July 10th and from September 20th to October 10th spring and summer rice were harvested, respectively, after which the soil was plowed and harrowed for the subsequent crops, leading to very high SC in these periods. From October onwards, upland soils were dry and cassava plots were completely covered, thus effectively protecting the soil; hence, the main sources of soil

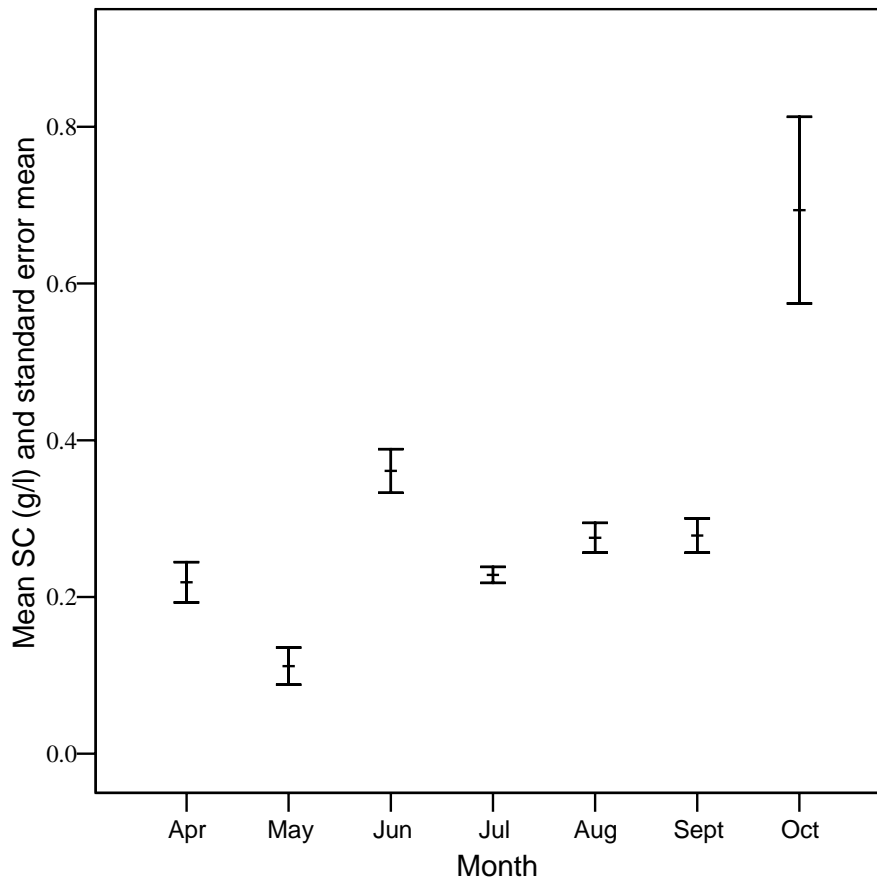


Figure 5. Monthly average sediment concentration and standard error (error bars) in 2004–05.

erosion in this period were the paddy fields. In August, both the uplands and the paddy fields were well covered, so that substantial sediment loads were associated only with events of very high rainfall volume and intensity. Combining these results with total runoff and sediment yields from Table 4, allows examination of the relation between land use dynamics and soil erosion. Such information may form the basis for formulation and analysis of new land use scenarios for soil conservation, for instance, decreasing agricultural land use, redistribution of land use based on pedological information, slope, and potential soil erosion (Stolte et al., 2005); designing new crop rotations, inter-crop activities, production techniques, and animal production activities (Dogliotti et al., 2004). Whether or not such alternatives are actually adopted depends on incentives, economically- and/or environmentally-driven.

CONCLUSIONS

In this study, field measurements of runoff and sediment yield were carried out to assess the magnitude of soil erosion from field plots, sub-watershed and main watershed in Quan Dinh watershed. Runoff volume and sediment yield from the SW

were 75 to 95% and 88 to 99% lower, respectively than at plot scale. Runoff from MW was higher than from SW, because of the rice fields with their temporary storage and release effects. The rice fields also acted as green filters to trap sediment from uphill and from high terraces, and thus had large effects on both runoff and soil loss.

Total runoff ranged from 538 to 3324 m³ ha⁻¹ yr⁻¹ and sediment yield from 163 to 1722 kg ha⁻¹ yr⁻¹, in agreement with results from other studies in the district and the region. Soil erosion in 2004 represents a value at the low end of the range (with a low annual rainfall of 1172 mm) and that in 2005 at the medium to high end (with annual rainfall of 1560 mm), as rainfall may reach 2000 mm. Threats for natural hazards occurred in August and September, with events of very high rainfall volume and intensity, causing flash floods and large-scale soil erosion.

Sediment concentrations were significantly higher in April, June and late September/October, when crop cover was low and the soil surface was disturbed. The data also revealed that it is highly likely that high erosion rates would occur in April and/or October, if rainfall occurs early or late. This indicates risks associated with current land use distribution and crop calendars. Alternatives may be proposed, that may be derived from scenario studies.

CHAPTER 4

Simulation of soil erosion in Quan Dinh watershed in Tam Duong district, north Vietnam *

V.T. Mai^{1,4}, R. Hessel², H. Van Keulen^{1,3}, C. Ritsema², R.P. Roetter²

- ¹ Plant Production Systems Group, Wageningen University, P.O. Box 430, 6700 AK Wageningen, The Netherlands
- ² Soil Science Centre, Alterra Green World Research, Wageningen University and Research centre, P.O. Box 47, 6700 AA Wageningen, The Netherlands
- ³ Plant Research International, Wageningen University and Research centre, P.O. Box 16, 6700 AA Wageningen, The Netherlands
- ⁴ National Institute for Soils and Fertilizers (NISF), Dong Ngac, Tu Liem, Hanoi, Vietnam

Abstract

The soil erosion model LISEM was applied to simulate soil erosion in a 248.9 ha complex watershed, including terraces and lowland paddy fields in Quan Dinh village, Tam Duong district, northern Vietnam in the period 2004–05. Soil erosion was also simulated for a 19.1 ha sub-watershed bordering the main watershed, to examine soil erosion at different scales and to study effects of terraces and paddy fields within the watershed. The model has been calibrated for five events and validated for four additional events. For hydrology, LISEM yielded satisfactory results for the sub-watershed, which consists of sloping land. Peak runoff time, peak runoff and total discharge were all simulated satisfactorily. For the main watershed, results were also satisfactory for peak runoff time and peak runoff, but total discharge was grossly underestimated. The reason is that throughflow in the terraces and storage in and release from the paddy fields are not taken into account in the model. These processes not only delay overland flow from the upper hills, but also contribute more surface runoff to the watershed outlet. Soil loss was overestimated for the sub-watershed, because sediment concentrations were overestimated, and it was underestimated for the main watershed, because of underestimation of total runoff.

Keywords: Rice-based cropping systems, soil erosion modelling, LISEM

* This chapter has been submitted to CATENA Journal.

INTRODUCTION

Northern Vietnam is a region where sloping lands are combined with a tropical climate, characterized by large rainfall amounts and high rainfall intensity. In the region, land cover is decreasing, and agricultural activities are increasing, which in combination with high rainfall, results in serious soil erosion. Soil erosion rates of up to 200 Mg ha⁻¹ have been measured at plot scale, and the area of degraded soils is increasing (Siem and Phien, 1999). Soil erosion has been measured at various sites, and for various landscapes, slope angles, soil types, land uses, and rainfall regimes, with the aim to properly assess the erosion problem and to identify measures to conserve the soil resources. Such measurements (mostly at plot scale) require many long-term experiments for combinations of different crops, soil types and slope angles, and are therefore demanding in terms of human and financial resources. However, soil erosion can also be assessed using soil erosion modelling, based on selected measurements from the field. Using models, both spatial and temporal variation in soil erosion can be simulated, requiring less human and financial resources, and yielding results useful for soil and water quality management.

In developing models of soil erosion by water, increasing emphasis is placed on appropriate representation of the physical processes involved in erosion. Some models represent space in a simplified way, such as the Universal Soil Loss Equation (USLE; Wischmeier and Smith, 1978), the Revised Universal Soil Loss Equation (RUSLE; Renard et al., 1991) and the Erosion-Productivity Impact Calculator (EPIC; Williams, 1985). These are lumped models, assuming, in principle, a spatially homogeneous uniform hill slope, although they may be applied to more complex terrain. The GLEAMS (Groundwater Loading Effects of Agricultural Management Systems; Leonard et al., 1987) and CREAMS (Chemicals, Runoff and Erosion from Agricultural Management Systems; Knisel, 1991) models are both based on on-field management, such as conservation tillage, terracing, contouring, a single land use, relatively homogeneous soils and spatially uniform rainfall. Recently, the Water Erosion Prediction Project (WEPP; Flanagan et al., 2001), the KINematic runoff and EROSION model (KINEROS2; Smith et al., 1995) and the EUROpean Soil Erosion Model (EUROSEM; Morgan et al., 1998) models have adopted a basically similar element-based calculation method.

With the expansion of geographical information system (GIS) capabilities, spatially distributed catchment models have been developed to simulate runoff and erosion dynamics of larger and more complex catchments. Such models allow identification of the source and sink areas of water, sediment and associated chemicals within a catchment. They are also adapted to catchment scale by increasing the number of elements and catering for special elements, such as channels and ponds (Jetten et al., 2003).

Models such as the Limburg Soil Erosion Model (LISEM; De Roo et al., 1996a, b; Jetten and De Roo, 2001), the 3D erosion model (EROSION3D; Schmidt et al., 1999), the Areal Non-point Source Watershed Environmental Response Simulation model (ANSWERS; Beasley et al., 1980), the catchment water discharge and soil water model (TOPMODEL; Beven and Freer, 2001) and MIKE-SHE (Refsgaard and Storm, 1995) are based on regular grids of equal-sized raster cells. These models are based on water and sediment balances that produce runoff and (suspended) sediment for each spatial element, which is then routed towards the outlet using a kinematic wave routine. LISEM, a raster-based model, has been calibrated and validated for various watersheds in tropical conditions (De Roo and Jetten, 1999; De Roo et al., 1996b). It was therefore selected to simulate soil erosion in our study area in Vietnam.

In Chapter 3, soil erosion measurements were reported for two years, 2004 and 2005 in Quan Dinh watershed (21°26' N, 105°36' E), Tam Duong district, northern Vietnam. In that study, water height and sediment concentration were measured at the sub-watershed and the main watershed outlets, for calculation of total discharge and sediment yield. The results showed that total discharge and sediment yield at both the sub-watershed and watershed scales, were much lower than at field plot scale. Total discharge in the main watershed was higher than in the sub-watershed, because there was slow storage release to the watershed outlet from bunded paddy fields where rain water was temporarily stored. This mechanism has not often been simulated in soil erosion models, although such watersheds, including upland hill slopes, sub-watersheds and paddy fields are common in mountainous areas in northern Vietnam and South-east Asia in general. To increase understanding about soil erosion in this complex watershed, to reduce damage, and to avoid losses from soil erosion, this study focused on (i) testing the soil erosion model LISEM for the main watershed and the sub-watershed and (ii) simulating soil erosion in the main watershed.

MATERIALS AND METHODS

Study area

Quan Dinh main watershed (MW) is located in the hilly land of Tam Duong district, 72 km north of Hanoi (Figure 1). The watershed has a total area of 248.9 ha, and elevation ranges from 28 to 70 m above sea level (asl). A small watershed (referred to as sub-watershed, SW) of 19.1 ha, located just north of and sharing a drainage divide with MW, was also selected.

Soil and land use

Geomorphologically, the study area consists of hilly land and medium to low terraces.

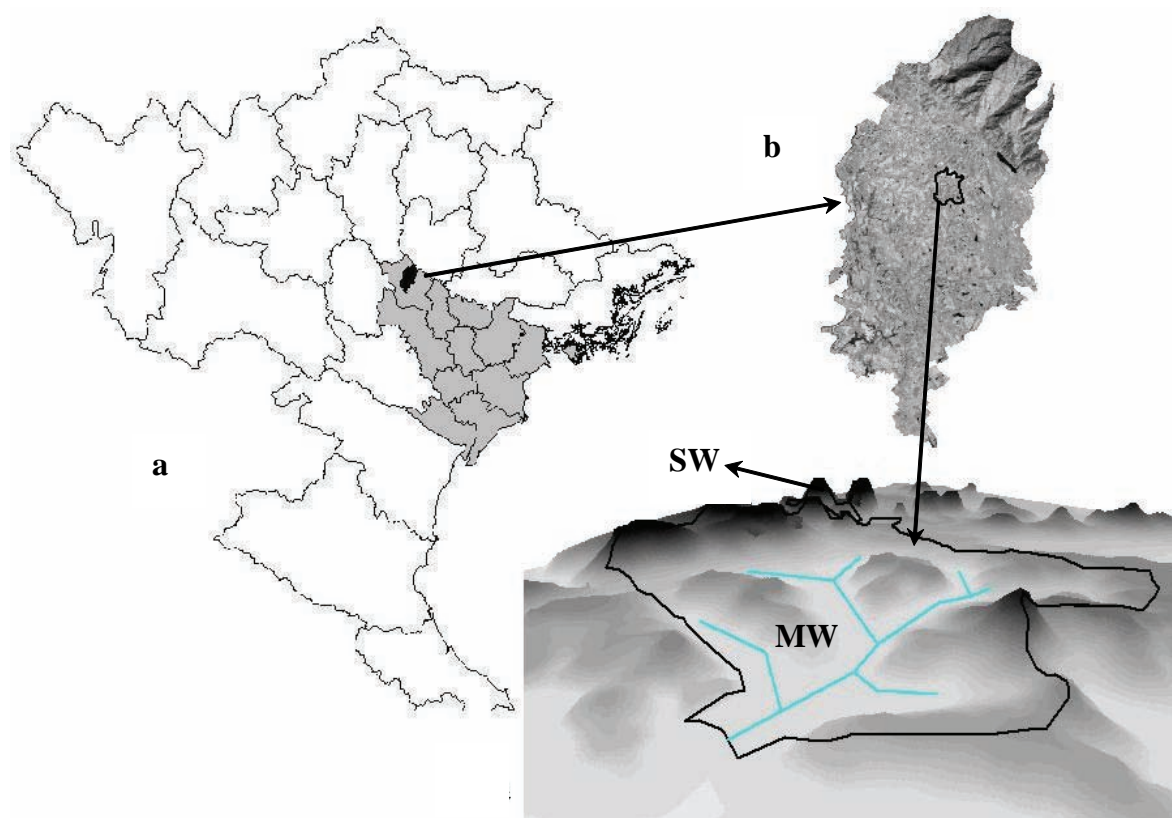


Figure 1. Schematic representation of the study area, with: Red River Delta in grey located in north Vietnam (a), satellite image LANDSAT TM of Tam Duong district (b), Main Watershed (MW) in three dimensions, and Sub-Watershed (SW) without paddy fields.

Table 1. Soil types and land use types in the study area.

	Main watershed (MW)		Sub-watershed (SW)	
	Area (ha)	Fraction (%)	Area (ha)	Fraction (%)
Soil type				
Endogleyic Albic Arenosols	88.3	35.5	19.1	100.0
Albi Gleyic Cambisols	0.5	0.2		
Epilithi Ferralic Acrisols	66.2	26.6		
Endolithi Ferralic Acrisols	73.7	29.6		
Hapi Ferralic Acrisols	20.2	8.1		
Land use				
Rice	62.5	25.1		
Upland crops	22.4	9.0	4.5	23.6
Perennial crops	10.7	4.3		
Forest	74.3	29.9	9.9	51.6
Mixed gardens	64.9	26.1	4.7	24.8
Non-cultivated land	14.1	5.7		

Dominant soils in the study area are arenosols and Acrisols (FAO, 1976; FAO/UNESCO, 1974). On the upper hills, major land use is second and third generation eucalyptus (*Eucalyptus globulus*), which has a poor land cover of 20 to 30%. Because of the tropical rainfall in the area, soils have been strongly eroded and degraded, with compacted surfaces and low organic matter contents (Mai et al., 2005). On the slope faces, fruit trees, such as lichi, longan and custard are grown, on the high terraces, cassava and peanut. Around the farms, mixed gardens are found, that occupy about three fourths of the total homestead area. On middle and low terraces that lie along the watershed drainage network, slopes are gentle and soils are suitable for annual crops, i.e. rice, maize and beans, with the main land use type being double rice and winter maize. The temporal pattern of land use here is spring rice from January/February to June, summer rice from July to September and winter maize from September 20th to the middle of January. Transition time between crops is about 10 to 20 days for land preparation and transplanting/sowing, with substantial soil surface disturbance. Since 25% of the watershed area is occupied by paddy rice (Table 1), MW differs considerably from other upland watersheds, because paddy rice fields are usually wet or waterlogged in the growing season. In the SW, however, there is only hilly land, with steeper slopes, which is suitable for three land use types: forest, mixed gardens and upland crops.

Field measurements

Rainfall was measured with a resolution of 0.2 mm, using a ‘stand-alone’ tipping bucket rain gauge placed at the outlet of MW. The data were retrieved from the data logger using a notebook computer, and were converted to standard input files for the LISEM model at 5 minute resolution. Water heights at the SW and MW outlets were measured at 5 minute resolution with a water height data logger (WT-HR), using a capacitive sensor (Intech). Flow velocity at the outlets was measured for various water levels and a linear relationship between water height and flow velocity was established. This relationship was used to estimate flow velocity for events for which flow velocity could not be measured. Discharge was calculated as product of wet area of the outlet, which depends on water height, and water velocity.

Water samples were taken at the outlets for determination of sediment concentration from the start of runoff, every 10 minutes during periods of rapidly changing water level and every 30 minutes during more gradually changing conditions. Soil loss at the outlets was computed as product of runoff volume and associated sediment concentration. Measurements of soil erosion were also performed on an event basis at two small (1 × 2 m) plots on cassava and eucalyptus (Chapter 3).

The LISEM model requires a number of soil physical characteristics. Saturated

hydraulic conductivity (K_{sat}) was determined by the constant head method (Stolte, 1997). Random roughness (RR), the standard deviation of soil surface height, was measured at two-weekly intervals. The median texture of the soil (D_{50} ; μm) was calculated from soil particle size distribution, determined by the pipette method (Day, 1965). As it was not possible to determine soil aggregate stability using the drop method suggested by Hessel (2002), the wet sieve method (Kemper and Rosenau, 1986) has been used to have the same unit for model input. Soil aggregate stability was then calculated as a linear function of the percentage of the 3.5 mm aggregate class, as found by Liu et al. (2003).

Crop characteristics, such as soil cover, plant height, and leaf area index (LAI) are also very important factors influencing soil erosion. These characteristics were measured at 15-day time intervals (Hessel, 2002).

LISEM model

LISEM is a physically-based runoff and erosion model (Figure 2) for research, planning and conservation purposes that simulates the spatial effects of rainfall events on small watersheds. The model is fully described by Jetten (2002) and Jetten and de Roo (2001) and is briefly described in the following.

Rainfall and interception

Rainfall is added to the current water height (h) in each cell, but because the rain falls on a horizontally projected surface, while the actual terrain has a slope, a correction is needed:

$$h = h + P \times \cos(a) \quad (1)$$

where, P is rainfall in that time step (mm) and a is the slope angle in degrees.

Interception by the vegetation is simulated by regarding the canopy as a simple storage device, and is subtracted from rainfall.

Infiltration and surface storage

Rainfall that reaches the soil surface can either infiltrate or can be (temporarily) stored in micro depressions. Infiltration can be calculated with several sub-models, such as Holtan (Beasley and Huggins, 1982), Green and Ampt (Li et al., 1976) for one or two layers, and the SWATRE model, which is a finite difference solution of the Richard equation (Belmans et al., 1983). The input is, for all equations, in the form of maps with soil hydrological properties, such as initial moisture content, porosity, and saturated conductivity for each soil layer. Selection of the infiltration model is mostly based on the type of data available and the user's experience.

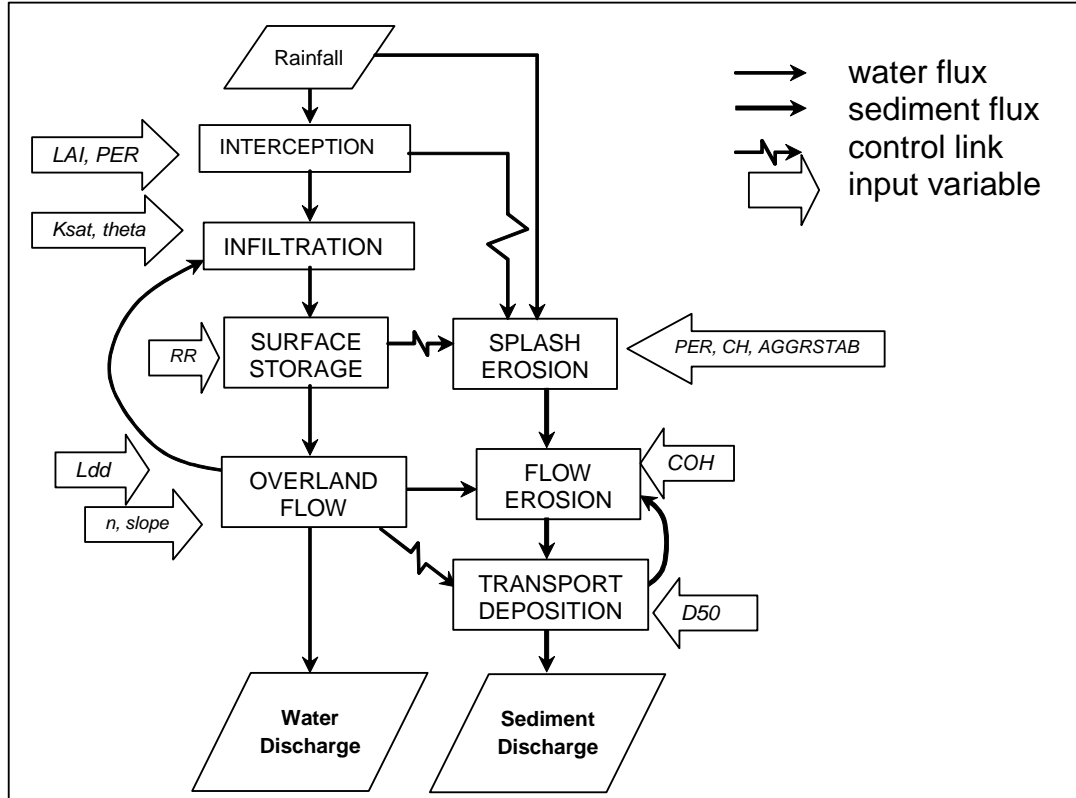


Figure 2. Flow diagram of the physically-based hydrological and soil erosion model LISEM (Hessel, 2002), LAI = Leaf Area Index, PER = Plant Cover, Ksat = soil hydraulic conductivity, theta = initial soil water content, RR = random roughness, ldd = drainage direction, n = Manning's n coefficient, slope = slope gradient, AGGRSTAB = aggregate stability, CH = plant height, COH = cohesion of the soil, D50 = median texture of the soil.

Surface storage is calculated based on random roughness. Excess water that cannot be stored, and does not infiltrate becomes runoff.

Overland flow

Flow velocity V (m s^{-1}) is calculated with Manning's formula:

$$V = \frac{\sqrt[3]{R^2 \times \sqrt{S}}}{n} \quad (2)$$

where, R is hydraulic radius (m) calculated from the flow width and average water height, S sine of the slope (fraction) and n is Manning's n (dimensionless).

The discharge Q ($\text{m}^3 \text{s}^{-1}$) per cell is then calculated with Chow et al. (1988):

$$A = \alpha \times Q^\beta \quad (3)$$

$$\alpha = \left(\left(\frac{n}{\sqrt{S \times P}} \right)^{2/3} \right)^\beta \quad \text{where, } A \text{ is wet cross section (m}^2\text{), } \beta = 0.6 \quad (4)$$

Erosion and deposition

Detachment modelling is developed applying a generalized erosion-deposition equation, as described by Morgan et al. (1998), identical to that in the EUROSEM model, whereas transport capacity concentration of the runoff is assumed to be a balance between erosion and deposition (D_p). Erosion is the sum of splash detachment by rain drops (D_s) and flow detachment by runoff (D_f). Total sediment in suspension (e) is then calculated as:

$$e = D_s + D_f - D_p \quad (5)$$

Splash detachment D_s (g s^{-1}) is simulated as a function of soil aggregate stability, rainfall kinetic energy, and depth of the surface water layer (Jetten, 2002).

Soil detachment by flow and deposition during flow, expressed in terms of settling velocity and transport capacity is described as:

$$D = Y \times (T_c - C) \times V_s \times w \times dx \quad (6)$$

where, D is D_f or D_p (in kg s^{-1}), Y a dimensionless efficiency factor, T_c the volumetric transport capacity of the flow (kg m^{-3}), C the sediment concentration in the flow (kg m^{-3}), V_s the settling velocity of the particles (m s^{-1}), w the width of flow (m), and dx pixel size. The Y coefficient depends on soil cohesion, and accounts for the fact that detachment can be limited by the cohesion of the soil material. Therefore, Y equals 1 for deposition, but is smaller than 1 for detachment.

The transport capacity of overland flow (in rills) is modelled as a function of unit stream power (Govers, 1990):

$$T_c = \delta_s \times c \times (\omega - \omega_c)^d \quad (7)$$

where, δ_s is the material density (2650 kg m^{-3}), ω the stream power (calculated as flow velocity \times energy slope), ω_c the critical stream power defined by Govers (1990) for a fairly wide range of materials to be approximately 0.4 cm s^{-1} , and c and d are empirical coefficients, depending on the median texture (D50) of the material. The value of c decreases with increasing D50, while the value of d increases with increasing D50.

To avoid calculation of an incorrect D_f or D_p , two checks are included in LISEM. The amount of erosion or deposition in a time step depends on the settling velocity V_s . First, within a time step that is too large, all sediment may have settled already before the end of the time step. Therefore, deposition can never exceed the amount of sediment in suspension. Second, in the case of detachment, the amount of detached soil can not exceed the remaining carrying capacity of the flow. The net sediment in suspension is transported between grid cells with the kinematic wave.

Channel detachment and deposition

Erosion and deposition in channels is treated in the same way as on land. There is no separate detachment equation for channels in LISEM, although the stream power concept was initially developed for rills. The same equations are used, but with the hydraulic radius, velocity, discharge, and transport capacity based on channel maps for cross-sectional shape, bed-gradient and Manning's n . Detachment efficiency is calculated with the channel cohesion.

Model calibration and validation

The LISEM model was run with 5 m grid size, as dictated by the available elevation data, for both MW and SW. A digital elevation map (DEM), as detailed as possible, was based on contour intervals of 5 m, the smallest interval available. LISEM version 2.35 was used, with a time step of 5 minutes and using the Green & Ampt infiltration equation. This time step is acceptable for the main watershed, but long for the sub-watershed. The same time step length was nevertheless applied for SW and MW to allow comparison of simulation results for both areas. In addition, in the study area, rainfall events can last for many hours, even days. Simulating such events with shorter time steps might result in very long calculation times and might cause problems with limited computer memory, especially for the MW.

In the calibration process, the main parameters used were saturated hydraulic conductivity, initial and saturated soil moisture content, Manning's n , soil cohesion, root cohesion, and median soil particle size. Multiplication factors were used to modify watershed characteristics, while maintaining the (measured) relative differences between different land use types. Calibration was based on the watershed outlet data. The simulated hydrograph and sedigraph were visually compared to the measured data, until no further improvement in simulated results could be discerned.

Erosion rates measured on the 1 × 2 m plots for cassava (*Manihot esculenta*) and eucalyptus (*Eucalyptus globulus*) were converted to Mg per hectare. The location of these plots was determined on the SW map. The calculated soil erosion values from these cells were compared to the measured plot data for each event.

Soil erosion occurred between April and October and was dependent on environmental conditions in the watershed, soil characteristics and crop cover at different development stages (Chapter 3). Therefore, LISEM was calibrated for different periods separately, using average calibration (Hessel et al., 2003b) for each period. These periods were: April, when soils in the hilly areas are dry and bare, and crops are very young at both the middle and low terraces; May, August and the first 20 days of September, when soil cover is high, and soil surfaces have minimum disturbance; June, July, the last 10 days of September and October, when many

activities, such as harvesting, ploughing, harrowing and weeding take place. LISEM was then validated by simulating the other events within these periods. Simulated soil erosion results for individual events were added, to yield annual erosion rates.

RESULTS

Input parameters

Saturated hydraulic conductivity (Ksat)

Ksat, representing infiltration capacity, is the most important parameter in simulating infiltration. However, Ksat varied strongly spatio-temporally for the different soil and land use types (Table 2). For most upland soils, Ksat was lowest late in the rainy season (from September to October), following a period with high rainfall and very little soil surface disturbance. Soil status such as sealing/crusting exerts a strong influence on infiltration capacity that is difficult to measure on samples taken from the field (Hessel et al., 2003b). In eucalyptus (Table 2), field observations showed severe surface cracking during the dry season (November to April), resulting in much faster water movement. During the rainy season, soil cracks disappeared due to swelling of the clay and infilling with fine soil particles eroding from the upper slope. Moreover, in this land use type, sealing and crusting aggravated with increasing rainfall. Cassava is planted in March/April, causing substantial soil surface disturbance during ploughing, hoeing and weeding. The soil surface was very soft at the beginning of the crop season, but was compacted through rainfall and became very firm in August and September. In November, the soil dried out, resulting in cracking again, due to both dry air and massive cassava roots. In rice fields, the soil is ploughed in January, in preparation for spring rice, following harvesting of the winter crops, and again in June in preparation for summer rice. Ksat was high during land preparation, because tillage

Table 2. Measured Ksat (cm d^{-1}) in eucalyptus, cassava and rice plots at different sampling dates.

Date	Eucalyptus	Cassava	Rice
16-January	957.6	421.2	514.9
17-April	1200.0	565.2	420.7
6-May	246.0	173.2	16.5
25-June	148.6	143.0	40.0
10-August	51.8	65.7	2.9
8-November	1178.1	357.6	37.8

activities make the soil more porous. After transplanting, soils were wetted/submerged by either rainfall or irrigation water. The soil surface was smoothed and became densely packed, especially after long rainy periods, so that Ksat was low until harvesting.

Initial soil moisture content (Theta-init)

Soil samples were collected before expected rainfall events (based on weather forecasts and local observations), for determination of soil moisture content. Most soils in the watershed are characterized by very low organic matter content and therefore low water holding capacity. The soil surface dried very rapidly after the end of rainfall and reached very low water content after one week. Nevertheless, during periods with frequent rainfall events, the soil surface could still be wet, even close to saturation, at the start of the next event.

Random Roughness (RR)

Random roughness strongly varies among land use types (Figure 3d), and mostly decreased when plant height increased. In the eucalyptus plot, RR was very stable throughout the study period. In the cassava plot, RR was high at planting time, and decreased with time, as the surface was smoothed due to rainfall detachment and sealing effects. In the rice plot, RR was very high in January, June and September following ploughing. RR declined very fast following harrowing and transplanting. The soil surface was completely flat about one month after transplanting. Some soils, in which upland crops such as peanut or beans were planted, were also intensively tilled in the harvest and land preparation periods.

Soil cohesion (Coh)

Soil cohesion is one of the indices of soil resistance, which represents the soil's ability to resist removal by flowing water. Soil cohesion is related to factors, such as soil type, organic matter content, and soil water content, while it varies for different land use types and in different years (Liu et al., 2003). Cropland exhibited the lowest cohesion values, and was thus the most erodible land use type, while wasteland and woodland showed the highest values. In the study area, soil strength was determined using penetrometer resistance (Herrick and Jones, 2002; IBSRAM, 1998).

Aggregate stability (Aggrstab)

Soil aggregate stability is closely related to anti-scourability and erodibility. It shows a close positive correlation with organic matter content, but varies for different soil types and land use types. Aggrstab of rice soils in the middle terraces was much lower

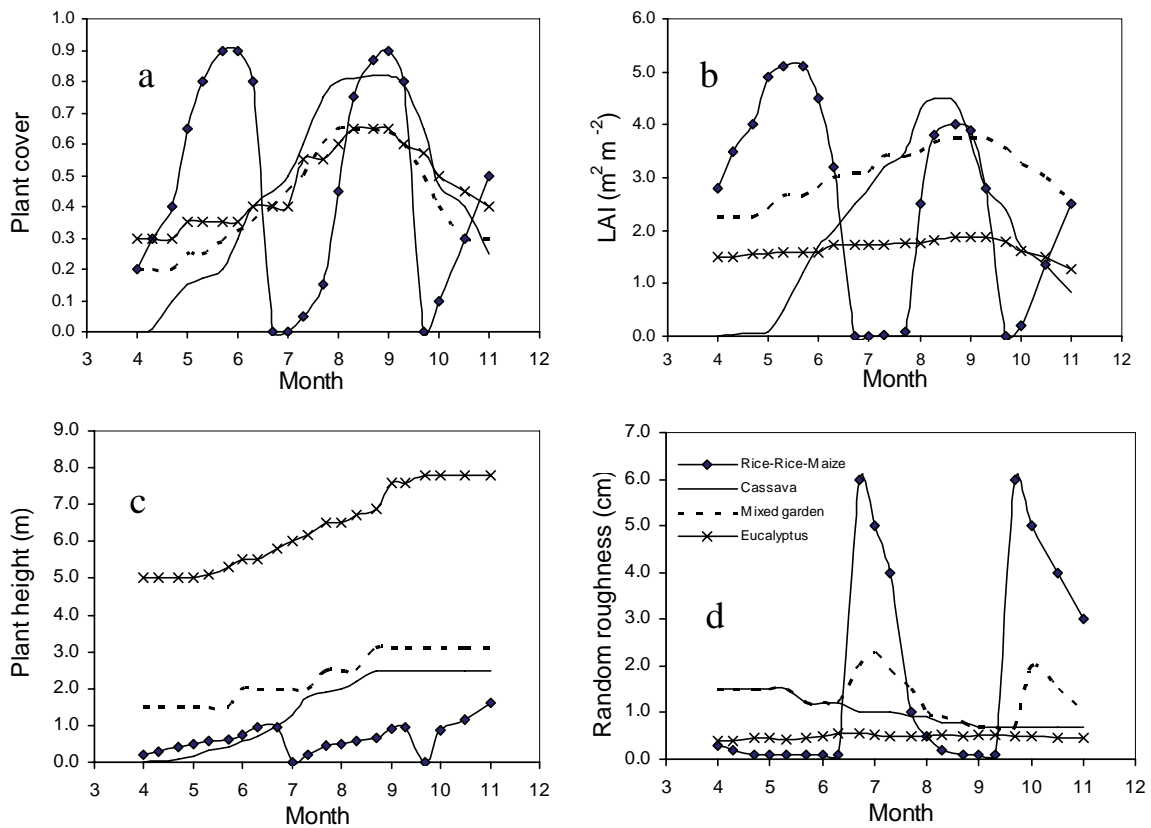


Figure 3. (a) Plant cover, (b) LAI, (c) plant height and (d) random roughness dynamics of rice-rice-maize, cassava, mixed gardens and eucalyptus systems.

than that in the low terraces, because of the higher organic matter and clay contents in the low terraces. On the slope faces, aggrstab was higher for the mixed gardens than for the cassava plots. Aggrstab was especially low on the upper hill and/or sandy soils which had very low organic matter contents.

Mean soil particle size (D50)

The median texture of the soil is used in simulating the settling velocity, i.e. determining sediment deposition in the runoff water. Measured D50 was 81, 85, 83, 76 and 85 μm for rice, upland crops, forest, mixed-garden and non-cultivated land, respectively.

Manning's n

Manning's n determines the velocity of flow, and therefore influences the timing of the runoff peak. It also influences the shape of the hydrograph and total discharge, because with increasing residence time of the water in the watershed, infiltration increases. In a small watershed on the Chinese Loess Plateau, Hessel et al. (2003a) obtained values of

Manning's n of 0.104 for cropland, 0.076 for fallow, 0.09 for orchard, 0.211 for woodland and 0.084 for wasteland. As no measurements were available from the study area, these values were adopted for the present simulations. Using this set of values for Manning's n , LISEM performed well for SW with simulated discharge comparable to measured discharge. However, simulated discharge at the MW outlet was much lower than measured. The most plausible reason is that infiltration in paddy fields is very low when they are waterlogged, but the values for Manning's n that were used might also not be representative for paddy fields, and were therefore changed during calibration.

Crop parameters

Other LISEM input parameters, such as soil cover, leaf area index (LAI), and plant height (Figure 3) affect rain interception, storage capacity of the plant canopy, and kinetic energy in splash erosion. Crop cover and LAI varied strongly for each crop between the dry and wet seasons, and between the early and mature crop stages. Plant height and LAI increased in the course of the growing seasons for the annual crops, but were zero in the transition periods. For eucalyptus, plant cover, LAI and height increased continuously over time. Cassava and mixed gardens were harvested in late November and December, therefore plant height slightly increased and the soil surface was undisturbed in the late rainy season.

Model calibration

Selection of Manning's n values and good hydrograph

Sensitivity analyses results showed that Ksat strongly influences peak discharge, and also discharge duration, as it determines how fast rain water infiltrates. Saturated soil moisture content determines water holding capacity of the soil, while initial soil moisture content determines soil storage capacity during infiltration, which influences the time needed to reach peak discharge. Manning's n value represents the surface resistance to flow, i.e. a high value implies that water flow is retarded by the resistances of the rough surfaces and their cover, resulting in later peak discharge and a prolonged falling limb (recession curve) of the hydrograph. However, when Manning's n is increased, peak discharge will become lower, as the increased residence time allows more time for infiltration. To correct for this effect, Ksat needs to be adjusted to retain a correct peak discharge with simulation of higher total discharge.

Simulation results for SW for event 170804 (Figure 4a) showed good agreement with measured peak discharge, time to the peak and shape of the hydrograph. Results for MW (Figure 4b) showed, however, that no calibration settings could be identified that resulted in satisfactory simulations of peak discharge, total discharge, and time to

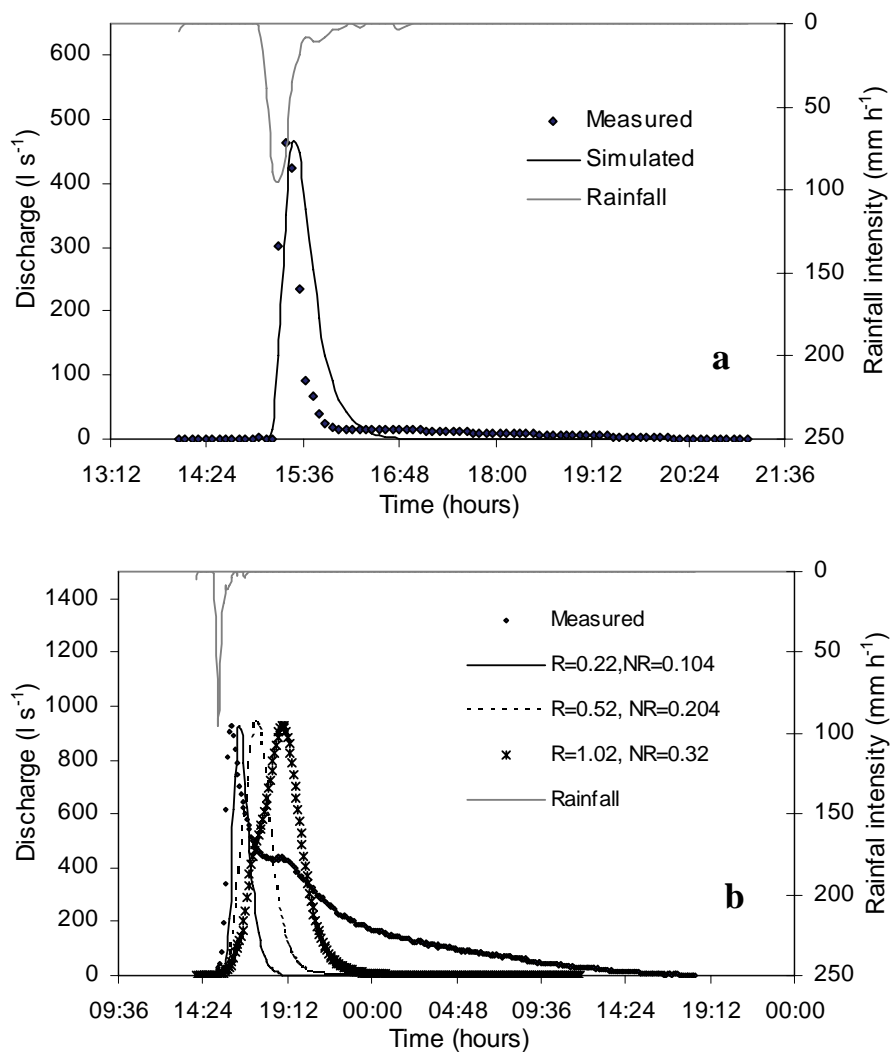


Figure 4. (a) Precipitation (starting at 14:02) and measured and simulated discharge for the event 170804 in the sub-watershed (SW), (b) precipitation, measured and simulated discharge with different values for Manning's n for rice (R) and non-rice (NR) crops (Manning's n values for the other land use types equal to those for SW) in the main watershed (MW).

the peak simultaneously. Different curves show calibration results for different sets of input parameters for rice and non-rice crops. As the SW simulation showed good results, only input data for crops were changed. Input data for, e.g. forest remained the same. The solid line hydrograph gives the best fit for peak time and peak runoff, but not for total discharge. The discrepancy between simulated and measured total discharge can be explained by the effect of paddy rice fields and agricultural crops on the terraces (Chapter 3). Paddy fields act as small reservoirs that store rain and runoff water from the upper terraces, which is gradually released to lower fields and drainage systems through passing the bunds and lateral percolation from higher to lower fields.

A higher total discharge can be generated by the model by increasing the flow resistance (Manning's n values) of paddy fields and terraces (Figure 4b), but this also results in a longer delay of the peak, so that K_{sat} and θ_{init} would have to be recalibrated to obtain good fits of time to peak and peak discharge. Initial soil moisture content could probably be adjusted to delay peak runoff to some extent. However, for MW, a satisfactory fit for both peak and total discharge could not be attained simultaneously. The solid line (Figure 4b), with the first values of Manning's n , was selected as most satisfactory, because the corresponding hydrograph best explained the real processes. This hydrograph represents fast overland flow, which is the process that LISEM simulates and therefore, discrepancies between this simulation and observed discharge may be explained by processes that are not simulated by LISEM, such as storage release from paddy fields.

For event 300804 (Figure 5), precipitation included three single events. In MW, only one hydrograph was generated, as runoff from the subsequent rainfall events was superimposed on runoff from the first event at the watershed outlet. In SW, runoff was generated only in the first event, because rainfall intensity exceeded infiltration rate in this event but not in the following ones.

Sediment concentration (SC)

Calibration of sediment concentration is complicated, as the quantity of sediment transported depends not only on flow conditions, but also on detachment and transport capacity. The most sensitive calibration parameter for SC is D50, although cohesion and aggregate stability also affect simulation results. LISEM is intended for D50-values between 25 and 300 μm (Jetten, 2002). To examine the effect of variations in D50 on simulated SC, sensitivity analyses were performed for a range in D50-values, including values below 25 and above 300. As can be seen in Figure 6a, the model performed satisfactorily over a very wide range of D50-values for SW (i.e. from 25 μm to very large) and within a very narrow range for MW (i.e. from 7 to 40 μm). Within these ranges, SC exponentially decreased with increasing D50. In SW, the reduction in SC was small when D50 exceeded 300. In MW, SC was almost zero at values of D50 exceeding 40 μm . However, model performance was not satisfactorily with D50-values below the ranges, as that resulted in delayed and late ending simulated sedigraphs.

Sensitivity was also analysed of transport capacity, calculated from Eqn 7 (Figure 7b) on D50, which showed that at a slope of 10 degree, transport capacity exponentially decreased with increasing D50 at a flow less than 1 m s^{-1} , whereas it was always high at flows exceeding 1 m s^{-1} . As stream power is the product of energy slope and flow velocity, transport capacity is higher in SW than in MW due to its steeper slopes.

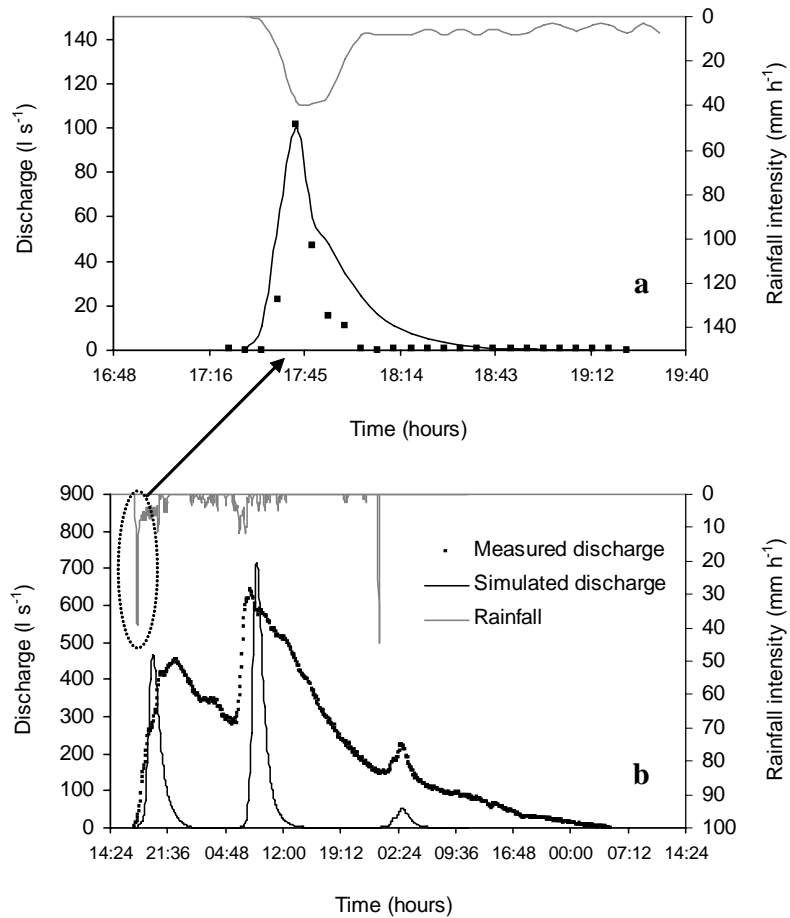


Figure 5. (a) Precipitation (starting at 17:23), measured and simulated discharge generated from the first single event in the sub-watershed; (b) precipitation, measured and simulated discharge for the event 300804 that included three single events in the main watershed.

Table 3. LISEM input data (plant and soil characteristics) for the 170804 event.

Parameter	Land use				
	Rice	Beans	Cassava	Mixed garden	Eucalyptus
Aggregate stability (drops)	12.00	12.00	12.00	10.00	14.50
Cohesion (kg cm ⁻²)	7.19	7.19	6.20	5.19	12.20
Random roughness (cm)	0.20	0.20	0.80	0.90	0.52
Manning's <i>n</i> (-)	0.22	0.22	0.10	0.09	0.21
Leaf Area Index (-)	3.80	3.00	4.50	3.60	1.90
Plant cover (fraction)	0.75	0.55	0.81	0.65	0.65
Plant height (m)	0.60	0.40	2.20	2.50	6.70
Ksat (cm hr ⁻¹)	0.89	3.19	3.20	0.89	3.92
Theta-init (cm ³ cm ⁻³)	0.41	0.31	0.37	0.37	0.34
D50 in MW(μm)	24.00	15.00	15.00	12.00	9.00
D50 in SW(μm)	-	425.00	425.00	405.00	380.00

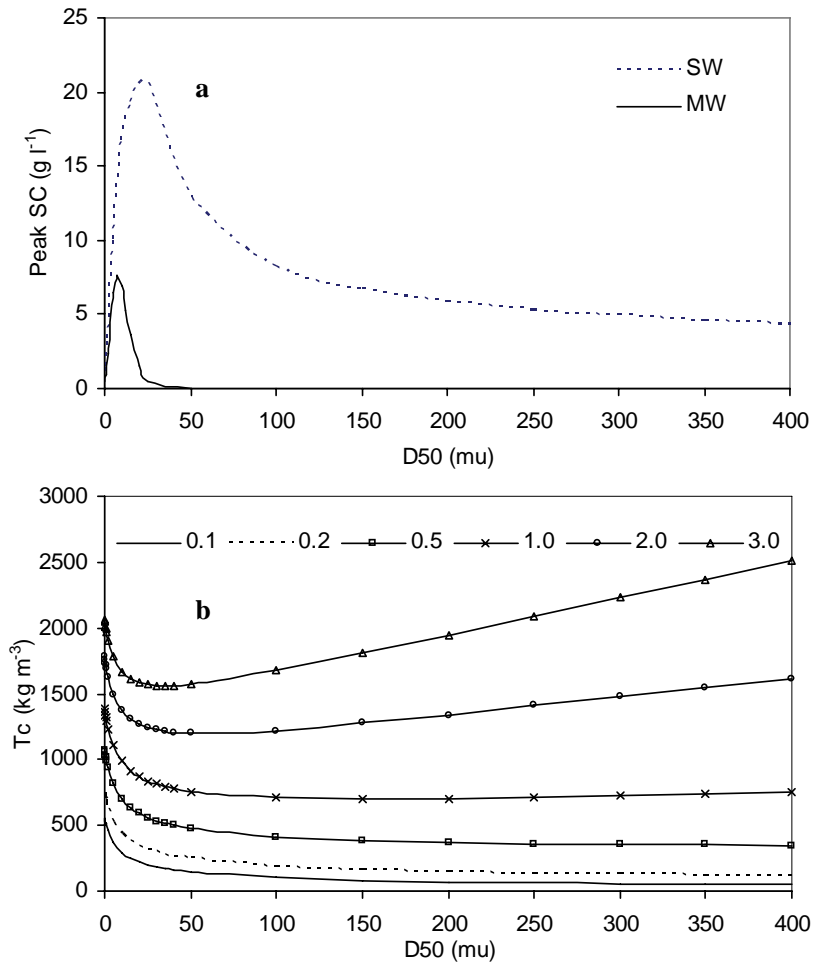


Figure 6. (a) Influence of different D50s on sediment concentration at the sub-watershed and main watershed outlets, and (b) influence of different D50s on transport capacity (Tc) at a slope of 10 degree and different flow velocities.

Because of differences in measured SC in SW and MW, and because of the differences in model response mentioned above, the calibrated values for D50 should be different for SW and MW (Table 3). As predicted SC for SW was generally too high, D50 was increased to increase settling velocity and decrease transport capacity and soil loss. In MW, however, simulated SC was generally too low, and D50 was therefore reduced to reduce settling velocity and increase transport capacity and soil loss. This resulted in large differences in calibrated D50 for SW and MW.

Figure 7 shows simulated SC dynamics that are representative for most calibration results. Hence, the shapes of the simulated sedigraphs are different from those of the measured sedigraphs, and simulated concentrations at the SW outlet are still higher than measured, while simulated SCs at the MW outlet are, in general, similar to the measured values, although performance strongly varies among events.

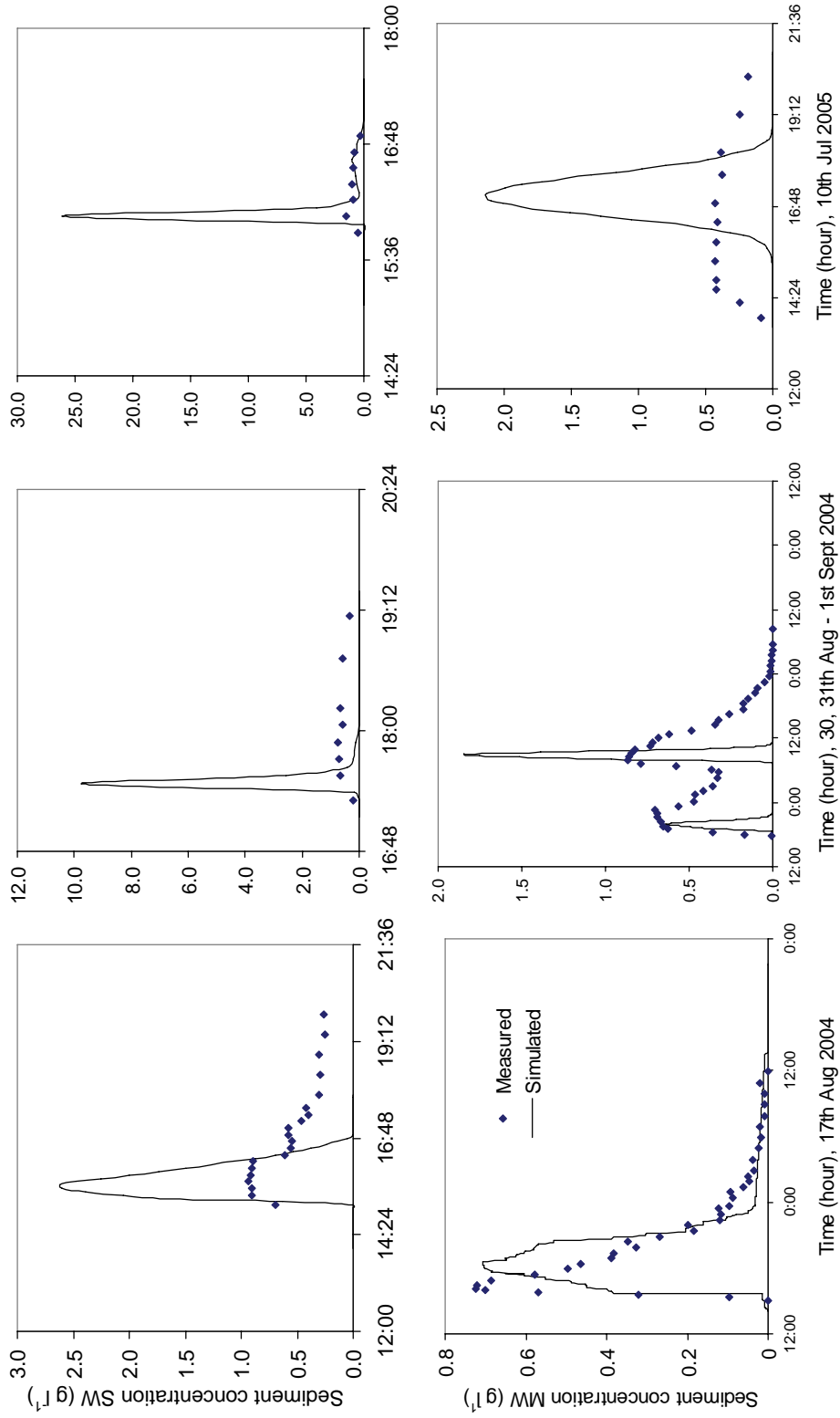


Figure 7. Measured and simulated sediment concentration for events of 170804, 300804, and 100705 at sub-watershed (first row) and main watershed (second row) outlet, (the events on the upper row are the same events as those on the lower row).

Model validation

LISEM was calibrated for five events, i.e. 050404, 170804, 260804, 100705 and 310705, and validated for four other events, i.e. 250804, 300804, 250705 and 040805 for both SW and MW (there was no measurement for SW of event 050404). For SW, simulated peak runoff time, peak runoff and total runoff (Table 4) agreed well with the measured values, but simulated soil loss was overestimated. All hydrographs and sedigraphs for SW were generated from single events, resulting in total runoff and soil loss also pertaining to single events, while in MW, the runoff water from event 260804 was superimposed on event 250804, resulting in a combined hydrograph and sedigraph with one value for total runoff and soil loss. For MW, simulated total discharge and soil loss were much lower than measured, even though peak time and peak runoff were simulated well (Figures 4b and 5b; Table 4). The events 300804 and 250705 each included two peaks of the hydrograph and sedigraph. Timing and magnitude of the second peaks were not only influenced by rainfall volume and intensity of the associated rainfall events, but also by the initial soil moisture content resulting from preceding events. Simulated peak time and peak runoff for SW were closer to the measured values than for MW, presumably because overland flow is the dominant runoff type in SW. Simulated SC was very high at the peak of event 100705, resulting in substantial overestimation of soil loss. At that moment, the soil was bare and the soil surface was strongly disturbed in the low terraces and paddy rice fields. Simulated soil loss was overestimated for SW associated with overestimation of SC (Figure 7) and underestimated for MW (Table 4), associated with underestimation of total runoff (Figures 4b and 5b).

Comparison of simulated cells and field plot measurement

The positions of the two measured plots (cassava and eucalyptus) were identified on the SW map. Simulated soil loss from the corresponding cells in SW was compared to measured soil loss of the two plots for 8 events (Table 5). However, the size of the plots (2 m²) was much smaller than pixel size (25 m²).

For all events (except event 310705), simulated soil losses for the plots were (much) higher than measured. Several reasons can be identified. Firstly, the soil surface in the eucalyptus plot was covered by a mixture of plant roots and mosses, protecting the soil surface from rain detachment, a mechanism not included in the model. Secondly, the slope in the DEM was (somewhat) steeper than the real slope in the field (Table 5). Thirdly, in the cassava plot, the soil was partly covered by dry litter, which reduced detachment by rain water. Fourthly, plots were probably too small to adequately measure rill erosion, which needs a certain slope length to fully develop. Consequently, comparison of model results with small-scale plot measurements is wrought

Table 4. Calibration and validation results, showing rainfall (mm), observed (Obs) and simulated (Sim) peak runoff time (Tpeak in minutes), peak discharge (Qpeak in $l\ s^{-1}$), total discharge (Qtot in m^3) and soil loss (kg) in SW and MW for the different events.

Event	Rainfall	Tpeak		Qpeak		Qtot		Soil loss	
		Obs	Sim	Obs	Sim	Obs	Sim	Obs	Sim
Sub-watershed									
Calibration									
170804	34.8	80.0	85.0	465.9	462.7	670.6	792.1	522.6	982.2
260804	10.2	25.0	20.0	22.5	21.4	35.1	40.8	17.6	50.3
100705	13.2	25.0	25.0	35.4	35.7	64.0	52.2	37.1	78.0
310705	24.3	30.0	20.0	177.6	150.1	130.3	285.9	121.1	286.4
Validation									
250804	31.0	50.0	45.0	19.3	21.1	13.4	23.0	5.2	12.2
300804	55.0	20.0	25.0	101.3	102.1	46.4	170.8	32.8	194.2
250705	11.9	25.0	25.0	250.4	257.6	136.8	424.3	107.6	340.5
040805	17.8	25.0	20.0	16.7	17.0	20.3	23.7	8.3	12.5
Main watershed									
Calibration									
050404	15.0	270.0	310.0	139.9	142.8	2000.0	1812.0	244.8	151.2
170804	34.8	115.0	145.0	927.9	930.8	16890.8	3722.4	5514.8	1816.0
260804*	10.2	60.0	90.0	253.5	258.4	14971.2	1812.2	1009.0	453.0
100705	13.2	70.0	90.0	103.8	105.9	1152.4	980.5	448.0	1072.6
310705	24.3	85.0	100.0	403.5	424.6	2603.5	2173.5	558.7	218.4
Validation									
300804	55.0	50.0	105.0	156.0	452.9				
		890.0**	940.0	646.0	713.6	46754.5	8078.4	19840.3	11827.2
250705	11.9	600.0	550.0	271.9	257.1				
		855.0**	130.0	296.3	262.7	6300.0	10856.0	3381.9	1686.5
040805	17.8	285.0	220.0	253.5	258.3	4828.7	1461.1	448.0	295.1

* Events 250804 and 260804 yielded a combined hydrograph and sedigraph for MW.

** Second peak (events 300804 and 250705 included two events with two peaks). There is no measurement for SW in event 050404.

with difficulties: differences in size, in slope, and in local conditions that cannot be captured by the model. There were probably also differences in erosion mechanism,

Table 5. Comparison of simulated soil loss (Mg ha^{-1}) in cells on the map and field plot measurements on cassava and eucalyptus for different events.

Event	Cassava		Eucalyptus	
	Measured	Simulated	Measured	Simulated
Slope (degree)	5.000	5.000*	5.000	6.000*
170804	0.238	0.848	0.211	0.795
250804	0.053	0.733	0.032	0.722
260804	0.046	0.225	0.032	0.222
300804	0.454	1.234	0.143	2.554
100705	0.207	0.862	0.150	0.849
250705	0.103	0.660	0.082	5.162
310705	0.194	0.142	0.001	2.761
040805	0.066	0.721	0.032	0.711

* Slope (degree) in DEM map.

with rill erosion being more important in the model than in the plot. However, analysis of the differences in simulated and observed results did lead to identification of possible reasons that could form the basis for improvement of the model to reduce the gap between the model and the real system.

Simulation of soil erosion for the MW

To simulate soil erosion for the two-year period, the model was parameterized on the basis of the calibrated values for the different time periods (Table 6).

Simulated discharge and soil loss were lower than measured. However, the results for 2004 were closer to measured than those for 2005, especially for soil loss. The results show that the higher rainfall and rainfall intensity, the larger the difference between simulated and measured values (e.g. August and September 2005). As shown in Figures 4 and 5, the main reason for the differences is underestimation of total discharge. The shape of both hydrographs shows discrepancies in hydrological processes, such as retardation of the flow in MW, associated with flow through terraces and storage in paddy fields. In the rainy season, the soil is wet and more water is released to the watershed outlet, while in the dry season, less water is released to the watershed outlet because the soil can store more water due to its low moisture content.

Sensitivity analysis

To examine the influence of throughflow and storage in different situations (time in the season and soil conditions), the model was calibrated for both, time to peak

Table 6. Selected calibrated parameters for continuous simulation.

Time period	Average calibrated parameters
April, November	050404
May, August	170804, 250804, 040805
June, July, September 20 th – October	100705, 250705, 310705
September 1 st to 19 th	300804

Table 7. Monthly measured and simulated (Sim.) discharge and soil loss for MW for the years 2004–05.

Month	2004				2005			
	Discharge (m ³ ha ⁻¹)		Soil loss (kg ha ⁻¹)		Discharge (m ³ ha ⁻¹)		Soil loss (kg ha ⁻¹)	
	Measured	Sim.	Measured	Sim.	Measured	Sim.	Measured	Sim.
1	0.0	0.0	0.0	0.0	0.0	0.0	0.0	0.0
2	0.0	0.0	0.0	0.0	0.0	0.0	0.0	0.0
3	0.0	0.0	0.0	0.0	0.0	0.0	0.0	0.0
4	8.0	7.3	1.0	0.6	63.0	12.7	27.0	5.4
5	5.0	5.3	0.6	0.9	0.0	0.0	0.0	0.0
6	6.5	6.9	3.3	2.3	68.0	13.8	38.8	7.8
7	70.3	34.1	22.4	14.9	132.0	49.2	39.2	21.3
8	350.8	101.0	122.1	80.7	367.0	97.9	232.7	4.7
9	97.6	20.2	13.4	3.4	2586.0	413.9	1296.0	168.6
10	0.0	0.0	0.0	0.0	108.0	36.4	88.2	37.1
11	0.0	0.0	0.0	0.0	0.0	0.0	0.0	0.0
12	0.0	0.0	0.0	0.0	0.0	0.0	0.0	0.0
Sum	538.2	174.8	162.8	102.8	3324.0	633.9	1721.9	244.9

discharge and total discharge (Figure 8). Three events were simulated; these events representative for the late dry season, with very dry soils (Figure 8a), the middle of the rainy season, with wet soils (Figure 8b) and the beginning of the dry season, with drying soils (Figure 8c). Input parameters were used for each period as shown in Table 6. In the first situation, the storage effect was strong, and release was negligible, because the soil was dry. The dominant process was throughflow, combined with limited release in the low paddy fields near the watershed outlet. In the second situation, when soil moisture was high, release was much higher. In the third situation, when wet soil was drying, water was also stored in the soil but the low fields were not submerged because of winter crops. As a result, the storage effect was smaller than in

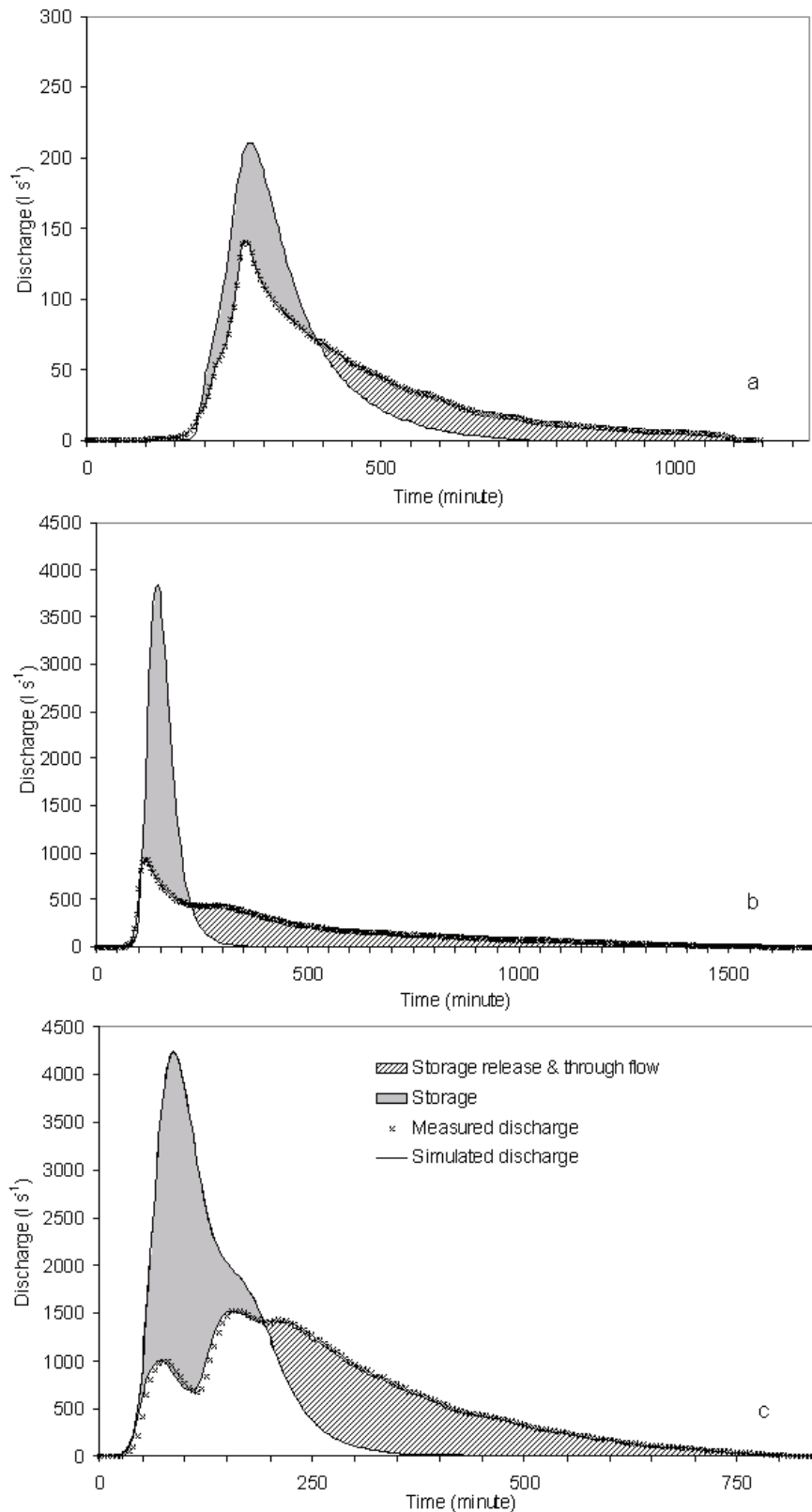


Figure 8. Storage (gray polygon), storage release and throughflow (dashed polygon) as delayed discharge in the measured hydrograph for MW for events (a) 050404 (late dry season, (b) 170804, middle of the rainy season and (c) 041005, beginning of the dry season. The gray and dashed polygons have the same area.

the first situation, but stronger than in the second. These effects are also expressed by the ratio of simulated (see Section Model calibration) and measured total discharge that was 0.91, 0.22 and 0.34, respectively for the events 050404, 170804 and 041005 (see details in Figure 8).

To improve the simulation of total discharge, values of Manning's n can be increased, and values of Ksat can be decreased. However, such adjustments lead to either higher predicted peak runoff (with higher sediment concentrations) or a delay in peak discharge and consequently modified total discharge.

DISCUSSION

Soil surface and infiltration

Many calibration studies and sensitivity analyses of LISEM (De Roo and Jetten, 1999; De Roo et al., 1996b; Hessel et al., 2003b; Jetten et al., 2003) have shown that saturated conductivity is the most sensitive variable, through its effect on infiltration rate and therefore on runoff volume. In the study area, Ksat was spatio-temporally variable, i.e. for a given soil type, it can spatially vary strongly depending on soil surface conditions, organic matter content and land use type and management, especially for orchards, mixed gardens and rice. For eucalyptus and cassava, the temporal variation in Ksat was large, as illustrated in Table 2. In the late rainy season, the soil surfaces generally settled, under the impact of cumulative rainfall and the absence of soil disturbance. This reduced pore space, and thus Ksat, resulting in high runoff coefficients in August and September.

Hydrology

The poor performance of LISEM for MW is due largely to the effects of storage and release of water from paddy fields, and to throughflow through the terraces, that occurred during most events. Water was transported from the hills, through the upper terraces and paddy fields, to the lower ones through the sandy sub-soils. In MW, in many paddy fields, bunds, varying in height from 0.05 to 0.2 m, were constructed by farmers to store water for land preparation and rice growth. Paddy fields and terraces cover about 35% of MW, and thus have a strong influence on catchment hydrology. All runoff from uphill has to pass through the rice fields before reaching the watershed outlet (except for some sub-watersheds that have direct flow to the drainage system). Rain water first ponds in the fields; and starts contributing to overland flow only when the water level exceeds the height of the bunds. Paddy fields will be filled faster when runoff from uphill is added to rainfall. Hence, runoff at the MW outlet will be lower than expected (compared to that at SW outlet) if rice fields have no or a low level of

standing water, and higher if rice fields are full of water. Moreover, water stored in the fields is continuously released through throughflow and seepage, through and below the bunds (Bouman et al., 1994; Wopereis et al., 1994; Huang et al., 2003). The rates of these flows depend on the altitude difference between fields, conductivity of the soil and firmness of the bunds, and on the activity of animals, such as field crabs, mice, and rats. Especially in fields with permeable sandy soils, seepage can be high (Bouman et al., 1994). The lower flow rates of throughflow and release flow, compared to direct runoff, cause delayed discharge at the MW outlet, leading to lower peak discharge and longer falling limbs of hydrographs, but not to lower total discharge. Throughflow on terraces was presumably relatively stable in most events, because the configuration of the terraces is not changing over time, while storage and release vary among events, in dependence of actual water storage capacity of the paddy fields (i.e. the difference of bund height and standing water depth), soil moisture content, and canopy interception. For reliable simulation of runoff and soil erosion for this type of watershed, the model should be extended with throughflow and storage sub-models.

Soil loss

The D50s used for SW were larger than those used for MW (Table 3), despite the fact that soil types are quite similar. The reason is that in SW soil erosion originates from a small area, with short flow routes and few opportunities for deposition, while in MW erosion originates from a much larger area, with a more complex geometry, comprising concave slopes and road systems, where the sediment can be trapped. As the larger particles deposit first, it can be expected that D50 of the sediment carried in suspension is, in reality, also larger in SW than in MW.

Simulated SC in the runoff depends on detachment, deposition and transport capacity (T_c). T_c strongly depends on stream power, which is computed from flow velocity and slope, and particle size (Eqn 7). At low stream power, T_c is low and decreases with increasing D50, because in Eqn 7 the effect of decreasing c outweighs the effect of increasing d . However, if stream power is high, the effect of increasing d starts to outweigh the effect of decreasing c for larger D50s. In the study area, stream power is high in SW because of steep slopes, and much lower in MW because of very gentle slopes in the terraces. As a result, transport capacity is higher in SW, leading to higher SC at the SW outlet. This difference in stream power might also explain the observed difference between D50 and T_c for SW and MW (Figure 6).

Thus, both D50 and T_c can be expected to be different for SW and MW, but the exact effect on simulated soil loss is difficult to determine, as in the simulation, flow conditions and transport capacity will vary, both in time and among pixels. Simulated concentrations at the SW outlet were higher than measured for most events, despite the

very large D50s that were used, while simulated SCs at the MW outlet were, in general, of the correct order of magnitude, when very small D50s were used (Figure 7). Thus, it was not possible to simulate correct SCs for SW by calibrating D50 within plausible limits. For MW, in contrast, the values used for D50 were low, but given the large opportunities for sedimentation in e.g. the paddies, these values do not seem unrealistic.

This result seems surprising, as hydrology of SW was simulated more accurately than that of MW. However, overprediction of soil loss has also been reported in earlier applications of LISEM (De Roo and Jetten, 1999; Stolte et al., 2003). In those studies also sediment concentrations were over-predicted. The present version of the model has been improved and more sub-models have been added. Nevertheless, in recent studies (i.e. Hessel et al., 2005) soil loss calculations appeared still inaccurate and need to be improved. Overestimation of soil loss in SW could be associated with overestimated detachment and underestimated deposition.

CONCLUSIONS

In this study, the LISEM model was applied to simulate soil erosion for a sub-watershed and the main watershed in Quan Dinh village in Vietnam. The model was calibrated for 5 events and validated for another 4 events. The model satisfactorily predicted peak runoff time, peak runoff and total runoff in the sub-watershed, which consist of sloping land. For the main watershed, that included low terraces and paddy fields, simulated total discharge was underestimated, although simulated peak runoff time and peak runoff were satisfactorily simulated. The shorter duration and lower falling limb of the simulated hydrograph indicate that delayed flow as a result of throughflow and storage release, is responsible. These processes are not taken into account in the current version of LISEM.

There was an opposite trend in simulated soil loss in the upland sub-watershed and the main watershed in which paddy rice is present. Soil loss was overestimated for the sub-watershed, due to high sediment concentrations in the runoff water, resulting from strong detachment and transport processes, and was underestimated for the main watershed, due to underestimation of discharge, which was generated from the low terraces and the flat paddy fields.

Despite problems that were identified, LISEM can be used to predict and compare soil erosion rates for different periods of the year, and to analyse spatio-temporal variability of soil erosion that results from changing land use and changing crop calendars. Thus, LISEM can support identification of the best land use pattern for soil erosion control.

CHAPTER 5

Nitrogen leaching in intensive cropping systems in Tam Duong district, Red River Delta of Vietnam *

V.T. Mai^{1,4}, H. Van Keulen^{1,3}, R.P. Roetter², H.H. Bui⁴, V.B. Nguyen⁵

- ¹ Plant Production Systems Group, Wageningen University, P.O. Box 430, 6700 AK Wageningen, The Netherlands
- ² Soil Science Centre, Alterra Green World Research, Wageningen University and Research centre, P.O. Box 47, 6700 AA Wageningen, The Netherlands
- ³ Plant Research International, Wageningen University and Research centre, P.O. Box 16, 6700 AA Wageningen, The Netherlands
- ⁴ National Institute for Soils and Fertilizers (NISF), Dong Ngac, Tu Liem, Hanoi, Vietnam
- ⁵ Vietnam Academy of Agricultural Science, Thanh Tri, Thuong Tin, Hanoi, Vietnam

Abstract

An experiment was conducted in the Red River Delta of Vietnam, on five different crops of rose, daisy, cabbage, chili and a rice – rice – maize rotation during 2004 and 2005. Core soil samples were taken periodically in 20 cm increments to a depth of 1 m and analysed for nitrate-nitrogen and ammonium-nitrogen. The results indicate appreciable leaching losses in high rainfall and irrigation conditions, especially when fertilizer application is not well synchronized with the dynamics of crop nitrogen demand. Highest annual leaching losses were recorded in flowers with 185–190 mm of percolation and 173–193 kg N ha⁻¹, followed by vegetable (cabbage and chili) with 120–122 mm of percolation and 112–115 kg N ha⁻¹, while it was lowest in rice with about 50 kg N ha⁻¹. It was shown that a relatively simple combined water and nitrogen balance model is a useful tool for quantifying the risks of nitrogen leaching and can be applied with confidence to explore the scope for improvements in soil and crop management.

Keywords: Horticulture, flowers, vegetables, rice, nitrate, nitrogen losses, modelling

* This chapter has been submitted to Nutrient Cycling in Agroecosystems.

INTRODUCTION

Nutrient losses and nutrient efficiencies are important issues in agriculture in many regions of the world (Janssen, 1998; Smaling et al., 1999; Carberry et al., 2002; Mosier, 2002; Sheldrick et al., 2002). Especially the fate of nitrogen has received extensive attention, because of its crucial role in crop production (potentials) and its possible negative environmental impacts (Mosier et al., 2004). Plant recovery efficiencies of fertilizer N vary strongly, depending on cropping system, environmental conditions and fertilizer management (Neeteson, 1995; Janssen, 1998). In rice-based systems, values are on average 30–40% (Dobermann et al., 2002). One of the loss pathways in the nitrogen cycle is nitrate leaching from the soil. The magnitude of leaching also strongly varies, depending on such factors as soil type, cropping system, weather conditions and fertilizer regime (Di and Cameron, 2002; Hauggaard-Nielsen et al., 2003; Verloop et al., 2006). High leaching losses from intensive agriculture may cause high nitrate concentrations in groundwater, which potentially carries health risks. Tripathi et al. (1997) calculated nitrogen leaching losses from heavily fertilized rice-vegetable systems in the range of 34 to 549 kg ha⁻¹, with the largest losses from rice-sweet pepper and rice-tomato rotations. Similar results were recorded in China, with leaching losses roughly between 30 and 450 kg ha⁻¹, at annual fertilizer inputs of 350 kg N ha⁻¹ for double rice and 920 kg ha⁻¹ in horticulture (Fang et al., 2005). Comparing nitrate leaching from different land use domains in Japan, Babiker et al. (2004) established the highest mean nitrate concentrations in groundwater in vegetable fields with 57.1 mg l⁻¹, followed by urban areas with 30.8 and paddy fields with 24.2.

Measuring nitrate leaching from agricultural non-point sources is complicated and requires extensive field and laboratory measurements. Five methods are potentially suitable, i.e. porous ceramic cups, pan/trench samplers, lysimeters, large-scale drainage collection and soil coring (Addiscott, 1990), each with its typical advantages and difficulties in terms of implementation, costs, reproducibility, relevance, effect, and interpretability. N leaching can also be calculated in many ways, e.g. Tripathi et al. (1997) calculated total apparent N losses as the balance of the sum of available soil N before cropping, fertilizer N applied and N addition from weed residues and the sum of N removed and residual N in the soil after crop harvest. Liu et al. (2003) calculated nitrate-nitrogen loss on the basis of measured nitrate-nitrogen concentrations in the course of time at different soil depths, and Chikowo et al. (2004) used differences in mineral N concentration at different sampling dates to calculate N leaching per soil layer and for the whole soil profile. Increasingly, models are being used to simulate nitrogen dynamics and leaching from the soil profile, based on water balance models (Addiscott and Whitmore, 1987; Jemison et al., 1994; Ersahin and Rustu Karaman, 2001; Helwig et al., 2002). Such models simulate both, water and nitrogen balances

with short time intervals and take into account other processes important in the nitrogen cycle, such as nitrogen mineralization, crop uptake, nitrogen volatilization and denitrification to calculate nitrogen losses, as well as potential pollution to groundwater (Chowdary et al., 2004).

Tam Duong district, located upstream in the Red River Delta of northern Vietnam (21°26' N, 105°36' E), is characterized in recent years by strong population and economic growth. Population increased by 9% in the period 1990–95, 5% in 1995–2000 and 3% in 2000–03. Population increase in the rural areas was about 1.5% per year, while urban growth was very fast, i.e. from 5 to 7% per year. Thus, demand for food in the urban sector continuously increases, both in terms of quantity and in number of commodities. One of the fast growing commodities is vegetables, of which cultivated area and yield have been increasing, e.g. from 300 ha and 13.7 Mg ha⁻¹ in 1990, via 499 and 14.0 in 1995 to 719 ha and 16.2 Mg ha⁻¹ in 2003. Farmers' income from vegetables is much higher than that from other commodities (IRMLA, 2005). The increase in cultivated area and in crop yield is associated with a dramatic increase in the use of agro-chemicals, such as fertilizers and pesticides (Van Wijk et al., 2006). The consequences are declining fertilizer use efficiency and increasing environmental impact, such as pollution of soil and water. In this study, nitrate and ammonium dynamics in the soil profile were monitored in intensive agricultural systems with the objective to assess nitrogen losses and environmental effects.

MATERIALS AND METHODS

Study area

The study was conducted in Van Hoi commune, a flat area in Tam Duong district, about 70 km north-west of Hanoi, Vietnam. The soil is a sandy loam, derived from old alluvial deposits of the Red River system. It is classified as an Albi dystric plinthosol (FAO/UNESCO, 1974; FAO, 1976) and has been used traditionally for rice cultivation, but is considered suitable for vegetables and horticulture (Chi and Bo, 2002). The soil profile is strongly developed; clay content sharply increases with depth, while organic carbon and plant nutrient contents decrease (Table 1).

Experimental setup

The experiment included five cropping systems:

- Long-term rose cultivation in its third and fourth year,
- Daisy flowers, grown annually from September to May,
- Six successive cabbage crops per year,
- Chilis (hot pepper), grown annually from September to August,

- Spring rice–summer rice–winter maize, the traditional rotation in the area.

Soils were sampled six times annually, based on the growing periods of the six cabbage crops, i.e. in 2004 on March 21st, May 9th, July 6th, September 18th, November 13th; and in 2005 on January 11th, March 26th, May 9th, July 6th, September 18th, November 28th, and January 19th 2006. Rainfall, irrigation and nitrogen fertilizer applied to each crop in each period are shown in Figure 1.

Field sampling, soil and data analysis

Soils were sampled with augers in 20-cm increments to a depth of 1 m. In each field, soil was sampled in triplicate and the samples bulked for each depth. Sub-samples were taken to the laboratory in polyethylene bags and stored at 4 °C prior to extraction, usually within 2 days of collection. Above-ground plant samples were taken at the same dates, for determination of nitrogen content.

Twenty grams of field-moist soil were extracted in 50 ml 0.5 M KCl via shaking on a rotary shaker for one hour, followed by filtering through Whatman no. 1 filter paper into polyethylene containers. Nitrate nitrogen (NO₃-N) and ammonium nitrogen (NH₄-N) in KCl extracts were determined by the steam distillation method. Another sub-sample of soil was dried at 105 °C for 24 h to determine moisture content. Plant samples were oven-dried (65 °C) for 12 hours and weighed. N was determined by the micro-Kjeldahl method (Bremner, 1996).

Data of NO₃-N and NH₄-N in all systems from each soil layer were analysed using one-way ANOVA analysis of variance, using the Genstat statistical package (Lawes Agricultural Trust, 2003). Total mineral nitrogen (N_{min}) in each soil layer was calculated as the sum of NO₃-N and NH₄-N.

Table 1. Soil properties at the experimental site.

Soil depth	Particle size distribution (%)			Bulk density (g cm ⁻³)	OC* (%)	N total (%)	P total (% P ₂ O ₅)	K total (% K ₂ O)
	Clay	Silt	Sand					
0–20	8.3	20.9	70.8	1.31	1.5	0.09	0.130	0.22
20–40	16.9	13.6	69.5	1.29	1.8	0.05	0.045	0.15
40–60	24.4	11.8	63.8	1.29	1.0	0.04	0.018	0.37
60–80	34.8	11.9	53.3	1.25	0.6	0.05	0.017	0.63
80–100	39.9	9.0	51.1	1.25	0.4	0.05	0.018	0.97

*Organic Carbon.

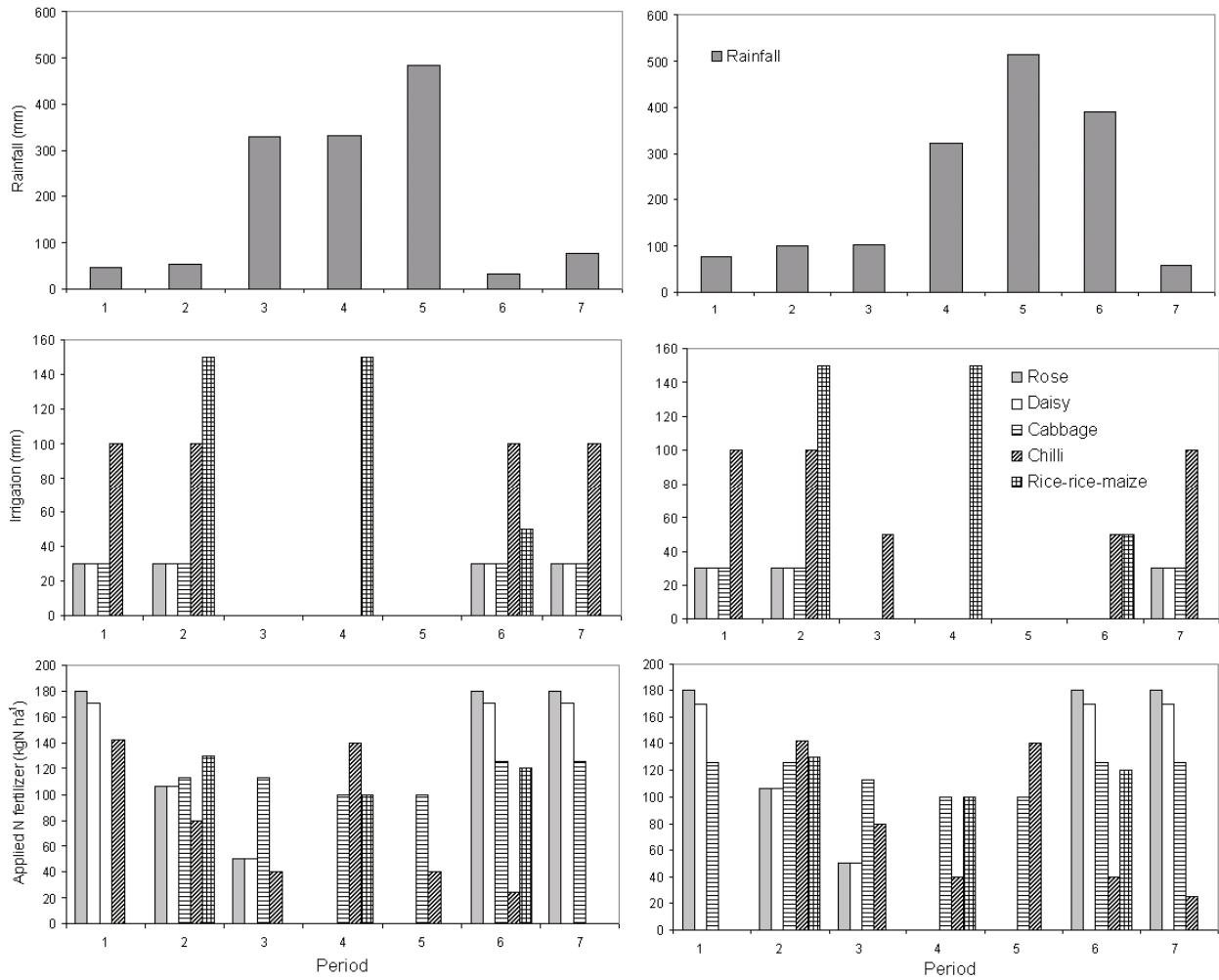


Figure 1. Rainfall (mm), irrigation (mm) and applied N fertilizer (kg N ha^{-1}) in different periods ending on Jan 1st, Mar 21st, May 9th, Jul 7th, Sept 18th, Nov 13th in 2004 (left) and Jan 11st, Mar 26th, May 05th, Jul 6th, Sept 18th, Nov 28th in 2005 and Jan 19th 2006 (right). Period 1 in 2005 is identical to period 7 in 2004

Nitrogen transport model

Water balance

Nmin dynamics were simulated based on a water balance model with daily time step, for a 1 m soil profile with compartments of 0.2 m. Soil water (SW) in each soil layer at time t was calculated as the sum of soil water in that layer at time $t-1$ and net flow (NFL) into the layer at time t . Net flow into the i^{th} soil layer was calculated as the balance of inflow (FL), outflow (i.e. inflow into the $i+1^{\text{th}}$ soil layer) and evapotranspiration from the i^{th} layer.

$$SW_{i,t} = SW_{i,t-1} + NFL_{i,t} \times \Delta t \quad (1)$$

$$NFL_i = FL_i - FL_{i+1} - ET_i \quad (2)$$

For the surface layer, inflow equals:

$$FL_1 = R + IRR - Q \quad (3)$$

where, SW_i is soil water content in the i^{th} layer (mm), R rainfall ($mm\ d^{-1}$), IRR irrigation ($mm\ d^{-1}$), ET_i contribution of i^{th} layer to evapo-transpiration ($mm\ d^{-1}$), FL_i , FL_{i+1} flow over upper and lower boundary of layer i ($mm\ d^{-1}$), respectively, Δt the time step of the model (d) and Q surface runoff ($mm\ d^{-1}$).

Total ET was calculated using the Penman-Monteith method (Allen et al., 1998). Hasegawa and Kasubuchi (1993) showed that water extraction by roots varies in time with variations in root distribution in the soil profile. Models of water extraction by roots have been reviewed by Molz (1981), including the empirical model proposed by Molz and Remson (1970):

$$s = \frac{-1.6 \times T}{v^2} \times z + \frac{1.8 \times T}{v} \quad (4)$$

where, s is root water extraction, T transpiration rate, z soil layer depth and v the depth of the root zone. If the root zone is divided in four layers of equal thickness, this equation indicates that water extracted from the successive layers is 40, 30, 20, and 10%, respectively, of the transpiration rate (Hasegawa and Kasubuchi, 1993).

Following this principle, in our model, total root water extraction was partitioned in the proportions 0.4, 0.3, 0.2, and 0.1 over four soil layers, each representing a quarter of the total rooting depth.

Flow into the i^{th} soil layer, either saturated or unsaturated, depending on soil moisture content (Radcliffe et al., 1998), is described by Darcy's law:

$$FL_i = -k_i \frac{dh_i}{dz} \quad (5)$$

$$k_i = ks_i \text{ if } \theta_i = \theta_{s_i} \quad (6)$$

$$k_i = kr_i \times ks_i \text{ if } \theta_i < \theta_{s_i} \quad (7)$$

$$kr_i = \left(\frac{\theta_i - \theta_{r_i}}{\theta_{s_i} - \theta_{r_i}} \right)^\lambda \quad (\text{Averjanov, 1950; Brutsaert, 1966}) \quad (8)$$

where, FL_i is water flow into soil layer i ($mm\ d^{-1}$), k_i soil hydraulic conductivity of soil layer i ($mm\ d^{-1}$), dh_i/dz the moisture potential gradient between layers i and $i-1$, kr_i the proportionality factor for actual soil hydraulic conductivity ($0 \leq kr_i \leq 1$), θ_i , θ_{r_i} , θ_{s_i} are water contents in the i^{th} layer to which kr_i applies, residual water content and water content at saturation, respectively ($cm^3\ cm^{-3}$); θ_r is defined as the water content in the soil that does not participate in flow (immobile water). In practice, θ_r corresponds to the content at which the moisture capacity of the soil approaches zero ($d\theta/dh \rightarrow 0$)

(Zaradny, 1993) and it varies from 0.005 for light-textured soils to 0.1 for heavy-textured soils (Lal and Shukla, 2004); λ is an empirical coefficient of 3.5 (Averjanov, 1950) or $2 \leq \lambda \leq 5$ (Brutsaert, 1966).

In this flat area, individual fields are surrounded by bunds, so that surface runoff only occurs when rainfall exceeds bund height (Chowdary et al., 2004). Surface runoff is estimated by:

$$Q = \text{Max}(0, R + \text{IRR} + (\text{SW}_1 - \text{POR}_1 - \text{BH})/\Delta t) \quad (9)$$

where, SW_1 , POR_1 are soil water content (mm) and saturated soil water content in the first layer; BH is bund height (mm), in this study set to 50 mm for flowers and cabbage and 100 mm for chili and rice, the crops for which rain water is stored in the field.

Nitrogen balance

Nitrogen uptake by the crop is calculated as the product of transpired water volume and mineral nitrogen concentration in each soil layer. Transpiration (T_i) is calculated from potential evapo-transpiration (ET_i), taking into account current leaf area index (LAI). The partitioning between T_i and soil evaporation (E) was derived from WOFOST, a crop growth model (Boogaard et al., 1998) that was calibrated for rice and maize for the study area (Mai et al., 2007). Simulated T_i is a very small fraction of ET_i at the onset of crop growth and increases with increasing LAI, to account almost completely for ET at the time of maximum LAI. Based on these results, an equation was derived to calculate T_i from ET_i :

$$T_i = \frac{\min(t, \text{Du_LAI}_{\max})}{\text{Du_LAI}_{\max}} ET_i \quad (10)$$

where, t is time after sowing (d), Du_LAI_{\max} the duration (d) of the period from sowing till maximum LAI (Table 2), and ET_i is ET from the i^{th} soil compartment.

The dominant influences on movement of Nmin in the soil are those due to mass transport, uptake by the plants and microbial biomass and gaseous losses; redistribution in the soil profile by diffusion is ignored as is adsorption on negatively charged soil particles. Only downward transport of nitrogen is considered on the basis of the “perfect mixing”-principle, as described by Van Keulen and Seligman (1987):

$$S_n = S_{ni} - S_{no} \quad (11)$$

$$S_{ni} = N_{i-1} \times \text{FL}_i \quad (12)$$

$$S_{no} = N_i \times \text{FL}_{i+1} \quad (13)$$

where, S_n is rate of change in nitrogen content in i^{th} layer due to transport ($\text{kg ha}^{-1} \text{d}^{-1}$), S_{ni} rate of inflow of nitrogen in i^{th} layer ($\text{kg ha}^{-1} \text{d}^{-1}$), S_{no} rate of flow of nitrogen out of

Table 2. Cropping calendars (sowing, maximum LAI and harvest dates) for different crops.

Crop	Date		
	Sowing	LAI _{max}	Harvest
Rose	Sept 15 ^{th*}	Oct 30 th	After Oct 30 th
Daisy	Sept 15 th	Nov 15 th	May 15 th
Cabbage**	Feb 5 th	March 15 th	March 21 st
Chili	Sept 1 st	Dec 1 st	Jul 15 th
Spring rice	Feb 5 th	May 5 th	Jun 5 th
Summer rice	Jun 25 th	Aug 19 th	Sept 19 th
Winter maize	Sept 20 th	Dec 5 th	Jan 10 th

* For rose, sowing date is starting time for fertilizer application;

** For cabbage, planting is repeated after harvesting of the preceding crop.

i^{th} layer ($\text{kg ha}^{-1} \text{d}^{-1}$), FL_i , FL_{i+1} rate of water flow into the appropriate soil layer (mm d^{-1}), N_i , N_{i+1} the nitrogen concentrations in the appropriate soil layer ($\text{kg ha}^{-1} \text{mm}^{-1}$).

All nitrogen present in a soil layer and that flowing into it are mixed with all the moisture associated with it, to calculate an average nitrogen concentration. For the present purpose, this description adequately represents the transport dynamics of nitrogen in the soil. Diffusion along developing concentration gradients, which will generally result in downward movement, particularly in the case of fertilizer application, will be partly compensated by upward movement of nitrogen with moisture evaporating at the soil surface. The distribution of nitrogen in the soil profile calculated in this way, will be different from that achieved with detailed process models, but that will hardly affect its availability to the crop that has access to mineral nitrogen over the whole rooted depth. Upward movement of nitrate from below the rooted depth to the root zone is unlikely to contribute substantially to plant-available nitrogen and can be ignored.

The total mineral nitrogen balance for a soil layer is now described by:

$$C_{ni} = S_n + R_{nfi} + R_{nsi} - T_i \times N_i - N_{di} - N_{gas} \quad (14)$$

where,

C_{ni} rate of change in nitrogen in the i^{th} layer ($\text{kg ha}^{-1} \text{d}^{-1}$);

R_{nfi} , R_{nsi} rate of release of mineral nitrogen during decomposition of fresh and stable organic material, respectively, in the i^{th} soil layer ($\text{kg ha}^{-1} \text{d}^{-1}$);

T_i rate of moisture uptake (transpiration) from i^{th} soil layer (mm d^{-1});

N_{di} rate of nitrogen uptake by diffusion from the i^{th} layer ($\text{kg ha}^{-1} \text{d}^{-1}$);

N_{gas} rate of nitrogen loss to the air by volatilization and denitrification ($\text{kg ha}^{-1} \text{d}^{-1}$).

Uptake via diffusion, which strongly depends on conditions such as water flow and N-concentration, is assumed to contribute 20% to total uptake (Miller and Gardiner, 2001).

In the cropping systems considered here, green manure and straw were not applied, while the contribution of residual root biomass was ignored, therefore, supply of fresh organic material was assumed to be zero. Stable organic material was applied in the form of FYM that also contains mineral nitrogen, which was directly added to the mineral nitrogen pool, while the organic component was assumed to gradually decompose. Decomposition is assumed to take place in the upper soil layer, and is simulated according to Yang's model (Yang, 1996):

$$R_{\text{nsi}} = R_9 \times f \times (f \times t)^{-S} \quad (15)$$

$$Y_t = Y_0 \times e^{-R_9 \times (f \times t)^{1-S}} \quad (16)$$

$$f = 2^{(T-9)/9} \quad \text{for } 9 < T \leq 27 \text{ }^\circ\text{C} \quad (17)$$

where, R_9 is defined as the initial relative mineralization rate (d^{-1}) at a temperature (T) of $9 \text{ }^\circ\text{C}$, set to 0.82 for FYM (Yang, 1996), f temperature correction factor, S rate of ageing or decrease in decomposability of the substrate, set to 0.49 for FYM (Yang, 1996). Y_0 and Y_t are quantities of substrate at times zero and t , respectively (mg kg^{-1}). For the roses and daisy, 'manure' consisted of slurry, a mixture of faeces and urine, nitrogen-rich materials such as bean residues and food processing wastes. Organic carbon content (%), total nitrogen content (%) and mineral nitrogen content (mg l^{-1}) of this material were 6.25, 1.39 and 346, i.e. higher than the 2.96, 0.53 and 147, respectively, for FYM. As no data were available for decomposition of this material, relative mineralization rate and rate of ageing have been set to 0.4 and 0.2, respectively.

Mineral nitrogen may be lost from the upper soil layer through volatilization, as part of the ammonium produced during hydrolysis is transformed into gaseous form. In the denitrification process, NO_3 is converted to NO , N_2O and N_2 , which may partly be lost to the atmosphere. The rates of these processes depend on the concentrations of NH_4 and NO_3 in the soil, aeration, and soil pH, and mostly follow first-order dynamics (Chowdary et al., 2004). Reported values of rate constants vary from 1.54×10^{-4} (Chin and Kroontie, 1963) to 0.3 d^{-1} (Jemison et al. 1994) for volatilization and from 0.0027 (Rolston and Marino, 1976) to 0.2 (Jansson and Anderson, 1988) for denitrification. In this study, gaseous nitrogen loss to the atmosphere, accounting for both volatilization and denitrification was assumed to depend on N_{min} in the first layer (0.2 m), following first-order dynamics. Hence, the rate of the gaseous nitrogen loss in these processes (N_{gas} in $\text{kg N ha}^{-1} \text{ d}^{-1}$) is:

$$N_{\text{gas}} = k_{\text{gas}} \times N_{\text{min}} \times e^{-k_{\text{gas}} \times t} \quad (18)$$

where, K_{gas} is a combined rate constant for both volatilization and denitrification, with an assumed value of 0.01 per day, t is time.

Model calibration and simulation

In the water balance model, the strongest determining factor is k (Radcliffe and Rasmussen, 2000) that determines inflow and outflow of water for each soil layer, while soil porosity determines soil water holding capacity. Because of the strong textural gradient in the soil profile, k decreases with increasing soil depth (Table 3), especially below 40 cm, which restricts water flow, and thus N leaching from the root zone.

Through trial-and-error, best-performing values, in terms of soil N dynamics, for ks were established. This yielded multiplication factors for ks for each layer (Table 4).

For the rice system, downward flow of water and hence transport of N strongly depends on the puddling effect, that was defined by Chen and Liu (2002) and Wopereis et al. (1992) as the presence of an ‘impermeable’ layer with a thickness of about 7.5 cm and a saturated hydraulic conductivity ranging from 0.027 to 0.083 cm d^{-1} , i.e. 20 to 30 times lower than that of the sub-soil. In the study area, such an impermeable layer is present in most of the rice soils at a depth between 15 and 22 cm, therefore the calibrated ks was very low for the first layer, and higher for the deeper layers (Table 4).

RESULTS

Measured nitrogen dynamics

NO₃-N dynamics

Figure 2 shows appreciable differences in NO₃-dynamics between 2004 and 2005, as a result of differences in rainfall, i.e. 1172 mm in 2004, and 1560 in 2005. Patterns are more similar from July onwards, i.e. the rainy season, during which most nitrogen leached in 2004, while it started earlier in 2005.

Rose is a perennial crop with a total life span from 5 to 7 years that is cut weekly from late October until April. As mentioned, it was heavily fertilized before the production period with nitrogen-rich mixed manure. The sludge was applied every ten days, combined with ‘bucket irrigation’ of urea fertilizer solution. During the summer season, growth was minimal, because the crop was damaged by very high radiation and rainfall, but nitrogen content in the surface layer remained high, because of the residual manure. Hence, N leaching continued throughout the year.

Table 3. Saturated hydraulic conductivity (ks), porosity, and field capacity (FC) of the soil in the experiment.

Soil layer (cm)	Soil texture class	ks (cm d ⁻¹)	Porosity (%)	FC (cm ³ cm ⁻³)
0–20	Loamy sand	146.40	43.7	33.3
20–40	Loamy sand	62.10	45.3	33.3
40–60	Sandy clay loam	10.32	39.8	60.6
60–80	Sandy clay loam	10.32	39.8	60.6
80–100	Sandy clay	2.88	43.0	65.0

Table 4. Initial soil moisture content (SW) (cm³ cm⁻³) and initial soil mineral nitrogen content (mg kg⁻¹) for the simulation model for the various crops and calibration factors for ks (see text for explanation).

Crop	Layer				
	1	2	3	4	5
	Initial SW				
For all crops	0.18	0.16	0.18	0.18	0.19
	Initial N				
Rose	131.6	60.6	53.6	57.5	63.6
Daisy	117.7	59.9	53.6	57.5	63.6
Cabbage	113.6	60.2	53.6	57.5	63.6
Chili	65.6	50.8	45.4	48.7	63.6
Rice	113.6	57.5	30.9	35.4	48.9
	ks				
Rose	0.8	1.0	1.0	2.0	2.0
Daisy	0.5	1.0	1.0	1.0	1.0
Cabbage	0.5	4.0	0.2	2.0	2.0
Chili	0.5	3.0	1.5	2.0	2.5
Rice (without puddling)	0.5	1.0	1.0	2.0	1.5
Rice (with puddling)	0.005	0.4	1.0	5.0	1.0

The production period for daisy largely overlaps with that for rose, but the daisy is an annual crop, planted in September and uprooted at the end of May, with the soil being fallow in the intercrop period. Fertilizer regime was similar to that for roses, in both quantity and timing.

Cabbage is an intensive crop, with six harvests per year, where seedlings are produced in a corner of the field. A high dose of manure was applied as a basal dressing, followed by weekly applications of high doses of urea fertilizer by bucket irrigation until 25 days after planting. Soil NO₃-N was high in the rainy season because of continuous high fertilizer application and lower in dry season, when crop uptake is high.

Chili is sown in August and transplanted in early September. A high dose of manure was applied at 40 days after planting, followed by bi-weekly fertigation of urea fertilizer. Manure was applied again after the onset of flowering by dissolving it into the standing water; this was repeated every two months from November to April, when yields are high. From May to July very little or no fertilizer was applied, the crop growing on residual nutrients. In addition, chili was irrigated abundantly during the dry season, resulting in high NO₃-N contents deeper in the profile in the dry season, exceeding those in summer.

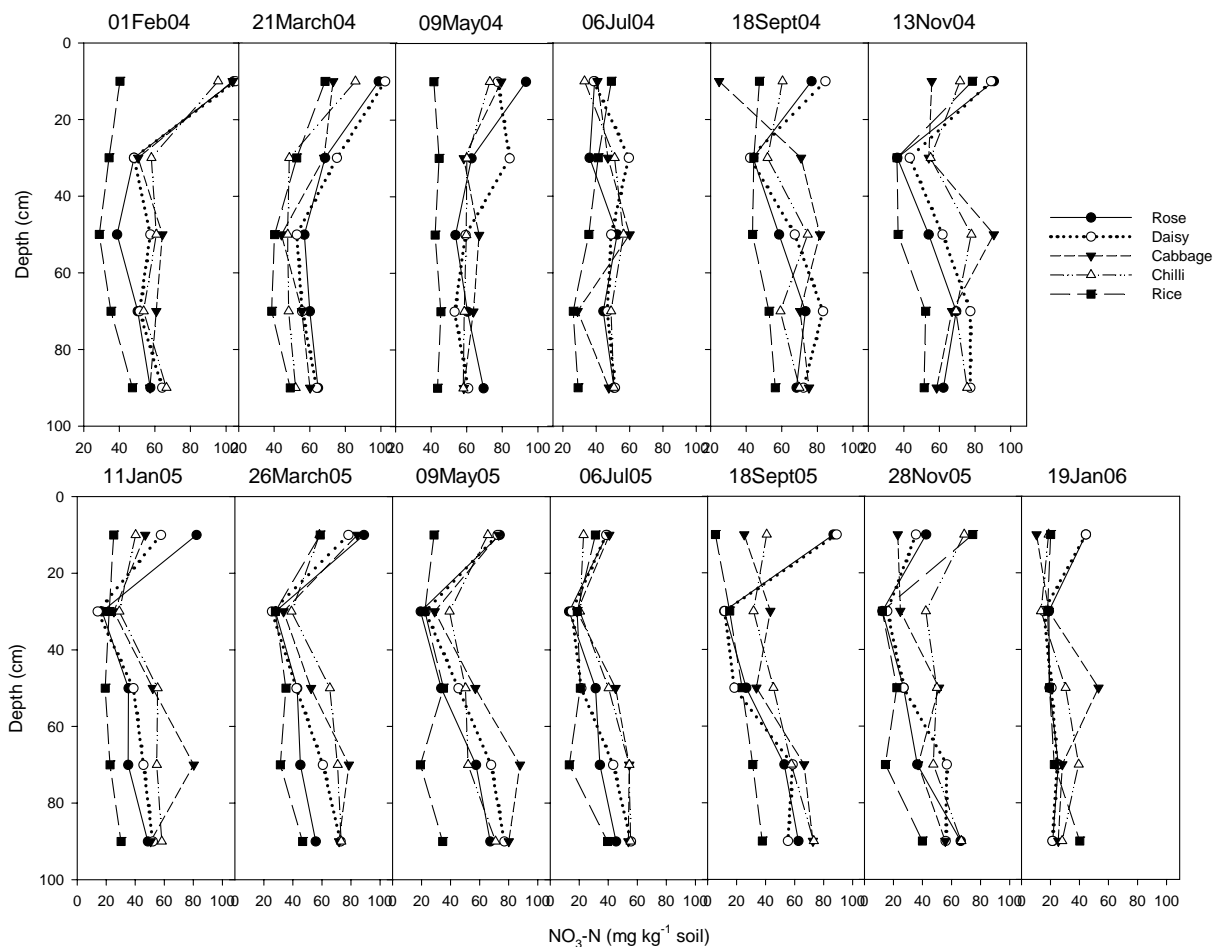


Figure 2. Nitrate-N concentrations (mg N kg^{-1} soil) at different soil depths in 2004 (top) and 2005 (bottom) for five land-use types (Note: concentration scales are different).

In the rice rotation, fertilizer application was high for spring rice in March, for summer rice in June and July, and for winter maize in September and November. The $\text{NO}_3\text{-N}$ concentrations in this rotation were lower than in the other crops. However, occasionally the $\text{NO}_3\text{-N}$ concentration was high (Figure 2), due to high fertilizer application and low nitrogen uptake, i.e. in the tillering period of rice (March, July) and after planting of maize (October).

NH₄-N dynamics

Soil $\text{NH}_4\text{-N}$ is much lower than $\text{NO}_3\text{-N}$. It is generally higher in the upper layers, because most $\text{NH}_4\text{-N}$ derives from fertilizer hydrolysis and is subsequently taken up by the crop. Under dry conditions it is easily transformed to NH_3 , which volatilizes. Under aerobic conditions it is nitrified to NO_3^- and easily leaches to deeper soil layers and the groundwater. When the $\text{NH}_4\text{-N}$ concentrations are high, and conditions conducive to leaching, it may leach to deeper layers in a short time (Miller and Gardiner, 2001). NH_4 in flowers was high in the rainy season, while in chili it was

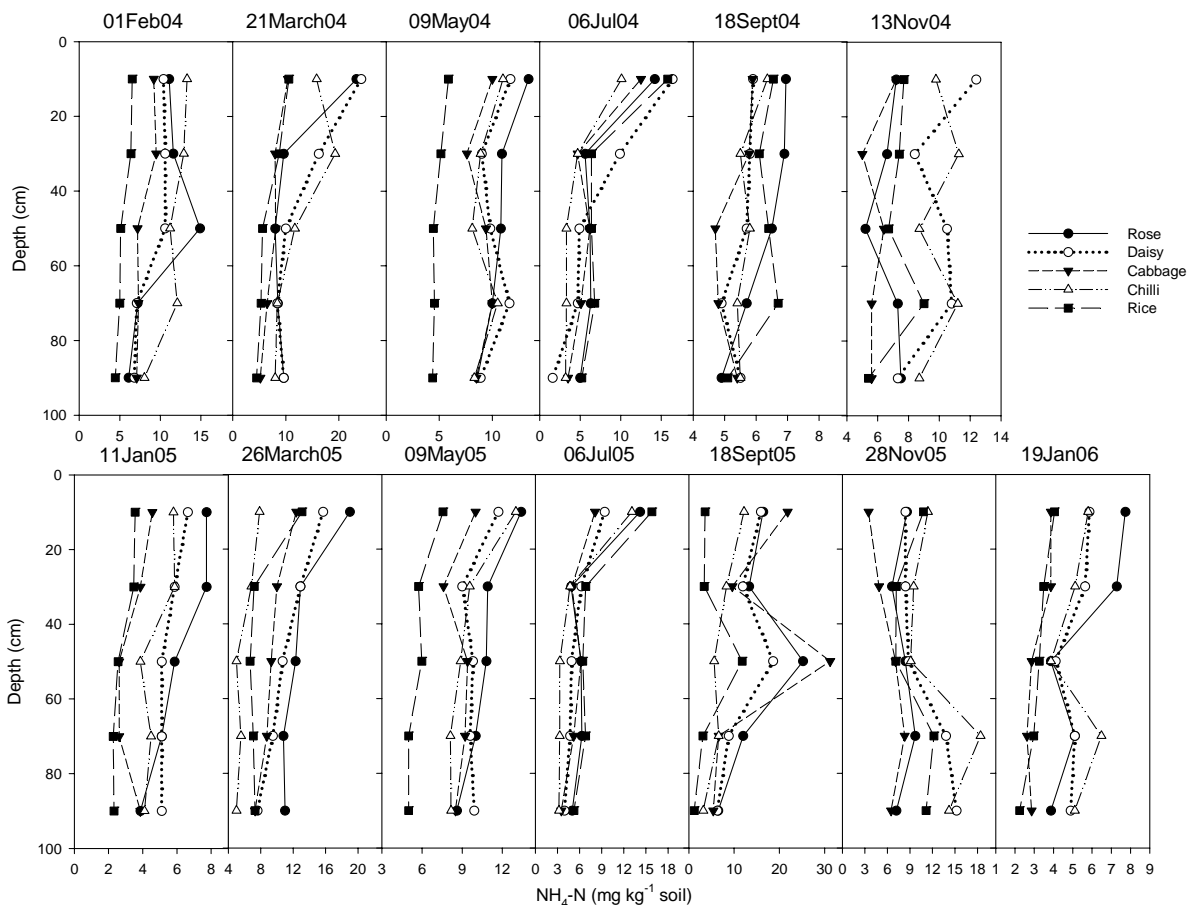


Figure 3. $\text{NH}_4\text{-N}$ at different soil depths in 2004 (top) and in 2005 (bottom) for five land-use types (Note: concentration scales are different).

high in the dry season (Figure 3). This was related to high rainfall and the continuing high mineralization from manure in the rainy season for the flowers and the combination of high irrigation and high fertilizer application in the dry season for the chili. In other words, NH_4 was much higher in the rainy season of 2005 than of 2004, associated with the much higher rainfall in 2005.

Simulated nitrogen dynamics

Water and mineral nitrogen (Nmin) balances were simulated for five crops with a daily time step during two years. Daily weather data from Vinh Yen station (2 km from the study area), crop calendars (Table 2), and soil properties (Table 3) were used.

Nitrogen dynamics in flowers

Simulated Nmin in the roses agreed well with the measured values for time course, pattern as well as magnitude (Figure 4). In summer, simulated Nmin in the first layer was slightly underestimated, but it was satisfactory for the other layers. For the deeper layers, Nmin dynamics and magnitude were simulated satisfactorily, although the variation was smaller than in the measured values that also showed a strong spatial variation (data not shown).

The pattern of Nmin in the daisies (Figure 5) was very similar to that of the roses, as production period, irrigation, and fertilizer regime were similar. However, as in summer the daisy land was fallowed and not fertilized, simulated Nmin in the surface layer is very low in this period. In reality, a substantial proportion of the manure remained on the soil surface and continued to be decomposed and supply Nmin to the soil.

Nitrogen dynamics in vegetables

The two vegetable species planted in the area each require specific management. Cabbage is a shallow-rooting crop that requires frequent irrigation, especially with hand sprinkler and bucket irrigation, while chili is deeper-rooting and thrives on high beds, but requires high water and organic matter contents. Manure was therefore applied to cabbage as a basal dressing on the soil surface under aerobic conditions, while for chili it was surface-applied in the course of the growing period, dissolving in the standing water.

The dominant N fertilizer applied to cabbage was urea, contributing more Nmin to the surface layer than manure. Simulated Nmin in this layer closely followed measured values (Figure 6), i.e. it was high in the early growth stages, when crop demand was low, declined in late summer as a result of high rainfall and lower fertilizer application in this period, and was very low in winter with intensive cabbage cultivation with high

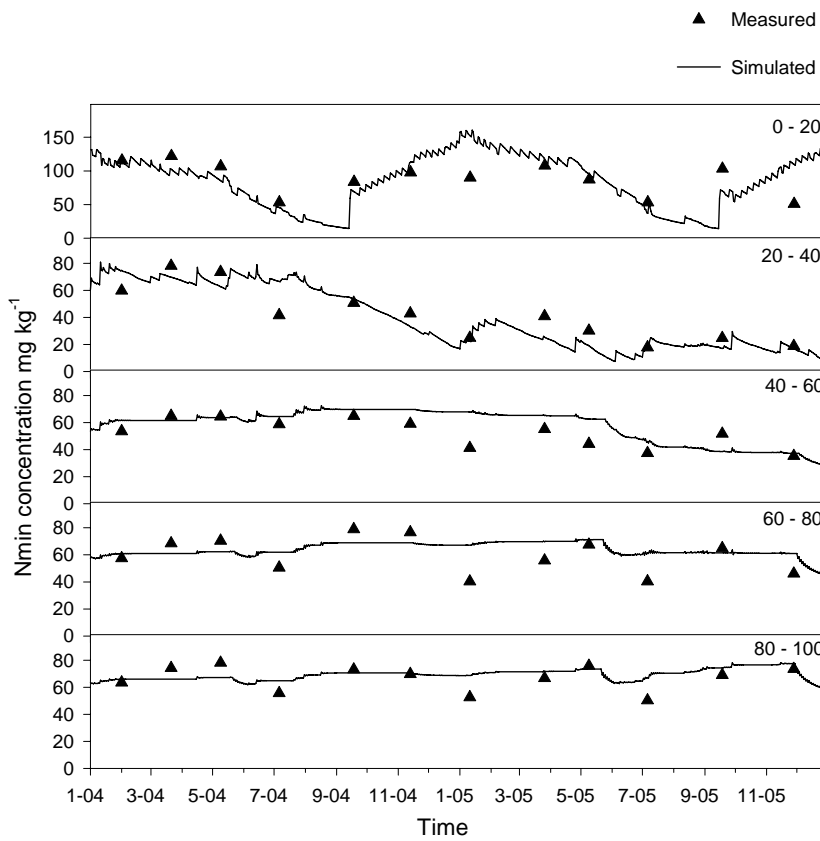


Figure 4. Measured and simulated mineral nitrogen concentration (mg kg^{-1}) at different depths for roses.

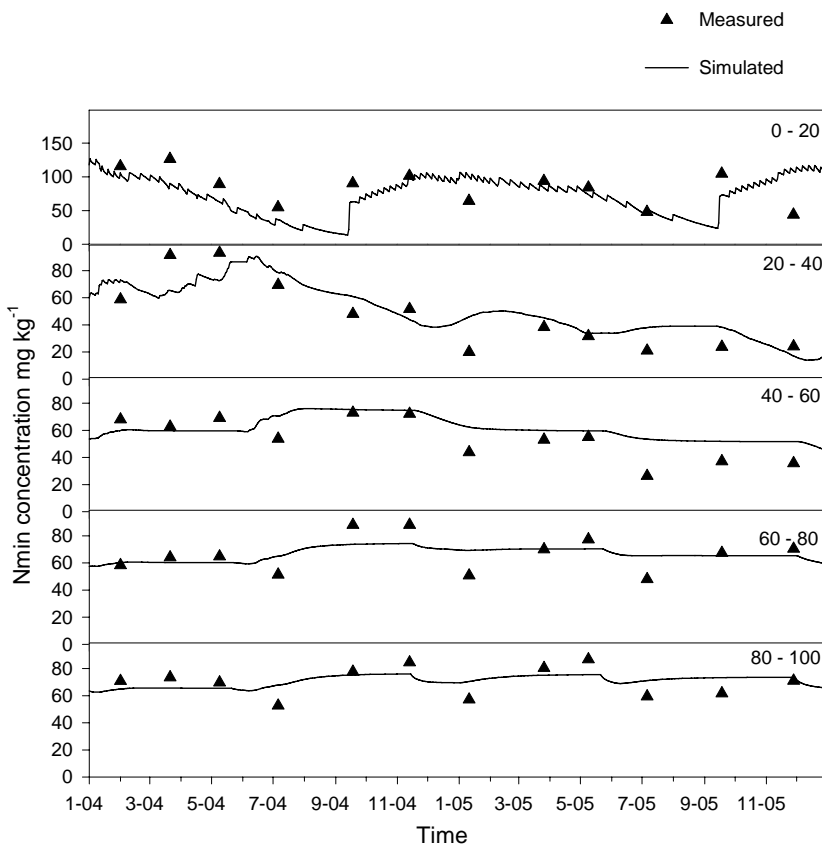


Figure 5. Measured and simulated mineral nitrogen concentration (mg kg^{-1}) at different depths for daisies.

fertilizer doses. Hence, N leaching was inversely related to N application, i.e. higher in summer than in winter, associated with the higher percolation in summer under high rainfall, whereas in winter, irrigation was rarely in excess of crop water requirement, hence percolation was limited.

In chili, manure was applied at high doses; N_{min} was slightly underestimated in the first layer for some time in the dry season (Figure 7), associated with a period of very high crop uptake. In the deeper layers, simulated N_{min} agreed well with the measured values. The water balance sub-model showed (results not shown) that percolation was higher in the rainy season than in the dry season, but N_{min} in the deeper soil layers was lower in the rainy season, for two reasons: (i) in the rainy season, less fertilizer is applied, while percolation is high, so that N_{min} is diluted, (ii) irrigation in the dry season was in excess of crop water requirements, high fertilizer doses were applied early in the dry season, which continued until the end of this season. As a result, large quantities of N_{min} were transported from the surface layers to the deeper soil layers.

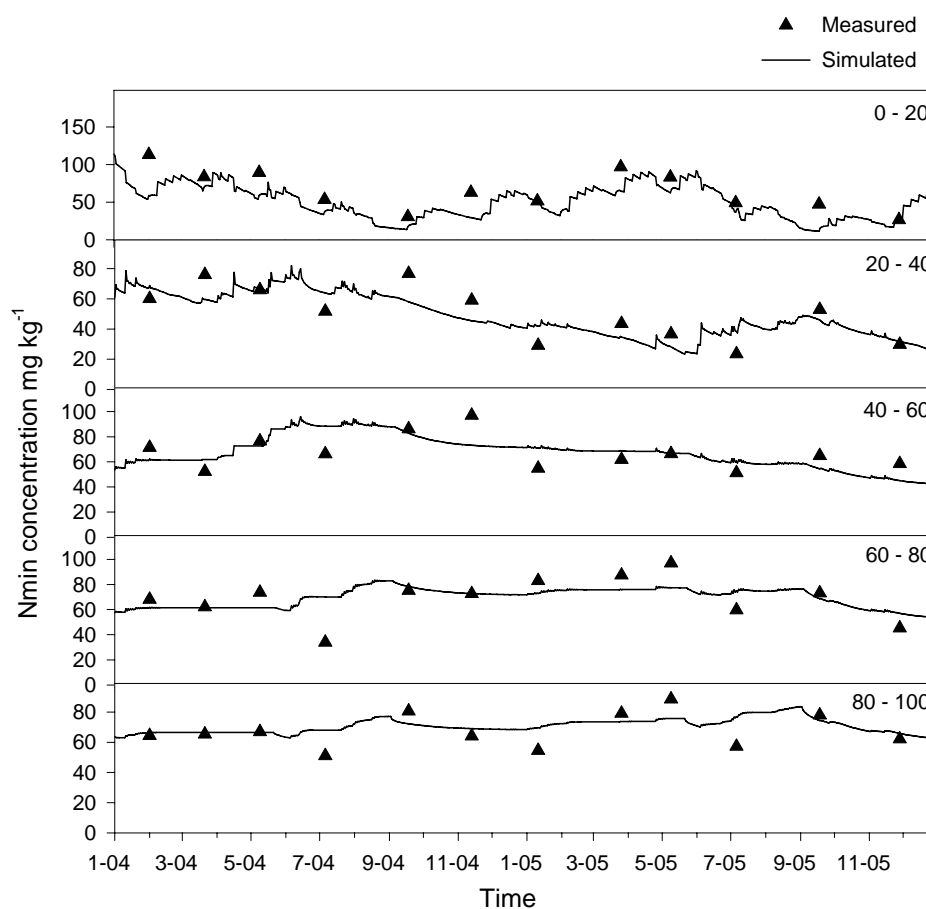


Figure 6. Measured and simulated mineral nitrogen concentration (mg kg^{-1}) at different depths for cabbage.

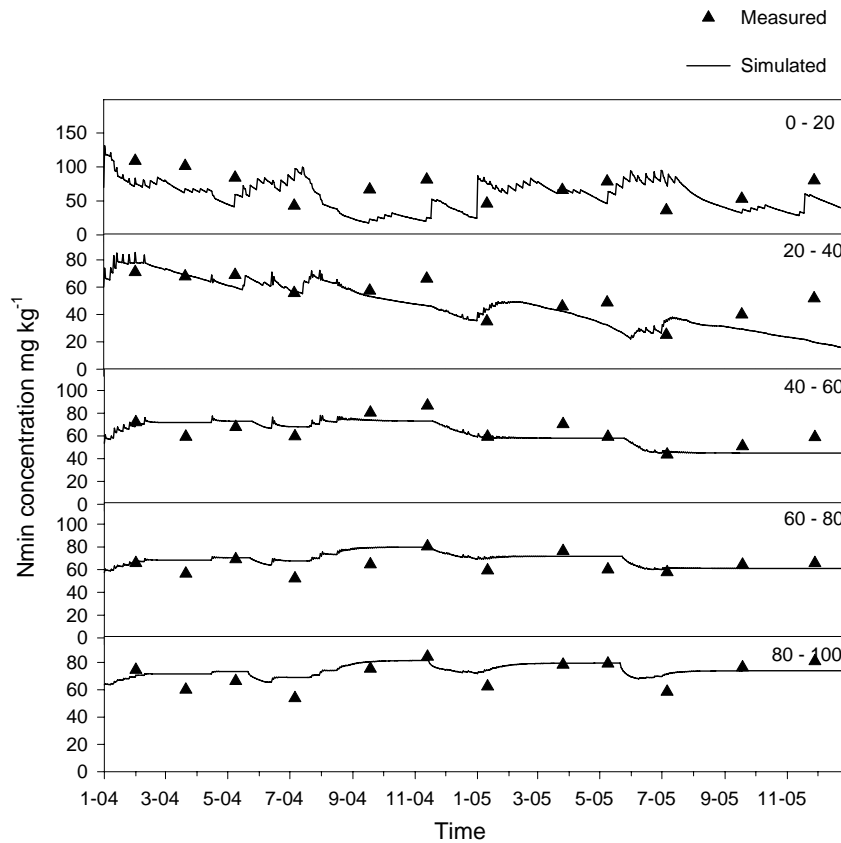


Figure 7. Measured and simulated mineral nitrogen concentration (mg kg^{-1}) at different depths for chili.

Nitrogen dynamics in rice

Rice receives mostly mineral fertilizer (urea) that is rapidly hydrolysed, leading to high available nitrogen levels. Simulated Nmin in the surface layer agrees well with measured values (Figure 8). Without the puddling effect, Nmin in the second layer was strongly underestimated and in the deeper layers overestimated (Figure 8, left). Inclusion of the puddling effect, reducing the k value in the first layer and increasing it in deeper layers, resulted in substantially improved model performance (Figure 8, right). In these layers, simulated Nmin is fairly constant, associated with stable downward water movement.

Nitrogen leaching losses

Nitrogen leaching losses were calculated by multiplying simulated daily outflow from the bottom of the soil column (mm) and the simulated Nmin concentration (mg l^{-1}) in the bottom layer. Annual nitrogen leaching losses were accumulated from the daily losses (Table 5).

In annual percolation, three classes can be distinguished (Table 5): High values in

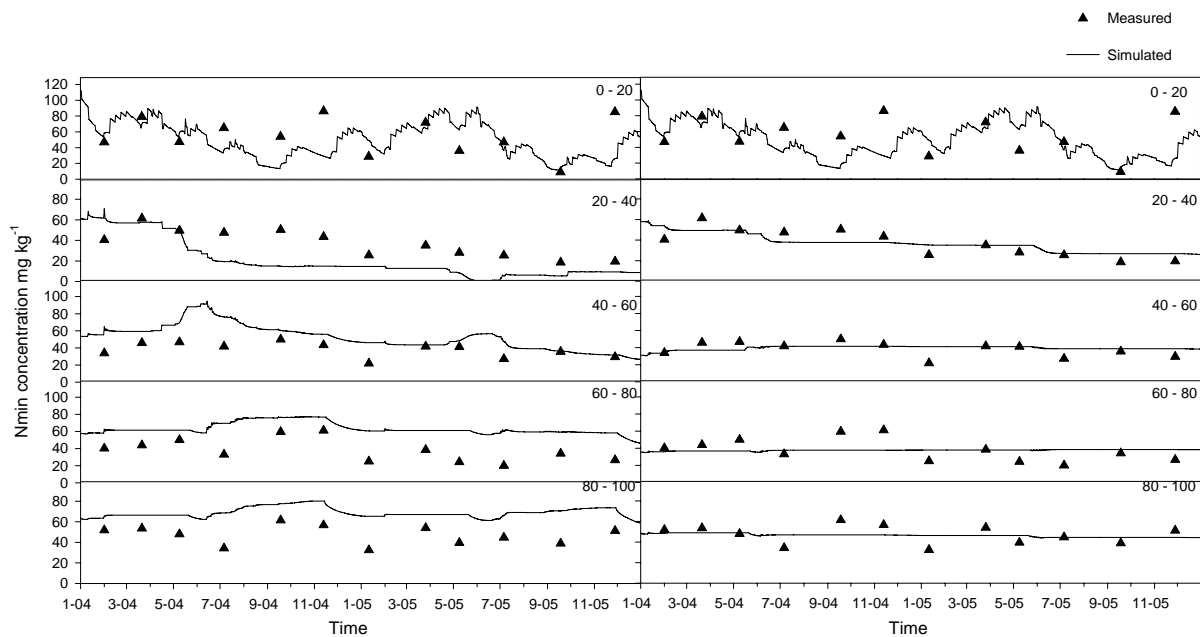


Figure 8. Measured and simulated mineral nitrogen concentrations (mg kg^{-1}) at different depths for rice without (left) and with puddling effect (right).

rose and daisy ($185\text{--}190 \text{ mm yr}^{-1}$), medium values in cabbage and chili ($120\text{--}122 \text{ mm yr}^{-1}$); and low values in rice (60 mm yr^{-1}). Rice without puddling effect (NP, given for illustrative purposes only) yields a very high value (243 mm yr^{-1}). Total annual percolation and maximum rate of percolation are not strongly correlated, as length of the growing period is a confounding factor.

Annual percolation and annual N leaching losses are correlated (Table 5), with high leaching losses in rose and daisy ($173\text{--}193 \text{ kg ha}^{-1} \text{ yr}^{-1}$), medium values in vegetables ($112\text{--}115 \text{ kg ha}^{-1} \text{ yr}^{-1}$), and low in rice ($40 \text{ kg ha}^{-1} \text{ yr}^{-1}$).

DISCUSSION

Soil mineral nitrogen dynamics

Mineral nitrogen includes both ammonium and nitrate that are both very soluble in water (Miller and Gardiner, 2001). The negatively charged nitrate ion is very mobile and easily leaches with percolating water. Part of the positively charged ammonium ions is adsorbed at the cation exchange sites and thus less susceptible to leaching.

Leaching losses of nitrate increase as percolation increases, as a result of either high rainfall or irrigation (Angle, 1990; Granlund et al., 2000) and when plant growth is insufficient to absorb the nitrates produced (Miller and Gardiner, 2001). $\text{NO}_3\text{-N}$ is usually present in higher concentrations in the soil solution than $\text{NH}_4\text{-N}$ (Pierzynski et

Table 5. Annual percolation (mm), maximum percolation rate (Max. Per. Rate; mm d⁻¹), nitrogen leaching losses (Leached N; kg ha⁻¹ yr⁻¹), and maximum nitrogen leaching rate (Max. L. rate; kg ha⁻¹ d⁻¹) for rose, daisy, cabbage, chili and for rice without (NP) and with puddling effect (P), in 2004 and 2005.

Leaching types	Year	Crop					
		Rose	Daisy	Cabbage	Chili	Rice	
						NP	P
Percolation	2004	123.1	177.5	118.4	109.5	230.7	47.6
	2005	247.6	203.5	125.9	131.4	255.3	73.0
Max. Per. rate	2004	5.5	3.2	3.5	4.3	6.0	1.7
	2005	11.8	3.3	15.0	0.4	6.1	6.9
Leached N	2004	101.2	160.4	106.8	100.6	207.4	31.0
	2005	284.7	185.8	122.8	122.9	214.2	48.8
Max. L. rate	2004	4.8	3.2	2.9	3.6	3.8	1.1
	2005	11.5	3.3	14.7	0.4	3.6	4.8

al., 2005). The highest concentrations were observed in the second, fourth, and sixth sampling periods in the rice rotation, when high fertilizer doses were applied, while crop uptake was low. It was high in flowers in most of the rainy season, when rainfall was high, nitrogen continued to be mineralized from manure, and crop uptake very low. N concentrations were also very high for most of the time in cabbage, where a new crop started every one and a half month, with high fertilizer doses and in chili in the rainy season with high rainfall. Ammonium accumulated mainly in the surface layer. The highest ammonium concentrations were recorded in the rainy season, especially in 2005, associated with the very high rainfall and the consequently high percolation. In September, cabbage, rose, and daisy received fertilizers at the start of the production period. High rainfall in this period generated high percolation rates, transporting excess NH₄-N to the deeper soil layers. Subsequently, rainfall rapidly declined, and only in chili, excess irrigation water continued to generate percolation, transporting NH₄-N downwards.

Modelling nitrogen leaching losses

The combined effects of environmental factors on soil and plant processes and the consequences for nitrogen transport in the soil are made explicit in the nitrogen transport model. The model fairly accurately reproduced the observed dynamics of mineral nitrogen in the soil profile, and the calculated leaching losses can thus be considered with confidence. The model showed continuous downward movement of

water under saturated conditions, similar to other models (Chen et al., 2002; Chowdary et al., 2004), while the flow rate decreased with a decrease in soil moisture content and the associated reduction in hydraulic conductivity (Mantovi et al., 2006; Yu et al., 2006). However, the model is incomplete, as capillary rise from the groundwater table and lateral flow are not included. Moreover, inclusion of a dynamic crop growth model would have improved performance of the transpiration and evapo-transpiration calculations in the water balance sub-model. The transport model, based on the perfect mixing principle, worked well for calculating nitrogen flows between soil layers. Simulated results for percolation and N leaching with the puddling effect are in agreement with reported data (Wopereis et al., 1992, 1994; Chen et al., 2002; Chen and Liu, 2002) and illustrate the advantage of an impermeable or hardpan layer in increasing water and nutrient use efficiencies.

CONCLUSIONS

Rapid expansion of intensive agriculture, with application of ever increasing fertilizer doses, increases the risk for negative environmental impacts, such as water pollution, from both overland flow and leaching of chemical fertilizers and pesticides. This study, focusing on leaching of nitrogen from the root zone was initiated to provide a scientific basis for land use planning and an environmental protection campaign. The results indicate appreciable leaching losses in high rainfall and irrigation conditions, especially when fertilizer application is not well synchronized with the dynamics of crop nitrogen demand.

It was shown that a relatively simple combined water and nitrogen balance model is a useful tool for quantifying the risks of nitrogen leaching and can be applied with confidence to explore the scope for improvements in soil and crop management.

CHAPTER 6

Nitrogen leaching and nitrogen losses in rice-rice-maize systems on sandy loam soil in Tam Duong, Red River Delta, Vietnam*

V.T. Mai^{1,4}, H. Van Keulen^{1,2}, R.P. Roetter³

- ¹ Plant Production Systems Group, Wageningen University, P.O. Box 430, 6700 AK Wageningen, The Netherlands
- ² Plant Research International, Wageningen University and Research centre, P.O. Box 16, 6700 AA Wageningen, The Netherlands
- ³ Soil Science Centre, Alterra Green World Research, Wageningen University and Research centre, P.O. Box 47, 6700 AA Wageningen, The Netherlands
- ⁴ National Institute for Soils and Fertilizers (NISF), Dong Ngac, Tu Liem, Hanoi, Vietnam

Abstract

The objective of this study was to quantify nitrogen leaching losses from rice-based production systems on sandy terraces in Vietnam, highly susceptible to nutrient losses due to surface runoff and leaching. Experiments were carried out with three fertilizer levels in a rice – rice – maize rotation, during two years, 2004 and 2005. Soil samples were taken in 20 cm increments up to 1 m depth to analyse nitrate and ammonium concentrations, just before transplanting, at maximum tillering, at flowering, and after harvest for rice; pre-sowing, 9th-leaf stage, flowering, and after harvest for winter maize. Results showed that nitrate leaching was the main type of nitrogen loss. Nitrate accumulation in the deeper soil layers was highest in the periods from transplanting to maximum tillering of rice, and from sowing to the 9th-leaf stage for maize. Percolation and nitrogen leaching losses below the soil profile were simulated using water and nitrogen balance sub-models. Simulated results showed trends in nitrogen dynamics similar to the measured data, and indicated high losses under current management, i.e. 52 and 60, 56 and 114, and 58 and 154 kg N ha⁻¹ yr⁻¹ in 2004 and 2005, for low, medium and high fertilizer inputs, respectively. Risks of nitrogen leaching can be substantially reduced by cautious management, with respect to fertilizer application and irrigation, (especially) in the early crop growth periods. To reduce losses, chemical fertilizer should be replaced by manure and inorganic fertilizer should be applied in split doses to increase agronomic efficiency and optimize economic returns.

Keywords: Rice-based cropping system, nitrate, nitrogen losses, modelling water balance, modelling nitrogen transport

* This chapter has been submitted to Nutrient Cycling in Agroecosystems.

INTRODUCTION

Nutrient losses from agricultural systems create serious problems (Sheldrick et al., 2002) and the study of nutrient use efficiencies and strategies to improve them are important issues in this context. Nitrogen (N) requires special attention, since the system is open for the element, i.e. crops need large quantities and large quantities cycle through the system with the associated (risks for) losses. Moreover, nitrogen exerts negative influences on the environment through its contribution to acid rain and eutrophication and its negative effect on the quality of drinking water. A study of N use efficiency in intensive rice-based systems has shown that apparent recovery efficiencies of N fertilizer, i.e. the proportion of the applied N accumulated in the aboveground plant parts at harvest are, on average, about 30–40% (Dobermann et al., 2002). A large proportion of the complementary fraction is lost. Leaching is one of the loss pathways, that may result in high nitrate concentrations in groundwater, under intensive agricultural systems (Kumazawa, 2002; Verloop et al., 2006). High leaching losses may result from excessive N fertilizer applications under conditions of high rainfall, high infiltration capacity, and low crop growth rates. For example, under pea and barley on sandy soil in a temperate region, annual NO_3 leaching losses ranging from 61 to 76 kg N ha⁻¹ have been reported (Hauggaard-Nielsen et al., 2003). Comparing N losses from different land use types, Di and Cameron (2002) concluded that nitrate leaching potential typically increases in the order forest < cut grassland < grazed pastures < arable cropping < ploughed pasture < market gardens. In a study on nitrogen dynamics in intensive lowland rice systems in the Philippines, annual N losses from the top 1 m ranged from 34 to 549 kg ha⁻¹ depending on crop rotation, with the highest values in rice-sweet pepper and rice-tomato (Tripathi et al., 1997).

Nitrate leaching losses are directly associated with percolation of water and fertilizer application. Zhu et al. (2000) reported that in a rice-wheat rotation in China, nitrate in percolation water increased when the field was drained. Nitrate leaching was particularly high in early spring, when rainfall starts, following fertilizer application at tillering. Xing and Zhu (2000) showed that in paddy fields in China, total leaching losses ranged from 6.75 to 27.0 kg N ha⁻¹ yr⁻¹, while runoff losses were between 2.45 and 19.0 kg ha⁻¹ yr⁻¹. Leaching is particularly high in the most intensive farming systems: N leaching losses were 28.2 kg ha⁻¹ in double rice with fertilizer doses of 350 kg N ha⁻¹ and 449.1 kg ha⁻¹ in annual horticultural crops with fertilizer doses of 920 kg N ha⁻¹ (Fang et al., 2005).

Recently, various studies in Asia have shown a positive correlation between fertilizer application rates and NO_3^- leaching (Kumazawa, 2002; Zhu et al., 2003; Hai, 2004). In the Red River Delta of Vietnam, NO_3 concentrations in groundwater under rice fields of 57 mg l⁻¹ in the dry season and 84 mg l⁻¹ in the rainy season have been

recorded (Tau, 1997). Following rain events, NO_3 concentrations increased to 116 mg l^{-1} . Nitrogen leaching from paddy soils has received less attention than that from upland soils (Zhu et al., 2000), and very few such studies have been conducted in Vietnam, although paddy rice-based systems cover a large area of the cultivated terraces in northern Vietnam. These terraces, the main resource for food production in the hilly and mountainous areas, consist of sandy soils, characterized by high infiltration capacities and low N fertilizer use efficiencies (Phuong, 2003; Son et al., 2004). The current study was initiated to fill the information gap on N use efficiencies and N losses in rice-based cropping systems in the Red River Delta, as one of the building blocks for designing more sustainable land use systems, in terms of nutrient balances. The specific objectives of the study were: (i) determination of nitrate and ammonium dynamics in a rice-rice-maize rotation on a sandy soil on terraces in the hilly area of northern Vietnam, (ii) quantification of N leaching losses at different levels of fertilizer input.

MATERIALS AND METHODS

Study area

The study was conducted in Tam Quan commune, Tam Duong district, about 70 km north-west of Hanoi, Vietnam ($21^{\circ}26' \text{ N}$, $105^{\circ}36' \text{ E}$), on the middle terraces, between the upper hills and the low terraces and flat lands. The soil is classified as an Albic Arenosol (FAO/UNESCO, 1974; FAO, 1976), very sandy, low in organic carbon and poor in plant nutrients (Table 1). The soil profile is weakly developed with slight gradients in clay content, color, organic matter content, bulk density and porosity with depth. Soil nutrients can be lost through overland flow in the rainy season, and through leaching during the rice growing period, associated with water logging.

Rainfall volume and distribution varied among seasons and years (Figure 1), i.e. earlier and higher rainfall in spring 2004 than in 2005, much higher in summer and winter 2005 than in 2004.

Experimental setup

The experiment was set up as a randomized complete block design with three treatments and three replicates, for the triple crop rotation spring rice – summer rice – winter maize during 2004 and 2005. Fertilizer recommendations have been formulated for the whole district, but not specifically for these sandy soils on the rice terraces. Therefore, based on the results of fertilizer trials of Dai and Trang (2003), on the same soil type in a neighbouring district, 10 Mg of manure $\text{ha}^{-1} \text{ crop}^{-1}$, and 100 and 70 kg inorganic fertilizer N ha^{-1} for spring and summer rice, respectively were

Table 1. Soil properties at the experimental site.

Horizon	Particle size distribution (%)			Bulk density g cm ⁻³	OC ¹ %	N total %	P total (P ₂ O ₅) %	K total (K ₂ O) %
	Clay	Silt	Sand					
0–20	20.8	9.8	69.4	1.20	1.25	0.034	0.107	0.042
20–40	14.2	8.8	77.0	1.29	1.41	0.073	0.013	0.042
40–60	12.2	7.8	80.0	1.29	0.98	0.039	0.007	0.066
60–80	12.6	6.0	81.4	1.29	0.58	0.028	0.009	0.060
80–100	13.2	7.4	79.4	1.29	0.36	0.034	0.122	0.084

¹ Organic Carbon.

recommended. These high fertilizer doses, aiming at realization of the climatic yield potentials can be afforded only by some rich farmers. The fertilizer treatments in the experiment (Table 2) were based on results of a production survey in the study area: (T0), the lowest level, practiced by very poor farmers; (T1), the medium level, practiced by the ‘average farmer’, and (T2) the high level, double the T1 inputs, applied by the few farmers that can afford high inputs.

Field sampling

Soil samples were taken (two replicates per plot) in 0.2 m increments to a depth of 1 m at four points in time: just before transplanting, at maximum tillering, at flowering, and after harvest for rice; pre-sowing, 9th-leaf stage, flowering, and after harvest for winter maize. Sub-samples were taken to the laboratory in polyethylene bags and stored at 4 °C prior to extraction, usually within 2 days of collection. Plants were sampled concurrently with the soil samples, for determination of nitrogen uptake.

Laboratory analyses

Twenty grams of field-moist soil were extracted in 50 ml 0.5 M KCl. Samples were shaken on a rotary shaker for one hour and then filtered through Whatman no. 1 filter paper into polyethylene containers. Nitrate-nitrogen (NO₃-N) and ammonium-nitrogen (NH₄-N) in the extracts were determined following steam distillation. Another sub-sample was dried at 105 °C for 24 hours to determine field moisture content. Plant samples were oven dried (65 °C) for 12 hours and weighed. N was determined by micro-Kjeldahl (Bremner 1996).

Data analysis

NO₃-N and NH₄-N concentrations from all treatments and replicates in each soil layer

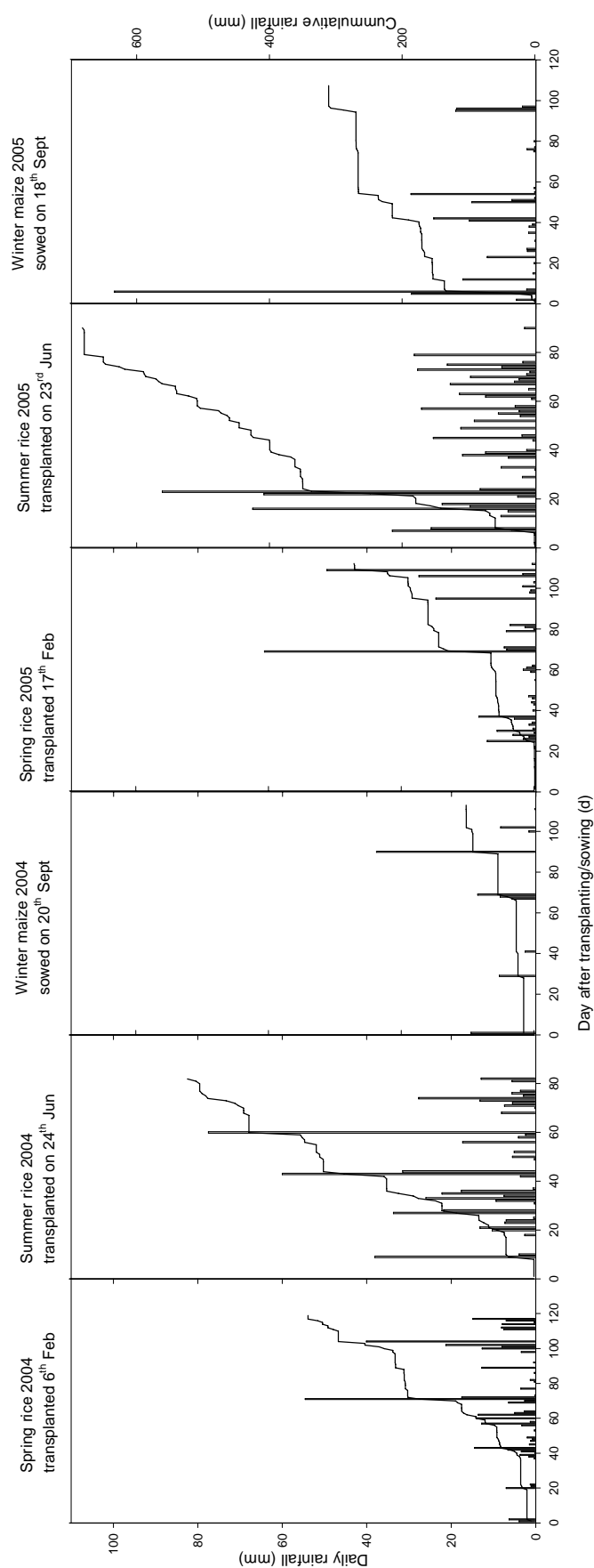


Figure 1. Daily rainfall (left hand Y axis) and cumulative rainfall (continuous line, right hand Y axis) for all cropping periods in 2004 and 2005.

Table 2. Fertilizer application dates and doses for the three treatments and the three crops in two years.

Crop	Date		Fertilizer	Dose (kg ha ⁻¹)		
	2004	2005		T0	T1	T2
Spring rice	Feb 06	Feb 17	Manure ¹	5500	5500	11000
			N	0	25	50
			P ₂ O ₅	0	45	90
	Mar 01	Mar 11	N	0	25	50
	Mar 16	Mar 27	K ₂ O	0	15	30
Summer rice	Jun 19	Jun 17	Manure	5500	5500	11000
			N	0	4	8
			P ₂ O ₅	0	10	20
			K ₂ O	0	5	10
	Jun 29	Jun 27	N	0	31	62
Winter maize ³	Sep 20	Sep 23	Manure	5500	5500	11000
			N	0	20	40
			P ₂ O ₅	0	20	40
			K ₂ O	0	5	10
	Sep 30	Oct 03	Urine ²	0	250	500
			N	0	20	40
	Oct 05	Oct 08	N	0	7.5	15
	Oct 10	Oct 13	Urine	0	250	500
			N	0	20	40
	Oct 15	Oct 18	N	0	25	50
P ₂ O ₅			0	20	40	
K ₂ O			0	5	10	

¹ Manure contained 2.96% C, 0.5 % N, 0.025 % P₂O₅ and 0.49 % K₂O.

² Urine (1 ha⁻¹) from pig and cow stables contained 4.19 g I⁻¹ total N and 345.8 mg Nmin I⁻¹.

³ Fertilizers were applied to maize in combination with bucket irrigation.

were analysed using one-way ANOVA analysis of variance. Crop yields of the three treatments and replicates were analysed using the Genstat statistical package (Lawes Agricultural Trust, 2003). Average nitrate and ammonium concentrations per soil depth were calculated for each growing period. Total mineral nitrogen (Nmin) in each soil layer was calculated as the sum of nitrate and ammonium nitrogen.

Calculation of nitrogen leaching losses

Accurately quantifying nitrogen losses is very demanding, requiring expensive equipment, such as a special lysimeter to measure downward water flow from the root zone (Cameron et al., 1996; Aronsson, 2001). Nitrogen leaching is affected by many

processes, such as mineralization from soil organic matter, fertilizer application, plant uptake, volatilization and denitrification, and rainfall and irrigation. In this study, N leaching losses were calculated by a one-dimensional simulation model containing water and N balance sub-models, as described in detail in Chapter 5. In the model, percolation is calculated as the balance of daily rainfall, irrigation, overland flow and evapo-transpiration. Overland flow is described as the water from rainfall/ irrigation in excess of the storage capacity provided by the field bunds (Chowdary et al., 2004), which in the study area are 50 mm on average. Crop transpiration and soil surface evaporation are calculated by WOFOST (Boogaard et al., 1998), a crop growth model for simulation of potential and water-limited yields. WOFOST has been calibrated for spring rice, summer rice and winter maize in the study area with relevant crop calendars, varieties and production levels (Mai et al., 2007).

RESULTS

Nutrient uptake and crop yield

Temperature is an important growth-determining factor in the spring season. Low temperatures affect both, above- and below-ground crop production, by retarding phenological development, reducing tiller formation and delaying panicle initiation (Grist 1986). They also adversely affect nutrient uptake due to slow development of new roots and increased root resistance (Street and Bollich, 2003). As shown in Figure 2 for spring rice, the patterns of cumulative total biomass and N uptake in 2004 and in 2005 are different. In spring 2004, both growth and phenological development of the rice crop were slow after transplanting, because of low temperatures. As a result, it took 72 days to reach flowering, compared to 59 days in 2005. The longer duration of the tillering stage and the relatively high growth rate late in that period, resulted in higher biomass at maximum tillering in 2004 than in 2005 (Figures 2a, b). In the next period (from maximum tillering till flowering), growth rate was lower in 2004 than in 2005, so that total biomass at flowering was practically the same in the two years. These differences in growth and N uptake rates may have consequences for soil-N status. In the spring season, crop yield was much higher for the manure + inorganic fertilizer treatments (T1 and T2) than for the manure-only treatment (T0). Grain yield was highest in the high fertilizer treatment (T2), but the difference with T1 was rather small (Table 3).

In summer, at higher temperatures and radiation, and more available water, plants quickly recovered after transplanting and growth rates were high in the pre-flowering period (Figures 2c, d). The pattern of both, cumulative total biomass and N uptake was the same in both years. Total biomass was similar in both years for T0, was lower in

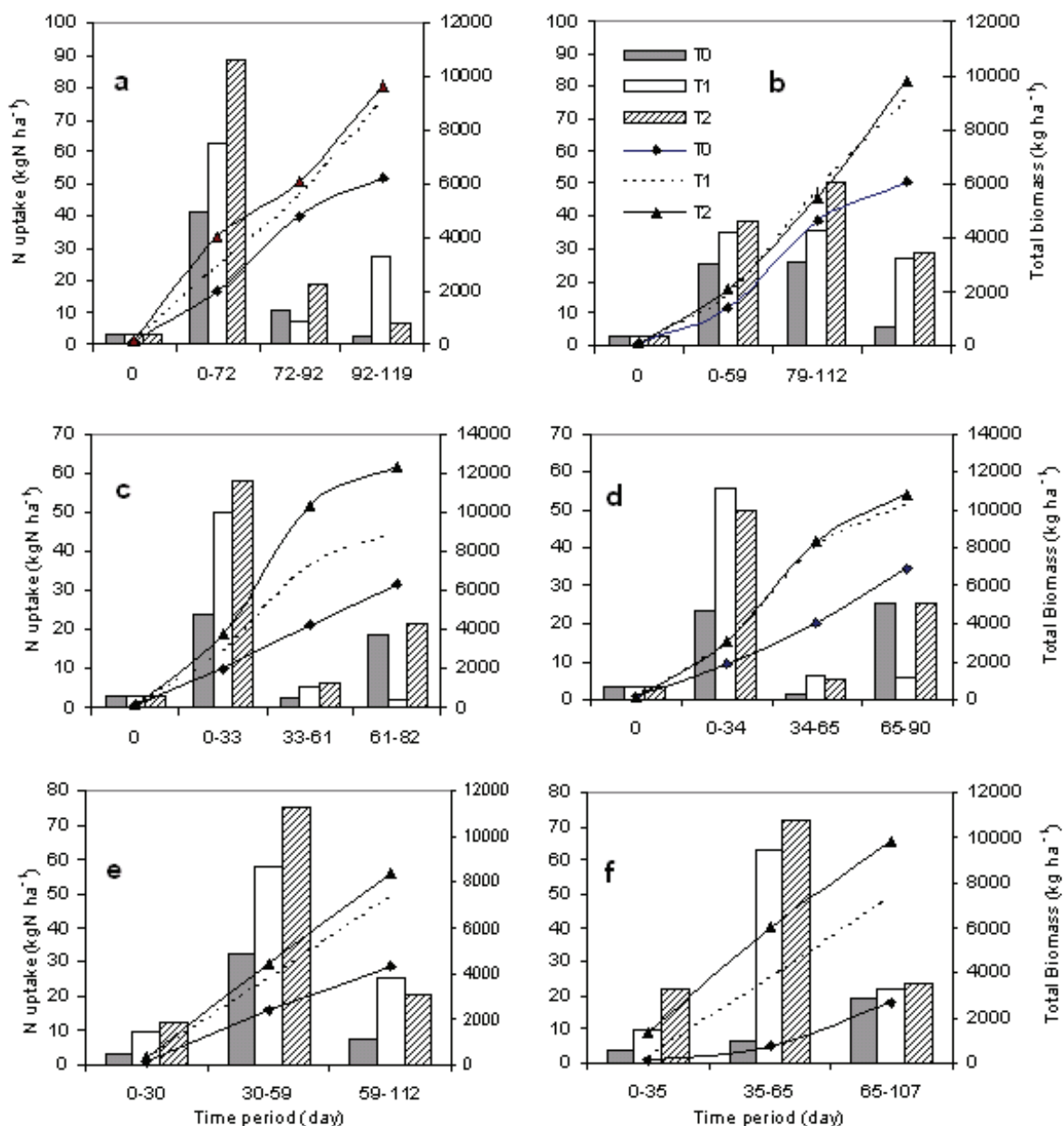


Figure 2. Nitrogen uptake (kg N ha^{-1} , vertical bars relating to left-hand Y-axis) and cumulative total biomass (kg ha^{-1} , continuous lines relating to right-hand Y-axis) at the tillering, flowering and ripening stages of (a) spring rice 2004, (b) spring rice 2005, (c) summer rice 2004, (d) summer rice 2005, (e) winter maize 2004 and (f) winter maize 2005.

2004 than in 2005 for T1, and higher for T2. In this season, the treatment differences in grain yield were small, even though grain yield was highest at the highest fertilizer dose.

In winter, the major constraint for crop growth is water availability. However, the maize crop was adequately irrigated, either through furrow or bucket irrigation with

Table 3. Grain yields in the experiments in 2004 and 2005.

Crop	Yield in dry matter (kg ha ⁻¹)			LSD _{0.05}
	T0	T1	T2	
Spring rice 2004	3057	5325	5425	482.7
Summer rice 2004	3078	3791	4360	268.2
Winter maize 2004	2065	4556	5172	186.4
Spring rice 2005	3047	5320	5740	159.1
Summer rice 2005	3415	4445	4778	103.5
Winter maize 2005	1333	4575	5056	71.6

fertilizers. Mineralization of nutrients from soil organic matter was limited due to low temperatures. Consequently, the manure-only treatment yielded 2.0 and 1.3 Mg ha⁻¹, compared to 5.2 and 5.0 Mg ha⁻¹ in the high fertilizer treatment (Table 3). The differences between treatments were larger in 2005 than in 2004, illustrating the stronger yield response to fertilizer, associated with the low production in the manure-only treatment (Figures 2e, f).

In spring, grain yields in 2004 and 2005 were similar for T0 and T1, but for T2 higher in 2005 (Table 3). In summer, grain yields were higher in 2005 than in 2004 in all treatments, the main reason being the much higher rainfall in summer 2005 (Figure 1). In winter, grain yields were slightly higher in 2005 than in 2004 for T1, but lower for T0 and T2. Note the very heavy rain after sowing of winter maize in 2005 (see Figure 1), resulting in compaction and sealing of the soil, and retarded growth of maize in the first ten days.

The pair-wise relations (Figure 3) between N application, N uptake and grain yield averaged per season, are given in a so-called three-quadrant graph (Van Keulen, 1982). Agronomic efficiency (AE), defined as grain production per kg of N applied, was highest in spring rice, followed by summer rice and winter maize (quadrant c). At the lowest fertilizer rate, AE in winter was appreciable lower than in spring and summer, due to both, a lower recovery (quadrant b) of fertilizer and less ‘dilution’ (quadrant a). The ‘degree of dilution’, expressed in the slope of the uptake-yield curve (physiological efficiency), was lowest in winter and highest in spring. However, the (apparent) recovery fraction (defined as the quantity of a certain nutrient element taken up from fertilized soil minus the quantity taken up from the same but unfertilized soil divided by the quantity of that element contained in the fertilizer) was lower at the highest application rate than at the lower application rate in all three seasons (quadrant b), even though the uptake-yield curve does not suggest that the crop is saturated with N, although the slope slightly decreases (quadrant a). As a result, grain yield was only

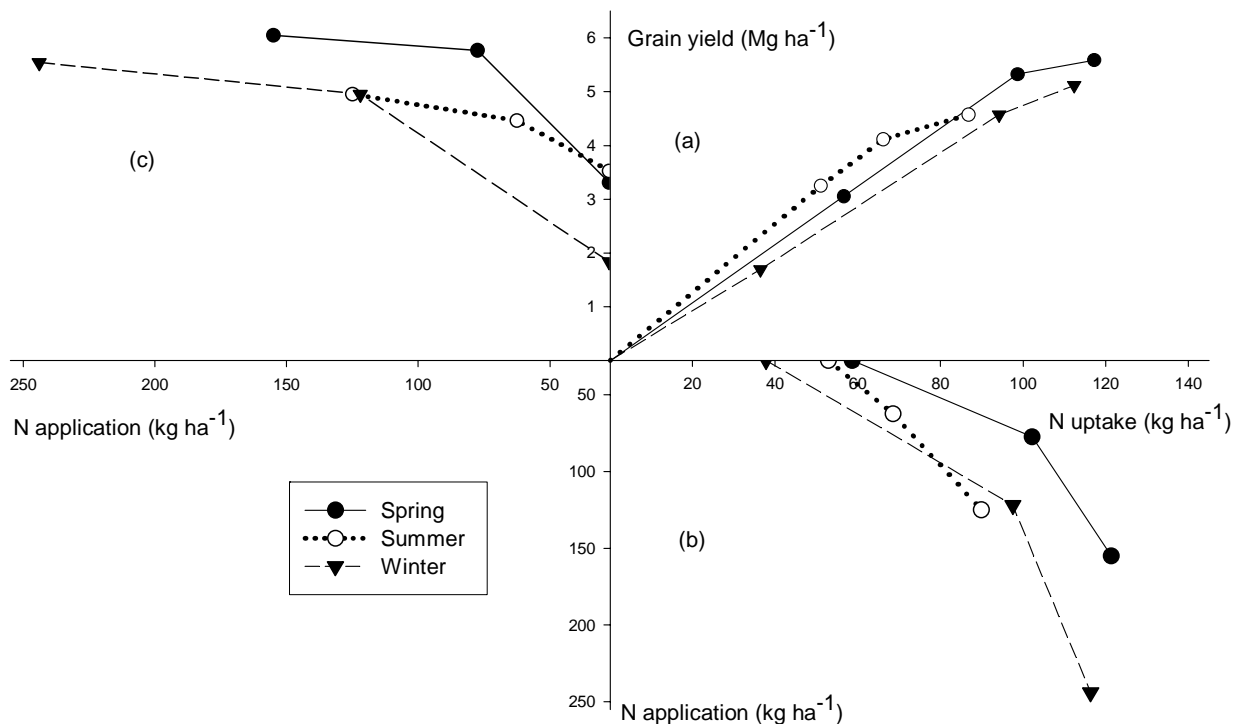


Figure 3. Three-quadrant graph for three seasons. quadrant (a): grain yield vs. N-uptake; quadrant (b): N-uptake vs. N fertilizer application; quadrant (c): grain yield vs. N fertilizer application.

slightly higher at T2 (quadrant c). This levelling off of grain yield on sandy soils is associated with observations of unhealthy plants in T2 at harvest. Dilution was strongest in summer, possibly associated with high rainfall in this season that allowed extended assimilation. On the other hand, levelling off of all three relations in Figure 3 suggests that the attainable yield of summer rice is rather low, as the very sandy nature of the soil restricts the buffering capacity for both water and nutrients.

Nitrogen dynamics

Nitrogen dynamics in the spring season

The nitrate-nitrogen concentration in the soil profile before transplanting of spring rice in 2004 (Figure 4a) was low, and relatively homogeneous in space (not significantly different, $P > 0.05$), and slightly increased with increasing depth, while, with a similar pattern, it was much higher in 2005. At maximum tillering (72 DAT in 2004, 59 DAT in 2005), $\text{NO}_3\text{-N}$ was very high (treatments different at $P < 0.01$), and remained high

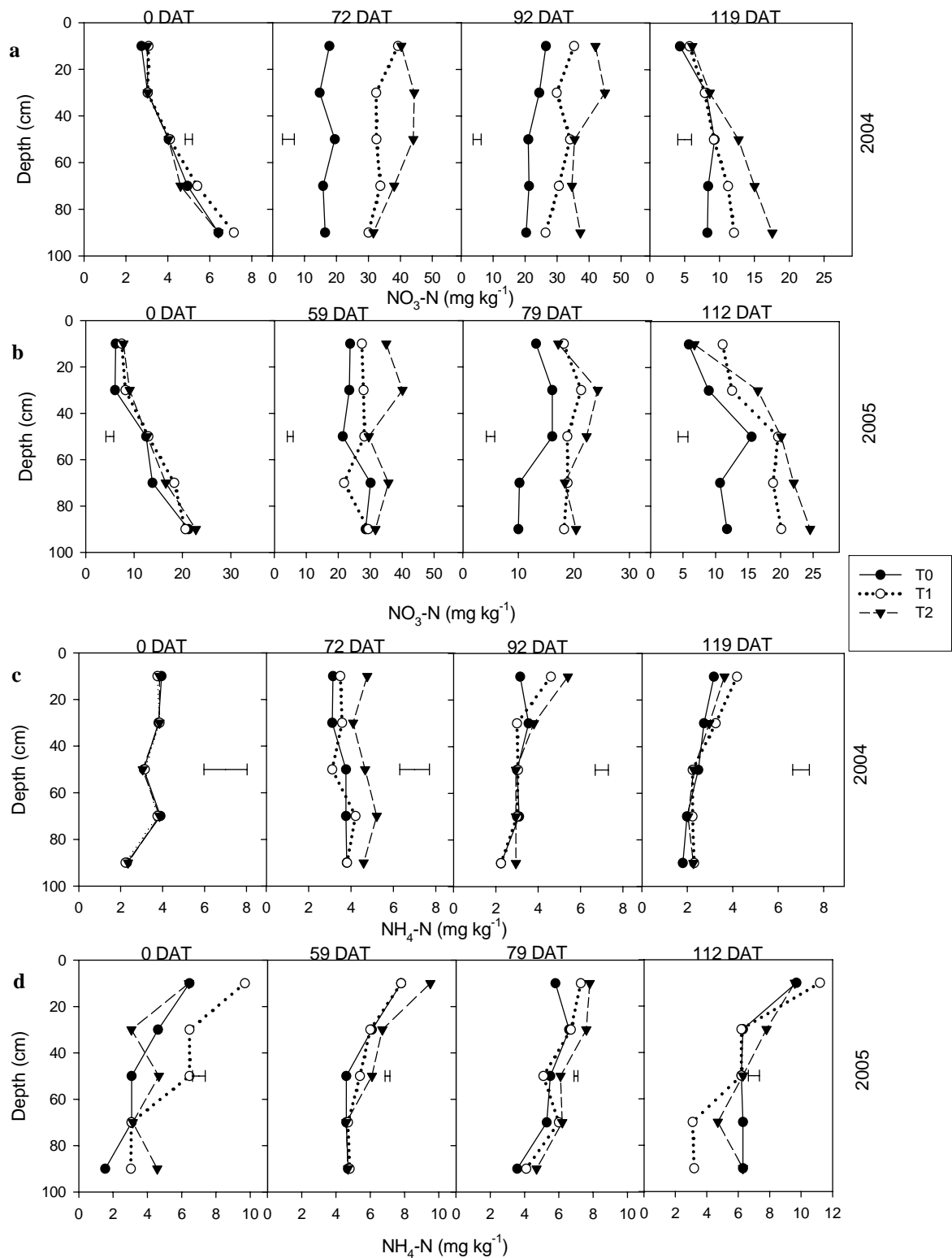


Figure 4. NO₃-N concentrations under spring rice 2004 (a) and 2005 (b); NH₄-N concentrations under spring rice 2004 (c) and 2005 (d), at different soil depths for three treatments. Each error bar represents LSD_{0.05} for all depths for the respective sampling dates. (NOTE: concentration scales are different).

for all treatments until flowering ($P < 0.05$). At harvest time (119 DAT in 2004 and 112 DAT in 2005), $\text{NO}_3\text{-N}$ was low again, especially in the top layers, as soil-N was partly taken up by the crop and partly leached to deeper soil layers ($P < 0.05$). The dynamic pattern of soil $\text{NO}_3\text{-N}$ in both years was qualitatively similar, but quantitatively different (Figure 4a, b), because of differences in rainfall distribution and crop nitrogen uptake.

The ammonium-nitrogen concentration in the soil profile was much lower than that of $\text{NO}_3\text{-N}$. It decreased with increasing depth, as it easily volatilizes and is converted to nitrate in the upper layers. Nitrate, produced through nitrification processes in the upper layers, subsequently moves downward and accumulates in deeper layers (Miller and Gardiner, 2001; Pierzynski et al., 2005). In 2004 (Figure 4c), the variation in $\text{NH}_4\text{-N}$ was small at all fertilizer levels, except at 72 and 92 DAT ($P < 0.05$), which is probably associated with high fertilizer doses and low N uptake. In 2005 (Figure 4d), however, the variation in $\text{NH}_4\text{-N}$ among treatments in all growth periods was large, with significant treatment differences ($P < 0.01$) at all sampling dates.

Nitrogen dynamics in the summer season

About 20% of the spring rice straw was ploughed in, after which the soil was submerged for 15 to 20 days before transplanting of summer rice. Under the high rainfall and temperature conditions, part of the soil organic matter and the rice straw were decomposed. In this process, Nmin is first immobilized in growing microbial biomass (Van Keulen and Seligman, 1987), and subsequently mineralized, following death of the microbes. As a result, the $\text{NO}_3\text{-N}$ content at transplanting was high (Figures 5a and b).

All manures, and small doses of inorganic N fertilizer for T1 and T2, were applied at transplanting (Table 2). Most of the inorganic N fertilizer was applied at 10 days after transplanting. In combination with the nitrogen mineralized from decomposing manure, this resulted in high $\text{NO}_3\text{-N}$ concentrations in the soil profile that exceeded crop requirements in this period. At maximum tillering (33 and 34 DAT; Figures 5a and b), $\text{NO}_3\text{-N}$ was still very high. Subsequently, it declined through crop uptake, overland flow, and leaching while no further fertilizer was applied. At flowering (61 DAT in 2004, 65 DAT in 2005), $\text{NO}_3\text{-N}$ in the upper layers was higher in 2004 than in 2005, which could be associated with differences in rainfall distribution, i.e. evenly distributed in 2004 and very high and early (i.e. a skewed distribution) in 2005 (see Figure 1). In 2004 (Figure 5a), treatment differences were significant ($P < 0.01$) at 33 and 82 DAT but not at 0 and 61 DAT ($P > 0.05$), while in 2005 (Figure 5b), treatment differences were significant ($P < 0.01$) at all dates.

The dynamic patterns of soil $\text{NH}_4\text{-N}$ were quite different in the two years, as in

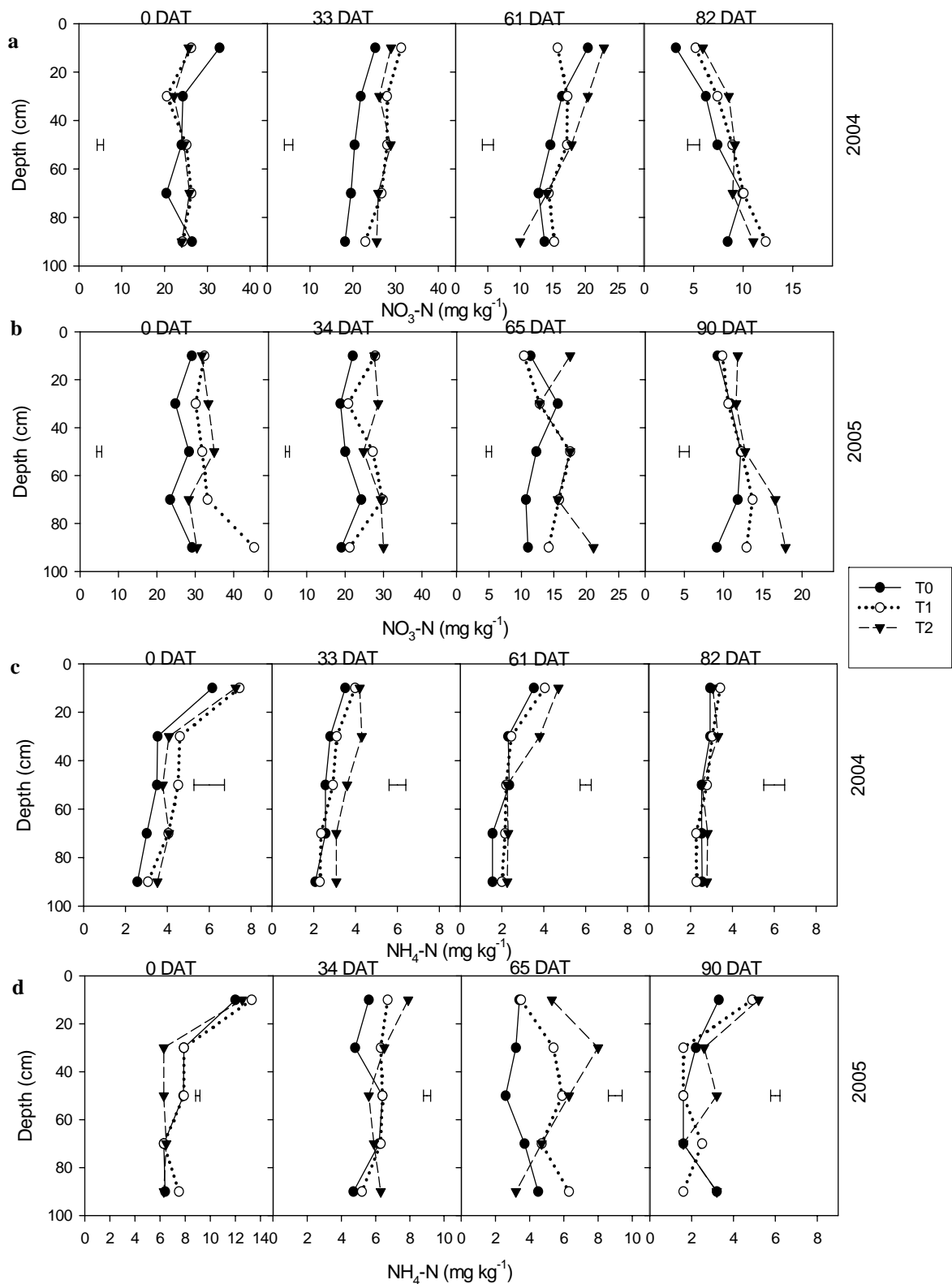


Figure 5. NO₃-N concentrations under summer rice 2004 (a) and 2005 (b); NH₄-N concentrations under summer rice 2004 (c) and 2005 (d), at different soil depths for three treatments. Each error bar represents LSD_{0.05} for all depths for the respective sampling dates. (NOTE: concentration scales are different).

2005, with higher rainfall, $\text{NH}_4\text{-N}$ concentrations in the deeper layers were higher. In 2004 (Figure 5c), the highest $\text{NH}_4\text{-N}$ in the soil profile was in T2, followed by T1, with treatment differences significant at 33 and 61 DAT ($P < 0.01$), but not at 0 and 82 DAT ($P > 0.05$). In 2005 (Figure 5d), $\text{NH}_4\text{-N}$ in the soil was significantly different among treatments ($P < 0.01$) at all dates, even though the dynamic $\text{NH}_4\text{-N}$ pattern varied among layers. At transplanting, the highest $\text{NH}_4\text{-N}$ was found in the top soil layers in both years, reflecting N mineralization from soil organic matter and ploughed-in crop residues, in the absence of crop uptake and with low leaching.

Nitrogen dynamics in the winter season

In winter, rainfall was very low, while humidity and temperature gradually declined, so that irrigation was increasingly needed to secure adequate water supply for crops. The soil was wetted at sowing and then gradually dried out due to low rainfall and high evapo-transpiration rates. Concurrently, lowering of the groundwater table in the region resulted in drying out of the subsoil and the deep layers. This led to downward moisture transport, due to developing (potential) gradients. Appreciable quantities of N were applied in manure, urine and inorganic fertilizer through ‘bucket irrigation’, concentrated in the period between 5 and 25 DAS (Table 2). As crop uptake in this period was low, very high $\text{NO}_3\text{-N}$ -levels (significant treatment differences at $P < 0.01$) of 59 and 54 mg N kg^{-1} soil were recorded at the 9th-leaf stage, 30 and 35 DAS, respectively. In 2004 (Figure 6a), $\text{NO}_3\text{-N}$ was concentrated mainly in the upper soil layers (especially in the period 30–60 DAS), whereas in 2005 (Figure 6b) it was more evenly distributed over the profile. Maize growth and nutrient uptake rates in the two years were similar, but rainfall was higher and earlier in 2005 (198 mm till 35 DAS and 292 till 65 DAS in 2005 vs. 15 mm till 30 DAS and 26 till 59 DAS in 2004). The high rainfall conditions in 2005 were conducive for nitrate leaching, which explains the shape of the $\text{NO}_3\text{-N}$ profile at 35 DAS. Subsequently, $\text{NO}_3\text{-N}$ decreased, but remained high throughout the growing period.

For ammonium, small changes in $\text{NH}_4\text{-N}$ in the deep soil layers indicate limited $\text{NH}_4\text{-N}$ leaching. The dynamic pattern of $\text{NH}_4\text{-N}$ in the soil varied among periods and years, especially for the periods of 30–35 and 59–65 DAS. In these periods, $\text{NH}_4\text{-N}$ seems evenly distributed over the whole soil profile, while it mostly accumulated in the second layer in 2005 (Figure 6d). At harvest time, $\text{NH}_4\text{-N}$ in the first three layers was very low, because of high crop uptake during the grain filling stage (42 days).

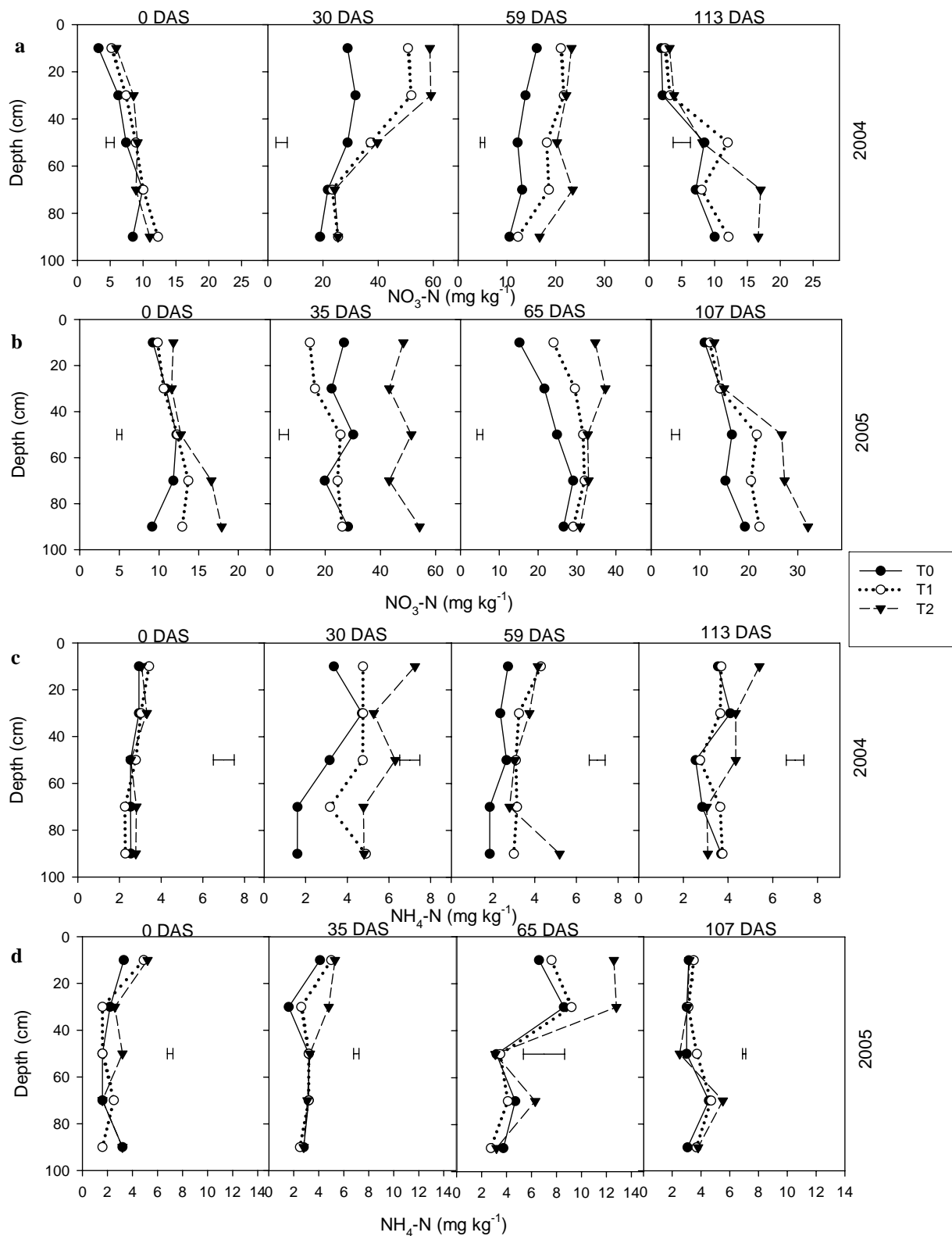


Figure 6. $\text{NO}_3\text{-N}$ concentrations under winter maize 2004 (a) and 2005 (b); $\text{NH}_4\text{-N}$ concentrations under winter maize 2004 (c) and 2005 (d), at different soil depths for three treatments. Each error bar represents $\text{LSD}_{0.05}$ for all depths for the respective sampling dates. (NOTE: concentration scales are different).

Model calibration and nitrogen leaching losses

Model calibration

The study area is characterized by sandy soils on terraces, with weakly developed profiles, in which the effects of puddling are negligible. Moreover, the fields were not always flooded, because of their position in the landscape and the sandy soil texture. Irrigation was applied in dependence of rainfall distribution and soil moisture conditions. The model was therefore calibrated for soil conditions in the absence of puddling, on the basis of the water and nitrogen balance sub-models via modification of soil hydraulic conductivity. Clay content in the soil profile decreased with increasing depth to 60 cm, after which it increased with increasing depth (Table 1). These variable clay contents determine hydraulic conductivity. On the other hand, the objective of the current calibration was to identify a parameter set resulting in the best fit between simulated and measured Nmin in each soil layer.

Values of hydraulic conductivity of 103.2, 100, 30, 30, and 12 mm d⁻¹ for the 5 successive layers resulted in the best simulation of water and nitrogen dynamics. Soil moisture content (in the dry season) was initialized throughout the profile at 0.18 cm³ cm⁻³. Initial Nmin was set to 17.7 mg kg⁻¹ for the second layer and 10.7 mg kg⁻¹ for the remainder of the profile. Calibration results (Figure 7) showed satisfactory agreement for the top layer of treatments T1 and T2, and reasonable agreement for T0 with a slight underestimation of Nmin. In T1 and T2 both, manure and inorganic fertilizer were applied, in which a very large proportion of Nmin originates from the inorganic fertilizer that easily hydrolyses. The contribution from inorganic fertilizers to mineral soil N is more easily estimated than that from manure, that contains different organic carbon and N pools with different decomposition and mineralization rates. In addition, other sources of N, such as rainfall, irrigation and fixation represented a significant proportion of total Nmin in T0, whereas they represented a small proportion in T1 and T2. These may be reasons for the less accurate Nmin simulations in the manure-only treatment. For the bottom layers (Figures 7b, d, and f), simulated results are satisfactory for all three treatments, albeit the temporal variation in measured Nmin is much higher than in the simulated values. In the manure-only treatment (Figure 7b), Nmin tends to decline with time, while it is stable in T1 (Figure 7d) and increases in T2 (Figure 7f), indicating declining soil fertility in T0, compared to stable and improving conditions in T1 and T2, respectively.

Nitrogen leaching losses

Following model calibration, a period of two years was simulated, covering two triple crop rotations. Cumulative leaching losses over each period (Table 4) were calculated

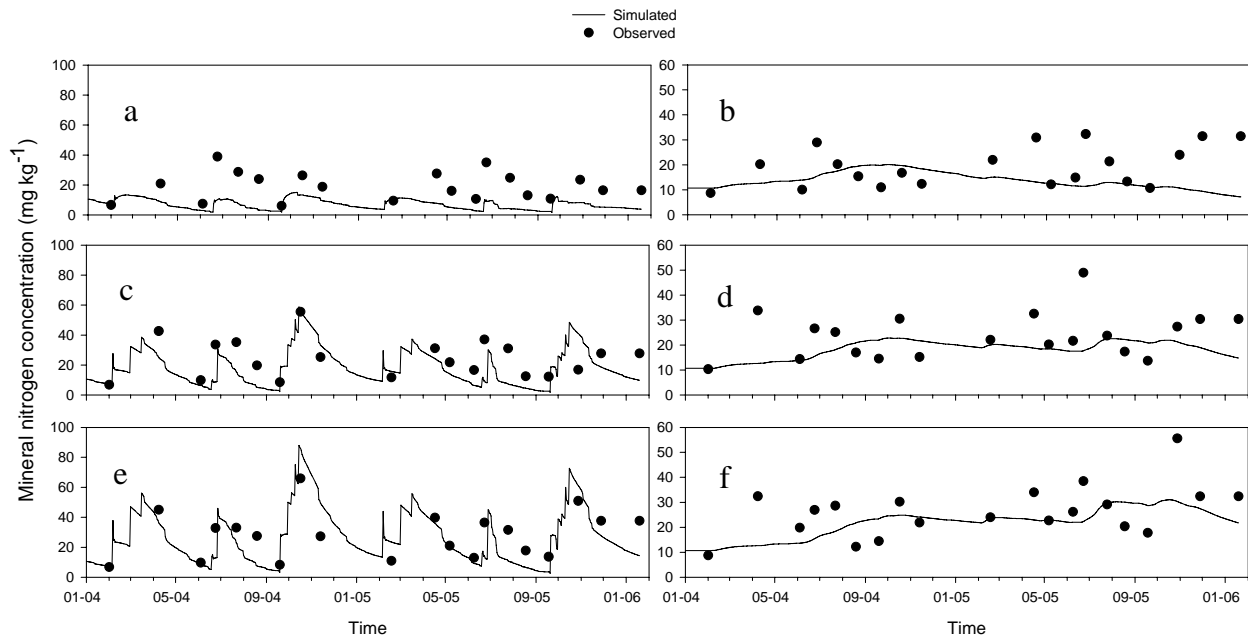


Figure 7. Simulated and observed N_{min} concentration in the soil ($mg\ kg^{-1}$) in (a) 0–20 and (b) 80–100 cm of treatment T0, (c) 0–20 and (d) 80–100 cm of treatment T1, and (e) 0–20 and (f) 80–100 cm of treatment T2, during 2004–05.

from simulated percolation flow volumes and the calibrated N_{min} concentrations in the soil solution.

High N leaching rates result from high percolation, associated with high rainfall and irrigation, combined with high fertilizer application. Growth periods with high N leaching, were 61–82 DAT for summer rice 2004, 0–59 DAS for winter maize 2004, 0–59 DAT for spring rice 2005, the whole summer of 2005 and winter maize in 2005. In general, N leaching was high during the growth periods of summer rice, characterized by very high rainfall (Figure 1), and during the early growth periods of winter maize, characterized by high irrigation and fertilizer application. The highest N leaching was calculated for the first period (0–35 DAS) of winter maize in 2005 (from 9.7 to 28.9 $kg\ ha^{-1}$). N leaching was low in the spring season, because of low rainfall, despite high fertilizer application in this period. However, N leaching was high in early spring 2005 (8.2 to 16.3 $kg\ ha^{-1}$), because of concurrent irrigation and high fertilizer application in the rice tillering stage.

With a total rainfall and irrigation of 1552 and 1780 mm in 2004 and 2005, respectively, calculated annual percolation values were 418.5 and 1005.5 mm in T0, 380.3 and 973.5 in T1, and 359.1 and 926.5 in T2. Annual N leaching losses were 52.4 and 59.5 $kg\ ha^{-1}\ yr^{-1}$ in T0, 55.9 and 114.0 in T1, and 58.1 and 153.9 in T2, respectively.

Table 4. Calculated percolation flow and nitrogen losses in each growing period of three treatments during two years (2004–05) and annual nitrogen losses in each rotation (simulation covered the period from 1st January 2004 to 19th January 2006).

Date	Season	DAT/ DAS*	Percolation (mm)			Nitrogen losses (kg ha ⁻¹)		
			T0	T1	T2	T0	T1	T2
01-02-04	Spring	0	0.10	0.10	0.10	0.01	0.01	0.01
18-04-04		72	9.00	9.01	8.81	0.92	0.92	0.90
08-05-04		92	12.27	11.01	9.76	1.33	1.19	1.05
04-06-04		119	12.05	10.50	9.16	1.35	1.17	1.02
24-06-04	Summer	0	16.55	15.21	13.61	1.99	1.84	1.64
22-07-04		33	37.25	35.43	34.31	5.04	4.94	4.82
19-08-04		61	61.61	58.24	54.74	8.84	9.07	8.93
19-09-04		82	83.49	79.65	75.74	11.63	12.77	13.22
17-10-04	Winter	30	81.19	77.76	74.29	10.42	12.23	13.29
13-11-04		59	70.58	67.37	64.17	8.02	9.85	11.04
11-01-05		112	34.42	15.97	14.39	2.90	1.95	2.17
17-02-05	Spring	0	58.94	56.67	51.24	4.61	6.68	7.57
17-04-05		59	113.78	113.05	106.98	8.19	13.20	16.26
7-05-05		79	16.01	15.69	14.77	1.01	1.73	2.17
9-06-05		112	49.20	47.19	43.70	2.97	5.10	6.35
23-06-05	Summer	0	21.06	19.62	17.61	1.22	2.09	2.54
25-07-05		34	97.87	94.49	89.93	6.17	11.80	15.58
18-08-05		65	97.08	94.78	91.77	6.25	12.80	17.60
18-09-05		90	116.67	113.12	108.84	6.96	14.55	20.20
18-09-05	Winter	0						
28-10-05		35	169.94	164.68	158.72	9.68	20.38	28.91
28-11-05		65	124.16	120.17	115.77	6.36	13.23	19.03
19-01-06		107	140.79	134.01	126.91	6.07	12.46	17.74
2004	Sum		418.53	380.26	359.09	52.44	55.94	58.08
2005	Sum		1005.50	973.46	926.24	59.49	114.01	153.94

* Days after transplanting (DAT) and days after sowing (DAS),
total rainfall + irrigation = 1552 and 1780 mm in 2004 and 2005, respectively.

DISCUSSION

The magnitude of nitrogen leaching, one of the main pathways for nitrogen losses from agricultural systems, is determined by complex inter-relationships among soil (type), crop, environment (rainfall, radiation and temperature, determining crop

demand), and management (fertilizer, i.e. dose, method, timing) and irrigation, that are not fully understood (Goulding, 2000; Delgado, 2002; Verloop et al., 2006). In rainfed lowland rice-based systems, Tripathi et al. (1997) found a wide range in both, soil nitrate and ammonium concentrations for different growth periods, crops and seasons, and concluded that N_{min} is most likely lost in the early growth stages, when crop N-demand is low. Nitrate leaching has been reported to increase with increasing fertilizer application in winter wheat-maize rotations in China (Liu et al., 2003), as has been confirmed in many other studies (Allaire-Leung et al., 2001; Aronsson, 2001; Dimitriou and Aronsson, 2004; Rimski-Korsakov et al., 2004), with however, large spatial and temporal variation (Ghosh and Bhat, 1998). Rimski-Korsakov et al. (2004) indicated that higher yields, associated with higher N-demands, reduce the risk for nitrate leaching. Our results indicate that NO_3-N is the main component of leaching losses, its concentration in soil being 8 to 10 times higher than that of NH_4-N (Figures 4 to 6). Temporally, nitrate concentration varied widely, i.e. very low before the cropping period, quickly increasing after transplanting/sowing associated with fertilizer application (Figures 4 to 6), even in the lower soil layers in this very sandy soil with high infiltration rate. For ammonium, the variation was smaller. In all seasons, NH_4-N accumulated in the upper layers, at tillering in rice or the 0 to 9th leaf-stage in maize, as a result of adding N fertilizers, but hardly in the lower layers (Figures 4 to 6). Therefore, it can safely be assumed that NH_4-N leaching is very small. In both, rice and maize, high N concentrations occurred in the early growth stages, due to excess fertilizer application and low plant uptake. In summer however, N leaching can be high in the later growth stages, due to late and high rainfall. Because, whatever the nitrate concentrations, leaching losses depend on percolation generated from rainfall and irrigation. Nitrogen leaching has been quantified on the basis of nitrogen balance calculations, i.e., Tripathi et al. (1997) calculated apparent N losses as the balance of initial available soil N, fertilizer-N applied and N mineralized from weed residues on one hand and N removed and residual mineral soil N on the other. Liu et al. (2003) calculated NO_3-N losses on the basis of measured NO_3-N concentrations at different soil depths, while Chikowo et al. (2004) used differences in N_{min} concentration at different sampling dates to calculate N leaching per soil layer and for the whole soil profile. Alternatively, under uniform irrigation conditions during two growing seasons, Allaire-Leung et al. (2001) found nitrate leaching, estimated by anion-exchange resin bags, to be positively correlated to soil NO_3-N content in different soil layers up to 1.2 m depth. However, such correlations are site- and time-specific and cannot be used for extrapolation. Therefore, as leaching is a dynamic process, accurate quantification requires a coherent description of all relevant processes in a dynamic model. The method applied in this study, combining field

measurements of $\text{NO}_3\text{-N}$ concentrations with model-calculated water balances and nitrogen transport, appears promising. Nonetheless, calculated leaching losses would have been more reliable with higher spatial and temporal resolution of sampling and inclusion in the model of other nitrogen transformation processes, such as volatilization and denitrification, as influenced by climatic conditions, and lateral flows. In addition, other N sources, such as rainfall, irrigation, and fixation should be taken into account. For instance, the underestimation of N concentration in the soil (Figure 7a) might be associated with omission of these terms in the model.

Percolation volume increases in the order $T_0 > T_1 > T_2$, whereas N leaching losses follow an inverse trend. Crop production follows the order $T_2 > T_1 > T_0$, which is thus also the order for evapo-transpiration, so that the quantity of water available for downward movement follows the order $T_0 > T_1 > T_2$. However, N leaching increases in the order $T_0 < T_1 < T_2$, because of the difference in N concentration, resulting from fertilizer application.

CONCLUSIONS

Understanding the dynamics of nitrogen leaching and quantitative information on actual leaching losses are indispensable for formulation of recommendations, aimed at increasing fertilizer use efficiency. Information on leaching losses from the four million ha of rice soils in Vietnam as a whole, and from rice soils on the sandy terraces in hilly and mountainous areas in particular, characterized by low N fertilizer use efficiencies, is scarce. These systems are highly susceptible to nutrient losses due to surface runoff and leaching. Our results indicate high N losses under current management, i.e. 52 to 60, 56 to 114 and 58 to 154 $\text{kg N ha}^{-1} \text{ yr}^{-1}$ for low, medium, and high fertilizer inputs, respectively. Risks for leaching losses can be substantially reduced by cautious management with respect to fertilizer application and irrigation in the early growth stages of all crops. To reduce losses, different types of fertilizer and application methods should be used. For example, farmers could apply more manure to increase water and nutrient holding capacity and gradually provide nutrients until the grain filling period; inorganic nitrogen fertilizers could be applied in split doses, synchronized with the demand of the crop, to increase fertilizer use efficiencies and maximize economic returns.

CHAPTER 7

Spatio-temporal prediction of nitrogen concentrations in shallow groundwater under intensive farming in northern Vietnam using regression-kriging

V.T. Mai^{1,5}, H. Van Keulen^{1,2}, U. Leopold^{3,6}, R.P. Roetter⁴

- ¹ Plant Production Systems Group, Wageningen University, P.O. Box 430, 6700 AK Wageningen, The Netherlands
- ² Plant Research International, Wageningen University and Research centre, P.O. Box 16, 6700 AA Wageningen, The Netherlands
- ³ Resource Centre for Environmental Technologies, Public Research Centre Henri Tudor, Technoport Schlassgoart, P.O. Box 144, 4002 Esch-sur-Alzette, Luxembourg
- ⁴ Soil Science Centre, Alterra Green World Research, Wageningen University and Research centre, P.O. Box 47, 6700 AA Wageningen, The Netherlands
- ⁵ National Institute for Soils and Fertilizers (NISF), Dong Ngac, Tu Liem, Hanoi, Vietnam
- ⁶ Institute for Biodiversity and Ecosystem Dynamics, University of Amsterdam, Nieuwe Achtergracht 166, 1018 WV Amsterdam, The Netherlands

Abstract

A study was conducted in Van Hoi commune, Tam Duong district, the Red River Delta in northern Vietnam. The objective of study was to determine nitrogen concentrations in shallow groundwater under various environmental conditions (soil and topography) and land use types. Water samples were taken at one meter depth during the growing season, using an open porous pipe and hand pump, at four sampling dates in two years (March, August 2004 and March, August 2005). Nitrate- and ammonium nitrogen concentrations were determined. Explanatory variables were partly derived from a stepwise backward linear regression as well as from expert knowledge, to improve the spatial predictions of nitrogen concentrations in groundwater. Semi-variograms were computed and appropriate models were established for original nitrogen concentrations, as well as for the residuals derived from regression analysis. Nitrogen concentrations were predicted using both, ordinary block kriging and regression block kriging. Regression block kriging yielded more accurate results, taking into account additional information in the generalized linear regression. Temporal changes in nitrogen concentrations in the groundwater were mainly the result of variations in environmental conditions, such as rainfall and land use with different irrigation and fertilizer regimes.

Keywords: Nitrate pollution, geostatistics, multiple regression, intensive farming

INTRODUCTION

In recent years, groundwater pollution due to human activities has been recognized as an increasing environmental threat in many countries throughout the world. In Asian countries intensive farming systems have developed in recent decades. Water for drinking and other domestic uses in many poor rural areas originates from polluted sources such as shallow aquifers under agricultural land (Pingali and Roger, 1993). A countrywide survey of the Vietnam Cancer Institute (NCI, 2002) showed that stomach cancer is the second leading form of cancer in males and the third one in females. The main cause of this disease is the consumption of food (in particular, vegetables and water) with high contents of nitrate and nitrite (Anh et al., 2002). Extensive research on groundwater quality problems has been conducted, by both agricultural and environmental scientists at farm, regional and national scales (Van Keulen, 2001; Ondersteijn et al., 2002; Sheldrick et al., 2002; Wolf et al., 2005). In Japan, $\text{NO}_3\text{-N}$ concentrations in well water have been recorded of up to 100 mg l^{-1} . These values tended to decrease following reductions in fertilizer application rates (Kumazawa, 2002). In China, ground- and drinking water were measured at 69 locations, covering $14,000 \text{ km}^2$ (Zhang et al., 1996); more than half of the samples showed NO_3 concentrations exceeding 50 mg l^{-1} (exceeding 300 mg l^{-1} at two locations). Moreover, residues of fertilizers and other chemicals from agriculture, that is increasingly intensified, represent non-point pollution sources to surface and groundwater. Xing and Zhu (2000) estimated that NO_3 -leaching from uplands in the north of China accounted for 0.5–4.2% of the applied chemical N-fertilizer. Values for paddy fields in the south ranged from 6.75 to $27.0 \text{ kg N ha}^{-1} \text{ yr}^{-1}$. Studies at farm level (Hack-ten Broeke and De Groot, 1998; El-Sadek et al., 2003; Verloop et al., 2006), corroborate that agriculture is a major contributor to NO_3 -leaching to groundwater. Fuentes et al. (2003) found in Washington State (USA) that after harvest, up to $90 \text{ kg NO}_3\text{-N ha}^{-1}$ can be leached to depths of 1.5 to 2.5 m, which was attributed to inefficient or excessive use of fertilizer.

Stored and flowing in the aquifers and soil pores, groundwater quality varies spatio-temporally under the influence of inputs and environmental factors, such as elevation, soil type, land use and geo-hydrological conditions (Pebesma and De Kwaadsteniet, 1997). Spatial variation can be mapped by interpolation from point observations. Different interpolation methods have been applied, such as moving averages, Thiessen polygons or distance-related algorithms (Goovaerts, 2000). Currently, geostatistics is the recommended method, in particular kriging techniques (Goovaerts, 1994; 2000; Hengl et al., 2004; Leopold et al., 2006). Geostatistical methods have been applied in various scientific disciplines for mapping soil properties (Goossens and Riksen, 2004; Lemke et al., 2004), rainfall distribution (Goovaerts, 2000), erosivity (Goovaerts,

1999), and groundwater quality (Pebesma and De Kwaadsteniet, 1997; Cinnirella et al., 2005). Kriging belongs to the family of generalized linear models; it uses weighted point observations to predict on the point or block support. The weights are determined from semi-variogram models and are calculated in such a way that the estimation error in each output pixel is minimized. For natural conditions, simple kriging can be applied for interpolation of N concentrations in shallow groundwater. As Pebesma and De Kwaadsteniet (1997) pointed out, in agricultural areas, many environmental factors can influence groundwater quality, such as soil type, land use, and geohydrological conditions (e.g. depth of groundwater table, infiltration or seepage, marine influence, precipitation) which have to be taken into account in interpolation procedures. The objectives of this study were to measure nitrogen concentrations in shallow groundwater under intensive agriculture with high fertilizer use and to produce spatial nitrogen concentrations for the whole area of 290 ha, using geostatistics.

METHODOLOGY

Study area

Van Hoi commune, with a total area of 290 ha, is located in the flat land of Tam Duong district, 60 km north of Hanoi (Figure 1). Soils in the commune consist of 224 ha (77.4%) Endogleyic Dystric Plinthosols and 66 ha (23.6%) Albi Dystric Plinthosols (FAO/UNESCO, 1974; FAO, 1976), while texturally they comprise 126 ha (53.8%) of sandy loam and 109 ha (46.2%) of clay loam as shown in Figure 3. The climate is characterized by two main seasons: a rainy season (May–September) and a dry season (October–April), with differences in rainfall, evaporation, temperature, and solar radiation.

Land use and fertilizer use

Land use in the area consists of paddy rice, vegetables, and other horticultural crops. The main rotation is triple cropping, including double rice and a winter crop. In well-irrigated soils, vegetables can be grown continuously. The number of harvests in such vegetable rotations depends on crop rotation, market opportunities, availability of labor and capital. The commune is situated very close to the provincial center, where purchasing power and consumption of food and vegetables are high. This situation allows farmers to intensify cultivation systems through introducing new high-value and high-yielding crops and investing in external inputs as fertilizers. Currently, nitrogen fertilizers are applied at different rates to different crops: the highest doses are applied to flowers (up to 984 kg N ha⁻¹ yr⁻¹), followed by chili and the ‘squash group’, consisting of cucumber, tomato and pumpkin (up to 817 kg N ha⁻¹ yr⁻¹), the ‘cabbage

group', consisting of paprika, cabbage, eggplant and kohlrabi (up to 645 kg N ha⁻¹ yr⁻¹), and paddy rice (up to 427 kg N ha⁻¹). During the main cropping season, from February till the end of September, rice fields are flooded and non-rice fields are adequately irrigated and sometimes flooded in the rainy season (from June till August). Under these conditions, percolation takes place and hence, nitrogen can be leached below the root zone, which causes nitrogen pollution of the groundwater.

Sampling design and chemical analysis

Water samples were taken at four moments, i.e. 6th March and 15th August 2004 and 26th March and 8th August 2005. March represents the early spring season that follows a long dry period, while August represents the mid-summer season with the highest rainfall in the year. At each occasion, 52 samples, distributed throughout the whole commune (Figure 1), were taken using porous pipes. PVC pipes, 3 cm in diameter, were inserted in pre-drilled holes into the soil to 1 m depth. Small PVC pipes (0.5 cm in diameter) were inserted into the wide pipes till the bottom. Before the sample was taken, the water in the porous pipes was pumped off several times. Water from the

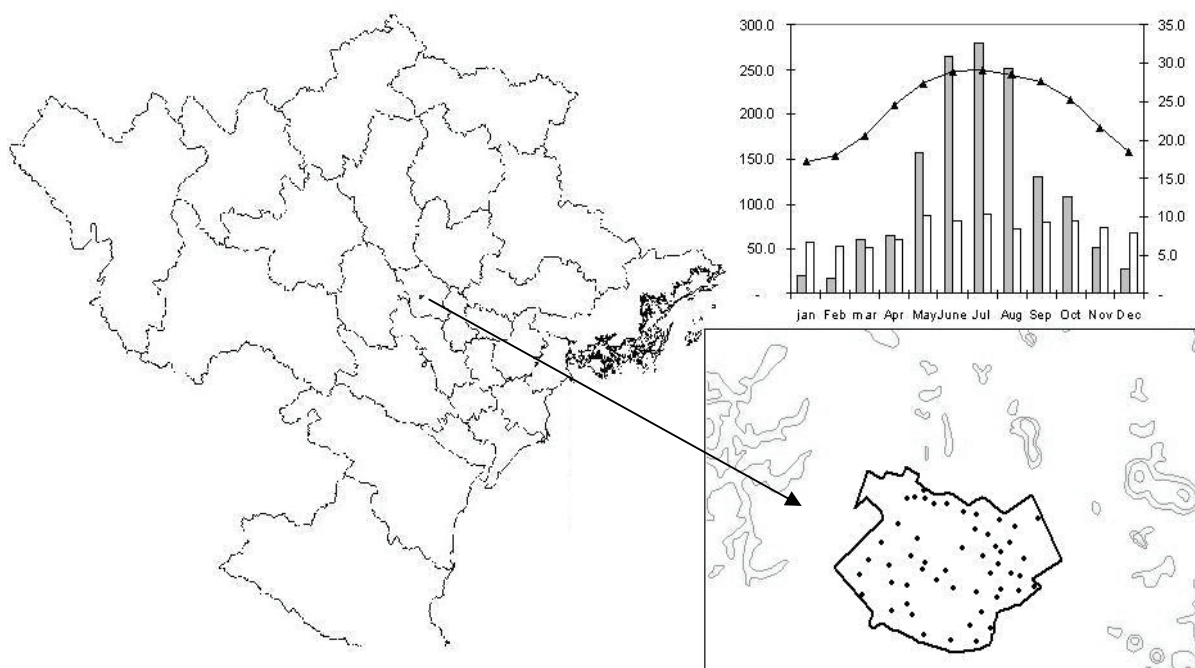


Figure 1. Study area location in the north of Vietnam; sampling point map overlaying the topographic map with contour lines. Average weather conditions in the study area are shown on the inset graph with monthly rainfall (solid bars; mm) and monthly potential evapotranspiration (blank bars; mm) on the left hand Y-axis, and monthly mean temperature (triangles; °C) on the right hand Y-axis.

pipe was collected by hand pump, through a vacuum bottle, transferred to plastic bottles and stored at 4 °C till chemical analysis. Water samples were filtered through 0.45 mm Whatman paper, and the extract was distilled for determination of NH₄-N and NO₃-N, using micro-Kjeldahl.

Spatio-temporal analysis and prediction

To take into account the spatial correlation of the observed NO₃ and NH₄ concentrations, for each sampling date semi-variograms were computed for the observations, as well as their residuals derived from stepwise generalized linear regression. The semi-variance is a measure of spatial auto-correlation and can be expressed as:

$$\gamma(h) = \sum_{i=1}^{n(h)} \frac{(z(x_i + h) - z(x_i))^2}{n(h)} \quad (1)$$

where, z is the random variable at location x_i and h is the lag distance in space between the points.

Ordinary block kriging (OBK) and regression block kriging (RBK) were used for prediction (Goovaerts, 1997; Hengl et al., 2004; Leopold et al., 2006) in order to yield averages for larger supports than the point support, as uncertainty of predictions increases with decreasing size of support and the number of available sampling locations used in this study. Ordinary kriging uses weighted linear combinations of the observations of Z to predict Z at unobserved locations. The weights are chosen such that the prediction error variance is minimized, under the condition of unbiasedness. The weights are a solution to the kriging system, and can be expressed in terms of semi-variogram values, that describe the spatial autocorrelation structure of Z . In mathematical terms, the ordinary kriging predictor is defined as:

$$\hat{Z}(B) = \sum_{i=1}^n \lambda_i Z(x_i) \quad (2)$$

where, $\hat{Z}(B)$ is the predictor of the average value of Z over a block B , obtained from the n observations $Z(x_i)$, using weights λ_i . In regression kriging, an extension of ordinary kriging, the mean of Z is taken as a non-constant trend, defined as a linear regression on explanatory variables. Thus, in regression kriging the random function Z is defined as the sum of a deterministic trend m and a zero-mean stochastic residual ε :

$$\hat{Z}(x) = m(x) + \varepsilon(x) = \sum_{k=0}^m \beta_k y_k(x) + \varepsilon(x) \quad (3)$$

where, β_k are regression coefficients and y_k explanatory variables (usually y_k is taken as 1, so that β_k is the intercept of the regression). Prediction, using regression block

kriging, follows from:

$$\hat{Z}(B) = \sum_{k=1}^m \hat{\beta}_k y(B)(x) + \sum_{i=1}^n \kappa_i \varepsilon(x_i) \quad (4)$$

The regression coefficients are estimated from the observations, using weighted least squares. We can possibly use the regression coefficients derived at the point support for estimations on the block support. The regression model is linear and thus, the block predictions and the corresponding prediction variance are not affected by a change in support (Heuvelink and Pebesma, 1999). The kriging weights k_i are solved by the kriging system, and are expressed as semi-variogram values of the residuals. The corresponding regression kriging variance incorporates the uncertainty on the estimation of the regression coefficients (Leopold et al., 2006). To compare regression kriging to ordinary kriging and plain regression for three target variables, i.e. soil organic matter, pH, and soil thickness, Hengl et al. (2004) used six relief parameters (DEM, slope, mean topographic index, stream power index, watershed) and 9 soil mapping units. Regression kriging gave better results than ordinary kriging and plain regression methods. In this study, candidate explanatory variables for NO_3 and NH_4 were elevation, soil type, soil texture class, and land use type. The soil and land use maps were obtained by reclassification of the original soil and land use maps, to achieve reliable estimates of the regression coefficients. Soil type and land use were categorical variables and were transformed to binary variables of zero and one to be used in Eqn 3.

Explanatory variables were selected for linear regression analysis, using the statistical software package Genstat (Lawes Agricultural Trust, 2003). Residuals at observation locations were computed by subtracting the fitted regression line from the observations. Experimental semi-variograms were computed for the original observations, as well as for the residuals. Variogram models were fitted by ordinary least squares, selecting the correct values for the parameters nugget, range, and sill. Finally, the N concentrations were interpolated and aggregated using OBK and RBK as in Eqns 1 and 3. Gstat software (Pebesma, 2001) was used to compute and model the semi-variograms and perform the kriging predictions.

RESULTS

Data analysis

Data used in the analysis were $\text{NO}_3\text{-N}$ and $\text{NH}_4\text{-N}$ concentrations in groundwater in March and August 2004 and March and August 2005. For environmental variables, Soil and land use types are very important, influencing N concentrations spatially

(Diodato and Ceccarelli, 2004; Hengl et al., 2004). Groundwater quality also varies in some managed ecosystems. Histograms of N concentration showed a normal distribution only for the NO₃-N concentration in March 2004. For the other sampling dates, data would have to be log-transformed (Figure 2) to be normally distributed. However, untransformed data were used, because the back-transform of N concentrations for averaged block values does not equal the log-transform of the point observations and bias could be introduced (Leopold et al., 2006).

Figures 3a-d show the spatial distribution of the explanatory variables selected for regression, i.e. land use type (a), elevation (b), soil texture (c) and soil type (d). In the central part, soils are suitable for non-rice crops (Chi and Bo, 2002), such as cabbage, chili, flowers and squash, because of their low clay content. Elevation gradually declines from north-east to south-west. Irrigation and drainage systems are designed in association with this topographical trend. Soil type and soil texture are classified as two separate characteristics, as shown in Figure 3.

Linear regression analysis for all sampling dates of NO₃ and NH₄ was performed for the full set of 10 explanatory variables (5 land use types, 1 elevation, 2 soil types and 2 soil texture groups). Fertilization and irrigation regimes are associated with land use, for instance, in flowers high inputs of fertilizers are used, causing high N leaching. Percolation continuously takes place in rice soils. Differences in elevation cause lateral flows. Percolation rate is higher in sandy loam than in the clay loam. The analysis showed different equations for NO₃ and NH₄, as linear functions of selected explanatory variables, with significant differences ($P < 0.05$) at high correlation coefficients (R^2). The minor explanatory variables, showing no significant differences and low correlations with NO₃- and NH₄-concentrations, were removed from the candidate list for the kriging models. These variables are Albi dystric Plinthosols soil type and clay loam soil texture. They have no significant influence in the regression analysis, because of small sample size and high variation in N concentration. For appropriate comparison of NO₃ and NH₄ concentrations at all sampling dates, the final linear models were chosen, for both NO₃ and NH₄. These models are based on stepwise regression and expert knowledge, using the following explanatory variables: elevation, cabbage group, chili, flower, squash group, rice, soil1 and texture1, as shown in Table 1.

Spatio-temporal prediction

Experimental semi-variograms and the fitted models for the ordinary and regression kriging are shown in Figures 4a and b as an example. The nugget-, sill- and range values in the semi-variogram for the observations are relatively larger than for the semi-variogram of the residuals (Figure 4b). This is in accordance with observations of

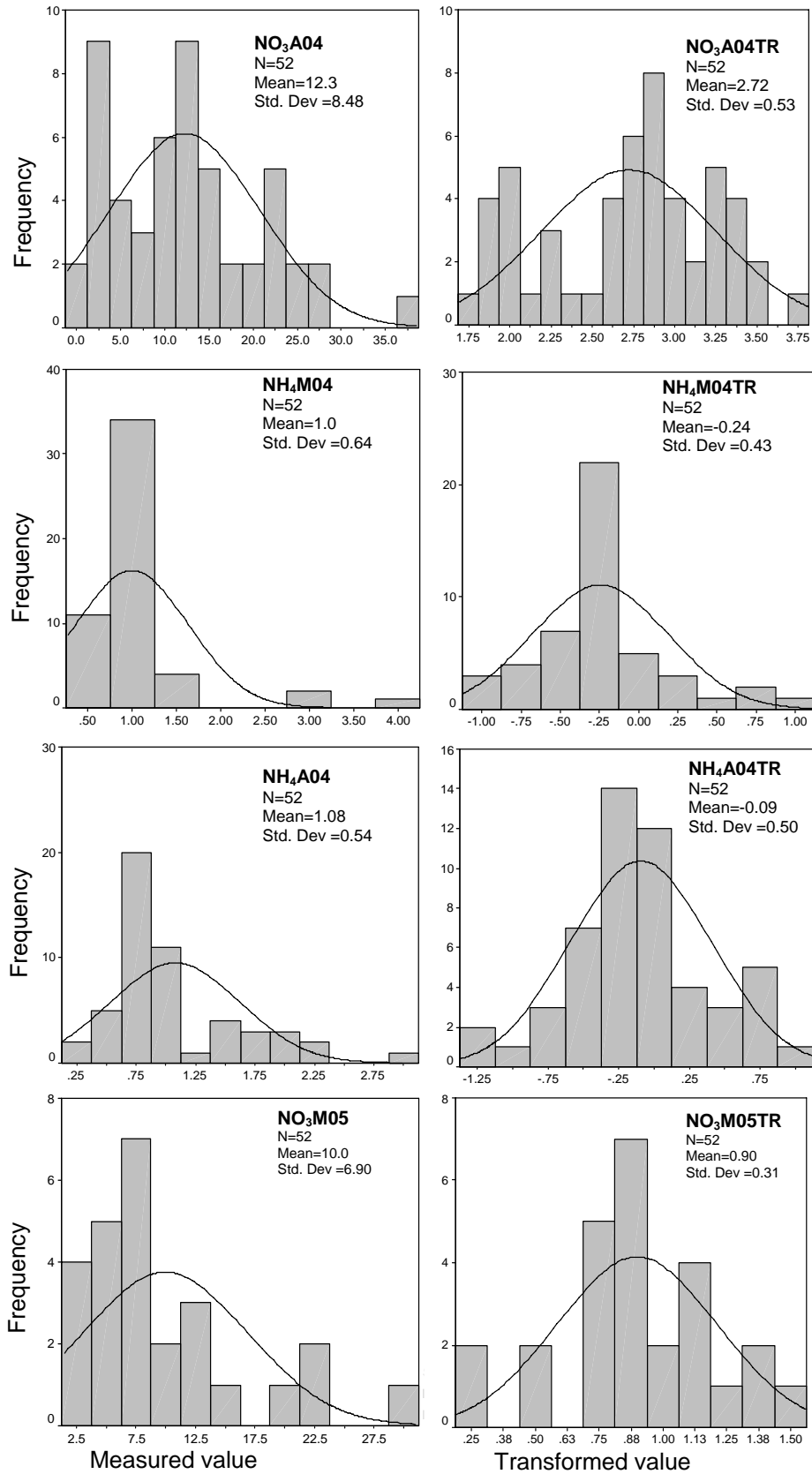


Figure 2. Histogram of N concentration (left) and its log-transformation (right) for NO₃-N in August 2004, NH₄-N in March 2004, NH₄-N in August 2004 and NO₃-N in March 2005.

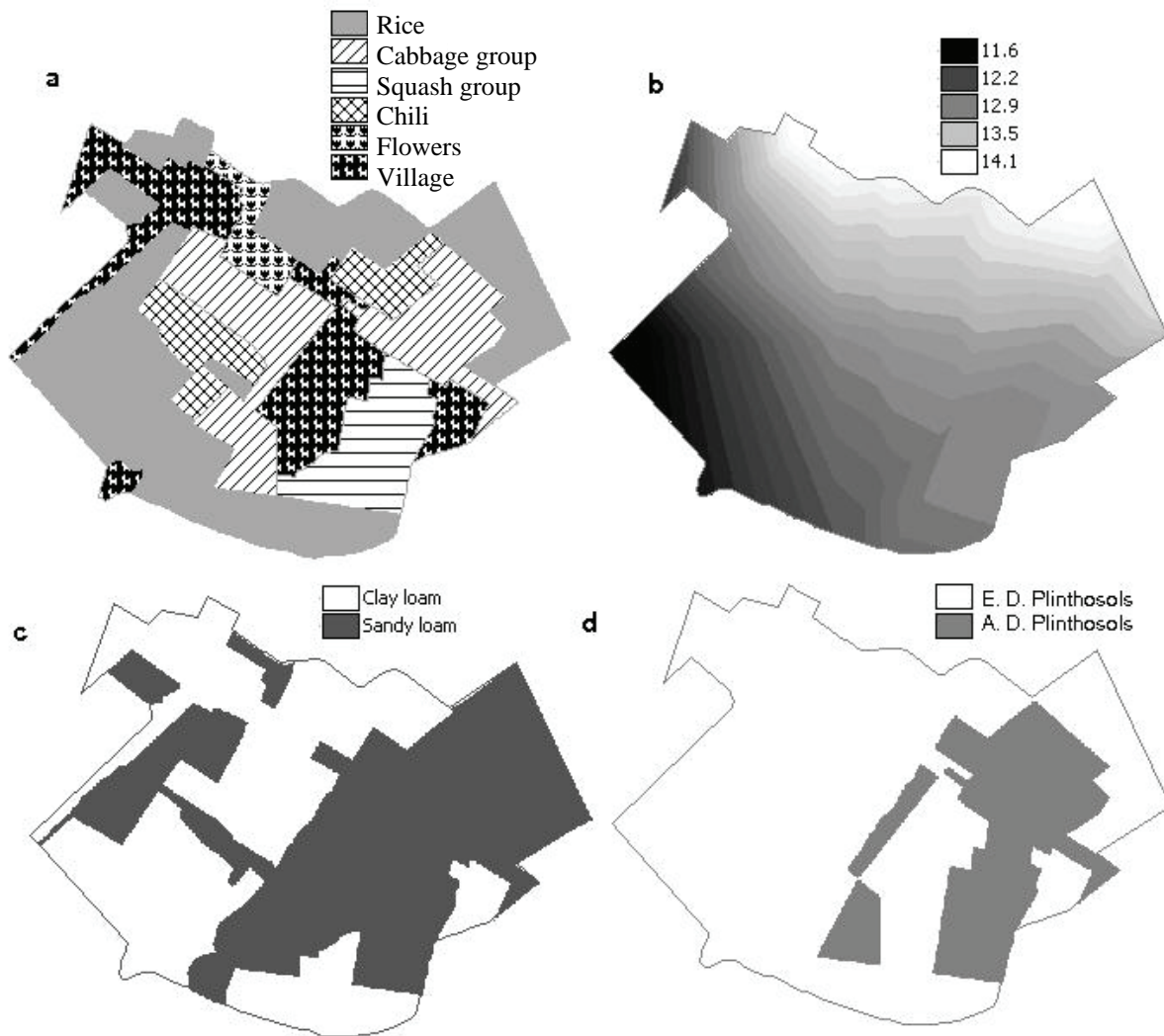


Figure 3. Maps for explanatory variables used in regression block kriging of $\text{NO}_3\text{-N}$ and $\text{NH}_4\text{-N}$: (a) land use, (b) elevation (m), (c) soil texture and (d) and soil type, including Endogleyic dystric (E. D.) plinthosols and Albi dystric (A. D.) plinthosols.

Hengl et al. (2004) and Leopold et al. (2006) that semi-variograms for residuals result in lower nugget and sill values when the deterministic trend has been removed by regression.

OBK and RBK have first been applied to the $\text{NO}_3\text{-N}$ concentration in August 2004, and prediction results and variances are given (Figures 5a-d). Block size, which is not only depending on the outcomes of the semi-variogram analysis, but also on the resolution of available additional information, such as the digital elevation model and land use (5 m resolution), was chosen as 40 m. OBK predicts a smooth spatial distribution of $\text{NO}_3\text{-N}$ concentration over the area (Figure 5a). RBK results in a more detailed picture, where $\text{NO}_3\text{-N}$ concentration varies under the influence of the

Table 1. Coefficients (intercept and slope) of the linear regression models and correlation coefficients (R^2) for nitrate and ammonium concentrations and determining factors (see text for explanation) for the four sampling dates.

Time step	Slope										R^2
	Intercept	Cabbage	Chili	Elevation	Flower	Rice	Soil	Squash	Textl		
NO ₃ M04*	12.10	7.990	7.680	0.220	27.570	8.130	-4.600	10.340	-3.710	0.65	
NO ₃ A04	94.90	-11.080	-9.460	-6.200	18.070	1.370	7.880	-8.370	-1.850	0.57	
NO ₃ M05	8.00	2.640	7.480	-0.300	20.950	1.850	2.640	0.050	0.710	0.37	
NO ₃ A05	-2.90	2.200	1.390	0.811	3.310	0.800	-2.140	0.500	-0.240	0.74	
NH ₄ M04	2.87	-0.617	-0.715	-0.102	0.897	-0.582	0.500	-0.946	-0.340	0.82	
NH ₄ A04	3.39	-0.880	-0.951	-0.108	-0.266	-0.867	0.198	-0.794	-0.356	0.78	
NH ₄ M05	1.95	-0.455	0.246	-0.111	0.717	0.064	0.425	-0.316	0.139	0.68	
NH ₄ A05	0.70	-0.174	-0.096	0.005	0.234	-0.155	-0.128	0.096	0.169	0.84	

* M04 – March 2004; A04 – August 2004, M05 – March 2005; A05 – August 2005

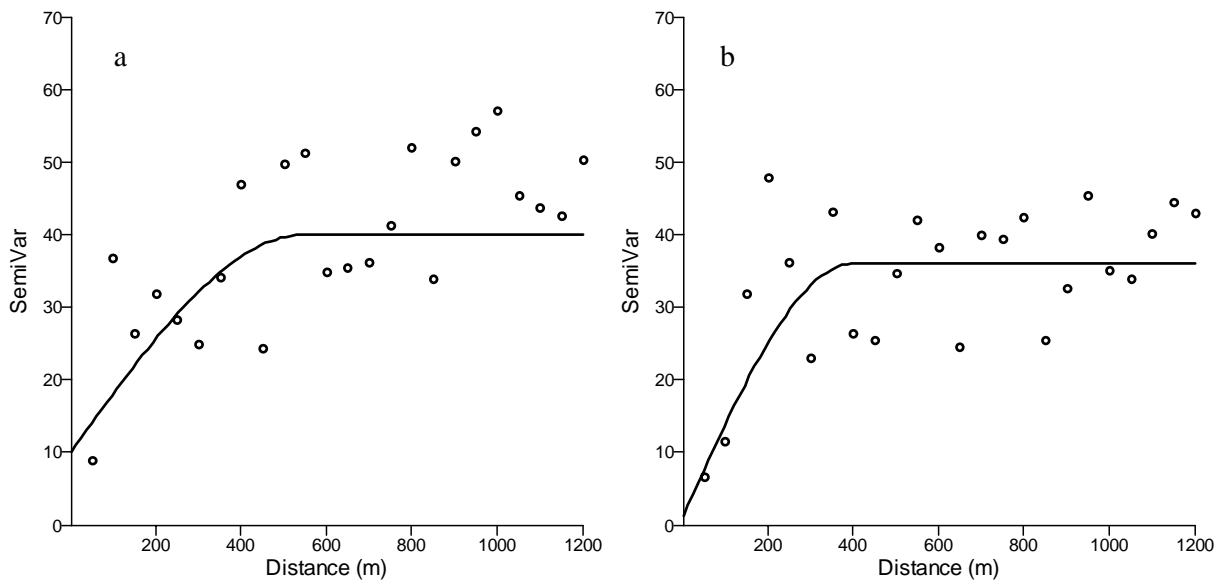


Figure 4. Experimental semi-variogram (dots) and fitted model (solid line) of $\text{NO}_3\text{-N}$ observations (a) and $\text{NO}_3\text{-N}$ residuals (b) in August 2004.

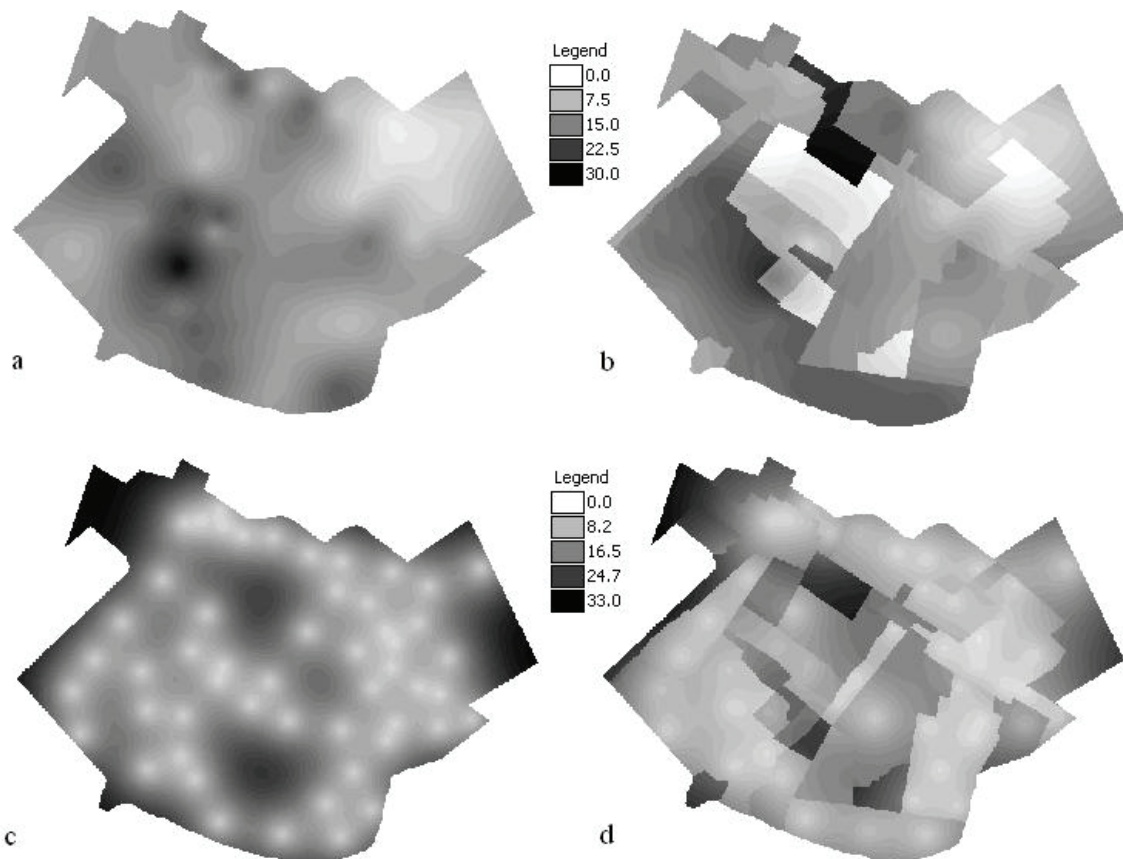


Figure 5. Kriging predictions for $\text{NO}_3\text{-N}$ (mg l^{-1}) and kriging variances (mg l^{-1})² in August 2004; (a) ordinary block kriging, (b) regression block kriging, (c) ordinary block kriging variance and (d) regression block kriging variance.

explanatory variables (Figure 5b). High $\text{NO}_3\text{-N}$ was predicted from the very intensive agro-ecosystems with high inputs of fertilizer. Overall, OBK gives a mean variance of $15.24 \text{ (mg l}^{-1}\text{)}^2$ compared to $12.40 \text{ (mg l}^{-1}\text{)}^2$ for RBK. The patterns of variance distributions are clearly illustrated in Figures 5c and d, showing very much difference between OBK and RBK variances.

Based on this comparison, RBK was selected for continuous interpolation of $\text{NO}_3\text{-N}$ and $\text{NH}_4\text{-N}$ for the other data sets. The semi-variogram model parameters used for each prediction are shown in Table 2.

$\text{NO}_3\text{-N}$ and $\text{NH}_4\text{-N}$ at all sampling dates were interpolated from measured points using RBK, following the semi-variogram models (Figure 6). The N concentrations clearly show their dependence on explanatory variables, such as soil type, elevation, and land use. These explanatory variables influence the N concentration, for instance, high inputs of fertilizer in some land use types significantly contribute to N-leaching to the groundwater. Moreover, predicted NO_3 and NH_4 concentrations at different sampling dates show that N in groundwater dramatically varies with time and environmental conditions.

Both, predicted NO_3 and NH_4 appear clearly higher in flowers than in the other land use types, at all sampling dates. For the other land use types, N concentration varied in both space and time, for example, NO_3 in rice was only slightly lower than in flowers in March 2004 but very much lower in March 2005.

In addition, kriging provides an error estimate associated to the kriging prediction for each sampling date shown in Figure 7. These variance values are much higher with larger spatial variation for NO_3 than NH_4 (Table 3). Figure 7 also shows very large variation among sampling dates for NO_3 ; the highest variances obtained were $78 \text{ (mg l}^{-1}\text{)}^2$ in March 2004, 33 in August 2004, 32 in March 2005, and 8 in August 2005. For NH_4 , the highest variances were $0.37 \text{ (mg l}^{-1}\text{)}^2$ in March 2004, and 0.18 for the other sampling dates. In both, the NO_3 and NH_4 variance maps, the spatial patterns are very similar for all sampling dates, because they are derived from the same sampling scheme.

DISCUSSION

NO_3 and NH_4 concentrations varied over time, with lower N concentrations in 2005 than in 2004. Intercepts and slopes from linear regression equations for each sampling date (Table 1), showed different weights for each environmental variable that, moreover, varied for different sampling dates. These variations are associated with variations in the environmental variables, for example, N concentration is dependent on percolation that is the balance of rainfall, irrigation, surface runoff, and evapotranspiration. It also depends on fertilizer regimes, crop uptake, and crop calendars.

Table 2. Semi-variogram model parameters, i.e. nugget, sill and range for all regression-kriging models (see Table 1 for explanation).

Time step	Model	Nugget	Sill	Range
NO ₃ M04	Spherical	35.00	60.0	500
NO ₃ A04	Spherical	10.00	30.0	550
NO ₃ M05	Spherical	2.00	25.0	600
NO ₃ A05	Spherical	2.00	4.00	500
NH ₄ M04	Spherical	0.10	0.25	800
NH ₄ A04	Spherical	0.01	0.13	600
NH ₄ M05	Spherical	0.05	0.10	500
NH ₄ A05	Spherical	0.00	0.12	400

Table 3. Average variance (mg l⁻¹)² and standard deviation from variance maps for all sampling dates (see text for explanation).

Time step	Mean variance	Standard deviation
NO ₃ M04	49.44	19.74
NO ₃ A04	12.40	5.75
NO ₃ M05	11.64	6.11
NO ₃ A05	3.45	1.60
NH ₄ M04	0.12	0.06
NH ₄ A04	0.05	0.03
NH ₄ M05	0.07	0.03
NH ₄ A05	0.05	0.03

However, relatively high R²-values for most of the regressions show high correlations between N concentration and environmental variables.

As shown in Figure 5, example of August 2004, the predicted and variance maps are totally different, in both pattern and value, between two methods. In RBK, the spatial distribution widely varies for different land use types with sharp changes at the boundaries (Figures 5b and d), in response to differences in land management. In contrast, in OBK, predicted NO₃ changes smoothly in space, not showing clear influences of land management (Figures 5a and c). This agrees with the conclusion of Hengl (2004) that ordinary kriging maps show rather gradual transitions with a fairly low level of detail, whereas regression kriging maps reflect changes in elevation, slope, and exposition; and thus, regression kriging maps yield more detail than ordinary kriging maps. The kriging variance (Figures 5c and d), that can be used as a

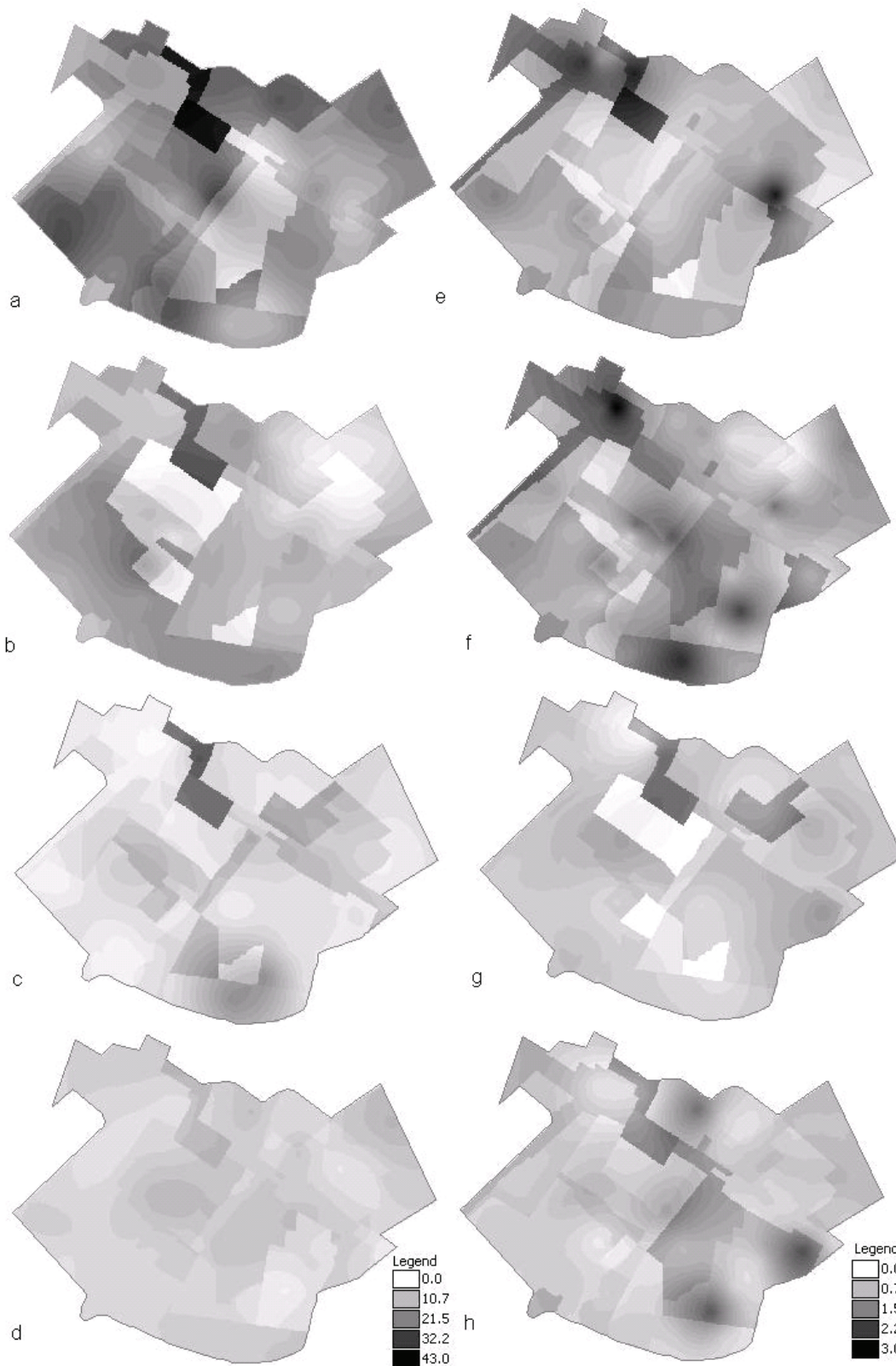


Figure 6. Prediction results of N concentration (mg l^{-1}) in shallow groundwater using regression block kriging (RBK) for $\text{NO}_3\text{-N}$ in March 2004 (a), $\text{NO}_3\text{-N}$ in August 2004 (b), $\text{NO}_3\text{-N}$ in March 2005 (c), $\text{NO}_3\text{-N}$ in August 2005 (d); $\text{NH}_4\text{-N}$ in March 2004 (e), $\text{NH}_4\text{-N}$ in August 2004 (f) and $\text{NH}_4\text{-N}$ in March 2005 (g) and $\text{NH}_4\text{-N}$ in August 2005 (h).

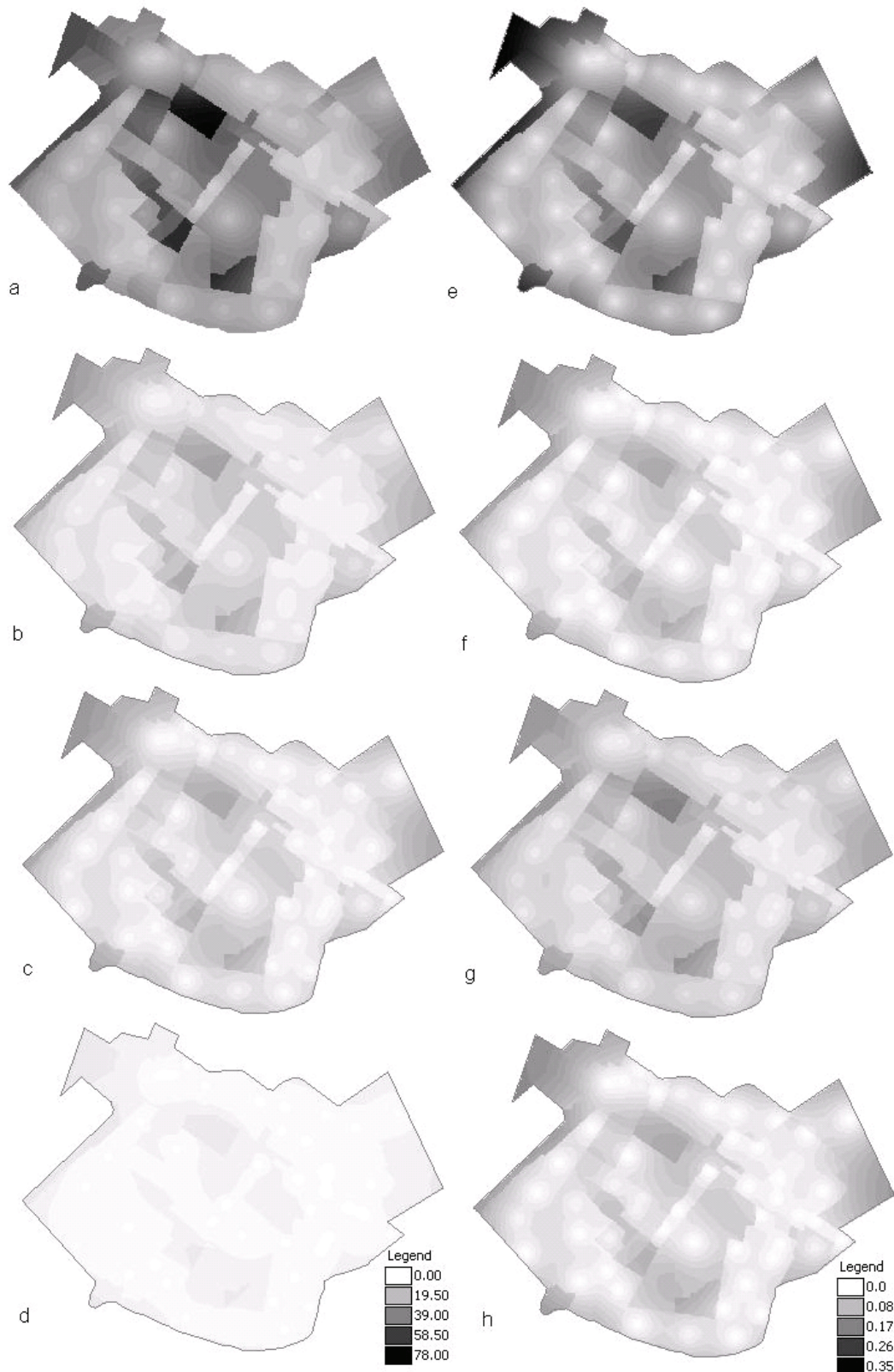


Figure 7. Kriging variance (mg l^{-1})² maps calculated from prediction for NO₃-N in March 2004 (a), NO₃-N in August 2004 (b), NO₃-N in March 2005 (c), NO₃-N in August 2005 (d); NH₄-N in March 2004 (e), NH₄-N in August 2004 (f) and NH₄-N in March 2005 (g) and NH₄-N in August 2005 (h).

criterion for the goodness of prediction, is lower for RBK than for OBK. It provides information on the uncertainties associated with the predictions. Spatial patterns are reproduced more realistically with RBK than with OBK, according to expert judgment. This agrees with the conclusion of Hengl et al. (2004) that regression kriging achieved a higher accuracy of prediction and a smaller bias for prediction than ordinary kriging. Therefore, RBK was used to predict N concentrations in groundwater for all other dates. However, our data did not permit independent establishment of the most accurate method, as no further independent data sets for validation were available, neither on the point nor on the block support. Cross-validation enables evaluation of the goodness of a defined geostatistical model used for kriging. But this only holds for the support at which data have been gathered. As we predicted for the block support, cross-validation for point support would not have added any value to the accuracy of the prediction (Chiles and Delfiner, 1999). In contrast, the prediction error maps give useful information about the associated uncertainties for each prediction.

Nitrogen concentrations varied over time, due to changing environmental conditions. The value of the intercept in the linear regression (Table 1) and those of the range and sill in the semi-variogram models (Table 2) show a decreasing trend with time, indicating the decrease in N concentration over time. The trend is also clear in the maps of predicted N concentration (Figures 6a-h). The maps also show that land use is a major variable influencing N concentration and leaching in this situation, where the soil is relatively homogenous, and almost flat. Moreover, N concentrations varied temporally as a result of variation in rainfall, irrigation, crop status, and fertilizer regimes. For example, irrigation and fertilizer application for rice were high in the tillering period, and low in the grain filling period, and flowers were irrigated and fertilized in the productive period, but not outside that period (Figure 3a).

Comparison of Figures 6a and 6b shows higher $\text{NO}_3\text{-N}$ concentrations in March 2004 than in August 2004. In March 2004, basal fertilizers, comprising manure and chemical nitrogen fertilizer, were applied to almost all crops. As temperatures were low in this period, crop growth rate was low, as was nitrogen uptake. In August, in the rainy season, fertilizer application was lower and temperatures were higher, so that the rates of crop growth and nitrogen uptake were higher. Hence, quantities of $\text{NO}_3\text{-N}$ and $\text{NH}_4\text{-N}$ in the soil solution, available for leaching, were smaller and consequently, N concentrations in the groundwater were lower. In 2005, temperatures in early spring were higher than in 2004, so that crop growth started earlier, inducing higher N-uptake, resulting in less available N for leaching (Figures 6a and c). The trends are similar for $\text{NH}_4\text{-N}$ in Figures 6d, e and f, but $\text{NH}_4\text{-N}$ concentrations are much lower than those of $\text{NO}_3\text{-N}$, because nitrification generally proceeds fast under these conditions and NH_4 , being a cation, is adsorbed at the soil colloids (Mulvaney, 1994).

Depending on the regression model used for each prediction date, the prediction errors vary which indicates sensitivity of the regression-kriging to temporal changes as shown in Figure 7.

CONCLUSIONS

Taking into account various explanatory variables for predicting spatial distributions of N concentration, RBK gave more realistic results, with lower kriging variance than OBK; RBK results, according to expert knowledge, also better resembled the true spatial variation. Land use appeared the most influential factor for the spatial distribution of N concentrations, because it determines the water balance components, such as runoff, evapo-transpiration and percolation. The fertilizer and irrigation regimes, in interaction with crop growth, also strongly affected the magnitude of N leaching and, thus, N-concentrations in groundwater. Concentrations of $\text{NH}_4\text{-N}$ were very low, but those of $\text{NO}_3\text{-N}$ fairly high, associated with favorable conditions for nitrification and the relatively high mobility of the ion. The accuracy of the predictions depends on both, the environmental variables taken into account, and the number of sampling points. Furthermore, the predictions are only representative for a given period of time with relative stable environmental conditions. Therefore, the accuracy could be improved by increasing the number of sampling points and the frequency of sampling. That would improve the prediction of N loss due to leaching under various land use types and environmental conditions, such as soil type, rainfall, elevation, etc. The method aims at determining uncertainty in other areas, where the determining factors are strongly influenced by environmental conditions and management. For example, in peri-urban areas in Vietnam different crop types are subjected to different irrigation and fertilization regimes, or different land units are irrigated from different waste water sources. Moreover, predicted maps from different sampling dates could be used instead of ground truth data, for calibration and validation of spatial dynamic models that spatio-temporally simulate changes in N concentration in soil or groundwater. These models usually take into account other dynamic processes, such as crop growth with actual transpiration and nutrient uptake, nitrogen application and its transformation in soil and water.

CHAPTER 8

Spatial dynamics of nitrogen in shallow groundwater under intensive farming in northern Vietnam

V.T. Mai^{1,5}, H. Van Keulen^{1,2}, C.T. Hoanh³, R. Hessel⁴, R.P. Roetter⁴

- ¹ Plant Production Systems Group, Wageningen University, P.O. Box 430, 6700 AK Wageningen, The Netherlands
- ² Plant Research International, Wageningen University and Research centre, P.O. Box 16, 6700 AA Wageningen, The Netherlands
- ³ International Water Management Institute, Regional Office for South-east Asia c/o The World Fish Center, Jalan Batu Maung, Batu Maung, 11960 Bayan Lepas, Penang, Malaysia
- ⁴ Soil Science Centre, Alterra Green World Research, Wageningen University and Research centre, P.O. Box 47, 6700 AA Wageningen, The Netherlands
- ⁵ National Institute for Soils and Fertilizers (NISF), Dong Ngac, Tu Liem, Hanoi, Vietnam

Abstract

In this study, a spatial dynamic model was developed, to simulate nitrogen dynamics in Van Hoi commune, Tam Duong district, Vietnam, for different soil and land use types, under different irrigation and fertilizer regimes. The model has been calibrated using measured nitrogen concentrations in soil solution in March and August 2004 and validated for data from March and August 2005. Lateral flow was low in this level area. Percolation was the main process leading to high nitrogen leaching losses to groundwater. Calculated annual leaching losses varied from 88 to 122 kg N ha⁻¹ in flowers, 64 to 82 in vegetables of the cabbage group, 51 to 76 in chili, 56 to 75 in vegetables of the squash group, and 36 to 55 in rice. Model accuracy needs to be improved through further calibration in both vertical and lateral dimensions and more combinations of soil and land use.

Keywords: Vegetables, rice, lateral flow, percolation, GIS simulation, PCRaster, regional scale

INTRODUCTION

High fertilizer and manure use in intensive agriculture is one of the main sources of nutrient leaching losses to the environment, and the associated reduction in groundwater quality (Wolf et al., 2005). In many regions the annual leaching load exceeded 20 kg ha^{-1} (Lin et al., 2001), while in about 2.5% of the land area occupied by terrestrial ecosystems it exceeded 30 kg ha^{-1} ; especially in areas with heavy fertilizer application, such as the United States, Europe, and China, the maximum leaching load was $133 \text{ kg ha}^{-1} \text{ yr}^{-1}$. In Vietnam, the population has rapidly increased, leading to increased food demand. In response, agriculture has intensified, increasing the pressures on soil and environment. In northern Vietnam, Vinh Phuc province is one of these rapidly developing regions. The population in the province increased from 642,000 in 1990 via 1,106,000 in 2000 to 1,143,000 in 2004, while livestock population increased from 2,402,000 in 1990, via 5,616,000 in 2000 to 6,679,000 in 2004, 85–90% of which was poultry. Crop yields also increased, i.e. for rice, maize, and fresh vegetables from 2.6, 1.8 and 13.7 Mg ha^{-1} in 1990 to 4.8, 3.4 and 16.2 in 2004. Intensification of farming is associated with strongly increasing inputs of nitrogen fertilizer. A countrywide survey on fertilizer use and management (Hien and Thoa, 2003) showed that from 1985 to 2000, fertilizer use annually increased by 7.2% for nitrogen, 13.9% for phosphorus, and 23.9% for potassium. The annual increase in total fertilizer use ($\text{N} + \text{P}_2\text{O}_5 + \text{K}_2\text{O}$) was 9%. In the coming years an annual increase of 10% is expected.

Various studies in Asia have shown a positive correlation between fertilizer application rates and NO_3 leaching (Zhu et al., 2003; Hai, 2004). In a groundwater quality assessment by the Vietnamese Mineral Geology Department, covering an area of 800 km^2 in the middle part of the Red River Delta (Minh and Hoc, 1997), the area with NH_4^+ concentrations exceeding 10 mg l^{-1} increased from 22.3 km^2 in 1992, through 41.1 in 1993 to 68.0 in 1994. In intensive rice fields in the Red River Delta, NO_3 concentrations in groundwater have been recorded of 57 mg l^{-1} in the dry season and 84 mg l^{-1} in the rainy season (Tau, 1997).

Nitrate contamination of drinking water may increase the risk of cancer (Yang et al., 1998; Weyer et al., 2001), because nitrate is endogenously reduced to nitrite, and subsequent nitrosation reactions result in increased concentrations of N-nitroso compounds that are highly carcinogenic. It has also been shown that high nitrate-containing vegetables increase the risk of gastric cancer (Kim et al., 2001). A national survey of the Vietnam Cancer Institute (NCI, 2002) showed that stomach cancer is the second leading form of cancer in males, and the third in females, and increases at an annual rate of 4.4% (Anh et al., 2002).

Nitrogen leaching from agriculture originates from non-point pollution sources and

is difficult to quantify. At plot scale, various methods for measuring N leaching have been applied, in different soils, and under different land use systems (Ross et al., 1995; Williamson et al., 1998; Riley et al., 2001; Chapter 6). Alternatively, N leaching has been estimated using decision support systems (Johnsson et al., 2002) and models at appropriate scales (Granlund et al., 2000; Ersahin and Rustu Karaman, 2001; El-Sadek et al., 2003), combining spatial and non-spatial data on soils, crops, and fertilization. At watershed scale, N leaching losses vary both temporally (different seasons, rainfall and fertilizer application regimes, and crop calendars), and spatially (different elevations, soils, land uses, rainfall patterns, irrigation and fertilizer patterns). Therefore, quantifying N leaching losses from agriculture requires appropriate methods for scaling up of spatial and temporal patterns. The objectives of this study were: (i) to develop a spatial-dynamic model for N leaching in an intensive agricultural region with high fertilizer use and (ii) to apply the model for quantifying N leaching losses from intensive farming systems, with very high irrigation and fertilizer inputs, in Van Hoi commune, Tam Duong district, northern Vietnam.

METHODOLOGY

Study area

Van Hoi commune is located in a flatland area of Tam Duong district (21°26' N, 105°36' E), 60 km north of Hanoi. The commune has a total area of 290 ha, with arable land belonging to two soil texture groups (Figure 1): clay loam (126 ha; 53.8%) and sandy loam (109 ha; 46.2%). Representative soil profiles were described for both the sandy loam and clay loam soils, including their properties, such as hydraulic conductivity, porosity, and field capacity (Table 1). Rainfall, temperature, radiation, wind speed, and sunshine hours were recorded at Vinh Yen meteorological station, about 2 km from the study area.

Table 1. Saturated hydraulic conductivity (ks), porosity, and field capacity (FC) of sandy loam (SL) and clay loam (CL) in Van Hoi commune, Tam Duong district, Vietnam

Soil depth (cm)	ks (cm d^{-1})		Porosity (%)		FC ($\text{cm}^3 \text{cm}^{-3}$)	
	SL	CL	SL	CL	SL	CL
0–40	146.4	102.1	43.7	45.3	33.3	33.3
40–80	10.3	10.3	39.8	41.2	59.2	60.6
> 80	3.6	2.9	43.0	43.7	63.7	65.0

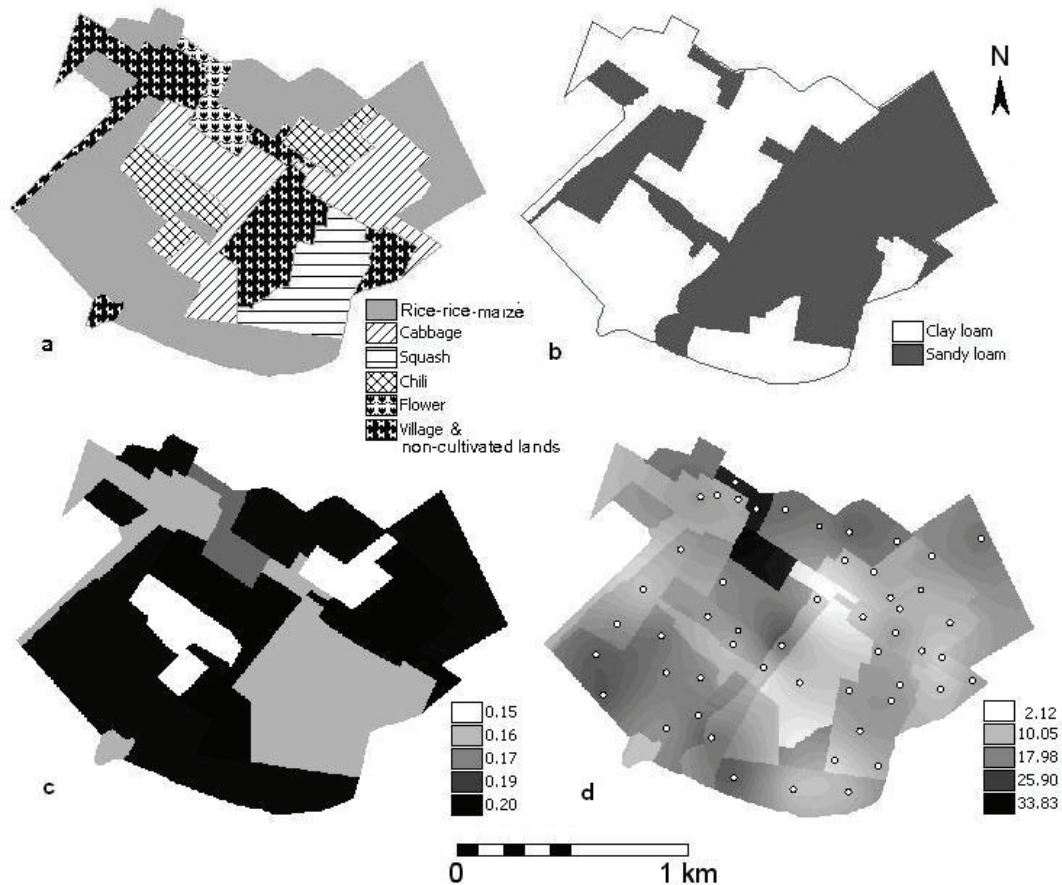


Figure 1. Land use map (a), soil map (b), initial soil moisture content (c, $\text{cm}^3 \text{cm}^{-3}$), and initial soil Nmin (d; mg kg^{-1}) with measurement points (100 cm depth) in Van Hoi commune, Tam Duong district, Vietnam.

Land use and fertilizer use

The dominant cropping pattern in the past was double rice. Farmers have shifted to more than 2 crops in the rotations to increase income per unit area (Figures 1 and 2). Currently, the main rotation is double rice followed by an upland crop, such as maize, potato, sweet potato, or vegetables during winter. Where irrigation is possible, vegetables are grown continuously. The number of crops and crop types in the rotations (Figure 2) are adapted flexibly, depending on market conditions, availability of labour and capital.

Average fertilizer use for different crops in the commune is shown in Table 2. For vegetables, high value crops, with very high fertilizer and biocide inputs, two groups are distinguished: group 1 ('cabbage' group) consisting of paprika, cabbage, egg plant, and kohlrabi, in which cabbage is the major crop; group 2, including chili, cucumber, tomato, and squash, with chili and squash as major crops.

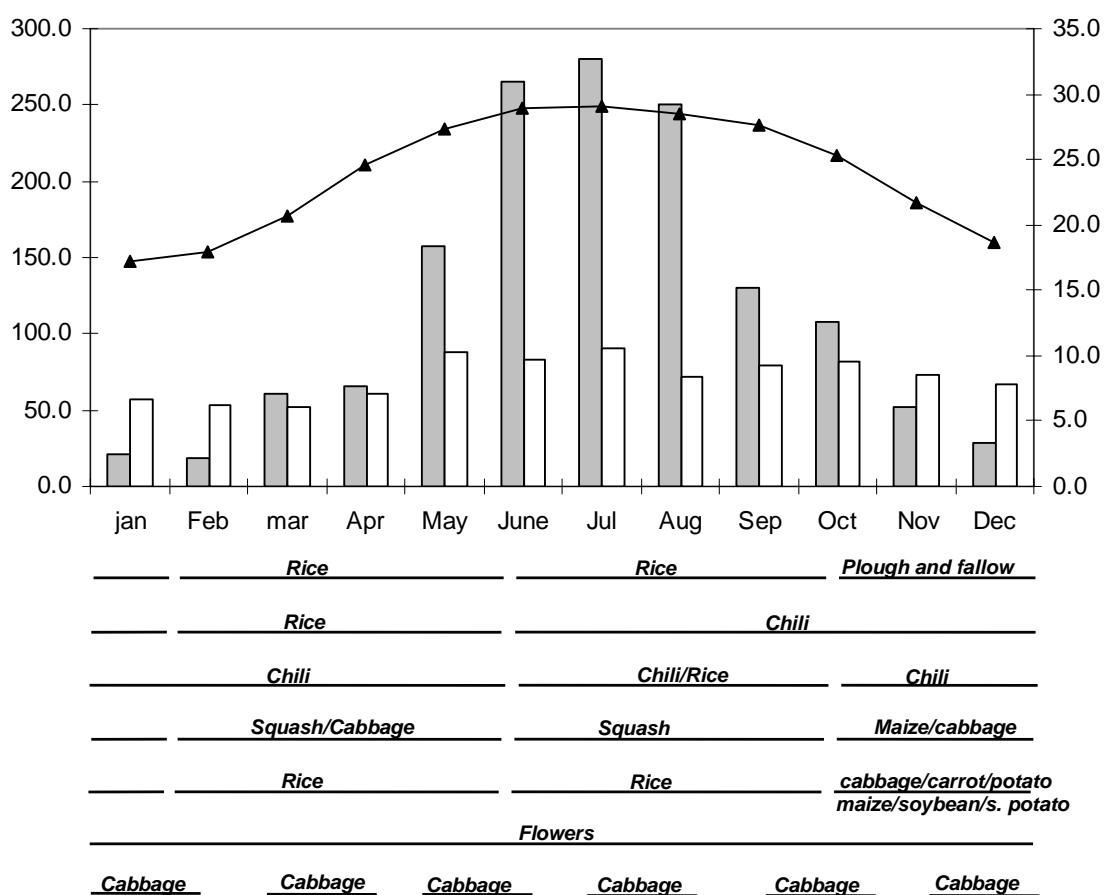


Figure 2. Weather conditions in the study area: monthly rainfall (solid bar; mm) and monthly evaporation (blank bar; mm) referring to left hand Y-axis. Monthly temperature (triangles; °C) referring to right hand Y-axis. Lower part: Cropping calendars of land use systems in Van Hoi commune, Tam Duong district, Vietnam.

For rice, all farm yard manure (FYM), all phosphorus, and 20 to 30% of the N fertilizer is applied as basal dressing. The remaining N fertilizer is applied in 2 to 3 splits, at the start of tillering and before booting. For spring rice, in addition to the basal dose, FYM is also applied as top dressing during tillering, as a slow release nutrient source to avoid nutrient deficiency at later stages. For maize, mostly grown in the winter season, FYM and phosphorus fertilizer are applied as basal dressing, while chemical N fertilizers are applied each week, till the 9-leaf stage, through ‘bucket irrigation’. Peanut and soybean cover small areas and receive small doses of fertilizers. For vegetable group 1, all FYM and phosphorus fertilizer are applied at planting, whereas dissolved N fertilizers are applied in the early stages through ‘bucket irrigation’. Cabbage is grown very intensively with up to seven harvests per year. In chili, FYM is applied as basal dressing under submerged conditions between the beds,

Table 2. Fertilizer and biocide use for different crops in Van Hoi commune, Tam Duong district, Vietnam.

Crop	N kg ha ⁻¹	P kg ha ⁻¹	K kg ha ⁻¹	FYM ¹ Mg ha ⁻¹	Herbicide (10 ³ VND ² ha ⁻¹)
Spring rice	76.3	28.2	62.0	7.9	111.8
Summer rice	84.2	24.2	66.9	5.4	86.9
Maize	59.5	15.9	30.2	2.9	ND ³
Soybean	30.0	0.0	0.0	0.0	ND
Peanut	40.0	0.0	0.0	0.0	ND
Vegetable group 1 ⁴	63.7	25.0	34.1	9.3	ND
Vegetable group 2 ⁵	254.2	57.8	26.9	20.0	139.0
Sweet potato	20.3	11.7	10.9	4.1	0.0
Flowers ⁶	568.0	240.0	360.0	30.0	ND

¹ FYM (Farm Yard Manure) has 0.53% N, 0.025% P₂O₅ and 0.49% K₂O;

² VND = Vietnamese Dong; 15,000 VND = 1 US\$ (in 2002);

³ ND = Not Determined;

⁴ Vegetable group 1: paprika, cabbage, egg plant, kohlrabi;

⁵ Vegetable group 2: chili, cucumber, tomato, squash;

⁶ Fertilizer dose per year.

followed by monthly additions, while chemical nitrogen fertilizer is applied weekly on the soil surface. In cucumber, tomato and squash, FYM and phosphorus are surface-applied before planting, followed by weekly applications of sludge and chemical N fertilizers through 'bucket irrigation'. Flowers (mainly rose and daisy) require high doses of fertilizers to compensate for nutrient export in the weekly cuttings. Liquid compost, consisting of a mixture of manure, N-rich materials such as bean residues, urine, and food processing wastes are surface-applied each week through 'bucket irrigation'.

The price of urea, the main N fertilizer in the study area, increased from 2800 VND (Vietnamese Dong)* in March 2004, via 4400 in December 2004 to 5900 in June 2005. Many poor farmers could no longer afford the fertilizer, so that average application rates decreased by 10 to 20%. Moreover, fertilizer management changed, i.e. priority was given to important crop growth stages, such as root development, tillering, and flowering.

Field measurements

Groundwater samples (at 52 locations, randomly selected; Figure 1d), at 1 m depth,

* 1 US\$ = 15,200 VND in 2004 and 15,800 in 2005.

were taken at four dates, 6th March and 15th August 2004, and 26th March and 8th August 2005, using an open porous pipe and a hand pump, and were analysed for nitrate- and ammonium-nitrogen content (Chapter 7). Irrigation and fertilizer application were recorded for each land use type as inputs for calculation of the water and soil mineral nitrogen balances. Soil samples were taken on 1st February 2004 (assuming very little change from 1st January to 1st February, because of the very dry conditions), and analysed for Nmin as initial condition for the simulation model.

Model description

To allow analysis in the specific geo-morphological conditions of the study area, a spatial dynamic model was developed. It simulates N leaching, using PCRaster, a computer language for construction of dynamic spatio-temporal environmental models (Van Deursen, 1995; Karssenberget al., 1996; Wesseling et al., 1996). It includes water and nitrogen modules and uses a daily time step (Figure 3). Both, the water and nitrogen module have been applied in simulations at plot scale (Chapter 6). In spatial dynamic simulation, three main components are distinguished: the space dimension, the time dimension, and the dynamic process.

In the soil profile, three horizons are distinguished (Table 1), while the model consists of four compartments, with thickness of 40, 40, 20 and 300 cm, respectively (Figure 3).

Water balance

In the water balance sub-model, net flow into the i^{th} soil layer is calculated as the balance of inflow (FL), outflow (i.e. inflow into the $i+1^{\text{th}}$ soil layer), and evapotranspiration (ET) from that layer:

$$SW_{i,t} = SW_{i,t-1} + NFL_{i,t} \times \Delta t \quad (1)$$

$$NFL_i = FL_i - FL_{i+1} - ET_i \quad (2)$$

For the surface layer, inflow equals:

$$FL_1 = R + IRR - Q \quad (3)$$

where, SW_i is soil water (mm) in the i^{th} layer, Δt the time step of the model (1 d), R rainfall (mm d^{-1}), IRR irrigation (mm d^{-1}), ET_i contribution of i^{th} layer to evapotranspiration (mm d^{-1}), FL_i , FL_{i+1} flow over upper and lower boundary of layer i (mm d^{-1}), respectively, and Q surface runoff (mm d^{-1}).

Total ET has been calculated outside the model using the Penman-Monteith method (Allen et al., 1998). Total root water extraction is partitioned in the proportions 0.4, 0.3, 0.2 and 0.1 over the four successive quarters of the total rooting depth, starting

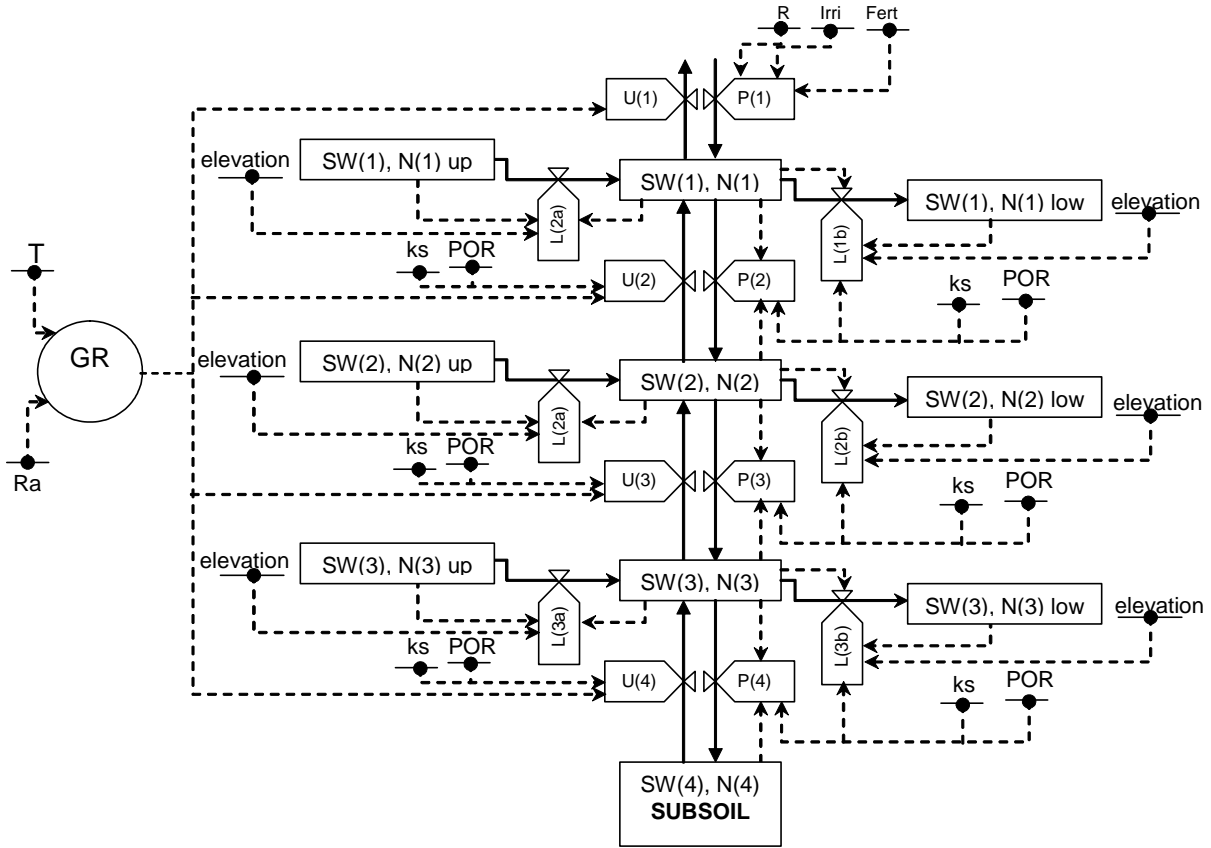


Figure 3. Relational diagram for soil moisture and nitrogen dynamics in the soil; where R is rainfall; Irri, irrigation; Fert, fertilizer, SW(1), soil water content (layer); L(1a), lateral inflow rate; N, nitrogen concentration; P, percolation and leaching rates; U, evapo-transpiration and nitrogen uptake rates; T, temperature; Ra, radiation; GR, crop growth; ks, soil conductivity; L(1b), lateral outflow; and POR, is soil porosity.

from the top (Molz and Remson, 1970; Molz, 1981; Hasegawa and Kasubuchi, 1993; Chapter 6).

Flow into the i^{th} soil layer (Radcliffe et al., 1998) is described by Darcy's law:

$$FL_i = -k_i \frac{dh_i}{dz} \quad (4)$$

$$k_i = ks_i \quad \text{if } \theta_i = \theta_{s_i} \quad (5)$$

$$k_i = kr_i \times ks_i \quad \text{if } \theta_i < \theta_{s_i} \quad (6)$$

$$kr_i = \left(\frac{\theta_i - \theta_{r_i}}{\theta_{s_i} - \theta_{r_i}} \right)^\lambda \quad (\text{Averjanov, 1950; Brutsaert, 1966}) \quad (7)$$

where, k_i is soil hydraulic conductivity of soil layer i (mm d^{-1}), dh_i/dz the moisture potential gradient (unitless) between layers i and $i-1$, kr_i the proportionality factor between actual and saturated soil hydraulic conductivity ($0 \leq kr_i \leq 1$), θ_i , θ_{r_i} , θ_{s_i} water

content in the layer to which kr_i applies, residual water content and water content at saturation, respectively ($\text{cm}^3 \text{cm}^{-3}$); θr is defined as the water content in the soil that does not participate in flow (immobile water). In practice, θr corresponds to the water content at which the soil moisture capacity approaches zero ($d\theta/dh \rightarrow 0$) (Zaradny, 1993) and varies from 0.005 for light-textured soils to 0.1 for heavy-textured soils (Lal and Shukla, 2004); λ is an empirical coefficient of 3.5 (Averjanov, 1950).

Daily water extraction from layer i for transpiration (T_i ; mm d^{-1}) is calculated as a function of daily ET_i , time after sowing (d), and duration to maximum leaf area index (Du_LAI_{\max} ; Table 3):

$$T_i = \frac{\min(t, Du_LAI_{\max})}{Du_LAI_{\max}} ET_i \quad (8)$$

In this level area, individual fields are surrounded by bunds; therefore, surface runoff is assumed to only occur when the first layer is saturated and surface water depth exceeds bund height (Chowdary et al., 2004):

$$Q = \max(0, R + IRR + Q_{\text{up}} + (SW_1 - POR_1 - BH)/\Delta t) \quad (9)$$

where, Q_{up} is runoff from upstream (mm d^{-1}); SW_1 , POR_1 soil water content (mm) and saturated soil water content in the first layer; BH is bund height (mm), in this study set to 50 mm for flowers and cabbage and 100 mm for chili and rice, the crops for which rain water is stored in the field.

Water is also transported laterally within the compartment; in the model, the rate of lateral flow from one cell (the smallest unit of the raster map) to the neighbouring

Table 3. Crop calendars (dates of sowing, maximum LAI and harvest) for various crops in Van Hoi commune, Tam Duong district, Vietnam.

Crop	Date		
	Sowing	LAI _{max}	Harvest
Flowers	Sept 15 th	Oct 30 th	After Oct 30 th
Tomato	Sept 15 th	December 15 th	January 15 th
Squash/cucumber*	February 5 th	June 5 th	August 5 th
Cabbage**	Feb 5 th	March 15 th	March 21 st
Chili	Sept 1 st	Dec 1 st	Jul 15 th
Spring rice	Feb 5 th	May 5 th	Jun 5 th
Summer rice	Jun 25 th	Aug 19 th	Sept 19 th
Winter maize	Sept 20 th	Dec 5 th	Jan 10 th

* Squash/cucumber and tomato are in the same rotation;

** Cabbage is transplanted directly following harvest of the preceding cabbage.

downstream cell, in layer i (LF_i , mm d^{-1}) is calculated (Hoffmann et al., 2006) from hydraulic conductivity (k , mm d^{-1}) and the difference in hydraulic head (dh) between two cells (dL = cell size):

$$LF_i = -k \frac{dh_i}{dL} \quad (10)$$

A Digital Elevation Model (DEM) was generated, from which the local drainage network map (Idd; Table 4) was derived. At each layer, for each cell, elevation/soil water content was assigned the value of the neighbouring downstream cell, where downstream cells were determined using the local drain directions on Idd. Differences in elevation/soil water content between upper and lower cells were calculated from original and downstream elevation/soil water content maps (Karssenberget al., 1996). Outflow from the upper cell is calculated with the accucapacityflux function (Karssenberget al., 1996). This function calculates outflow from the upstream cell (which equals inflow into the downstream cell) as a function of transport capacity. Water content in a cell is compared to transport capacity, and that part of the water that can be transported moves over the boundary.

Nitrogen balance

The net rate of change in nitrogen (N_{NFL}) in a cell in layer i is defined as:

$$N_{NFLi} = N_{ferti} + N_{lat_upi} + N_{leach(i-1)} - N_{uptakei} - N_{gasi} - N_{leachi} - N_{lat_lowi} \quad (11)$$

where, N_{fert} is fertilizer application ($\text{kg ha}^{-1} \text{d}^{-1}$), N_{lat_up} inflow from upper cells ($\text{kg ha}^{-1} \text{d}^{-1}$), defined as the product of lateral inflows and appropriate N concentrations in the upper cells, N_{uptake} uptake by the crop ($\text{kg ha}^{-1} \text{d}^{-1}$), defined as the product of transpired water and N concentration, N_{gas} gaseous losses due to volatilization and denitrification ($\text{kg ha}^{-1} \text{d}^{-1}$), $N_{leach(i-1)}$, $N_{leach(i)}$ downward transport ($\text{kg ha}^{-1} \text{d}^{-1}$) from the appropriate layer, i.e. the product of FL_{i-1} and N concentration in layer $i-1$ and the product of FL_{i+1} and N concentration in layer i , respectively, and N_{lat_low} outflow to the lower cell ($\text{kg ha}^{-1} \text{d}^{-1}$), defined as the product of lateral outflow and appropriate N concentration in that cell.

N fertilizer application, comprising N from manure and urea, the only chemical nitrogen fertilizer used in the study area, is read daily from the file Fert.tss (Table 4). Organic N from manure is mineralized following first-order kinetics as described by Yang (1996). The raster map of initial Nmin in the soil solution was interpolated from point measurements using regression kriging (Chapter 7).

The rates of volatilization (NH_3) and denitrification (NO , N_2O , N_2) depend on the concentrations of NH_4 and NO_3 in the soil, aeration, and soil pH, and mostly follow

first-order kinetics (Addiscott and Whitmore, 1987; Chowdary et al., 2004). In the model, these processes are approximated by:

$$N_{\text{gas}} = k_{\text{gas}} \times N_{\text{min}} \times e^{-k_{\text{gas}} \times t} \quad (12)$$

where, k_{gas} is a combined rate constant for volatilization and denitrification, set to 0.01 per day.

Model calibration and validation

The most important parameter influencing percolation and N transport rates is ks . As no data were available for calibration of lateral flows, N mineralization and transformation of nitrogen into gaseous form, only ks was used for calibration. Goodness of fit of simulated values was calculated following Jørgensen and Bendoricchio (2001):

$$Y = \sqrt{\frac{\sum (\chi_c - \chi_m)^2}{\frac{\chi_{m,a}}{n}}} \quad (13)$$

where, χ_c is simulated Nmin, χ_m the corresponding measured Nmin, $\chi_{m,a}$ average measured Nmin, and n the number of samples.

RESULTS

Model calibration and validation

Data from 2004 were used for calibration; input files with model parameters are given in Table 4.

Via trial-and-error, calibration was performed according to two procedures, (i) using different ks -values for the two soil types, and (ii) using different ks -values for 13 land units, derived from overlaying the soil and land use maps.

For each of the two procedures, output maps of simulated Nmin concentration in the soil solution were extracted for two dates, 6th March and 15th August 2004, for which measured values (for the third layer, i.e. 1 m depth) were available. Goodness of fit between simulated and measured Nmin-values was calculated (Figure 4), and the ks values were adjusted successively, until no further improvement in goodness of fit was obtained.

The multiplication factors for both, soil type-specific ks and land unit-specific ks associated with the best fit are shown in Table 5. Simulated Nmin was closer to the measured values with the second procedure (Figure 4a), with $Y=1.58$ (Eqn 13), compared to $Y = 2.29$ with the first procedure.

Table 4. Input parameters for the model (all maps are in raster mode with a resolution of 5 m).

Input file	Description
Rain.tss	Daily rainfall
Irrig.tss	Daily irrigation for each land use type
Evap.tss	Daily evapo-transpiration for each land use type (calculated outside the model)
Fert.tss	Daily fertilizer application for each land use type, 15% reduced in 2005
Soil.map	Soil map
Soil.tbl	Attribute table with different soil properties for each soil type
Dem.map	Digital elevation map
Ldd.map	Local drainage network map derived from Dem.map, which is raster-formatted with codes from 1 to 9 showing drain directions to the neighbouring cells (Karsenberg et al., 1996)
Landuse.map	Land use map that is linked to the irrig.tss, evap.tss and fert.tss files through land use types (Figure 1)
Landunit.map	Overlay from soil and land use type maps
Kslandunit.tbl	Multiplication factor for ks values in each land unit
InitSW.map	Initial soil water map (Figure 1)
InitN.map	Initial nitrogen concentration (mg kg^{-1}) map from soil samples taken on 1 st February 2004 at 1 m depth

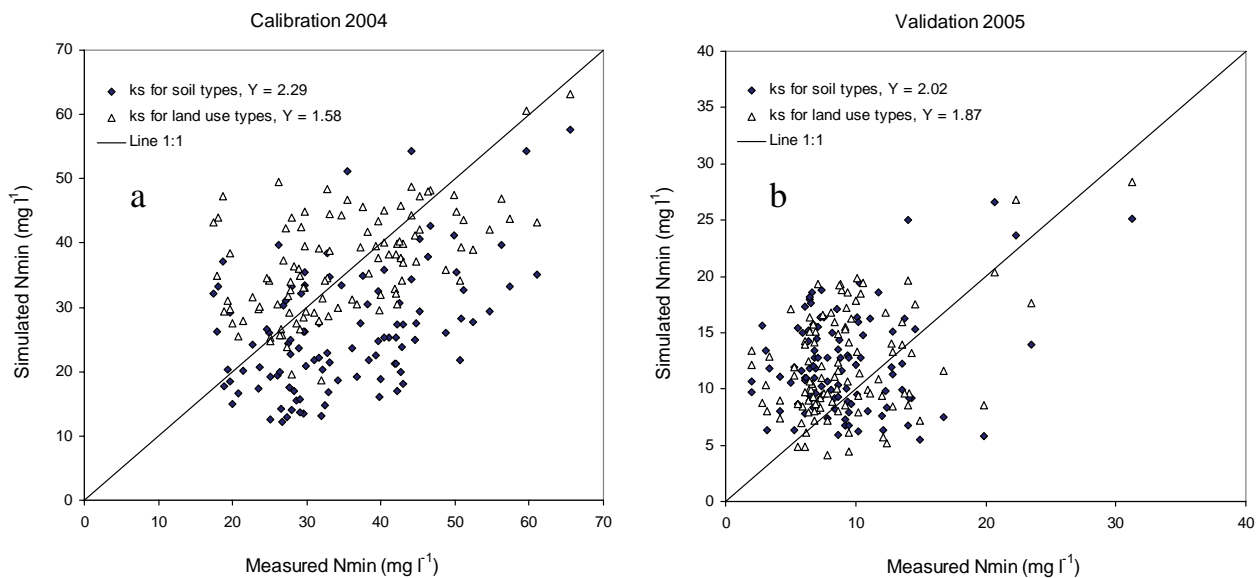


Figure 4. Calibration (2004, a) and validation (2005, b) results: correlation between measured soil mineral nitrogen concentration (Nmin, mg l^{-1}) at 52 points and 4 sampling dates and (solid symbols) simulated Nmin (mg l^{-1}) with different ks for the two soil types and (open symbols) simulated Nmin with different ks for the thirteen land units, created by overlaying soil and land use maps.

Table 5. Calibration factors for soil type-specific k_s and soil and land use type-specific k_s .

Soil compartment	Sandy loam			Clay loam		
	Rice	Other	Rice	Rice	Other	Other
Compartment 1	0.0003	0.0049	0.0003	0.0003	0.0075	0.0075
Compartment 2	0.030	0.130	0.030	0.030	0.130	0.130
Compartment 3	0.310	0.455	0.310	0.310	0.364	0.364

For soil and land use type-specific k_s	Flowers		Squash		Cabbage		Chili		Rice	
	Flowers	Squash	Flowers	Squash	Flowers	Squash	Flowers	Squash	Flowers	Rice
Compartment 1	0.0049	0.0049	0.0049	0.0049	0.0049	0.0024	0.0075	0.0075	0.0075	0.0024
Compartment 2	0.120	0.120	0.120	0.120	0.120	0.003	0.130	0.130	0.130	0.003
Compartment 3	0.457	0.447	0.437	0.437	0.455	0.478	0.400	0.354	0.341	0.437

As fertilizer use was reduced in practice, inorganic nitrogen fertilizer input was reduced by 15% in 2005. Applying the calibrated ks -values to 2005, the goodness of fit between simulated and measured N_{min} was lower than for 2004 (Figure 4b), and again Y was smaller for the procedure with land unit-specific ks (1.87) than for the procedure with soil type-specific ks (2.02).

Spatial N distribution

The spatial distribution of simulated N_{min} concentrations in the third layer for March 6th 2004 and March 26th 2005 is shown in Figure 5, illustrating the calibration and validation results. In general, N_{min} was lower in 2005 than in 2004. Overall, the spatial patterns were similar, but in 2004, N_{min} was similar in rice soil and in vegetable soil, whereas in 2005 it was lower in rice.

In the simulations, the rate of lateral nitrogen transport along the local drainage network (Idd; Table 4) was low, i.e. lateral water and N flows were less than 0.2 mm d⁻¹ and 0.032 kg ha⁻¹ d⁻¹ in the first, 0.11 and 0.06 in the second, and 0.03 and 0.012 in the third layer, respectively. The highest rates usually occurred during irrigation of specific crops, creating moisture content gradients between plots with different land use types. However, at some locations, cumulative lateral N_{min} transport was substantial (Figures 5c and d), due to frequent soil moisture gradients between the upper and lower cells. On the other hand, surface runoff also results in redistribution of soil water and nitrogen.

Nitrogen transport and leaching

Simulated percolation rates reached values up to 55.1 mm d⁻¹ in the first layer, 1.74 in the second, and 0.9 in the third, with associated N leaching rates of 0.7 kg ha⁻¹ d⁻¹ in the first layer, 0.65 in the second, and 0.45 in the third. Percolation was more frequent than lateral flow and strongly associated with rainfall events. However, the rates vary spatially, due to differences in elevation, soil type and land use type, as well as temporally, due to differences in rainfall, irrigation, evapo-transpiration and crop uptake.

Total annual N leaching was higher in 2004 than in 2005 (Figures 5e and f) and varied among crops (Table 6), as a result of differences in percolation volume under different irrigation and fertilizer regimes, i.e. from 88 to 122 kg N ha⁻¹ yr⁻¹ in flowers, 64 to 82 in the cabbage group, 51 to 76 in chili, 56 to 75 in the squash group, and 36 to 55 in rice.

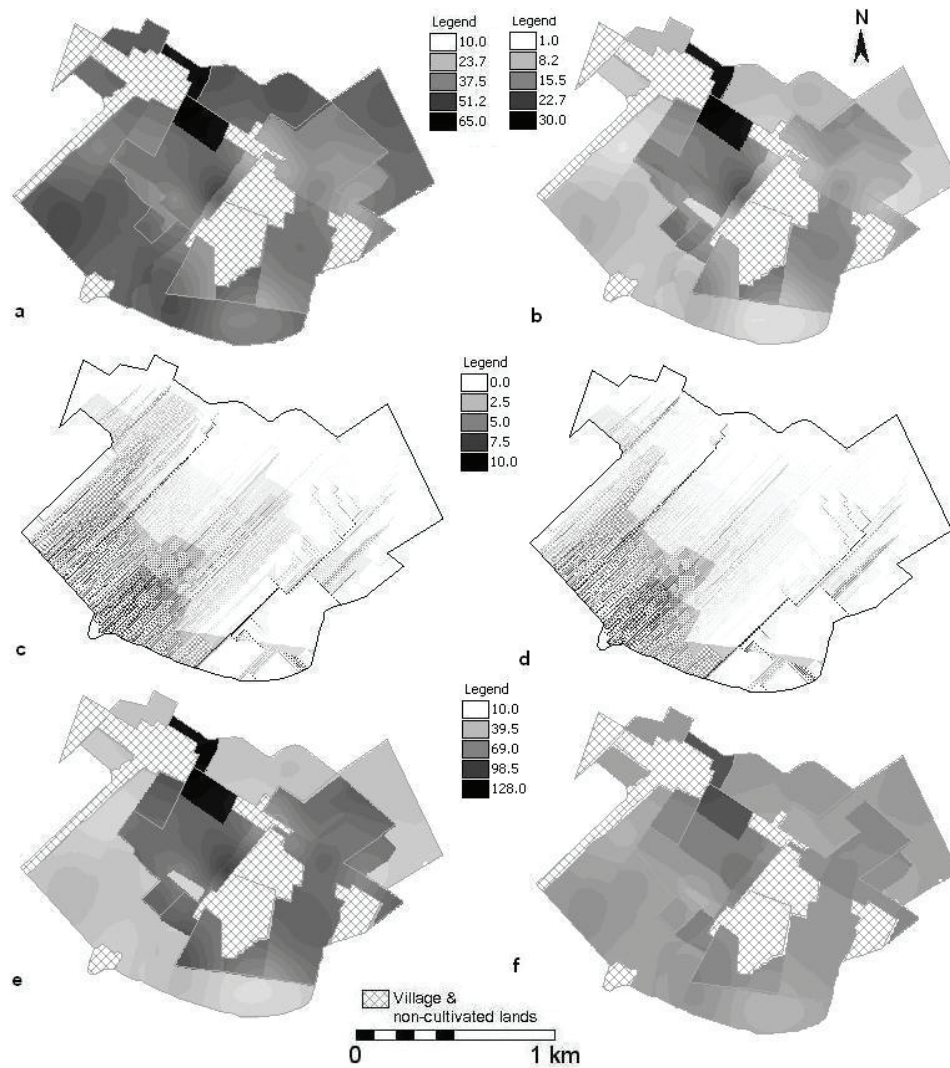


Figure 5. Simulated soil mineral nitrogen concentration (Nmin, mg l⁻¹) on 6th March 2004 (a), and 26th March 2005 (b); simulated cumulative lateral N transport (kg ha⁻¹ yr⁻¹) in 2004 (c) and in 2005 (d); and simulated annual N leaching (kg ha⁻¹ yr⁻¹) in 2004 (e), and in 2005 (f).

Table 6. Simulated annual nitrogen leaching losses (kg ha⁻¹) for different crops on sandy loam (SL) and clay loam (CL).

Land use	N leaching			
	2004		2005	
	SL	CL	SL	CL
Flowers	121.5	121.0	89.8	87.9
Squash	75.4	71.2	58.7	55.7
Cabbage	81.6	76.7	69.9	63.9
Chili	76.1	72.6	56.1	51.1
Rice	36.7	36.1	54.8	52.9

DISCUSSION

Modelling is a suitable way for quantifying nitrogen leaching from non-point sources as presented by intensive agriculture. The results become more accurate when more determining factors, such as environmental factors, i.e. climate, soil type, land use, and crop management, i.e. irrigation and fertilizer regimes, are taken into account. Up-scaling from individual plot level is essential in environmental assessment, and requires taking into account topography, spatial variability, temporal dynamics and interactions among factors that do not play a role at plot level (El-Sadek et al., 2003). For example, in our study area, nitrogen was transported laterally from north-east at higher elevation to south-west at lower elevation (Figures 5c and d). Particularly for the lands along the depressions, lateral flow may be important, although in general it is very low in the study area, due to the small differences in elevation.

Land use is the single most important factor influencing N leaching, as shown by significant differences in N-concentrations in the profile among crops (Chapter 6). Also in multiple correlation analysis, land use had a higher weight than other environmental factors (Chapter 7). Among the cropping systems in this study, flowers showed the highest susceptibility to N leaching, because of the very high fertilizer doses applied. Large quantities of nitrogen-rich manure were applied that remained on the soil surface during the rainy season. Vegetables, in both the cabbage and squash groups and chili show a similar range in N leaching, with the higher values for cabbage, associated with the intensive short-duration rotation and the relatively long residence time of the fertilizer on the soil surface. N leaching is lowest in rice, because of the presence of the low-permeability layer.

Land use type also strongly influences the water and nitrogen balances in the soil, through its effect on irrigation, evapo-transpiration, and fertilization. Soil moisture status varies among crops, as they are characterized by soil-type specific different rooting patterns, i.e. crops usually root deeper in sandy soil than in clay soil. Therefore, k_s should be calibrated for each soil horizon per combination of soil type and land use type.

For integrated environmental assessment, therefore, generating information relevant for policy makers and planners, a large number of system characteristics have to be combined. The PCRaster environment appears a very suitable tool for such applications, and can easily be combined with Geographic Information Systems.

These results show that the methodology is flexible and provides facilities for easily linking to and extracting information from spatial and non-spatial databases (Karssenbergh et al., 1996). For detailed and accurate identification of parameters, such as soil hydraulic properties (k_s , porosity, and water holding capacity) and to apply appropriate irrigation and fertilizer regimes, the land unit map, resulting from

overlaying the soil and land use maps should be used.

The model could be improved by incorporating the effects of drainage canal systems and watershed effects. Closer to the drainage network, soil moisture gradients are steeper and lateral flow is therefore higher near the canal. At watershed scale, the water and nitrogen balances would be more accurately simulated, if the drainage pathway through the local drainage network to the outlet of the watershed, which leads to N accumulation in the watershed outlet, would be incorporated.

CONCLUSIONS

A spatial dynamic model was developed in the PCRaster software environment to simulate nitrogen dynamics and leaching under intensive agriculture with high fertilizer use, and was applied for a period of two years to Van Hoi commune in a flatland area of Tam Duong district in Vietnam. The model is shown to be a suitable tool for quantifying nitrogen losses from agriculture and for environmental assessment at regional scale. It has been calibrated on the basis of measurements in March and August 2004 and validated for March and August 2005. Simulated result show that lateral flow was low, and that nitrogen leaching due to percolation was high. Simulated annual N leaching losses varied from 88 to 122 kg N ha⁻¹ yr⁻¹ in flowers, 64 to 82 in the cabbage group, 51 to 76 in chili, 56 to 75 in the squash group, and 36 to 55 in rice. Model accuracy might be improved through further calibration in both vertical and horizontal dimensions, and for more combinations of soil and land use.

CHAPTER 9

General discussion

INTRODUCTION

As population density in Tam Duong district in northern Vietnam has been increasing in the last decade, per capita available land has declined. To maintain family food security, production had to be increased, either to grow more food, or to increase income from the limited land area. The farming community has responded to this demand by intensification of agricultural production, i.e. by increasing the number of crops cultivated per year, and the use of external inputs, particularly chemical fertilizers and crop protection agents. This development has increased the risk for negative environmental impacts through losses of agro-chemicals. Erosion and leaching are the main processes contributing to high nutrient losses that, in turn, reduce income and soil quality. Annual losses through soil erosion at plot scale have been recorded from 227 to 599 kg ha⁻¹ for soil organic carbon, 29–52 for nitrogen, 20–26 for phosphorus, and 22–35 for potassium (Toan et al., 1998). Introduction of alternative crop management technologies could improve the situation. To design such technologies, increased insight in the relevant processes is required.

This study therefore dealt with the major processes involved in soil degradation at different scales, with the following objectives:

- To survey soil degradation dynamics in the study area, using remote sensing, to delineate the extent of different soil degradation types, as a basis for the design of effective soil conservation measures.
- To study soil erosion at different scales in hilly land watersheds, to assess effects of paddy fields on soil erosion in the watershed, and to simulate soil erosion in the watershed in the presence of paddy fields.
- To quantify nutrient losses due to leaching from different soils and agricultural systems through field experimentation and to develop a suitable model for estimation of nutrient leaching losses.
- To scale-up nitrogen dynamics and leaching losses in a small region, using geostatistics and a geographic information system (GIS).
- To make the new data and knowledge available for the design of sustainable land use systems that meet/contribute to achieving the multiple development goals of the region.

ASSESSING SOIL DEGRADATION THROUGH REMOTE SENSING

Satellite imagery (LANDSAT MSS in 1984 (4 bands), TM 1992, 1996 and 2000 (6 bands)) was applied for the assessment of the extent of soil degradation. Bare and degraded soils were identified and extracted from Colour Composite and Band Ratio images. Land use and soil degradation dynamics were assessed for 1984, 1992, 1996 and 2000, showing degraded soil areas in the district of 2437, 3282, 2185 and 2576 ha,

respectively. During the years 1990–92, large-scale reforestation took place (mostly eucalyptus for supply to the paper mill), with the associated higher land cover and biomass, reducing erosion and soil degradation. The productive forest has been harvested since 1996, resulting in larger bare soil areas and increased soil degradation. Ground truth data showed satellite imagery to be a useful tool to represent the degraded soil areas in the hilly land and the sandy soils on the high terraces, but not in the agricultural lowland, because on hilly and sandy terraces, soil organic matter and soil moisture contents were very low.

SOIL EROSION UNDER DIFFERENT CONDITIONS

Tam Duong is located in the transitional zone between the flat lowlands and the mountainous regions, and consists of a mosaic of mountains, hilly and flat lands. Despite relatively gentle slopes, soil erosion is severe in the zone, because of the prevalence of highly erodible soil types, very high and concentrated rainfall conditions, and scarce land cover during extended periods. Geographically, the mosaics of hilly lands and terraces form complex watersheds that are communally managed by the local population.

Soil erosion was measured at three scales (Chapter 3), i.e. plot, sub-watershed (SW), and main watershed (MW). The main watershed contains many sub-watersheds; the selected plots and the SW were situated on sloping land at an elevation of 70 to 80 m above sea level. Terraces are situated in the lower parts towards the main watershed outlet, including parts of sub-watersheds. Soil erosion at plot- and SW-scales was used as reference to assess the effects of (terraced) paddy fields on erosion at MW-scale. Soil erosion per unit surface at SW- and MW-scales was lower than at plot scale, partly explained by steeper slopes in SW and the experimental plots than in MW as a whole. Moreover, the presence of paddy fields strongly affected the soil erosion pattern in the MW. At plot scale, detachment is the dominant process, that determines the potential for soil erosion (Wischmeier and Smith, 1978). At SW-scale, in addition to detachment, transport and deposition processes determine the final sediment yield at the watershed outlet. Detachment, transport and deposition depend on the geometry of the watershed and vary in dependence of plot surface characteristics, slope angle and exposition, as well on soil type and land management. During transport of runoff, sediment can be deposited in depressions or trapped at field boundaries or densely vegetated areas; moreover, deposition rate varies for different soil and land use types. Hence, at MW-scale, the number and characteristics of terraces and paddy fields affect runoff and sediment regimes. The magnitude of peak discharge, total discharge, and soil loss strongly depends on the geometry of hedges on the terraces, height of the bunds around cultivated plots and their firmness and water levels in paddy fields.

Results of a soil erosion model (Chapter 4) showed that paddy fields act as temporary storage facilities for rain and runoff water, which is subsequently gradually released to the stream networks and watershed outlet. The dynamics of the storage and release processes depend on rainfall volume and intensity and can therefore not easily be predicted. Peak discharge, total discharge, and soil loss are further affected by the slopes and soil surface characteristics, i.e. random roughness, soil cohesion, soil particle size distribution, and aggregate stability that influence stream power, sediment concentration, and transport capacity of the runoff flow. Highest soil erosion was observed in August and September, coinciding with periods of highest rainfall. Runoff peaked in August and September because of high rainfall, whereas sediment concentration was usually higher in April, June, July, the end of September, and October, associated with low soil cover and strong soil disturbance.

Erosion occurs at certain rainfall volume and intensity. For example, in 2004, 10 events with runoff and soil loss were recorded, compared to 30 in 2005, associated with a higher number of rainfall events, with higher intensity and larger volume (Chapter 3). Analysis of data from 8 selected events in the two years showed that with a total rainfall of 173.2 mm, soil loss at plot scale was $1067.4 \text{ kg ha}^{-1}$, while it was 44.6 at SW- and 125.2 at MW-scale. At MW-scale, annual soil loss in 2004 was 163 to kg ha^{-1} and in 2005, 1722; the very high value in 2005 was associated with an extraordinary event with very high rainfall. These values are comparable to those reported from other studies in the region (Toan et al., 2005), and much lower than values at plot scale, as measured for instance by Toan et al. (1998) ranging from 17.5 to $37.2 \text{ Mg ha}^{-1} \text{ yr}^{-1}$.

The soil erosion model LISEM (De Roo et al., 1996a, b) was applied to simulate erosion in SW and MW. Runoff dynamics, i.e. peak runoff time, peak runoff amount and total runoff were simulated satisfactorily for SW, but not for MW. This difference in performance is associated with the difference in geomorphology between the two watersheds. The sub-watershed consists mainly of sloping lands, while the main watershed includes low terraces and paddy fields that delay flow as a result of through-flow, storage and release, processes not included in the current version of LISEM. The magnitude and patterns of runoff strongly depend on season (weather conditions), field/soil conditions, and crop characteristics. Discharge can start shortly after the onset of a rain event and attain high values when (paddy) fields are fully flooded, while it can be strongly delayed and remain low, if fields are dry. Soil loss was overestimated (on average 2.8 times) for SW and underestimated (on average 0.74 times) for MW (Chapter 4). The overestimation for SW was associated with very high simulated sediment concentrations, resulting from strong detachment and transport capacity in SW, while the underestimation for MW was associated with

underestimation of total runoff, as a result of the presence of terraces and paddy fields. This type of watershed is common in northern Vietnam; for satisfactory simulation of soil erosion under these conditions, the soil erosion model should be extended to incorporate, among others, the effects of paddy fields on runoff, such as the relation between field bund height, water level and runoff, the mechanism of through-flow in the terraces, and the filtering effect of crops on the terraces that leads to a reduction in sediment concentration.

NITROGEN LEACHING LOSSES AT PLOT SCALE

Following the introduction of the ‘đổi mới’ strategy, and stimulated by the growing demand for agricultural products from population centres, such as Vinh Yen town, farmers intensified production. To make a livelihood from the relatively small areas of land available, high-value crops, such as vegetables, became a major commodity, as horticulture generated a much higher income than traditional double rice and winter maize (Hengsdijk et al., 2005; IRMLA, 2005; Ponsioen et al., 2006; Van den Berg et al., 2007). In addition to soil erosion, nutrient leaching is an important problem in these intensive systems on sloping terraces with sandy soils, causing environmental problems, such as eutrophication and pollution of drinking water sources, with potential health risks, and contributing to low fertilizer use efficiencies. In these intensive agricultural systems, in which large amounts of irrigation water and high fertilizer doses are applied (Chapters 5 and 6), much higher nitrogen leaching was recorded than in the traditional agricultural systems, even though crops were not fully irrigated nor (for rice) the soil continuously flooded, due to the sloping lands and the very sandy soils with high infiltration capacity.

In the experimental study, no attention was paid to seepage and lateral nitrogen transport between terraces. However, lateral flow through paddy bunds has been shown to be an important component in the water balance of paddy rice systems in Asia (Bouman et al., 1994; Wopereis et al., 1994; Chen et al., 2002; Huang et al., 2003). This process results in redistribution of soil nitrogen, with export from the upper terraces and accumulation in the lower terraces. To take into account the specific conditions of the study area, with its typical features of terraces and banded fields, the associated typical runoff behaviour, and flexible irrigation regimes, a soil water and nitrogen model was developed that explicitly takes into account the combined effects of environmental factors on soil and plant processes, and the consequences for nitrogen transport in the soil. The model satisfactorily reproduced the behaviour of soil mineral nitrogen under the typical northern Vietnamese terrace conditions. However, before the model can be applied under quite different agro-ecological conditions, it needs to be expanded and extensively tested, as it does not yet deal with important

processes in the nitrogen balance, such as volatilization, nitrification, denitrification, and hydrolysis of urea. These processes are especially important in situations where frequent transformations of ammonium and nitrate take place, under alternate wet and dry conditions that regularly occur in these systems. Moreover, nitrogen contributions from rain and irrigation water have not explicitly been taken into account, which may be significant components in the nitrogen balance, especially in situations of overland flow from upper hills and terraces with high sediment concentrations. That holds particularly in situations where inputs through fertilizers and manure are low, and would be important therefore in evaluation of the consequences of introduction of alternative management practices, such as low external input techniques. Of particular interest in this context could be the role of rice fields in the watershed as biological filters, retaining sediment and nutrients from runoff.

The intensive farming systems in the district, with up to six crops annually (Chapter 5), are characterized by high inputs of both on-farm resources, including Farm Yard Manure, (composted) N-rich residues and food processing wastes and external chemicals, i.e. fertilizers and biocides. These systems thus represent high risks for negative environmental impacts through emission of chemicals, with particular vulnerability for the soil and groundwater environments. Our data (Chapters 5 and 6) indicate that nitrate is by far the most dominant species in nitrogen leaching to groundwater. The simple water and nitrogen balance models show that the risk for N leaching is highest in situations with simultaneously high rainfall/irrigation, high levels of soil amendments in organic and/or inorganic fertilizer, and low crop nitrogen demand. These situations occur during the early growth stages of flowers, cabbage, and chili in the rainy season (Chapter 5), up to maximum tillering for rice and from sowing to the 9th leaf stage for maize (Chapter 6).

UP-SCALING OF NITROGEN LEACHING LOSSES

Spatially, N distribution in the soil and leaching to groundwater varied strongly, depending on land use type, environmental conditions, such as soil type, elevation, and rainfall regime, and management, i.e. irrigation and fertilizer regimes (Chapter 7). Land management had the strongest influence on N concentration and N leaching to groundwater, through the land use type-specific fertilizer and irrigation regimes. Regression block kriging (RBK) appeared a better technique for spatial interpolation of N concentration than ordinary block kriging (OBK), as it allows the use of weighted effects of different environmental conditions, derived from linear regression. The kriging technique allows up-scaling of the site-specific information of plot measurements of N concentration to maps providing time-specific information. To combine these data, a spatial dynamic model was developed (Chapter 8) that integrates

vertical N leaching (Chapters 5 and 6) and lateral transport, working in a GIS simulation environment (Karssenberget al., 1996). The model has been calibrated and validated, both spatially and temporally, based on measured nitrogen concentrations. The correlation between validated and measured values was lower than that between calibrated and measured values, but it can be concluded that the model fairly accurately reproduced measured nitrogen concentrations. The simulated nitrogen concentration and the 'kriged' nitrogen concentration (Chapter 7), that was interpolated from point measurements, showed similar trends and patterns, i. e. high nitrogen concentrations in land use types with high inputs of irrigation and fertilizers such as flowers and vegetables. In the simulation model (Chapter 8), the concentration was continuously quantified, based on calculated water and nitrogen balances, taking into account lateral flows. The results of the model show that land use, through its effects on evaporation, transpiration, and nitrogen uptake and land management, such as irrigation and fertilizer input, are the most important characteristics that determine water and nitrogen transport processes and thus percolation and nitrogen leaching; therefore, using the high resolution land unit map, which is an overlay of the soil map and the land use map as a basis, will result in the best predicted spatial distribution of N concentration and leaching in this model. Lateral flow, however, is also an important component in the transport processes in these sloping areas, and should thus be calibrated and validated as well. The model should also take into account the drainage system networks that usually result in increased soil moisture gradients and increased percolation and lateral flow near the drainage system network.

CONCLUDING REMARKS

The research provided useful information on the extent and dynamics of soil degradation in Tam Duong district in northern Vietnam, identifying the most important types of soil degradation under different soil and land use conditions and providing quantitative information on soil loss and nutrient losses for different land use patterns. However, provision of sound information on soil erosion and nitrogen leaching, and other environmental processes, as required in comprehensive land use analysis, looking at options for more sustainable land use and rural development in the region, requires additional research.

Remote sensing appears a useful tool for mapping soil degradation (Graetz, 1987). It allows discrimination between different soil development and degradation levels (Leone and Sommer, 2000), determination of rapid surface change due to anthropogenic influences (Schmid et al., 2004) and assessment of forest degradation (Souza et al., 2003). Since soil erosion is the main cause of soil degradation in the study area, remote sensing can be used for estimating erosion surface features, i.e. by

linear mixture modelling (Metternicht and Fermont, 1998) or mapping complex patterns of erosion and stability (Hill and Schutt, 2000). Furthermore, remote sensing can support soil erosion modelling, soil erosion mapping, and soil degradation assessment through providing various soil surface and soil cover indices. It has been shown that various system characteristics can be derived from satellite images, such as Leaf Area Index (Gu et al., 2006), soil moisture content (Wang et al., 2004; Zhang and Wegehenkel, 2006), spatial distribution of surface roughness (Goyal et al., 1999), and canopy height (Anderson et al., 2004). High resolution satellite images can provide accurate information on the spatial distribution of such characteristics that may be used as model inputs (Jongschaap, 2006). With a short return period of the satellites, also temporal patterns of relevant characteristics can be generated, representing changes in environmental conditions, i.e. rainfall intensity, land preparation periods and crop characteristics, such as onset of the period of linear crop growth, flowering and maturity. Such information would allow simultaneous simulation of land use dynamics and soil erosion, as well as soil degradation dynamics, which might open possibilities for designing soil erosion and other degradation control measures to avoid degradation of the natural resource base. However, for recognition of soil degradation features, high resolution, especially hyper spectral images are preferred. Correlations of multi-date satellite images, soil erosion modelling, and soil erosion measurement should be established, to develop an operational tool for accurate mapping of soil degradation in the hilly area of northern Vietnam as a basis for conservation and reclamation.

Additional field work is necessary to increase understanding of the dynamics of runoff and soil erosion in complex watersheds, comprising such elements as terraces and paddy fields. For an adequate quantitative description of soil erosion in such watersheds that are common in Vietnam and other areas in South-east Asia, the soil erosion model should be extended with such features (Eiumnoh et al., 2003).

Performance of the nitrogen leaching model developed in the current study should be improved by incorporating modules for the description of crop growth and nitrogen emission, including the filtering effects of paddy fields on the terraces that can retain sediment and nutrients eroded from upper terraces.

In designing alternative cropping systems for Tam Duong district, also using the results of the current study, a number of recent developments in Vietnam have to be taken into account. The “Three Reductions, Three Gains” programme of the Vietnamese government that started in 2001, focuses on motivating farmers to *reduce* seed rates, fertilizer rates, and pesticide applications to *gain* high yields, improved product quality, and income. It has been evaluated as very successful and is expected to be implemented in 50% of the country’s rice area within the next 3 years (IRRI, 2006). Tam Duong district is one of the first regions in which the program was

successfully implemented. Large-scale adoption of the principles of this programme should lead to increased income on one hand and reduced negative impacts and environmental pollution on the other. In addition, the Vietnamese national IPM (Integrated Pest Management) programme has been implemented by the Plant Protection Department, Ministry of Agriculture and Rural Development, with FAO support, since 1992 (FAO, 2001). The programme has successfully been training groups of farmers, who are supposed to then act as trainers throughout the country. The programme stimulated farmers to minimize biocide use through precision application at the right time, based on frequent crop observations and knowledge of pests and diseases and beneficial organisms. Moreover, a balanced fertilizer regime was promoted. Most quantitative targets for the programme have been met and its continuation is strongly recommended. Recognizing the increasing competition for water (Bindraban et al., 2006), the agricultural sector, currently by far the largest user of fresh water, is actively researching the possibilities for water-saving technologies (Warner et al., 2006). For rice, a crop with very high water requirements, alternative irrigation techniques are being investigated, such as alternative wetting-drying and aerobic rice (Bouman, 2007). Such technologies can substantially reduce the water requirements of rice, with positive consequences also for leaching and erosion and could also be useful for Tam Duong district.

References

- Abdeen, M.M., Thurmond, A.K., Abdelsalam, M.G. and Stern, R.J., 2001. Application of ASTER Band-Ratio images for geological mapping in arid regions: The Neoproterozoic Allaqi Suture, Egypt, GSA In: The Geological Society of America, Annual Meeting, November 5-8, 2001, Boston, Massachusetts, USA.
- Abu-Zreig, M., Rudra, R.P. and Whiteley, H.R., 2001. Validation of a vegetated filter strip model (VFSSMOD). *Hydrological Processes* 15(5), 729-742.
- Addiscott, T.M., 1990. Measurement of nitrate leaching: A review of methods. In: Calviet R. (Ed.), *Nitrates-Agriculture-Eau*. INRA (Institut National de Recherches Agronomique), Paris-Grignon, France, pp. 157-168.
- Addiscott, T.M. and Whitmore, A.P., 1987. Computer simulation of changes in soil mineral nitrogen and crop nitrogen during autumn, winter and spring. *Journal of Agricultural Science, Cambridge* 109, 141-157.
- Akiyama, H. and Tsuruta, H., 2002. Effect of chemical fertilizer form on N₂O, NO and NO₂ fluxes from Andisol field. *Nutrient Cycling in Agroecosystems* 63, 219-230.
- Allaire-Leung, S.E., Wu, L., Mitchell, J.P. and Sanden, B.L., 2001. Nitrate leaching and soil nitrate content as affected by irrigation uniformity in a carrot field. *Agricultural Water Management* 48, 37-50.
- Allen, R.G., Pereira, L.S., Raes, D. and Smith, M., 1998. *Crop evapotranspiration: Guidelines for computing crop water requirements*. FAO Irrigation and Drainage Paper No 56. Food and Agriculture Organization of the United Nations, Rome, Italy.
- Amr, A. and Hadidi, N., 2001. Effect of cultivar and harvest date on nitrate (NO₃) and nitrite (NO₂) content of selected vegetables grown under open field and greenhouse conditions in Jordan. *Journal of Food Composition and Analysis* 14, 59-67.
- Angle, J.S., 1990. Nitrate leaching losses from soybeans (*Glycine max* L. Merr.). *Agriculture, Ecosystems & Environment* 31, 91-97.
- Anderson, M.C., Neale, C.M.U., Li, F., Norman, J.M., Kustas, W.P., Jayanthi, H. and Chavez, J., 2004. Upscaling ground observations of vegetation water content, canopy height, and leaf area index during SMEX02 using aircraft and Landsat imagery. *Remote Sensing of Environment* 92, 447-464.
- Anh, P.H., Nga, N.H., Truong, T.H., Hoa, T.T., Hanh, C.H. and Duong, B.H., 2002. Cancer incidence in Hanoi population of period 1996-1999. *Journal of Practical Medicine* 431, 4-11. (Vietnamese)
- Antikainen, R., Lemola, R., Nousiainen, J.I., Sokka, L., Esala, M., Huhtanen, P. and Rekolainen, S., 2005. Stocks and flows of nitrogen and phosphorus in the Finnish

References

- food production and consumption system. *Agriculture, Ecosystems & Environment* 107, 287-305.
- Aronsson, P.G., 2001. Dynamics of nitrate leaching and ^{15}N turnover in intensively fertilized and irrigated basket willow grown in lysimeters. *Biomass and Bioenergy* 21, 143-154.
- Averjanov, S.F., 1950. About permeability of subsurface soils in case of incomplete saturation. In: *English Collection*, Vol. 7 (1950), quoted by P.Ya. Palubarinova, 1962. *The theory of Groundwater Movement* (English translation by I.M. Roger DeWiest, Princeton University Press), pp. 10-21.
- Babiker, I.S., Mohamed, M.A.A., Terao, H., Kato, K. and Ohta, K., 2004. Assessment of groundwater contamination by nitrate leaching from intensive vegetable cultivation using geographical information system. *Environmental International* 29, 1009-1017.
- Bac, D.D., 1984. Zoning soil erosion in Central Vietnam, Ministry of Agriculture and Food Industry, Hanoi, Vietnam. (Vietnamese)
- Bat, L.T., 2001. Soil environmental state of Vietnam. *Vietnam Soil Science* 15, 146-153. (Vietnamese)
- Beasley, D.B. and Huggins, L.F., 1982. ANSWERS Users Manual. U.S. Environmental Protection Agency. Purdue University, Region V, Chicago, Illinois, West Lafayette, Indiana, 54 pp.
- Beasley, D.B., Huggins, L.F. and Monke, E.J., 1980. ANSWERS: A model for watershed planning. *Transactions of the American Society of Agricultural Engineers* 23(4), 938-944.
- Belmans, C., Wesseling, J.G. and Feddes, R.A., 1983. Simulation model of the water balance of a cropped soil: SWATRE. *Journal of Hydrology* 63, 271-286.
- Beven, K. and Freer, J., 2001. A dynamic TOPMODEL. *Hydrological Processes* 15(10), 1993-2011.
- Bindraban, P.S., Van Keulen, H. and Warner, J.F., 2006. Editorial. *Water Resources Development* 22, 1-2.
- Boogaard, H.L., Van Diepen, C.A., Roetter, R.P., Cabrera, J.M.C.A. and Van Laar, H.H., 1998. WOFOST 7.1: User's guide for the WOFOST 7.1 crop growth simulation model and WOFOST Control Center. DLO Winand Staring Centre, Wageningen, The Netherlands, 144 pp.
- Bouman, B.A.M., 2007. A conceptual framework for the improvement of crop water productivity at different spatial scales. *Agricultural Systems* 93, 43-60.
- Bouman, B.A.M., Wopereis, M.C.S., Kropff, M.J., Ten Berge, H.F.M. and Tuong, T.P., 1994. Water use efficiency of flooded rice fields. II. Percolation and seepage losses. *Agricultural Water Management* 26, 291-304.

- Bremner, J.M., 1996. Nitrogen-total. In: Sparks D.L., Page A.L., Johnston C.T. and Summer M.E. (Eds), *Methods of soil analysis. Part 3. Chemical Methods*. SSSA Book Series No. 5, SSSA, Madison, WI, USA, pp. 1085-1121.
- Brutsaert, W., 1966. Probability laws for pore-size distributions. *Soil Science* 101, 85-92.
- Byrnes, B.H., 1990. Environmental effects of N fertilizer use: An overview. *Fertilizer Research* 26, 209-215.
- Cai, G.X., Chen, D.L., Ding, H., Pacholski, A., Fan, X.H. and Zhu, Z.L., 2002. Nitrogen losses from fertilizers applied to maize, wheat and rice in the North China Plain. *Nutrient Cycling in Agroecosystems* 63, 187-195.
- Cameron, K.C., Rate, A.W., Noonan, M.J., Moore, S., Smith, N.P. and Kerr L.E., 1996. Lysimeter study of the fate of nutrients following subsurface injection and surface application of dairy pond sludge to pasture. *Agriculture, Ecosystems & Environment* 58, 187-197.
- Can, L.T., My, N.Q., 1982. Observation of soil erosion in Vietnam. Ministry of Agriculture, Hanoi, Vietnam. (Vietnamese)
- Carberry, P.S., Probert, M.E., Dimes, J.P., Keating, B.A. and McCown, R.L., 2002. Role of modelling in improving nutrient efficiency in cropping systems. *Plant and Soil* 245, 193-203.
- Cerdan, O., Bissonnais, Y.L., Souchère, V., Martin, P. and Lecomte, V., 2002. Sediment concentration in interrill flow: Interactions between soil surface conditions, vegetation and rainfall. *Earth Surface Processes and Landforms* 27(2), 193-205.
- Changhe, L., 2000. Breaking the spiral of unsustainability. An exploratory land use study for Ansai, the Loess Plateau of China. PhD Thesis, Wageningen University, Wageningen, The Netherlands, 257 pp.
- Chavez, P.S., 1988. An improved dark-object subtraction technique for atmospheric scattering correction of multispectral data. *Remote Sensing of Environment* 24, 459-479.
- Chen, S.-K. and Liu, C.W., 2002. Analysis of water movement in paddy rice fields. I. Experimental studies. *Journal of Hydrology* 260, 206-215.
- Chen, S.-K., Liu, C.W. and Huang, H.-C., 2002. Analysis of water movement in paddy rice fields. II. Simulation studies. *Journal of Hydrology* 268, 259-271.
- Chen, R.S., Pi, L.C. and Huang, Y.H., 2003. Analysis of rainfall-runoff relation in paddy fields by diffusive tank model. *Hydrological Processes* 17(13), 2541-2553.
- Chi, H.T. and Bo, L.V., 2002. Suitability map of Vanhoi commune. Soil and Fertilizer Research Station, Vinh Phuc Agricultural and Rural Development Department, Vinh Phuc province, Vietnam. (Vietnamese)
- Chikowo, R., Mapfumo, P., Nyamugafata, P. and Giller, K.E., 2004. Mineral N

References

- dynamics, leaching and nitrous oxide losses under maize following two-year improved fallows on a sandy loam soil in Zimbabwe. *Plant and Soil* 259, 315-330.
- Chiles, J.P. and Delfiner, P., 1999. *Geostatistics: Modeling spatial uncertainty*. Wiley and Sons, New York, USA, 695 pp.
- Chin, W. and Kroontje, W., 1963. Urea hydrolysis and subsequent loss of ammonia. *Soil Science Society of America Journal* 27, 316-319.
- Cho, J.-Y., 2003. Seasonal runoff estimation of N and P in a paddy field of central Korea. *Nutrient Cycling in Agroecosystems* 65, 43-52.
- Chow, V.T., Maidment, D.R. and Mays, L.W., 1988. *Applied hydrology*. McGraw-Hill, New York, USA, 572 pp.
- Chowdary, V.M., Rao, N.H. and Sarma, P.B.S., 2004. A coupled soil water and nitrogen balance model for flooded rice fields in India. *Agriculture, Ecosystems & Environment* 103, 425-441.
- Chung, D.V., 1978. The main factors influence to soil erosion. *Journal of Hydrology Science* 192, 26-31. (Vietnamese)
- Cinnirella, S., Buttafuoco, G. and Pirron, N., 2005. Stochastic analysis to assess the spatial distribution of groundwater nitrate concentrations in the Po catchment (Italy). *Environmental Pollution* 133, 569-580.
- Cohen, M.J., Shepherd, K.D. and Walsh, M.G., 2005. Empirical reformulation of the universal soil loss equation for erosion risk assessment in a tropical watershed. *Geoderma* 124, 235-252.
- Dai, N.V. and Trang, T.T., 2003. Research results of fertilizer and returned crop residues in some crop rotations on degraded soil. Annual report, National Institute for Soils and Fertilizers, Hanoi, Vietnam. (Vietnamese)
- Daura, M.M., Akintola, F.O., Areola, O. and Faniran, A., 1995. Comparative analysis of nutrient losses on experimental plots under cropping system [in Nigeria, at Ibadan university campus]. *Geo-Eco-Trop (Belgium)* 19, 91-104.
- Day, P.R., 1965. Particle fractionation and particle-size analysis. In: C.A. Black (Ed.), *Methods of soil analysis. Part 1. Agronomy Monograph*, American Society of Agronomy, Madison, WI, USA, pp. 545-567.
- De Koning, G.H.J., Van Diepen, C.A. and Reinds, G.J., 1995. Crop growth model WOFOST applied to potatoes. In: Kabat, P., Marshall, B., Van den Broek, B.J., Vos, J. and Van Keulen, H. (Eds), *Modelling and parameterization of the soil-plant-atmosphere system - a comparison of potato growth models*. Wageningen Press, Wageningen, The Netherlands, pp. 275-297.
- Delgado, J.A., 2002. Quantifying the loss mechanisms of nitrogen. *Journal of Soil and Water Conservation* 6, 389-398.
- De Ridder, N., Van Ittersum, M., Van Keulen, H., De Haan, J., Rossing, W., Schipper,

- R., Claassen, F., Hendricks, T. and Stoorvogel, J., 2002. Quantitative analysis of land use systems. QUALUS, Course PPS-30304, Plant Production Systems, Development Economics, Biological Farming Systems, Operational Research and Logistics, Soil Science and Geology, Wageningen University and Research centre, Wageningen, The Netherlands.
- De Roo, A.P.J. and Jetten, V.G., 1999. Calibrating and validating the LISEM model for two data sets from The Netherlands and South Africa. *Catena* 37, 477-493.
- De Roo, A.P.J., Offermans, R.J.E. and Cremers, N.H.D.T., 1996a. LISEM: A single-event, physically based hydrological and soil erosion model for drainage basins. II: Sensitivity analysis, validation and application. *Hydrological Processes* 10, 1119-1126.
- De Roo, A.P.J., Wesseling, C.G. and Ritsema, C.J., 1996b. LISEM: A single-event physically based hydrological and soil erosion model for drainage basins. I: Theory, input and output. *Hydrological Processes* 10, 1107-1117.
- Di, H.J. and Cameron, K.C., 2002. Nitrate leaching in temperate agroecosystems: Sources, factors and mitigating strategies. *Nutrient Cycling in Agroecosystems* 64, 237-256.
- Dimitriou, I. and Aronsson, P., 2004. Nitrogen leaching from short-rotation willow coppice after intensive irrigation with wastewater. *Biomass and Bioenergy* 26, 433-441.
- Diodato, N. and Ceccarelli, M., 2004. Multivariate indicator kriging approach using a GIS to classify soil degradation for Mediterranean agricultural lands. *Ecological Indicators* 4, 177-187.
- Dobermann, A., Witt, C., Dawe, D., Abdurachman, S., Gines, H.C., Nagarajan, R., Satawathananont, S., Son, T.T., Tan, P.S. and Wang, G.H., 2002. Site-specific nutrient management for intensive rice cropping systems in Asia. *Field Crops Research* 74, 37-66.
- Dogliotti, S., Rossing, W.A.H., Van Ittersum, M.K., 2004. Systematic design and evaluation of crop rotations enhancing soil conservation, soil fertility and farm income: A case study for vegetable farms in South Uruguay. *Agricultural Systems* 80(3), 277-302.
- Eiumnoh, A., Pongsa, S. and Sewana, A., 2003. A dynamic soil erosion model (MSEC 1): An integration of mathematical model and PCRaster - GIS. In: *Integrated watershed management for land and water conservation and sustainable agricultural production in Asia. Proceedings of the ADB-ICRISAT-IWMI Project Review and Planning Meeting. Hanoi, Vietnam*, pp. 241-251.
- El-Sadek, A., Feyen, J., Radwan, M. and El Quosy, D., 2003. Modelling water discharge and nitrate leaching using DRAINMOD-GIS technology at small

References

- catchment scale. *Irrigation and Drainage* 52, 363-381.
- Ersahin, S. and Rustu Karaman, M., 2001. Estimating potential nitrate leaching in nitrogen fertilized and irrigated tomato using the computer model NLEAP. *Agricultural Water Management* 51, 1-12.
- Fan, A.M. and Steinberg, V.E., 1996. Health implications of nitrate and nitrite in drinking water: An update on methemoglobinemia occurrence and reproductive and developmental toxicity. *Regulatory Toxicology and Pharmacology* 23, 35-43.
- Fang B., Wang G.H., Van den Berg M. and Roetter R. 2005. Identification of technology options for reducing nitrogen pollution in cropping systems of Pujiang. *Journal Zhejiang University Science* 6b, 981-990.
- FAO, 1976. A framework for land evaluation. *FAO Soils Bulletin No. 32*, FAO, Rome, Italy, 72 pp.
- FAO, 2001. Report of the twenty-second session of the Asia and Pacific Plant Protection Commission, 17th- 21st September, 2001, Ho Chi Minh City, Vietnam.
- FAO/UNESCO, 1974. Soil map of the world, 1:5,000,000, 10 volumes. UNESCO, Paris, France.
- Fiener, P., Auerswald, K. And Weigand, S., 2005. Managing erosion and water quality in agricultural watersheds by small detention ponds. *Agriculture, Ecosystems & Environment* 110(3-4), 132-142.
- Flanagan, D.C., Ascough, J.C., Nearing, M.A., Laflen, J.M., 2001. The Water Erosion Prediction Project (WEPP) model. In: Harmon, R.S., Doe, W.W. (Eds), *Landscape erosion and evolution modelling*. Kluwer Academic Publishers, New York, USA, pp. 145-199.
- Fuentes, J.P., Flury, M., Huggins, D.R. and Bezdicek, D.F., 2003. Soil water and nitrogen dynamics in dryland cropping systems of Washington State, USA. *Soil and Tillage Research* 71, 33-47.
- Gad, A., 2002. Characterizing the environmental conditions of land use/land cover classes towards the assessment of desertification: Case study in north-western coast of Egypt. In: Paper no 2114, Symposium no 46, 17th World Congress of Soil Science, 14-21 August 2002, Bangkok, Thailand.
- Ghosh, B.C. and Bhat, R., 1998. Environmental hazards of nitrogen loading in wetland rice fields. *Environmental Pollution* 102, 123-126.
- Gilabert, M.A., González-Piqueras, F.J., García-Haro, F.J. and Meliá, J., 2002. A generalized soil-adjusted vegetation index. *Remote Sensing of Environment* 82, 303-310.
- Goossens, D. and Riksen, M., 2004. Wind erosion and dust dynamics at the commencement of the 21th century. In: Goossens, D. and Riksen, M. (Eds), *Wind erosion and dust dynamics: Observations, simulation, modelling*. ESW

- Publications, Wageningen, The Netherlands, pp. 7-13.
- Goovaerts, P., 1994. Study of spatial relationships between two sets of variables using multivariate geostatistics. *Geoderma* 62, 93-107.
- Goovaerts, P., 1997. *Geostatistics for Natural Resources Evaluation*. Oxford University Press, New York, USA.
- Goovaerts, P., 1999. Using elevation to aid the geostatistical mapping of rainfall erosivity. *Catena* 34, 227-242.
- Goovaerts, P., 2000. Geostatistical approaches for incorporating elevation into the spatial interpolation of rainfall. *Journal of Hydrology* 228, 113-129.
- Goudriaan, J., Van Keulen, H. and Van Laar, H.H., 1997. SUCROS1: Crop growth model for potential production. In: SUCROS97: Simulation of crop growth for potential and water-limited production situations as applied to spring wheat, *Quantitative Approaches in Systems Analysis*. No. 14. C.T. de Wit Graduate School for Production Ecology and Resource Conservation, Wageningen, The Netherlands.
- Goulding, K., 2000. Nitrate leaching from arable land and horticultural land. *Soil Use and Management* 16, 145-151.
- Govers, G., 1990. Empirical relationships on the transporting capacity of overland flow. *Association of Hydrology Science Publication* 189, 45-63.
- Goyal, S.K., Seyfried, M.S. and O'Neill, P.E., 1999. Correction of surface roughness and topographic effects on airborne SAR in mountainous rangeland areas. *Remote Sensing of Environment* 67, 124-136.
- Graetz, R.D., 1987. Satellite remote sensing of Australian rangelands. *Remote Sensing of Environment* 23, 313-331.
- Granlund, K., Rekolainen, S., Gronroos, J., Nikander, A. and Laine, Y., 2000. Estimation of the impact of fertilisation rate on nitrate leaching in Finland using a mathematical simulation model. *Agriculture, Ecosystems & Environment* 80, 1-13.
- Grist, D.H., 1986. *Rice*. Longman, London and New York, UK and USA.
- Gu, Y., Belair, S., Mahfouf, J.-F. and Deblonde, G., 2006. Optimal interpolation analysis of leaf area index using MODIS data. *Remote Sensing of Environment* 104, 283-296.
- Ha, N.T., 1996. Determination of soil erosion factors and soil erosion prediction on sloping lands. PhD Thesis, Hanoi University of Hydrology, Hanoi, Vietnam, 187 pp. (Vietnamese)
- Hack-ten Broeke, M.J.D. and De Groot, W.J.M., 1998. Evaluation of nitrate leaching risk at site and farm level. *Nutrient Cycling in Agroecosystems* 50, 271-276.
- Hai, L.D., 2004. A twinge of conscience for Vietnam coastal zone. *Vietnam Environmental Protection* 65, 28-34. (Vietnamese)
- Hall, F.G., Strebel, D.E., Nickeson, J.E. and Goetz, S.J., 1991. *Radiometric*

References

- rectification: Toward a common radiometric response among multirate, multisensor images. *Remote Sensing of the Environment* 35, 11-27.
- Harahsheh, H. and Tateishi, R., 2000. Desertification mapping of west Asia: A GIS and Remote Sensing Application. <http://www.gisdevelopment.net/aars/acrs/2000/ts11/glc001b.shtml>. (consulted March 2004)
- Harmsen, K., 2004. Assessment of the use of RS and GIS in India, <http://www.gisdevelopment.net/magazine/gisdev/2004/april/assessment5.shtml>. (consulted March 2004)
- Hasegawa, S. and Kasubuchi, T., 1993. Water regimes in fields with vegetation. In: Miyazaki, T., Hasegawa, S. and Kasubuchi, T. (Eds), *Water flow in soils*. Marcel Dekker Inc., New York - Basel - Hong Kong, pp. 223-250.
- Hauggaard-Nielsen, H., Ambus, P. and Jensen, E.S., 2003. The comparison of nitrogen use and leaching in sole cropped versus intercropped pea and barley. *Nutrient Cycling in Agroecosystems* 65, 289-300.
- Helwig, T.G., Madramootoo, C.A. and Dodds, G.T., 2002. Modelling nitrate losses in drainage water using DRAINMOD 5.0. *Agricultural Water Management* 56, 153-168.
- Hengl, T., Heuvelink, G.B.M. and Stein, A., 2004. A generic framework for spatial prediction of soil variables based on regression-kriging. *Geoderma* 120, 75-93.
- Hengsdijk, H., Van den Berg, M., Roetter, R.P., Guanghuo, W., Wolf, J., Lu, C.H. and Van Keulen, H., 2005. Consequences of technologies and production diversification for the economic and environmental performance of rice-based farming systems in East and South-east Asia. In: Toriyama, K., Heong, K.L. and Hardy, B. (Eds), *Rice is life: Scientific perspectives for the 21st century*. World Rice Research Conference, Tsukuba 4-7 November 2004, Japan, WRRC 2004 Proceedings, Session 14, pp. 422-425.
- Herrick, J.E. and Jones, T.L., 2002. A dynamic cone penetrometer for measuring soil penetration resistance. *Soil Science Society of America Journal* 66, 1320-1324.
- Hessel, R., 2002. Modelling soil erosion in a small catchment on the Chinese Loess Plateau. PhD Thesis, Utrecht University, Utrecht, The Netherlands, 317 pp.
- Hessel, R., 2006. Consequences of hyperconcentrated flow for process-based soil erosion modelling on the Chinese Loess Plateau. *Earth Surface Processes and Landforms* 31(9), 1100-1114.
- Hessel, R., Van Dijk, S. and Van den Elsen, E., 2002. LISEM project: Field measurements manual. Alterra, Wageningen University and Research centre, Wageningen, The Netherlands, 42 pp.
- Hessel, R., Jetten, V. and Guanghui, Z., 2003a. Estimating Manning's n for steep slopes. *Catena* 54, 77-91.

- Hessel, R., Jetten, V., Liu, B., Zhang, Y. and Stolte, J., 2003b. Calibration of the LISEM model for a small Loess Plateau catchment. *Catena* 54, 235-254.
- Hessel, R., Van den Bosch, R. and Vigiak, O., 2005. Evaluation of the LISEM soil erosion model in two catchments in the East African Highlands. *Earth Surface Processes and Landforms* 31(4), 469-486.
- Heuvelink, G.B.M. and Pebesma, E.J., 1999. Spatial aggregation and soil process modelling. *Geoderma* 89, 47-65.
- Hien, B.H. and Thoa, V.T.K., 2003. Formulating the campaign for controlling and efficiency management fertilizers in Vietnam. Annual Report, Institute for Soils and Fertilizers, Hanoi, Vietnam, 55 pp. (Vietnamese)
- Higgs, G.K., 2004. Supervised classification of TM band ratio images and radar for geological interpretations of central Madagascar. In: Geological Society of America Abstracts with Programs 36, 7.
- Hill, J. and Schutt, B., 2000. Mapping complex patterns of erosion and stability in dry Mediterranean ecosystems. *Remote Sensing of Environment* 74, 557-569.
- Hoang Fagerström, M.H., Van Noordwijk, M., Phien, T. and Vinh, N.C., 2001. Innovations within upland rice-based systems in northern Vietnam with *Tephrosia candida* as fallow species, hedgerow, or mulch: Net returns and farmers' response. *Agriculture, Ecosystems & Environment* 86(1), 23-37.
- Hoang, P.T., Tan, P.N., Hai, N.Q. and Cuong, T.X., 1998. Using biological measures to improve degraded soil. Annual report, Institute for Soils and Fertilizers, Ha Noi, Viet Nam. (Vietnamese)
- Hoffmann, C.C., Berg, P., Dahl, M., Larsen, S.E., Andersen, H.E. and Andersen, B., 2006. Groundwater flow and transport of nutrients through a riparian meadow - Field data and modelling. *Journal of Hydrology* 331, 315-335.
- Hollger, E., Baginska, B. and Cornish, P.S., 1998. Factors influencing soil and nutrient loss in stormwater from a market garden. In: Proceedings of the 9th Australia Agronomy Conference, Wagga Wagga, Australia.
- Holtschlag, D.J., 2001. Optimal estimation of suspended-sediment concentrations in streams. *Hydrological Processes* 15(7), 1133-1155.
- Horowitz, A.J., 2003. An evaluation of sediment rating curves for estimating suspended sediment concentrations for subsequent flux calculations. *Hydrological Processes* 17(17), 3387-3409.
- Hossain, M. and Narciso, J.H., 2003. New rice technologies and challenges for food security in Asia and the Pacific. In: Dat Van Tran (Ed.), Sustainable rice production and food security. Proceedings 20th Session International Rice Commission. Bangkok, July 23-26, 2002.
- Hou, A.X. and Tsuruta, H., 2003. Nitrous oxide and nitric oxide fluxes from an upland

References

- field in Japan: Effect of urea type, placement, and crop residues. *Nutrient Cycling in Agroecosystems* 65, 191-200.
- Huang, H.C., Liu, C.W., Chen, S.-K. and Chen, J.S., 2003. Analysis of percolation and seepage through paddy bunds. *Journal of Hydrology* 284, 13-25.
- Hue, N. and Phien, T. 2005. Sloping land management, view from long-term researches. National Institute for Soils and Fertilizers, Hanoi, Vietnam, pp. 34-43. (Vietnamese)
- Huete, A., Gao, X., Kim, H.J., Miura, T., Borghi, C. and Ojeda, R., 2002. Characterization of land degradation in Central Argentina with hyperspectral AVIRIS and EO-1 data. In: Paper no 987, Symposium no 46, 17th World Congress of Soil Science, 14-21 August 2002, Bangkok, Thailand.
- Hung, N.T., 2001. Soil erosion by rain; its effect on soil fertility and crop yield. *Agriculture and Rural Development Monthly Journal* 5, 334-335. (Vietnamese)
- Huyen, T.G. and Toan, B.Q., 1965. Three year research results of soil erosion study on hilly rice in north-western Vietnam. *Journal of Agricultural Science and Technology* 6, 23-27. (Vietnamese)
- IBSRAM, 1998. First training workshop on site selection and characterization. IBSRAM Technical Notes No 1, Bangkok, Thailand.
- Intech, Intech Instruments LTD. <http://www.trutrack.com/intech/WT-HR.html> (consulted 15th March 2006).
- IRMLA, 2005. Country report from Tamduong project, Vietnam. http://www.alterra-research.nl/pls/portal30/docs/folder/irmla/irmla/p_frames_page.htm. (consulted in July 2006)
- IRRI, 2006. Vietnam adopts 'Three Reductions, Three Gains' as national policy, <http://www.irri.org/irrc/impact/3R%203G%20July4.asp> (consulted in January 2007).
- Janssen, B.H., 1998. Efficient use of nutrients: An art of balancing. *Field Crops Research* 56, 197-201.
- Jansson, J.M. and Anderson, T., 1988. Simulation of runoff and nitrate leaching from an agricultural district in Sweden. *Journal of Hydrology* 99, 33-47.
- Jemison, J.M., Jabro, J.D. and Fox, R.H., 1994. Evaluation of LEACHIM. II. Simulation of nitrate leaching from nitrogen-fertilized and manured corn. *Agronomy Journal* 86, 852-859.
- Jetten, V., 2002. LISEM: LImburg Soil Erosion Model, Windows version 2.x, User Manual. Utrecht University, Utrecht, The Netherlands, 64 pp. (Available on www.geog.uu.nl/lisem)
- Jetten, V. and De Roo, A.P.J., 2001. Spatial analysis of erosion conservation measures with LISEM. In: Harmon, R.S., Doe, W.W. (Eds), *Landscape erosion and evolution modelling*. Kluwer Academic Publishers, New York, USA, pp. 429-445.

- Jetten, V., Govers, G. and Hessel, R., 2003. Erosion models: Quality of spatial predictions. *Hydrological Processes* 17(5), 887-900.
- Jinno, Y. and Honna, T., 1999. Nitrate leaching and nitrogen balance in turfgrass field by lysimeters. *Japanese Journal of Soil Science and Plant Nutrition* 70, 297-305.
- Johnsson, H., Larsson, M., Martensson, K. and Hoffmann, M., 2002. A decision support tool for assessing nitrogen leaching losses from arable land. *Environmental Modelling & Software* 17, 505-517.
- Jongschaap, R.E.E., 2006. Integrating crop growth simulation and remote sensing to improve resource use efficiency in farming systems. PhD Thesis, Wageningen University, Wageningen, The Netherlands, 130 pp.
- Jørgensen, S.E. and Bendoricchio, G., 2001. *Fundamentals of ecological modelling*. Elsevier, Amsterdam, The Netherlands.
- Kalra, N., Aggarwal, P.K., Pathak, H., Kumar, S., Dadhwal, S.K., Sheghal, V.K., Harith, R., Krishna, M. and Roetter, R.P., 2001. Evaluation of regional resources and constraints. In: Aggarwal, P.K., Roetter, R.P., Kalra, N., Van Keulen, H., Hoanh, C.T. and Van Laar, H.H. (Eds), *Land use analysis and planning for sustainable food security with an illustration for the state of Haryana, India*. International Rice Research Institute, Los Baños, Philippines, pp. 33-60.
- Karssenbergh, D., Wesseling, C.G. and Van Deursen, W.P.A., 1996. PCRaster version 2, manual. Appr. 380 pp. (Available at <http://www.geog.uu.nl/pcraster>)
- Kemper, W.D. and Rosenau, R.C., 1986. Aggregate stability and size distribution. In: Campbell, G.S., Jackson, R.D., Mertland, M.M., Nielsen, D.R., Klute, A. (Eds), *Methods of soil analysis. Part 1: Physical and mineralogical methods*. Agronomy Monograph no 9 (2nd edition), American Society of Agronomy, Madison, WI., USA, pp. 425-442.
- Khang, N., 2005. Current and possibility of widening agricultural land in Vietnam. In: MARD (Ed.), *Research results of science and technology in Agriculture and Rural Development, period 1996-2000*. Science, Technology and Product Quality Department, Ministry of Agriculture and Rural Development, Agricultural Publishing House, Hanoi, Vietnam, pp. 23-38. (Vietnamese)
- Khang, N., Tan, N.V., Pho, N.C., Liem, T.V., Anh, N.T., Hai, N.V., Toan, N.D., Tu, V.A. and Hai, T.T., 1998. *Soil map of Vinhphuc province*. National Institute of Agriculture Planning and Projection, Hanoi, Vietnam. (Vietnamese)
- Khoa, L.V., 1993. Problem of land use and environmental protection in the midland of Vietnam. *Vietnam Soil Science* 3, 45-49. (Vietnamese)
- Kim, H.J., Woong, K.C., Kim, M.K., Lee, S.S. and Choi, B.Y., 2001. Dietary factors and gastric cancer in Korea: A case-control study. *International Journal of Cancer* 97, 531-535.

References

- Knisel, W.G., 1991. CREAMS/GLEAMS: A development overview. In: Beasley, D.B., Knisel, W.G., Rice, A.P. (Eds), Proceedings of the CREAMS/GLEAMS Symposium. Agricultural Engineering Department, University of Georgia, Athens, GA, USA, pp. 9-17.
- Kruseman, G. and Van Keulen, H., 2001. Soil degradation and agricultural production: Economic and biophysical approaches. In: Heerink, N., Kuiper, M. and Van Keulen, H. (Eds), Economic policy and sustainable land use, recent advances in quantitative analysis for developing countries. Physica-Verlag, Berlin, Germany, pp. 21-48.
- Külling, D.R., Menzi, H., Sutter, F., Lischer, P. and Kreuzer, M., 2003. Ammonia, nitrous oxide and methane emissions from differently stored dairy manure derived from grass- and hay-based rations. *Nutrient Cycling in Agroecosystems* 65, 13-22.
- Kumazawa K. 2002. Nitrogen fertilization and nitrate pollution in groundwater in Japan: Present status and measures for sustainable agriculture. *Nutrient Cycling in Agroecosystems* 63, 129-137.
- Lal, R., 1991. Myths and scientific realities of agroforestry as a strategy for sustainable management for soils in the tropics. *Advances in Soil Science* 15, 91-132.
- Lal, R. and Shukla, M.K., 2004. Principles of Soil Physics. Marcel Dekker Inc, New York, USA.
- Lanh, V.V., 1999. First assessment about sea pollution in the southern coastal zone of Vietnam. In: Ministry of Environmental and Resource Management (Ed.), Country workshop on environment. Science and Technology Publishing House, Hanoi, Vietnam, pp. 274-281. (Vietnamese)
- Lawes Agricultural Trust 2003. GenStat® Release 7.1 Reference Manual. VSN International, Wilkinson House, Jordan Hills Road, Oxford, UK.
- Lawlor, A.J. and Tipping, E.W., 1996. Synoptic studies of nutrient leaching from the soils of the catchment of Bassenthwaite Lake, Colombia. IFE Report WI/T11059 r7/1 to the National Rivers Authority (North West Region), Colombia, 16 pp. + Ann.
- Lemke, L.D., Abriola, L.M. and Goovaerts, P., 2004. Dense nonaqueous phase liquid (DNAPL) source zone characterization: Influence of hydraulic property correlation on predictions of DNAPL infiltration and entrapment. *Water Resources Research* 40, W01511.
- Leonard, R.A., Knisel, W.G. and Still, D.A., 1987. GLEAMS: Groundwater loading effects of agricultural management systems. *Transactions American Society of Agricultural Engineers* 30, 1403-1418.
- Leone, A.P. and Sommer, S., 2000. Multivariate analysis of laboratory spectra for the assessment of soil development and soil degradation in the Southern Apennines

- (Italy). *Remote Sensing of Environment* 72, 346-359.
- Leopold, U., Heuvelink, G.B.M., Tiktak, A., Finke, P.A. and Schoumans, O., 2006. Accounting for change of support in spatial accuracy assessment of modelled soil mineral phosphorus concentration. *Geoderma* 130, 368-386.
- Lesschen, J.P., Stoorvogel, J.J. and Smaling, E.M.A., 2004. Scaling soil nutrient balances. Enabling mesolevel applications for African realities. *FAO Fertilizer and Plant Nutrition Bulletin No. 15*, FAO, Rome, Italy, 132 pp.
- Li, R., Stevens, M.A. and Simons, D.B., 1976. Solutions to the Green and Ampt infiltration equation. *Journal of Irrigation and Drainage* 2, 239-248.
- Lillesand, T.M. and Kiefer, R.W., 1994. *Remote sensing and image interpretation*. John Wiley & Sons, Inc., London.
- Lin, B.-L., Sakoda, A., Shibasaki, R. and Suzuki, M., 2001. A Modelling Approach to Global Nitrate Leaching Caused by Anthropogenic Fertilisation. *Water Research* 35, 1961-1968.
- Liu, G., Xu, M. and Ritsema, C., 2003. A study of soil surface characteristics in a small watershed in the hilly, gullied area on the Chinese Loess Plateau. *Catena* 54(1-2), 31-44.
- Liu, X., Ju, X., Zhang, F., Pan, J. and Christie, P., 2003. Nitrogen dynamics and budgets in a winter wheat-maize cropping system in the North China Plain. *Field Crops Research* 83, 111-124.
- Loc, D.C., Phien, T., Siem, N.T. and Toan, T.D., 1998. Effect of farming techniques on steep lands in Hoa Binh province. In: Phien, T., Siem, N.T. (Eds), *Sustainable farming on sloping lands in Vietnam*. Agricultural Publishing House, Hanoi, Vietnam, pp. 23-44. (Vietnamese)
- Maglinao, A.R. and Valentin, C., 2003. Community-based land and water management systems for sustainable upland development in Asia. MSEC Phase 2, International Water Management Institute (IWMI) Southeast Asia Regional Office, Bangkok, Thailand.
- Mai, V.T., Nguyen, D.D., Van Keulen, H., 2005. Using LANDSAT images for studying land use dynamics and soil degradation. Case study in Tamduong district, Vinhphuc province, Vietnam. *International Journal of Geoinformatics* 1, 157-164.
- Mai, V.T., Van Keulen, H., Wolf, J., Roetter, R.P. and Son, T.T., 2007. Modelling yield levels and yield gaps of rice (*Oryza sativa* L.), maize (*Zea mays* L.) and soybean (*Glycine max* L.) in rice-based cropping systems in North Vietnam. (in prep.)
- Malhi, S.S., Harapiak, J.T., Nyborg, M., Gill, K.S., Monreal, C.M. and Gregorich, E.G., 2003. Light fraction organic N, ammonium, nitrate and total N in a thin Black Chernozemic soil under bromegrass after 27 annual applications of different N rates. *Nutrient Cycling in Agroecosystems* 65, 201-210.

References

- Mantovi, P., Fumagalli, L., Beretta, G.P. and Guermandi, M., 2006. Nitrate leaching through the unsaturated zone following pig slurry applications. *Journal of Hydrology* 316, 195-212.
- Markham, B.L. and Barker, J.L., 1985. Spectral characterization of Landsat Thematic Mapper Sensors. *International Journal of Remote Sensing* 5, 679-716.
- Metternicht, G.I. and Fermont, A., 1998. Estimating erosion surface features by linear mixture modeling. *Remote Sensing of Environment* 64, 254-265.
- Miller, R.W. and Gardiner, D.T., 2001. *Soils in our environment*. 9th edition. Prentice Hall, Upper Saddle River, USA.
- Minh, T. and Hoc, B., 1997. Quality of groundwater in Hanoi and the problem of nitrate pollution. *Journal of Vietnam Geology* 24, 18-22. (Vietnamese)
- Molz, F.J., 1981. Simulation of plant-water uptake. In: Iskandar I.K. (Ed.), *Modeling wastewater renovation: Land application*. Wiley, New York, USA, pp. 69-91.
- Molz, F.J. and Remson, I., 1970. Extraction term models of soil moisture use by transpiring plants. *Water Resources Research* 6, 1346-1356.
- Morgan, R.P.C., 1995. *Soil erosion and conservation*. Longman, Harlow, UK, 198 pp.
- Morgan, R.P.C., Quinton, J.N., Smith, R.E., Govers, G., Poesen, J.W.A., Auerswald, K., Chisci, G., Torri, D. and Styczen, M.E., 1998. The European soil erosion model (EUROSEM): A dynamic approach for predicting sediment transport from fields and small catchments. *Earth Surface Processes and Landforms* 23(6), 527-544.
- Mosier, A.R., 2002. Environmental challenges associated with needed increases in global nitrogen fixation. *Nutrient Cycling in Agroecosystems* 63, 1385-1314.
- Mosier, A.R., Syers, J.K. and Freney, J.R. (Eds), 2004. *Agriculture and the nitrogen cycle: Assessing the impacts of fertilizer use on food production and the environment*. SCOPE Nr. 65, Island Press, Washington DC, USA.
- Mulvaney, R.L., 1994. Nitrification of different nitrogen fertilizers. In: *Illinois Fertilizer Conference Proceedings, Annual Illinois Fertilizer and Chemical Association Conference, Peoria, Illinois, January 24-26, 1994*.
- NCI, 2002. *Statistics on cancer in Vietnam*. Vietnam National Cancer Institute, Ministry of Public Health, Hanoi, Vietnam.
- Neeteson, J.J., 1995. Nitrogen management for intensively grown arable crops and field vegetables. In: Bacon P.E. (Ed.), *Nitrogen fertilization in the environment*. Marcel Dekker Inc., New York, USA, pp. 295-325.
- Nelson, D.W. and Sommers, L.E., 1996. Total carbon, organic carbon, and organic matter. In: Sparks, D.L., Page, A.L., Johnston, C.T., Summer, M.E. (Eds), *Methods of soil analysis. Part 3. Chemical methods*. SSSA Book Series No. 5, SSSA, Madison, WI, USA, pp. 961-1010.
- Nhuan, C.T., 1996. *Agricultural and forestry land allocation in Vietnam*. Vietnam Soil

- Science. 7, 35-41. (Vietnamese)
- Nizeyimana, E. and Petersen, G.W., 1997. Remote sensing application to soil degradation assessment. In: Lal, R., Blum, W.H. and Valentine, C. (Eds), Method for assessment of soil degradation. *Advances in Soil Science*, CRC Press, Boca Raton, FL, USA, pp. 393-405.
- Oldeman, L.R., 1994. An international methodology for an assessment of soil degradation: Land georeferenced soils and terrain database. In: The collection and analysis of land degradation data. Report of the Expert consultation of the Asian Network on Problem Soils. Bangkok, Thailand, 25 to 29 Oct. 1993, pp. 35-60.
- Ondersteijn, C.J.M., Beldman, A.C.G., Daatselaar, C.H.G., Giesen, G.W.J. and Huirne, R.B.M., 2002. The Dutch Mineral Accounting System and the European nitrate directive: Implications for N and P management and farm performance. *Agriculture, Ecosystems & Environment* 92, 283-296.
- Paringit, E.C. and Nadaoka, K., 2003. Sediment yield modelling for small agricultural catchments: Land-cover parameterization based on remote sensing data analysis. *Hydrological Processes* 17(9), 1845-1866.
- Pebesma, E.J., 2001. Gstat user's manual, v. 2.3.3. Department of Physical Geography, Utrecht University, P.O. Box 80.115, 3508 TC Utrecht, The Netherlands, 100 pp.
- Pebesma, E.J. and De Kwaadsteniet, J.W., 1997. Mapping groundwater quality in The Netherlands. *Journal of Hydrology* 200, 364-386.
- Penn, B.S., 2002. Applying band ratios to hyperspectral imagery data. In: *Remote Sensing and Geographic Information Systems in the New Millennium: Their use in environmental and engineering geology*. Colorado Convention Center, October 30, 2002.
- Phien, T., Trinh, M.V., Vinh, N.C., Nguyen, L., Hai, T.S. and Mai, N.N., 2000. Soil erosion under different short fallow shifting cultivation systems on sloping land. *Vietnam Soil Science* 13, 109-116. (Vietnamese)
- Phien, T., Toan, T.D., Didier, O., Phai, D.D., Julien, M. and Rinh, P.V., 2002. Soil erosion management at the watershed level for sustainable agriculture and forestry. National Institute for Soils and Fertilizers, Hanoi, Vietnam. (Vietnamese)
- Phong, T.A., 1995. Open and bare lands in Vietnam. *Vietnam Soil Science* 5, 67-69. (Vietnamese)
- Phuong, L.T., 2003. Study macro nutrient efficiency for rice on degraded soil in Bac Giang province. Annual report, National Institute for Soils and Fertilizers, Hanoi, Vietnam. (Vietnamese)
- Pierzynski, G.M., Sims, J.T. and Vance, G.F., 2005. *Soils and environmental quality*. 3rd edition. Taylor & Francis, Boca Raton, USA.
- Pilotti, M. and Bacchi, B., 1997. Distributed evaluation of the contribution of soil

References

- erosion to the sediment yield from a watershed. *Earth Surface Processes and Landforms* 22(13), 1239-1251.
- Pingali, P.L. and Roger, P.A., 1993. Impact of pesticides on farmer health and the rice environment. IRRI, Los Baños, Philippines.
- Ponsioen, T., 2003. TechnoGIN: A technical coefficient generator for cropping systems in Ilocos Norte province, Philippines. MSc Thesis, Plant Production Systems Group, Wageningen University, Wageningen, The Netherlands, 57 pp. + Ann.
- Ponsioen, T.C., Hengsdijk, H., Wolf, J., Van Ittersum, M.K., Roetter, R.P., Son, T.T. and Laborte, A.G., 2006. TechnoGIN, a tool for exploring and evaluating resource use efficiency of cropping systems in East and Southeast Asia. *Agricultural Systems* 87, 80-100.
- Quat, N.X. and Nganh, B., 1964. Research results of soil erosion study in Cauhai, Phutho province. *Journal of Agricultural Science and Technology* 10, 25-30. (Vietnamese)
- Radcliffe, D.E. and Rasmussen, T.C., 2000. Soil water movement. In: Sumner, M.E. (Ed.), *Handbook of Soil Science*. CRC Press, Boca Raton, London, New York, Washington, DC.
- Radcliffe, D.E., Gupte, S.M. and Box, J.J.E., 1998. Solute transport at the pedon and polypedon scales. *Nutrient Cycling in Agroecosystems* 50, 77-84.
- Refsgaard, J.C. and Storm, B., 1995. MIKE SHE. In: Singh, V.P. (Ed.), *Computer models of watershed hydrology*. Water Resources Publications, Colorado, USA, pp. 809-846.
- Ren, D. and Abdelsalam, M.G., 2003. ASTER band-ratio images for geological mapping in arid regions: The Neoproterozoic Allaqi-Heiani Suture, southern Egypt. South-central section (37th) and southeastern section (52nd), GSA (The Geological Society of America) Joint Annual Meeting, March 12-14, 2003, Memphis, Tennessee, USA.
- Renard, K.G., Foster, G.R., Weesies, G.A. and Porter, J.P., 1991. RUSLE: Revised universal soil loss equation. *Journal Soil and Water Conservation* 46(1), 30-33.
- Riley, W.J., Ortiz-Monasterio, I. and Matson, P.A., 2001. Nitrogen leaching and soil nitrate, nitrite, and ammonium levels under irrigated wheat in Northern Mexico. *Nutrient Cycling in Agroecosystems* 61, 223-236.
- Rimski-Korsakov, H., Rubio, G. and Lavado, R.S., 2004. Potential nitrate losses under different agricultural practices in the pampas region, Argentina. *Agricultural Water Management* 65, 83-94.
- Ritsema, C.J., 2003. Introduction: Soil erosion and participatory land use planning on the Loess Plateau in China. *Catena* 54(1-2), 1-5.

- Roetter, R.P., Aggarwal, P.K., Tan, P.S., Hoanh, C.T., Cabrera, J.M.C.A. and Nunez, B., 1998. Use of crop simulation models and alternative yield estimation techniques for optimizing agricultural land use and resource management. In: Roetter, R.P., Hoanh, C.T., Luat, N.V., Van Ittersum, M.K. and Van Laar, H.H. (Eds), Exchange of methodologies in land use planning, SysNet Research Paper Series No. 1, IRRI, Los Baños, Philippines, pp. 15-29.
- Roetter, R.P., Hoanh, C.T., Laborte, A.G., Van Keulen, H., Van Ittersum, M.K., Dreiser, C., Van Diepen, C.A., De Ridder, N. and Van Laar, H.H., 2005. Integration of Systems Network (SysNet) tools for regional land use scenario analysis in Asia. *Environmental Modelling & Software* 20, 291-307.
- Rolston, D.E. and Marino, M.A., 1976. Simulation transport of nitrate and gaseous denitrification products in soil. *Soil Science Society of America Journal* 46, 860-865.
- Ross, S.M., Beadle, R.S. and Jewkes, E., 1995. Lysimeter studies of nitrogen leaching potential in wetland peats and clays in South-West Britain. In: Hughes, J.M.R. and Heathwaite, A.L. (Eds), *Hydrology and hydrochemistry of British Wetlands*. John Wiley & Sons Ltd, Chichester, UK, pp. 223-243.
- Roy, R.N., Misra, R.V., Lesschen, J.P. and Smaling, E.M.A., 2003. Assessment of soil nutrient balance. Approaches and methodologies. *FAO Fertilizer and Plant Nutrition Bulletin* 14, FAO, Rome, Italy, 87 pp.
- Schmid, T., Koch, M., Gumuzzio, J. and Mather, P.M., 2004. A spectral library for a semi-arid wetland and its application to studies of wetland degradation using hyperspectral and multispectral data. *International Journal of Remote Sensing* 25, 2485-2496.
- Schmidt, J., Werner, M.V. and Michael, A., 1999. Application of the EROSION 3D model to the CATSOP watershed, The Netherlands. *Catena* 37(3-4), 449-456.
- Sheldrick, W.F., Syers, J.K. and Lingard, J., 2002. A conceptual model for conducting nutrient audits at national, regional, and global scales. *Nutrient Cycling in Agroecosystems* 62, 61-72.
- Siem, N.T. and Phien, T., 1992. Deterioration risk of the uplands in Vietnam and research priorities for their management. *Vietnam Soil Science* 2, 32-34. (Vietnamese)
- Siem, N.T. and Phien, T., 1999. *Upland soils in Vietnam: Degradation and rehabilitation*. Agricultural Publishing House, Hanoi, Vietnam, 412 pp. (Vietnamese)
- Smaling, E.M.A., Oenema, O. and Fresco, L.O. (Eds), 1999. *Nutrient disequilibria in agroecosystems: Concepts and case studies*. CABI Publishing, Wallingford, UK.
- Smith, R.E., Goodrich, D.C. and Quinton, J.N., 1995. *Dynamic, distributed simulation*

References

- of watershed erosion: The KINEROS2 and EUROSEM models. *Journal of Soil and Water Conservation* 50(5), 517-520.
- Son, T.T., Chien, N.V., Thoa, V.T.K., Dobermann, A. and Witt, C., 2004. Site-specific nutrient management in irrigated rice systems of the Red River Delta of Vietnam. In: Dobermann A., Witt C. and Dawe D. (Eds), *Increasing productivity of intensive rice systems through site-specific nutrient management*. Science Publishers Inc. and International Rice Research Institute (IRRI), Enfield, N.H. (USA) and Los Baños (Philippines), pp. 217-242.
- Souza, C., Firestone, L., Silva, L.M. and Roberts, D., 2003. Mapping forest degradation in the Eastern Amazon from SPOT 4 through spectral mixture models. *Remote Sensing of Environment* 87, 494-506.
- Stolte, J., 1997. Determination of the saturated hydraulic conductivity using the constant head method. In: Stolte, J. (Ed.), *Manual for soil physical measurements*. Technical Document 37, Alterra, Wageningen University and Research centre, Wageningen, The Netherlands, pp. 27-29.
- Stolte, J., Liu, B., Ritsema, C.J., Van den Elsen, H.G.M. and Hessel, R., 2003. Modelling water flow and sediment processes in a small gully system on the Loess Plateau in China. *Catena* 54, 117-130.
- Stolte, J., Ritsema, C.J. and Bouma, J., 2005. Developing interactive land use scenarios on the Loess Plateau in China, presenting risk analyses and economic impacts. *Agriculture, Ecosystems & Environment* 105(1-2), 387-399.
- Street, J.E. and Bollich, P.K., 2003. Rice production. In: Smith C.W. and Dilday R.H. (Eds), *Rice origin, history, technology, and production*. Wiley & Sons, Hoboken, New Jersey, pp. 271-296.
- Tabacchi, E.L.L., Guilloy, H., Planty-Tabacchi, A.-M., Muller, E. and Décamps, H., 2000. Impacts of riparian vegetation on hydrological processes. *Hydrological Processes* 14(16-17), 2959-2976.
- Tateishi, R., 2003. Land cover data and desertification data of Asia. <http://www.arsrin.net/contents/mar2003/p69.htm> (consulted March 2004)
- Tau, T.C., 1997. Some remarks on the relationship between fertilizers and environment throughout determination of groundwater quality under crops. In: Bo, N.V., Thi, N.T. and Loc, D.T. (Eds), *Fertilizer and environment*. Institute of Social Science Information, Hanoi, Vietnam, pp. 73-80. (Vietnamese)
- Thu, D.C., Ha, Q.D. and Hai, D.N., 1997. Assessment of the efficiency of agro-forestry models applied on the improvement of barren land at Tamquan, Tamdao district, Vinhphu province. *Vietnam Soil Science* 8, 88-92. (Vietnamese)
- Toan, T.D., Nhan, H.D., Siem, N.T. and Phien, T., 1998. Integrated management practices for effective agricultural production and use continuum of the upland

- degraded soil in Tamdao, Vinhphu. In: Phien, T. and Siem, N.T. (Eds), Sustainable farming on sloping lands in Vietnam, research results 1990-1997. Agricultural Publishing House, Hanoi, Vietnam, pp. 80-88. (Vietnamese)
- Toan, T.D., Phien, T., Nguyen, L., Phai, D.D. and Ga, N.V., 2001. Soil erosion management at the watershed level for sustainable agriculture and forestry in Vietnam. In: Maglinao, A.R., Leslie, R.N. (Eds), Soil erosion management research in Asian catchments: Methodological approaches and initial results. Proceedings of the 5th Management of Soil Erosion Consortium (MSEC) Assembly, IWMI Southeast Asia Regional Office, Bangkok, Thailand, pp. 233-251.
- Toan, T.D., Podwojewski, P., Orange, D., Phuong, N.D., Phai, D.D., Bayer, A., Thiet, N.V., Rinh, P.V., Renaud, J., Koikas, J., 2005. Effect of land use and land management on water budget and soil erosion in a small catchment in northern part of Vietnam. In: Kheoruenromne, I., Riddell, A.J., Soitong, K. (Eds), SSWM 2004: Innovative practices for sustainable sloping lands and watershed management, 5-9 September 2004. Department of Agricultural Extension, Ministry of Agriculture and Cooperatives, Bangkok, Thailand, pp. 109-122.
- Tripathi, B.P., Ladha, J.K., Timsina, J. and Pascua, S.R., 1997. Nitrogen dynamics and balance in intensified rainfed lowland rice-based cropping systems. *Soil Science Society of America Journal* 61, 812-821.
- Truong, N.V., Dan, N.T., Phien, T. and Siem, N.T., 1998. Effect of farming methods on sloping lands in terms of water management, erosion, leaching and improvement of soil fertility in Ba Vi, Ha Tay. In: Phien, T. and Siem, N.T. (Eds), Sustainable farming on sloping lands in Vietnam, research results 1990-1997. Agricultural Publishing House, Hanoi, Vietnam, pp. 45-59. (Vietnamese)
- Van den Berg, M.M., Hengsdijk, H., Wolf, J., Van Ittersum, M.K., Wang, G. and Roetter, R.P., 2007. The impact of increasing farm size and mechanization on rural income and rice production in Zhejiang province, China. *Agricultural Systems* (in press).
- Van Deursen, W.P.A., 1995. Geographical Information Systems and dynamic models: Development and application of a prototype spatial modelling language. Utrecht University, Utrecht, The Netherlands, 190 pp.
- Van Dijk, A.I.J.M., Bruijnzeel, L.A., Vertessy, R.A. and Ruijter, J., 2005. Runoff and sediment generation on bench-terraced hillsides: Measurements and up-scaling of a field-based model. *Hydrological Processes* 19(8), 1667-1685.
- Van Ittersum, M.K., 1998. New concepts and directions in exploratory land use studies. In: Roetter, R.P., Hoanh, C.T., Luat, N.V., Van Ittersum, M.K. and Van Laar, H.H. (Eds), Exchange of methodologies in land use planning, SysNet Research Paper Series No. 1, IRRI, Los Baños, Philippines, pp. 3-13.

References

- Van Ittersum, M.K., Roetter, R.P., Van Keulen, H., De Ridder, N., Hoanh, C.T., Laborte, A.G., Aggarwal, P.K., Ismail, A.B. and Tawang, A., 2004. A systems network (SysNet) approach for interactively evaluating strategic land use options at sub-national scale in South and South-east Asia. *Land Use Policy* 21, 101-113.
- Van Keulen, H., 1982. Graphical analysis of annual crop response to fertiliser application. *Agricultural Systems* 9, 113-126.
- Van Keulen, H., 2001. (Tropical) soil organic matter modelling: Problems and prospects. *Nutrient Cycling in Agroecosystems* 61, 33-39.
- Van Keulen, H. and Seligman, N.G., 1987. Simulation of water use, nitrogen nutrition and growth of a spring wheat crop. *Simulation Monographs*, Pudoc, Wageningen, The Netherlands.
- Van Keulen, H., Van Ittersum, M.K. and De Ridder, N., 2000. New approaches to land use planning. In: Roetter, R.P., Van Keulen, H. and Van Laar, H.H. (Eds), *Systems research for optimizing land use in South and South East Asia*. SysNet Research Paper Series No. 3. IRRI, Los Baños, Philippines, pp. 3-20.
- Van Wijk, S., Milwain, G., Zhang, X., Van den Bosch, R., Quang, V.Q., Thao, V.T., Fu, X., Yang, J., Yakupitiyage, A., Hempattarasuwan, N., Kiattichaiprasop, O., Bumrungtum, O., Allbritton, A., Bakker, J. and Stallen, M., 2006. Opportunities and threats for safe vegetable markets in China, Vietnam and Thailand. MAPET Report 2, Alterra-report 1285-2, Alterra, Wageningen, The Netherlands.
- Verloop, J., Boumans, L.J.M., Van Keulen, H., Oenema, J., Hilhorst, G.J., Aarts, H.F.M. and Sebek, L.B.J., 2006. Reducing nitrate leaching to groundwater in an intensive dairy farming system. *Nutrient Cycling in Agroecosystems* 74, 59-74.
- Vi, V.V., 1983. Zoning watershed erosion on mud loading in the river systems of North Vietnam. National conference of soil erosion. Ministry of Agriculture and Food Industry. 30 pp. (Vietnamese)
- Walling, D.E., Russell, M.A., Hodgkinson, R.A. and Zhang, Y., 2002. Establishing sediment budgets for two small lowland agricultural catchments in the UK. *Catena* 47(4), 323-353.
- Wang, C., Qi, J., Moran, S. and Marsett, R., 2004. Soil moisture estimation in a semiarid rangeland using ERS-2 and TM imagery. *Remote Sensing of Environment* 90, 178-189.
- Wani, S.P., 2001. Integrated watershed management for sustaining crop productivity and reducing soil erosion in Asia. In: Maglinao, A.R., Leslie, R.N. (Eds), *Soil erosion management research in Asian catchments: Methodological approaches and initial results*. Proceedings of the 5th Management of Soil Erosion Consortium (MSEC) Assembly, IWMI Southeast Asia Regional Office, Bangkok, Thailand.
- Warner, J.F., Bindraban, P.S. and Van Keulen, H., 2006. Introduction: Water for food

- and ecosystems: How to cut which pie? *Water Resources Development* 22, 3-13.
- Wesseling, C.G., Karssenbergh, D., Van Deursen, W.P.A. and Burrough, P.A., 1996. Integrating dynamic environmental models in GIS: The development of a dynamic modelling language. *Transactions in GIS* 1, 40-48.
- Weyer, P.J., Cerhan, J.R., Kross, B.C., Hallberg, G.R., Kantamneni, J., Breuer, G., Jones, M.P., Zheng, W. and Lynch, C.F., 2001. Municipal drinking water nitrate level and cancer risk in older women: The Iowa women's health study. *Epidemiology* 12, 327-338.
- Wezel, A., Steinmuller, N. and Friederichsen, J.R., 2002. Slope position effects on soil fertility and crop productivity and implications for soil conservation in upland northwest Vietnam. *Agriculture, Ecosystems & Environment* 91(1-3), 113-126.
- Williams, J.R., 1985. The physical components of the EPIC model. In: El-Swaify, S.A., Moldenhauer, W.C., Lo, A. (Eds), *Soil erosion and conservation*. Soil Conservation Society of America, Ankeny, IA, USA, pp. 272-284.
- Williamson, J.C., Taylor, M.D., Torrens, R.S. and Vojvodic-Vukovic, M., 1998. Reducing nitrogen leaching from dairy farm effluent-irrigated pasture using dicyandiamide: A lysimeter study. *Agriculture, Ecosystems & Environment* 69, 81-88.
- Wischmeier, W.H. and Smith, D.D., 1978. Predicting rainfall erosion losses: A guide to conservation planning. *Agricultural Handbook No. 537*, U.S. Department of Agriculture, Agricultural Research Service, Washington DC, USA, 58 pp.
- Witt, C., 2003. Fertilizer use efficiencies in irrigated rice in Asia. IFA Regional Conference for Asia and the Pacific, Cheju Island, Korea, 6-8 October 2003.
- Wolf, J., Roetter, R. and Oenema, O., 2005. Nutrient emission models in environmental policy evaluation at different scales-experience from The Netherlands. *Agriculture, Ecosystems & Environment* 105, 291-306.
- Wopereis, M.C.S., Wösten, J.H.M., Bouma, J. and Woodhead, T., 1992. Hydraulic resistance in puddled rice soils: Measurement and effects on water movement. *Soil and Tillage Research* 24, 199-209.
- Wopereis, M.C.S., Bouman, B.A.M., Kropff, M.J., Ten Berge, H.F.M. and Maligaya, A.R., 1994. Water use efficiency of flooded rice fields. I. Validation of the soil-water balance model SAWAH. *Agricultural Water Management* 26(4), 277-289.
- Xing, G.X. and Zhu, Z.L., 2000. An assessment of N loss from agricultural fields to the environment in China. *Nutrient Cycling in Agroecosystems* 57, 67-73.
- Xiong, Z.Q., Xing, G.X., Tsuruta, H., Shen, G.Y., Shi, S.L. and Du, L.J., 2002. Measurement of nitrous oxide emissions from two rice-based cropping systems in China. *Nutrient Cycling in Agroecosystems* 64, 125-133.
- Yang, C.Y., Cheng, M.F., Tsai, S.S. and Hsieh, Y.L., 1998. Calcium, magnesium, and

References

- nitrate in drinking water and gastric cancer mortality. *Cancer Science* 89, 124-130.
- Yang, H.S., 1996. Modelling organic matter mineralization and exploring options for organic matter management in arable farming in northern China. PhD Thesis, Wageningen Agricultural University, Wageningen, The Netherlands, 159 pp.
- Yu, H.M., Li, Z.Z., Gong, Y.S., Mack, U., Feger, K.H. and Stahr, K., 2006. Water drainage and nitrate leaching under traditional and improved management of vegetable-cropping systems in the North China Plain. *Journal of Plant Nutrition and Soil Science* 169, 47-51.
- Zaradny, H., 1993. Groundwater flow in saturated and unsaturated soil. A.A. Balkema, Rotterdam, The Netherlands.
- Zeleke, G. and Hurni, H., 2001. Implication of land use and land cover for mountain resource degradation in the north-western Ethiopian highlands. *Mountain Research and Development* 21, 184-191.
- Zhang, W.L., Tian, Z.X., Zhang, N. and Li, X.Q., 1996. Nitrate pollution of groundwater in northern China. *Agriculture, Ecosystems & Environment* 59, 223-231.
- Zhang, Y. and Wegehenkel, M., 2006. Integration of MODIS data into a simple model for the spatial distributed simulation of soil water content and evapotranspiration. *Remote Sensing of Environment* 104, 393-408.
- Zhu, J.G., Han, Y., Liu, G., Zhang, Y.L. and Shao, X.H., 2000. Nitrogen in percolation water in paddy fields with a rice/wheat rotation. *Nutrient Cycling in Agroecosystems* 57, 75-82.
- Zhu, Y., Fox, R.H. and Toth, J.D., 2003. Tillage effects on nitrate leaching measured by pan and wick lysimeters. *Soil Science Society of America Journal* 67, 1517-1523.

Summary

The study was conducted in Tam Duong, an upstream district in the Red River Basin, located 50–60 km north-west of Hanoi in the transitional zone between the flat lowlands and the mountainous region in northern Vietnam. Population in Tam Duong district has been increasing steadily and there has been considerable economic growth in northern Vietnam during the last decades, leading to increasing demand for food, both in total quantity and in diversity of commodities. Within the agricultural sector the increasing population and industrialization have led to a serious decline in per capita land availability. The farming community has responded to these developments by diversification and intensification of agricultural production. Diversification through large-scale introduction of high-value crops, such as flowers and vegetables, intensification through increasing the number of crops cultivated per year, and the use of external inputs, particularly chemical fertilizers and crop protection agents. These developments have increased the risks for negative environmental impacts through emissions of agro-chemicals, particularly nutrients and biocides, both by overland flow and percolation to the groundwater.

The district comprises three geographical sub-regions: the flat southern part, characterized by paddy rice and vegetable cropping systems; the middle part with alternating flat and hilly (rolling) landscape, where mostly upland crops are cultivated, such as cassava, maize and soybean; and the northern high mountainous area with steep slopes, mostly cultivated with production forest. Within the hilly land, Quan Dinh watershed with a total area of 248.9 ha, ranging in elevation from 28 to 70 meter above sea level, representative for this part of the district, was selected for erosion measurements.

The study had four major goals: (i) examining soil degradation dynamics, using remote sensing; (ii) measuring soil erosion at different spatial scales and simulating soil erosion at sub-watershed and watershed scales in the presence of paddy fields; (iii) measuring nitrogen dynamics in different soil and land use types, and developing a suitable model for estimation of nitrogen leaching losses for current and alternative agricultural systems; and (iv) scaling-up nitrogen dynamics and nitrogen leaching losses in a small region, using geostatistics and a geographic information system.

The analysis of remote sensing images showed that soils in Tam Duong have strongly degraded since the 1980s. Classified band ratios from LANDSAT satellite images, evaluated with soil map and ground truth data, showed that with 3280 ha, the degraded area in the district was largest in 1992, associated with substantial deforestation and agricultural intensification in the preceding period. The area was

Summary

significantly smaller in 1996, as a consequence of re-forestation, particularly planting of eucalyptus plantations and then larger again in 2000, due, among others, to harvesting of production forests.

The main cause of soil degradation in the hilly area was soil erosion that was very severe at individual plot scale, but far less at sub-watershed and watershed scales, because of sediment trapping during transport. Annual runoff at watershed scale in the two years of measurement (2004 and 2005) was 538 and 3324 m³ ha⁻¹ and the associated sediment loss 163 and 1722 kg ha⁻¹. The high values for 2005 were associated with one extraordinary rainfall event, which illustrates that generalization of such experimental results is associated with great uncertainty. To allow a more extensive analysis of soil erosion in the area, the performance of the LISEM soil erosion model was evaluated. The results of the model showed differential performance at different scales. Simulated total runoff and soil loss were underestimated for the main watershed, characterized by a wide diversity in land use types of both upland and lowland fields and a complex geomorphology of hilly lands, terraces and paddy fields along the drainage systems from the middle terraces to the watershed outlet. Total soil loss, on the other hand, was overestimated for an upland sub-watershed. The main reason was the very high simulated sediment concentration in the sub-watershed, due to high detachment and transport capacity. The underestimation for the main watershed was caused by temporary storage and release in rice fields on the terraces - effects that were not included in the model.

Leaching of nitrogen (N) out of the root zone is another process on the terraces that may result in environmental pollution at both field and regional scales. N leaching is one of the causes of low nitrogen fertilizer use efficiency. Experimental results showed regular high N concentrations in deeper soil layers, indicative for substantial leaching losses, associated with high rainfall and/or irrigation, low crop demand and high fertilizer doses. Simulated results from a N balance model that recognizably reproduced experimental results in terms of N concentrations, showed increased N leaching with increasing fertilizer doses, i.e. in a rice–rice–maize rotation from 52 to 60 kg ha⁻¹, 56 to 114 kg ha⁻¹ and 58 to 154 kg ha⁻¹ for low, intermediate, and high fertilizer inputs, respectively.

N leaching is particularly high in the intensive high-value crops receiving very high doses of fertilizer, i.e. annual leaching losses were calculated of up to 193 kg ha⁻¹ in flowers and 115 in vegetables, compared to about 50 in rice.

Spatial distributions of nitrate- and ammonium N concentrations in shallow groundwater under various environmental conditions (soil and topography) and land use types were derived from a set of point measurements, using geo-statistics. The most important explanatory variable, identified through a stepwise backward linear

regression, combined with expert knowledge, appeared to be land use type, in addition to soil type and soil texture. Semi-variograms were computed and appropriate models were established for original N concentrations, as well as for the residuals derived from regression analysis. N concentrations were predicted using both, ordinary block kriging and regression block kriging. Regression block kriging yielded more accurate results, taking into account additional information in the generalized linear regression. Temporal changes in N concentrations in the groundwater were mainly the result of variations in environmental conditions, such as rainfall and land use with different irrigation and fertilizer regimes.

For exploring options for and consequences of introduction of alternative land use and management, a spatial dynamic model was developed. It simulates N dynamics at sub-regional scale, for combinations of different soil and land use types, combined with different irrigation and fertilizer regimes. The model was calibrated using measured N concentrations in one year and then applied to a subsequent year. The contribution of lateral flow to N redistribution was small in this flat area. Percolation was the main process leading to high N leaching losses to groundwater. Calculated annual leaching losses varied from 88 to 122 kg N ha⁻¹ in flowers, 64 to 82 kg N ha⁻¹ in vegetables of the 'cabbage group' (i.e. paprika, cabbage, eggplant, kohlrabi) 51 to 76 kg N ha⁻¹ in chili, 56 to 75 kg N ha⁻¹ in vegetables of the 'squash group' (i.e. cucumber, tomato, pumpkin), and 36 to 55 kg N ha⁻¹ in rice. The model is a useful tool for regional application, environmental assessment, and management support, but needs further calibration and validation before it can confidentially be applied to examine the consequences of adoption of alternative crop and soil management practices.

The study has indicated that the current agricultural developments in Tam Duong district present a number of serious threats for the quality of the natural resource base, particularly soil and water, and thus jeopardize the environmental sustainability of current land use practices. At the same time, it is realized that these developments are co-determined by efforts aimed at achieving (short-term) economic viability of the systems. The obvious and less obvious conflicts between the various (short- and long-term) land use objectives require more comprehensive analyses. Results as generated in this study can contribute to integrated analyses in which the various stakeholders, such as farmers ('organizations), local authorities, environmental protection agencies and national planners are involved to analyse trade-offs between different development goals to (ultimately) come up with truly sustainable land use and development options.

Samenvatting

Deze studie is uitgevoerd in Tam Duong, een district in de bovenstroom van de Red River Delta, gelegen in de overgangszone tussen vlak laagland en het bergachtige gebied in het noorden van Vietnam. De bevolkingsdichtheid in Tam Duong is de laatste tien jaar sterk gestegen, wat, gecombineerd met de sterke economische groei in Vietnam gedurende die periode, geleid heeft tot een toename in de vraag naar voedsel, zowel in hoeveelheid als in diversiteit van voedingsmiddelen. In de landbouwsector heeft de bevolkingstoename en de industrialisatie geleid tot een aanzienlijke afname in de bedrijfsgrootte. De sector heeft op deze ontwikkelingen gereageerd door diversificatie en intensivering van de productie. Diversificatie werd bereikt door het introduceren van gewassen met een hoge toegevoegde waarde, zoals bloemen en groenten; intensivering door het aantal gewassen per jaar te verhogen en door intensief gebruik van externe productiemiddelen, in het bijzonder kunstmest en chemische bestrijdingsmiddelen. Deze ontwikkelingen hebben het gevaar vergroot voor negatieve milieueffecten door emissies van agro-chemicaliën, vooral nutriënten en biociden, zowel door oppervlakkige afstroming als door uitspoeling.

Binnen het district kunnen geomorfologisch drie sub-regio's worden onderscheiden: het vlakke zuidelijke deel, waar voornamelijk rijst en groenten worden verbouwd, het middendeel dat afwisselend vlak en heuvelachtig is, en waar, op terrassen, voornamelijk regenafhankelijke gewassen worden verbouwd, zoals cassave, maïs en sojabonen, en het noordelijke bergachtige gebied, met steile hellingen, die voor een deel onder productiebos staan.

In het onderzoek is aandacht besteed aan vier componenten: (i) de dynamiek van bodemdegradatie, gebruik makend van remote sensing beelden, (ii) metingen van bodemerosie op verschillende ruimtelijke schalen (veld-, deelstroomgebied- en stroomgebiedsniveau) en het modelleren en simuleren van erosie op het niveau van een stroomgebied waarin omdijkte rijstvelden voorkomen en een deelstroomgebied in het heuvelachtige gebied; (iii) metingen van de dynamiek van minerale stikstof in verschillende bodemtypen en bij verschillende vormen van landgebruik en het ontwikkelen van een simulatiemodel van water- en stikstofbalansen om stikstofuitspoeling van verschillende huidige en alternatieve landgebruikssystemen te simuleren; en (iv) het opschalen van de stikstofdynamiek en verliezen van stikstof door uitspoeling, gebruikmakend van geo-statistiek en geografische informatiesystemen.

De analyse van remote sensing beelden liet zien dat bodemdegradatie in Tam Duong sterk is toegenomen in de 80-er jaren, en daarnaast een sterke dynamiek vertoont. De analyse van Landsatbeelden, op basis van de verhouding van signalen in

verschillende golflengten, liet zien dat de bodemdegradatie toenam tussen 1986 en 1992, samenhangend met sterke ontbossing en uitbreiding van het landbouwareaal; tussen 1992 en 1996 nam het gedegradeerde areaal af als gevolg van herbebossing vooral met *Eucalyptus plantages*; na 1996 nam het gedegradeerde areaal weer toe, in samenhang met het oogsten van productiebos.

De belangrijkste oorzaak van bodemdegradatie in het heuvelachtige deel van Tam Duong district is erosie. Erosie is daarom gemeten in Quan Dinh stroomgebied, in dit heuvelachtige gebied, met een totale oppervlakte van 248.9 ha, dat representatief is voor de bodems, het landgebruik en de landbouwpraktijk in het district. Erosie bleek buitengewoon ernstig op het niveau van individuele percelen, maar veel minder wanneer het betrokken wordt op de schaal van het deelstroomgebied of van het totale stroomgebied, als gevolg van bezinken van sediment gedurende het transport door het stroomgebied, vooral op terrassen en in omdijkte rijstvelden waar water tijdelijk kan worden opgeslagen. De jaarlijkse oppervlakkige afstroming in de twee jaren waarin metingen werden verricht (2004 en 2005) bedroeg 538 en 3324 m³ ha⁻¹ en het daarmee gepaard gaande grondverlies was respectievelijk 163 and 1722 kg ha⁻¹. De hoge waarden voor 2005 waren het gevolg van één buitengewoon grote regenbui, wat laat zien dat extrapolatie en generalisatie van gemeten waarden gepaard gaat met grote onzekerheden.

Om mogelijkheden te hebben voor een uitgebreidere analyse van de risico's van erosie, is het erosiemodel LISEM getest in het studiegebied. Modelgedrag en dus de resultaten van het model waren verschillend voor verschillende ruimtelijke schalen. Voor het totale stroomgebied, dat gekarakteriseerd wordt door een grote verscheidenheid in landgebruikstypen, zowel voor velden in het laagland als voor velden in de heuvels, en een complexe geomorfologie van heuvelachtig gebied, terrassen en omdijkte rijstvelden, werden totale afstroming en grondverlies onderschat door het model. Voor het deelstroomgebied, dat voornamelijk heuvelachtig gebied omvat, werd het grondverlies overschat. De voornaamste reden voor die overschatting was de hoge sediment-concentratie die gesimuleerd werd in het deelstroomgebied gerelateerd aan de hoge capaciteit voor detachement van bodemdeeltjes en voor transport. De onderschatting voor het totale stroomgebied was gerelateerd aan tijdelijke opslag van water en sediment in rijstvelden en terrassen, een proces dat niet in het model was opgenomen.

Uitspoeling van stikstof uit de wortelzone is een ander proces dat bijdraagt aan milieuverontreiniging, zowel op veld- als op regionaal niveau en wordt beschouwd als één van de oorzaken van lage efficiënties van kunstmestgebruik. Metingen op veldniveau toonden regelmatig hoge stikstofconcentraties in de diepere bodemlagen, een aanwijzing voor substantiële uitspoeling, samenhangend met hoge regenval en/of

grote hoeveelheden irrigatiewater, een lage behoefte aan stikstof van het gewas en hoge kunstmestgiften. Resultaten van een stikstofbalansmodel, waarvan de resultaten de gemeten waarden goed reproduceerden, gaven aan dat stikstofuitspoeling toenam met toenemende kunstmeststikstofgiften, i.e. in de rijst-rijst-maïs rotatie varieerde de uitspoeling, afhankelijk van de regenval, van 52-60 kg ha⁻¹ bij lage stikstofgiften, van 56 tot 114 bij intermediaire giften en van 58 tot 154 kg ha⁻¹ bij hoge giften.

De stikstofuitspoeling is vooral hoog onder de gewassen met een hoge toegevoegde waarde, die heel zwaar met stikstofkunstmest worden bemest. Jaarlijkse uitspoelingsverliezen tot 193 kg ha⁻¹ voor bloemen werden berekend en 115 voor groenten, vergeleken met ongeveer 50 voor rijst.

De ruimtelijke verdeling van de concentraties aan nitraat- en ammoniakstikstof in het bovenste grondwater onder verschillende omgevingsomstandigheden (bodem en topografie) en verschillende landgebruiksvormen is berekend op basis van een set van puntwaarnemingen. De belangrijkste verklarende variabelen bij deze interpolatie, geïdentificeerd via backward lineaire regressie gecombineerd met kennis van deskundigen, bleken landgebruiksvorm, bodemtype en bodemtextuur te zijn. Semi-variogrammen zijn berekend en geschikte modellen ontwikkeld voor de originele stikstofconcentraties en voor de residuele waarden, afgeleid van de regressieanalyse. De ruimtelijke verdeling van stikstofconcentraties werd 'voorspeld' via gewone 'block kriging' zowel als via regressie 'block kriging'. De resultaten van de laatste methode bleken nauwkeuriger, omdat additionele informatie gebruikt kon worden in de regressieanalyse. De temporele dynamiek van de stikstofconcentraties hing enerzijds samen met omgevingsfactoren, zoals regenval en anderzijds met het landgebruik en de daaraan gerelateerde irrigatie- en bemestingsregimes.

Voor het verkennen van de mogelijkheden voor en de gevolgen van het introduceren van alternatieve landgebruiksvormen en gewasbeheersvormen, is een ruimtelijk dynamisch model ontwikkeld waarmee de dynamiek van stikstof kan worden gesimuleerd op sub-regionaal niveau, waarbij het gebied bestaat uit een mozaiek van verschillende bodemtypen en landgebruikstypen, onder verschillende irrigatie- en bemestingsregimes. Het model is gecalibreerd op basis van gemeten stikstofconcentraties in één jaar, en vervolgens toegepast op een volgend jaar. De bijdrage van laterale stroming aan de herverdeling van stikstof was gering, omdat het studiegebied erg vlak is. Uitspoeling was dus het belangrijkste proces dat leidde tot grote verliezen van stikstof naar het grondwater. De berekende totale jaarlijkse uitspoelingsverliezen varieerden van 88 tot 122 kg N ha⁻¹ onder bloemen, van 64 tot 82 onder groenten behorend tot de 'koolgroep' (paprika, kool, aubergine, koolrabi), van 51 tot 76 onder chili, van 56 tot 75 kg onder groenten van de 'squashgroep' (komkommer, tomaat, pompoen) en van 36 tot 55 kg ha⁻¹ onder rijst.

Het model is een nuttig instrument voor het vaststellen van milieueffecten op regionaal niveau en voor managementondersteuning, maar, om het met vertrouwen te kunnen toepassen onder verschillende omstandigheden, moet het verder worden gekalibreerd en gevalideerd onder verschillende omgevingsomstandigheden.

De studie heeft duidelijk gemaakt dat de huidige landbouwkundige ontwikkelingen in Tam Duong district in Vietnam, die in sterke mate worden gestuurd door (korte termijn) economische overwegingen, een serieus gevaar inhouden voor de kwaliteit van de natuurlijke hulpbronnen, met name die van bodem en water, en dus een risico vormen voor de milieukundige duurzaamheid van de landbouwproductiesystemen. Hieruit blijkt dat er conflicten zijn tussen verschillende doelstellingen die nagestreefd kunnen worden bij het gebruik van het land. Om oplossingen te vinden voor dergelijke conflicten kunnen resultaten zoals gegenereerd in deze studie worden gebruikt om bij te dragen aan integrale analyses. Zulke integrale analyses van meervoudige doelen van landgebruik, waarbij alle belanghebbenden, zoals boeren(organisaties), lokale beleidsmakers, niet-gouvernementele organisaties, natuurbeschermingsorganisaties, en nationale beleidsmakers betrokken moeten worden, zijn noodzakelijk om opties voor duurzame ontwikkeling te verkennen.

Tóm tắt

Nghiên cứu “Xói mòn đất và rửa trôi đạm tại miền bắc Việt Nam: thí nghiệm và mô hình” được tiến hành tại Tam Dương, một huyện đầu nguồn của đồng bằng Sông Hồng, nằm trên vùng chuyển tiếp giữa miền đồng bằng và miền núi cao phía bắc Việt Nam. Vì dân số Tam Dương tăng nhanh trong những thập kỷ trước nên nhu cầu về lương thực, thực phẩm cũng tăng theo cả về số lượng và tính đa dạng. Đối với sản xuất nông nghiệp, gia tăng dân số còn kéo theo sự sụt giảm nghiêm trọng bình quân diện tích đất tính theo đầu người. Hệ thống canh tác nông nghiệp cũng phát triển cả về mức độ đa dạng và thâm canh, đáp ứng cho nhu cầu ngày một tăng này. Đa dạng hóa thông qua việc phổ biến rộng rãi các loại cây trồng có giá trị kinh tế cao như hoa và rau màu, thâm canh cao thông qua việc gia tăng số vụ gieo trồng trong năm và gia tăng đầu vào như sử dụng nhiều phân bón và hóa chất. Sự phát triển ngày càng tăng này ảnh hưởng đến môi trường do sự phát thải của hóa chất dùng trong nông nghiệp, đặc biệt là các chất dinh dưỡng, bằng cả hai con đường trên bề mặt và thấm sâu vào lòng đất.

Huyện Tam Dương được chia làm 3 tiểu vùng: tiểu vùng đồng bằng phía nam với đặc trưng là hệ thống canh tác lúa và rau màu; tiểu vùng đồi thấp xen kẽ đất bằng nằm ở giữa huyện với đặc trưng canh tác của hầu hết các loại cây như sắn, ngô, và đậu tương; và tiểu vùng núi cao phía bắc với địa hình dốc hầu hết được che phủ bởi rừng sản xuất. Lưu vực Quan Đình có diện tích 248,9 ha với độ cao từ 28–70 m so với mực nước biển trung bình, là một lưu vực đại diện cho vùng đồi núi của huyện Tam Dương, được lựa chọn nghiên cứu về xói mòn.

Mục đích của đề tài là: (i) nghiên cứu động thái thoái hóa đất bằng phương pháp sử dụng ảnh viễn thám; (ii) đánh giá xói mòn ở các quy mô khác nhau và mô phỏng xói mòn ở quy mô tiểu lưu vực và lưu vực có trồng lúa; (iii) xác định động thái của đạm trên các loại đất và cây trồng khác nhau, phát triển một mô hình phù hợp để tính toán lượng đạm bị rửa trôi trong các hệ thống sản xuất nông nghiệp; và (iv) mở rộng đánh giá rửa trôi đạm ở quy mô tiểu vùng sử dụng hệ thống thông tin và thống kê địa lý.

Kết quả phân tích ảnh viễn thám đã chỉ ra rằng đất ở Tam Dương đã bị thoái hóa mạnh trong các năm 1980. Những ảnh tỉ lệ đã phân loại, cùng với số liệu trong bản đồ đất và số liệu kiểm tra thực địa cho thấy diện tích đất bị thoái hóa ở Tam Dương lớn nhất vào năm 1992, chủ yếu do phá rừng hàng loạt để lấy đất sản xuất nông nghiệp vào những năm trước đó. Sau đó diện tích đất bị thoái hóa giảm đi vào năm 1996, nhờ kết quả của việc trồng rừng, đặc biệt là rừng bạch đàn. Tuy nhiên do thu hoạch đồng loạt bạch đàn nên diện tích đất bị thoái hóa lại tăng lên vào năm 2000.

Nguyên nhân chính của thoái hóa đất trên vùng đồi núi là do xói mòn. Quá trình này xảy ra nghiêm trọng ở quy mô ô thửa nhưng lại rất thấp ở quy mô tiểu lưu vực và lưu

vực, bởi vì đất được giữ lại trong quá trình vận chuyển. Dòng chảy mặt tại quy mô lưu vực đo được là 538 và 3.324 m³ ha⁻¹ năm⁻¹ trong năm 2004 và 2005. Dòng chảy này kéo theo lượng đất mất tương ứng là 163 và 1.722 kg ha⁻¹ năm⁻¹. Thể tích dòng chảy mặt và lượng đất mất trong năm 2005 cao do xuất hiện một số trận mưa lớn bất thường. Điều đó cho thấy việc suy diễn từ các kết quả như trên là không chắc chắn. Để phân tích cận kẽ hơn về xói mòn trong vùng nghiên cứu, mô hình xói mòn LISEM đã được sử dụng. Kết quả của mô hình đã cho thấy những kết quả mô phỏng theo hướng khác nhau cho các quy mô lưu vực khác nhau. Thể tích dòng chảy và lượng đất mất tính toán ở quy mô lưu vực thấp hơn so với thực đo do các loại hình sử dụng đất rất đa dạng ở cả vùng đất dốc và đất bằng, và địa hình địa mạo phức tạp, các loại bậc thang, ruộng lúa phân bố dọc theo hệ thống sông suối trải dài từ lưng chừng đồi đến cửa lưu vực. Trong khi đó lượng đất mất tính toán tại tiểu lưu vực đất dốc lại cao hơn thực đo. Nguyên nhân chính là do hàm lượng cận tính toán cao hơn so với hàm lượng thực đo vì sự công phá mạnh và khả năng vận chuyển cao của dòng chảy. Trong khi thể tích dòng chảy mặt và lượng đất mất tính toán tại lưu vực chính thấp hơn thực đo, bởi vì hiệu ứng đọng và nhả nước tại các ruộng bậc thang và ruộng lúa, một quá trình chính trong lưu vực chính, lại không bao gồm trong mô hình.

Hiện tượng rửa trôi đạm khởi tầng rễ là một quá trình khác trên các ruộng bậc thang, gây ra hậu quả ô nhiễm môi trường trên cả quy mô ô thửa và vùng, và làm giảm hiệu quả sử dụng phân đạm. Kết quả thí nghiệm đã chỉ ra hàm lượng đạm cao ở các tầng đất sâu, dấu hiệu của quá trình rửa trôi mạnh mẽ, dưới ảnh hưởng của lượng mưa và nước tưới cao, lượng cây hút thấp và lượng phân bón cao. Các kết quả mô phỏng từ mô hình cân bằng đạm được hiệu chỉnh với hàm lượng đạm thực đo đã cho thấy sự rửa trôi gia tăng khi lượng phân bón cao hơn, ví dụ trong hệ thống luân canh lúa-lúa-ngô đông lượng đạm bị rửa trôi ở các mức bón phân theo thứ tự thấp, trung bình và cao từ 52 đến 60, 56 đến 114 và 58 đến 154 kg ha⁻¹ năm⁻¹.

Hiện tượng rửa trôi đạm đặc biệt cao trên các cây trồng thâm canh với lượng phân bón rất cao. Lượng đạm bị rửa trôi hàng năm được tính toán lên đến 193 kg ha⁻¹ trên đất trồng hoa và 115 kg ha⁻¹ trên đất trồng rau so với khoảng 50 kg ha⁻¹ trên đất trồng lúa.

Phân bố hàm lượng đạm a môn và ni tơ rất trong nước ngầm tầng nông dưới các điều kiện môi trường (đất và địa hình) và các loại hình sử dụng đất khác nhau được xác định từ số liệu thực đo tại các điểm bằng phương pháp địa thống kê. Yếu tố môi trường quan trọng nhất xác định bằng phương pháp phân tích hồi quy tuyến tính nghịch (stepwise backward linear regression) kết hợp với kiến thức chuyên gia là loại hình sử dụng đất, loại đất và thành phần cơ giới đất. Các biểu đồ semi-variogram được tính toán và các mô hình tương ứng được thiết lập cho các hàm lượng đạm thực đo và các dư số (residuals) của kết quả tính toán hồi quy tuyến tính. Hàm lượng đạm được

phỏng đoán bằng hai phương pháp mô phỏng khối thông thường (ordinary block kriging; OBK) và mô phỏng khối hồi quy (regression block kriging; RBK). RBK cho kết quả chính xác hơn OBK vì phương pháp này có tính đến các thông tin phụ từ phép hồi quy. Sự thay đổi hàm lượng đạm trong nước ngầm theo thời gian chủ yếu phụ thuộc vào các yếu tố môi trường như mưa, sử dụng đất với các chế độ tưới và phân bón khác nhau.

Để phát triển và đánh giá các phương án sử dụng đất, một mô hình động thái không gian được xây dựng. Mô hình này mô phỏng động thái của đạm của một tiểu vùng có các loại đất và sử dụng đất khác nhau dưới các chế độ tưới và phân bón khác nhau. Mô hình được hiệu chỉnh với số liệu thực đo hàm lượng đạm trong năm thứ nhất và áp dụng cho năm thứ hai. Kết quả cho thấy dòng vận chuyển ngang có ảnh hưởng tương đối nhỏ so với sự tái phân bố đạm trong vùng đất bằng phẳng này. Thấm sâu mới là quá trình chính dẫn đến sự rửa trôi nhiều đạm xuống tầng nước ngầm. Lượng đạm bị rửa trôi hàng năm tính toán được thay đổi từ 88 đến 122 kg N ha⁻¹ trên đất trồng hoa, 64 đến 82 trên đất trồng rau 'nhóm cải bắp' (ví dụ cải bắp, cà, xu hào), 51 đến 76 trên đất trồng ớt, 56 đến 75 trên đất trồng rau nhóm bầu bí (ví dụ dưa chuột, cà chua, bí xanh), và 36 đến 55 trên đất lúa. Mô hình này là một công cụ hữu ích cho đánh giá tác động môi trường và hỗ trợ quản lý ở cấp vùng. Tuy nhiên, để có thể áp dụng rộng rãi, mô hình cần được hiệu chỉnh và đánh giá với những điều kiện đặc thù trước khi áp dụng để phân tích hậu quả của các phương án sử dụng đất và các biện pháp canh tác.

Nghiên cứu này đã chỉ ra rằng sự phát triển nông nghiệp hiện nay của huyện Tam Dương hàm chứa một số thiệt hại về chất lượng của nguồn tài nguyên thiên nhiên, đặc biệt là đất và nước, đe dọa sự bền vững về môi trường. Tuy nhiên, sự phát triển này là nỗ lực để đạt được những thành tựu kinh tế địa phương. Những mâu thuẫn xuất hiện khi chọn lựa các mục tiêu sử dụng đất đòi hỏi những phân tích toàn diện hơn trong đó có sự tham gia của nhiều đối tác có liên quan như nông dân, các tổ chức địa phương, các cơ quan bảo vệ môi trường và các nhà hoạch định chính sách.

PE&RC PhD Education Statement Form

With the educational activities listed below the PhD candidate has complied with the educational requirements set by the C.T. de Wit Graduate School for Production Ecology and Resource Conservation (PE&RC) which comprises of a minimum total of 22 credits (= 32 ECTS = 22 weeks of activities).



Review of Literature (4.2 credits)

- Nutrient losses in intensive farming in northern Vietnam

Writing of Project Proposal (7 credits)

- Soil erosion and nitrogen leaching in northern Vietnam: Experimentation and modelling

Post-Graduate Courses (10 credits)

- Soil ecology: Linking theory to practice; PE&RC, SENSE (2003)
- Wind and water erosion modelling and assessment; PE&RC (2004)
- Scientific writing; PE&RC (2004)
- The art of modelling; PE&RC (2006)
- Project and time management; PE&RC (2006)

Deficiency, Refresh, Brush-up and General courses (6 credits)

- System analysis, simulation and system management; PPS (2003)

Competence Strengthening / Skills courses (4 credits)

- Academic writing I; CENTA (2006)
- Academic writing II; CENTA (2006)

PhD Discussion Groups (4.2 credits)

- Sustainable land-use and resource management, with a focus on the tropics (2003)
- Methodology for soil erosion research in watershed (2004)
- A stakeholder meeting and discussion on land-use planning (2004)

PE&RC Annual Meetings, Seminars and Introduction Days (1.9 credits)

- PE&RC introduction weekend (2003)
- Soil fertility group meeting (2006)

International Symposia, Workshops and Conferences (8 credits)

- GIS IDEAS 2004 (international symposium on geoinformatics for spatial infrastructure development in earth and allied); Hanoi, Vietnam (2004)
- AIC International partners' meeting; Canada project, Mwanza, Tanzania (2004)
- ACRS2005, the 26th Asian Conference on Remote Sensing (ACRS); Hanoi, Vietnam (2005)

Curriculum vitae

Mai Van Trinh was born in Thai Binh province, Vietnam, on March 15th, 1967. He finished highschool in 1984 and studied for a Bachelor of Science degree in Agriculture, specializing in Soils and Fertilizers, at the Agricultural University No. 1, Hanoi, Vietnam. After obtaining his first degree in 1990, he worked as a research assistant in the Department of Soil Science and Agricultural Extension, Agricultural Extension Center, Thai Binh province. He participated in a soil mapping team for four districts for two years, and subsequently in a project for transfer of technology to farmers for three years. He then moved as a research scientist to the Institute for Soils and Fertilizers (ISF) in Hanoi, working for three years in soil erosion and soil conservation studies.

With an MSc scholarship from The Netherlands Fellowship Program (NFP) he studied Environmental Analysis and Monitoring (ESM2) at the International Institute for Geo-Information Science and Earth Observation (ITC) in Enschede, The Netherlands, where he graduated in April 2000. The study programme included watershed management, remote sensing and geographic information systems. He then returned to ISF. In January 2003, he started a PhD programme at the Plant Production Systems group (PPS) of Wageningen University with a scholarship from the Vietnamese Ministry of Education and Training (MOET).

Funding

Financial support for this thesis was received from project 322 of the Vietnam Ministry of Education and Training (MOET) through a PhD grant. Additional financial support came from the Vietcansol project, National Institute for Soils and Fertilizers (NISF), Vietnam and the Anne van den Ban Fund.